



# Light-regulated Pro-angiogenic Engineered Living Materials

Dissertation  
zur Erlangung des Grades  
des Doktors der Naturwissenschaften  
der Naturwissenschaftlich-Technischen Fakultät  
der Universität des Saarlandes

von  
Priyanka Dhakane  
Saarbrücken, 2023

Tag des Kolloquiums: 23.02.2024

Dekan: Prof. Dr. Ludger Santen

Berichterstatter: Prof. Dr. Aránzazu del Campo Bécares

Prof. Dr. Franziska Lautenschlager

Akad. Mitglied: Dr. Lorenz Latta

Vorsitz: Prof. Dr. Albrecht Ott

# **Light-regulated Pro-angiogenic Engineered Living Materials**

Priyanka Dhakane

Geb. In Maharashtra, India

DISSERTATION

INM- Leibniz Institut für Neue Materialien, Saarbrücken

I hereby declare that I wrote the dissertation submitted without any unauthorized external assistance and used only sources acknowledged in the work. All textual passages which are appropriated verbatim or paraphrased from published and unpublished texts as well as all information obtained from oral sources are duly indicated and listed in accordance with bibliographical rules. In carrying out this research, I complied with the rules of standard scientific practice as formulated in the statutes of Saarland University in Saarbrücken to ensure good scientific practice.

Priyanka Dhakane

## TABLE OF CONTENTS

<b>ACKNOWLEDGMENTS</b> .....	<b>4</b>
<b>ABSTRACT</b> .....	<b>6</b>
<b>ZUSAMMENFASSUNG</b> .....	<b>7</b>
<b>MOTIVATION</b> .....	<b>8</b>
<b>CHAPTER 1. INTRODUCTION: REVIEW OF PRO-ANGIOGENIC THERAPIES AND ADVANCES IN GROWTH FACTOR DELIVERY</b> .....	<b>11</b>
<b>1.1. USE OF GROWTH FACTORS IN REGENERATIVE MEDICINE</b> .....	<b>12</b>
<b>1.2. APPROACHES FOR CONTROLLED DELIVERY OF GFS BASED ON BIOMATERIALS IMMOBILIZATION</b> .....	<b>14</b>
1.2.1. PHYSICAL ENCAPSULATION/ IMMOBILIZATION OF GFS .....	15
1.2.2. ENGINEERING GFS FOR COVALENT ATTACHMENT TO BIOMATERIALS .....	15
1.2.3. ECM INSPIRED GF DELIVERY SYSTEMS. ....	16
<b>1.3. ANGIOGENESIS</b> .....	<b>16</b>
<b>1.4. IMPORTANCE OF VEGF IN ANGIOGENESIS</b> .....	<b>18</b>
<b>1.5. CHALLENGES INVOLVED IN ANGIOGENESIS THERAPIES</b> .....	<b>21</b>
1.5.1. ABNORMAL GROWTH OF BLOOD VESSELS IN TISSUES NOT TARGETED FOR TREATMENT. ....	21
1.5.2. VEGF THERAPY MAY LEAD TO THE DEVELOPMENT OF DYSFUNCTIONAL BLOOD VESSELS. ....	21
1.5.3. GROWTH OF NEOPLASMS .....	22
1.5.4. HYPOTENSION AND VASODILATION DURING SHORT TERM ADMINISTRATION OF VEGF.....	23
<b>1.6. ENGINEERED LIVING MATERIALS FOR SMART DELIVERY OF DRUGS</b> .....	<b>23</b>
<b>1.7. REFERENCES</b> .....	<b>28</b>
<b>CHAPTER 2. OPTOGENETIC ENGINEERING OF BACTERIA TO LIGHT-RESPONSIVELY SECRETE A PRO-ANGIOGENIC PROTEIN.</b> .....	<b>42</b>
<b>2.1. INTRODUCTION</b> .....	<b>43</b>
2.1.1. OPTOGENETIC CONTROL OF DRUG PRODUCTION IN BACTERIA .....	46
2.1.2. SECRETION OF PROTEINS FROM <i>E. COLI</i> .....	48
<b>2.2. DESIGN, CLONING AND PURIFICATION OF THE FUSION PROTEIN YEBF-CBD-QK (YCQ) AND THE CONTROL VARIANT</b> .....	<b>50</b>
2.2.1. DESIGN, CLONING AND DETECTION OF THE HIS-TAG VARIANT .....	50
2.2.2. ENGINEERING YCQ WITH STREP TAG .....	51
2.2.3. CHARACTERIZATION OF YEBF-MEDIATED SECRETION.....	53
<b>2.3. CONCLUSION AND DISCUSSION:</b> .....	<b>56</b>
<b>2.4. MATERIALS AND METHODS</b> .....	<b>58</b>
2.4.1. CONSTRUCTION OF PLASMIDS AND BACTERIAL STRAINS: .....	58
2.4.2. PURIFICATION OF YCQ AND YCX .....	59
2.4.4. SDS PAGE ANALYSIS OF THE SECRETED AND PURIFIED YCQ.....	60

2.4.4. ANALYSIS OF THE PROTEIN WITH WESTERN BLOT AND MASS SPECTOMETRY .....	62
2.4.5. PATTERNING OF COL-GEL MATRIX ON A GLASS SURFACE TO ASSESS BINDING OF YCQ: .....	63
<b>2.5. REFERENCES .....</b>	<b>67</b>
<b><u>CHAPTER 3. SECURE ENCAPSULATION AND CHARACTERIZATION OF ENGINEERED BACTERIA IN BILAYER THICK-FILM HYDROGEL CONSTRUCTS .....</u></b>	<b>76</b>
<b>3.1. INTRODUCTION .....</b>	<b>77</b>
<b>3.2. ENCAPSULATION OF BACTERIA IN THIN FILM SCAFFOLDS .....</b>	<b>81</b>
<b>3.3. METHODOLOGIES TO FABRICATE BILAYER THICK FILMS WITH DEFINED GEOMETRIES AND PLUDA COMPOSITIONS .....</b>	<b>82</b>
3.3.1. FABRICATING THE MOLDS FOR MAKING ELMs .....	82
3.3.2. MEDIA OPTIMIZATION FOR ELMs .....	85
<b>3.4. CHARACTERIZATION OF BACTERIAL GROWTH IN THE HYDROGEL CORE .....</b>	<b>87</b>
<b>3.5. STUDYING LIGHT REGULATED YCQ RELEASE AND BIOACTIVITY FROM THE BACTERIAL HYDROGELS .....</b>	<b>89</b>
3.5.1. ESTABLISHING ELISA-BASED ASSAY TO QUANTIFY YCQ RELEASE INTO THE MEDIUM .....	89
<b>3.6. QUANTIFICATION OF LIGHT-SWITCHABLE AND LIGHT-TUNABLE RELEASE OF YCQ .....</b>	<b>91</b>
3.6.1. YCQ QUANTIFICATION FROM HYDROGELS .....	91
<b>3.7. CONCLUSION AND DISCUSSION .....</b>	<b>97</b>
<b>3.8. MATERIALS AND METHODS: .....</b>	<b>98</b>
3.8.1. FABRICATION OF ELMs .....	98
3.8.2. ANALYSIS OF ELMs .....	100
<b>3.9. REFERENCES .....</b>	<b>102</b>
<b><u>CHAPTER 4. 2D NETWORK-FORMATION ASSAY WITH HUVECS TO STUDY THE BIOACTIVITY OF YCQ .....</u></b>	<b>106</b>
<b>4.1. IN VITRO MODELS TEST THE ANGIOGENIC POTENTIAL OF NEW MOLECULES. ....</b>	<b>107</b>
<b>4.2. SCREENING OF MATRICES FOR THE ANGIOGENESIS ASSAY .....</b>	<b>112</b>
4.2.1. MATRIGEL™ .....	112
4.2.2. GELATIN METHACRYLATE HYDROGELS .....	113
4.2.3. COLLAGEN-FIBRIN GELS .....	115
4.2.4. COLLAGEN-GELATIN GELS FOR ANGIOGENESIS .....	116
<b>4.3. SURFACE IMMOBILIZATION OF YCQ .....</b>	<b>120</b>
<b>4.4. ESTABLISHMENT OF FIXATION, IMMUNOSTAINING, AND IMAGE ANALYSIS PROTOCOLS.....</b>	<b>122</b>
<b>4.6. NETWORK FORMATION CAPABILITIES OF LIGHT-RESPONSIVELY SECRETED YCQ FROM LIQUID CULTURE AND PURE YCQ .....</b>	<b>127</b>
<b>4.7. NETWORK FORMATION CAPABILITIES OF LIGHT-RESPONSIVELY SECRETED YCQ FROM ELMs</b>	<b>131</b>
<b>4.8. CONCLUSION AND DISCUSSION .....</b>	<b>134</b>

<b>4.9. MATERIALS AND METHODS.....</b>	<b>135</b>
4.8.1. HUVEC NETWORK FORMATION ASSAY:.....	135
<b>4.9. REFERENCES .....</b>	<b>138</b>
<b>CONCLUSION AND OUTLOOK .....</b>	<b>146</b>

## Acknowledgments

The work was performed at the INM-Leibniz Institute for New Materials, Saarbrücken.

First, I would like to express my gratitude to Prof. Dr. Aránzazu del Campo for giving me the opportunity to work at the INM. Her guidance in the first year of PhD helped me to think critically about my own work to make it better. I would also like to thank her for continuous support and motivation throughout this journey. I am grateful that I could join and work with her interdisciplinary group which offered me a creative work environment.

I would like to express my deepest gratitude to my mentor Dr Shrikrishnan Sankaran, who conceived the project idea. This PhD journey would not have been possible without you. You supported me through the highs and lows of this beautiful journey. Thank you for motivating me and being patient when the results were not promising. It gave me hope and the strength to continue. I learnt a lot about science from our critical discussions about the results. I always think that you communicate science very well. I tried learning that from you and hope to carry it with me throughout my life. Thanks for always being there whenever I needed guidance. Thanks for providing me with resources to carry out this project successfully. I truly enjoyed working with the Bioprogrammable Materials Group because of its diverse environment and enthusiastic members.

Next, I would like to thank VarunSai Tadimarri. I supervised you during your master thesis in the lab and learnt a lot from you on this journey. The undying enthusiasm that you showed throughout the journey is highly commendable. We optimized critical experiments together, which was possible because of your positivity. You were always open to learning and exploring more. You contributed in many ways to make this project a success.

I would like to thank the group members of Dynamic Biomaterials and Bioprogrammable Materials. Shardul, Maria, Qiyang, Rocio, Adrian, Ana, Minye, Mitchell, Sam, you were the first people I met when I joined the group. You all made living in a foreign country easier for me. Varun, Florian, Marc, Varun, Ketaki, Zahra, Hanuman, Anwasha, we had a lot of fun times outside of work. I will forever remember our parties, gatherings, food outings and all the fun we had together.

I would like to thank my parents and my sister, Daksha for believing in me and for proving me with an unwavering support, lots of love and encouragement. You are a constant source of positivity in my life. You all gave me strength to explore my career in a foreign country.

Finally, I would like to thank my amazing husband, Navnath. We have known each other for years now and I constantly keep learning from you in many aspects of life. You contributed to my personal and professional growth in many ways. You supported me and believed in me when I did not believe in myself. I could handle the rough phases of this PhD journey because of you. Words will fall short to express my gratitude and appreciation for you.

## **Abstract**

The role of growth factors is important to stimulate regenerative cellular changes to rejuvenate damaged cells, tissues, and organs. Growth factor engineering and delivery systems are developed quite a lot for example, emergence of small protein like chains (peptidomimetics) and matrices for controlled release of growth factors. Despite these advancements, the use of growth factors in regenerative medicine is limited because of their low stability. In this thesis, angiogenesis inducing Engineered Living Materials (ELMs) are used as the strategy to overcome the limitations associated with traditional GF delivery methods. These ELMs contain living bacteria programmed to synthesize angiogenic protein in response to light. This thesis describes challenges and successes in developing light regulated Engineered Living Material that releases angiogenic protein. The bacteria were ontogenetically engineered to synthesize and secrete a Vascular Endothelial Growth Factor (VEGF) mimetic peptide (QK) attached to a Collagen Binding Domain (CBD). To create an ELM, the engineered bacteria were safely encapsulated in a bilayer hydrogel designed to help aid survival and to prevent bacterial escape from the material. It is proven that in-situ control over production of pro-angiogenic protein can be attained with light. Secreted protein can bind to collagen and promote endothelial cell network formation which is a hallmark of angiogenesis. These results highlight the potential of this light inducible ELM to support vascularization in endothelial cells.

## Zusammenfassung

Wachstumsfaktoren spielen eine wichtige Rolle bei der Stimulierung regenerativer zellulärer Veränderungen zur Verjüngung geschädigter Zellen, Gewebe und Organe. Die Entwicklung von Systemen zur Herstellung und Verabreichung von Wachstumsfaktoren ist weit fortgeschritten, z. B. die Entwicklung von kleinen proteinhaltigen Ketten (Peptidomimetika) und Matrizen zur kontrollierten Freisetzung von Wachstumsfaktoren. Trotz dieser Fortschritte ist die Regenerationsfähigkeit von Wachstumsfaktoren aufgrund ihrer geringen Stabilität im menschlichen Körper und der Notwendigkeit, ihre lokale Konzentration sorgfältig zu regulieren, um schädliche Auswirkungen zu vermeiden, begrenzt. In dieser Arbeit werden Angiogenese-induzierende lebende Materialien (ELMs) als Strategie zur Überwindung der mit den herkömmlichen GF-Verabreichungsmethoden verbundenen Einschränkungen verwendet. Diese ELMs enthalten lebende Bakterien, die darauf programmiert sind, als Reaktion auf Licht angiogenes Protein zu synthetisieren. In dieser Arbeit werden die Herausforderungen und Erfolge bei der Entwicklung eines ELMs beschrieben, das ein Angiogenese-induzierendes Protein auf lichtregulierte Weise freisetzt. Die Bakterien wurden ontogenetisch so verändert, dass sie ein mimetisches Peptid (QK) des vaskulären endothelialen Wachstumsfaktors (VEGF) synthetisieren und absondern, das an eine kollagenbindende Domäne (CBD) gebunden ist. Um ein ELM herzustellen, wurden die manipulierten Bakterien sicher in einem zweischichtigen Hydrogel eingekapselt, das das Überleben der Bakterien unterstützt und ihr Entweichen aus dem Material verhindert. Es wurde gezeigt, dass das Freisetzungsprofil des pro-angiogenen Proteins in-situ mit Hilfe von Licht gesteuert werden kann. Das sezernierte Protein kann an Kollagen binden und die Endotheli

## Motivation

Growth factors (GF) play an important role in stimulating and coordinating the changes necessary for regeneration of damaged tissue. Various cells secrete GFs which can bind to extracellular matrix as well as interact with the cell surface receptors. This interaction can initiate downstream signaling pathways that activate various processes, including cell proliferation, growth, differentiation, survival, adhesion, and migration.<sup>1-4</sup> A good example of this is VEGF promoting the formation of blood vessels by activating integrin, WNT and NOTCH signaling pathways.<sup>5</sup> Therefore, growth factors represent potent tools in the field of regenerative medicine. Nevertheless, their potential to drive significant cellular changes necessitates precise control over their concentration and localization. Failure to attain precise control over these factors can lead to overstimulation of target cells, which can then result into unwanted effects like necrosis or activation of dormant tumor.<sup>6,7</sup> There are some examples where clinically approved medical products have been reported to show side-effects, such as Regnarex based on PDGF (which is linked to an increased systemic cancer risk, cellulitis, and skin rash).<sup>8</sup> Beyond these adverse effects, growth factors are intricate, large proteins characterized by poor stability, which makes their storage and manufacturing expensive.<sup>7,9</sup> Due to these challenges there is limitation on implementation of growth factor based therapies in clinics.<sup>10</sup>

Two primary strategies have been employed to tackle these challenges. The use of drug-release systems is the first strategy used that allows localized and controlled delivery of drugs for prolonged periods of time. The second approach focuses on the development of peptidomimetics as an alternative, which are characterized by greater reduced complexity and greater stability as compared to conventional GFs. A great example of this can be found in VEGF based therapies where the aim is to repair the hypoxic tissue by regeneration of blood supply.<sup>9,11</sup> VEGF therapies are in the process of investigation for the treatment of peripheral vascular disease (PVD), a condition characterized by severe artery blockages in the lower extremities, which often result in high rates of limb amputation and mortality, with a generally poor prognosis.<sup>12</sup> However VEGF expressed in laboratory animals has been linked with unwanted effects like formation of dysfunctional blood vessels, swelling, uncontrolled blood vessel formation and thereby increasing the risk of cancer.<sup>13,14</sup> The controlled release of VEGF through a device that can be implanted in the body presents substantial challenges due to the protein's complexity and low stability in serum, resulting in elevated costs, limited density for packing, and insufficient control over release. Consequently, the clinical usage of VEGF for treating PVD has been significantly hampered by these problems, despite its promising potential.<sup>15,16</sup>

Currently, a shorter, cost-effective, and more robust molecular substitute for VEGF is under study in the form of a peptidomimetic known as QK (KLTWQELYQLKYKGI). Research has demonstrated QK's ability to stimulate angiogenesis, both *in vitro*<sup>17</sup> and *in vivo*<sup>18</sup>. When immobilized on hydrogel matrices, this 15-amino acid peptide exhibits a higher capability of driving angiogenic differentiation in endothelial cells as compared to its soluble form. QK effectively mimics VEGF's activity when bound to heparan sulfate within the extracellular matrix, and this immobilization ensures spatial confinement of its pro-angiogenic effects. It has been proven that bone graft materials releasing QK for a long period of time can induce angiogenesis in human endothelial for upto six days, highlighting the significant potential of QK in promoting angiogenesis.<sup>19</sup> Depending on the overall health of the patient, PVD shows variability in disease profile, therefore there is a pressing need for developing a flexible and cost-effective treatment strategy for delivering QK in spatial and time controlled manner.

Recently, there has been an increasing interest in the development of a cost-effective and controllable drug release strategy through engineered living materials (ELMs). ELMs are composite materials that incorporate living cells within non-living materials, endowing them with programmable and life-like functions.<sup>20</sup> In the context of drug delivery, ELMs utilize hydrogels containing genetically modified bacteria to produce and release drugs as needed, responding to external triggers such as chemical inducers or light. These engineered bacteria are designed to use the nutrients available on the disease site and they can be activated to produce drugs at required dosage at the time its needed. Various types of ELMs, including films, discs, patches, and 3D printed structures, have been developed using hydrogels like Pluronic F127, agarose or collagen, in combination by using bacteria such as *E. coli*, *L. lactis* and *B. subtilis* for covering a wide range of therapeutic requirements.<sup>21-25</sup> While many studies have primarily focused on the release of antimicrobial drugs from ELMs, a subset of research has already showcased the controlled release of BMP (Bone Morphogenetic Protein), regulated by a peptide-inducer called nisin.<sup>23,26</sup>

The primary objective of this thesis is to design ELMs capable of releasing a collagen-binding QK peptide upon exposure to light, and to illustrate their potential for angiogenesis.

This thesis has following concrete **objectives**:

- Engineering *ClearColi* (endotoxin free strain of *E. coli*) to secrete collagen binding QK in response to light. Quantify secretion of collagen binding QK from *ClearColi*.

- To encapsulate light-responsive *ClearColi* in hydrogels to build ELM prototypes using Pluronic F127 diacrylate as hydrogel precursor. The ELM design should prevent bacterial escape and allow release of collagen binding QK in a light switchable and light-tunable manner.
- To establish a cell based assay to test the activity of purified and secreted QK.
- To study the activity of QK released from ELMs and compare its angiogenic performance against VEGF.

The thesis is organized into four chapters as follows:

**Chapter 1** presents a literature review. It describes the use of growth factors in regenerative medicine, their delivery/presentation methods. It focuses on the role of VEGF in cardiovascular regeneration, VEGF based angiogenesis therapies and its peptidomimetics. It also describes the challenges faced in angiogenesis therapies and the need for on-site long term drug production and release. One strategy to achieve this is by employing ELMs, which is introduced as an upcoming technology for drug-release and examples of ELMs used in drug delivery options are provided.

**Chapter 2** describes the optogenetic engineering of bacteria to secrete a pro-angiogenic protein in response to light. It describes details of fusion protein design optimization. The fusion protein was designed to be secreted from *ClearColi* cells and to bind to extracellular matrix and to induce angiogenesis. For this purpose, the angiogenic peptide CBD-QK was attached to the C-terminus of YebF (known carrier protein in *E. coli*). To incorporate the light responsiveness, the fusion protein-YebF-CBD-QK (YCQ) was cloned in an optogenetic plasmid. The secretion of YCQ was quantified by different methods, including SDS-PAGE, Mass Spectrometry and Western Blot. Its ability to bind to collagen was tested by micropatterning collagen on a glass surface and staining the bound protein with anti-YebF antibodies.

**Chapter 3** describes the encapsulation of *ClearColi* in a hydrogel to create ELMs that support bacteria grow and secretion of YCQ do not allow escape of *ClearColi* from the ELM. It also describes release of YCQ from ELMs in a light switchable and light tunable manner.

**Chapter 4** describes testing the bioactivity of pure YCQ and YCQ secreted from ELMs. An endothelial cell network formation assay was developed for testing the activity of YCQ. This chapter also covers the selection of the most appropriate matrix for the assay that allows reproducible testing. Immunofluorescence staining for angiogenic markers PECAM-1 and actin and DAPI revealed the formation of endothelial cell networks.

**Chapter 1. Introduction: Review of  
pro-angiogenic therapies and  
advances in growth factor delivery**

## 1.1. Use of growth factors in regenerative medicine

Regenerative medicine is a rapidly developing research field focused on accelerating the repair of damaged cells, tissues, and organs to restore normal function and circumvent the need for transplantation. For this purpose, biomaterial scaffolds, stem cells or growth factors are provided to the site of damage in order to stimulate tissue regeneration.<sup>27-29</sup>

Growth factors are evolutionarily conserved, small, and stable peptides/proteins that are produced by cells in the body. They are either secreted by the cell into the extracellular space or remain membrane bound. Growth factors control a range of cellular behaviors such as survival, growth, differentiation, and migration via binding to specific receptors on the target cell.<sup>30-33</sup> On a larger scale, these growth factor simulated responses play a crucial role in development and are crucial for maintenance and angiogenesis<sup>34-37</sup>, wound healing, and organism development in adults.<sup>1,3,32,38</sup> Use of growth factors in tissue healing has demonstrated reliable results in pre-clinical trials but their success in clinics is not that effective.<sup>39</sup>

Growth factors	Expected function	Hal-life on blood	Harmful effects in humans
BMP-2	Osteogenic factor	1-4 hours	Abnormal bone formation, problems related to inflammation, elevated cancer risk <sup>40,41</sup>
BMP-7	Bone formation, regulation of neural cell proliferayion	1 to 4 hours	Not reported <sup>42,43</sup>
EGF	Stimulates differentiation and proliferation epithelial cells	<1 min	Not reported <sup>44,45</sup>
FGF-2	Induction of growth and differentiation of various cell lines, formation of new blood vessels	3 to 5 min	Not reported <sup>37,46</sup>
PDGF-BB	Synthesis of Extracellular Matrix, Proliferation of different cell types, angiogenesis	30 mins	Increase cancer risk <sup>47,48</sup>

VEGF-A	Induction of angiogenesis	30 mins	swelling, systemic hypertension, increased cancer risk <sup>34,35,49</sup>
--------	---------------------------	---------	--

**Table 1:** Important growth factors in regenerative medicine<sup>27</sup>

Translation of growth factor based therapies to clinics is often limited because of their rapid diffusion out of the delivery site, the short half-life of the GFs, and the high cost of the therapies.<sup>39,50</sup> Researchers have tried to circumvent some of these limitations by using them at supraphysiological doses of GFs but this has led to serious side effects in many cases<sup>55–58</sup>. There is a need for innovative technologies in order to improve ways to deliver growth factor and efficacy of delivery and reduce dosage and side effects.<sup>54</sup>

Amongst numerous strategies that have been developed some showing satisfying results include biomaterial-based delivery systems<sup>55</sup> and modification of GFs that enhance their bioactivity and stability.<sup>32</sup> The following are some examples of these strategies (Figure 1).

## 1.2. Approaches for controlled delivery of GFs based on biomaterials immobilization

One of the commonly used strategies for delivering/presentation growth factors is controlled release from biomaterials. Immobilization of GFs on or in a biomaterial provides the possibility of localized delivery and sustained release.<sup>50,51</sup> This approach needs less frequent doses and hence reduces the side effects. That's why multiple methods have been studied in order attain better interactions between biomaterials and GFs.<sup>51</sup>

For such delivery, two strategies have been applied to incorporate GFs in biomaterials: physical immobilization, covalent conjugation and ECM inspired immobilization. For biomedical applications, there are some most relevant delivery systems which are listed below.<sup>50,51,56</sup>

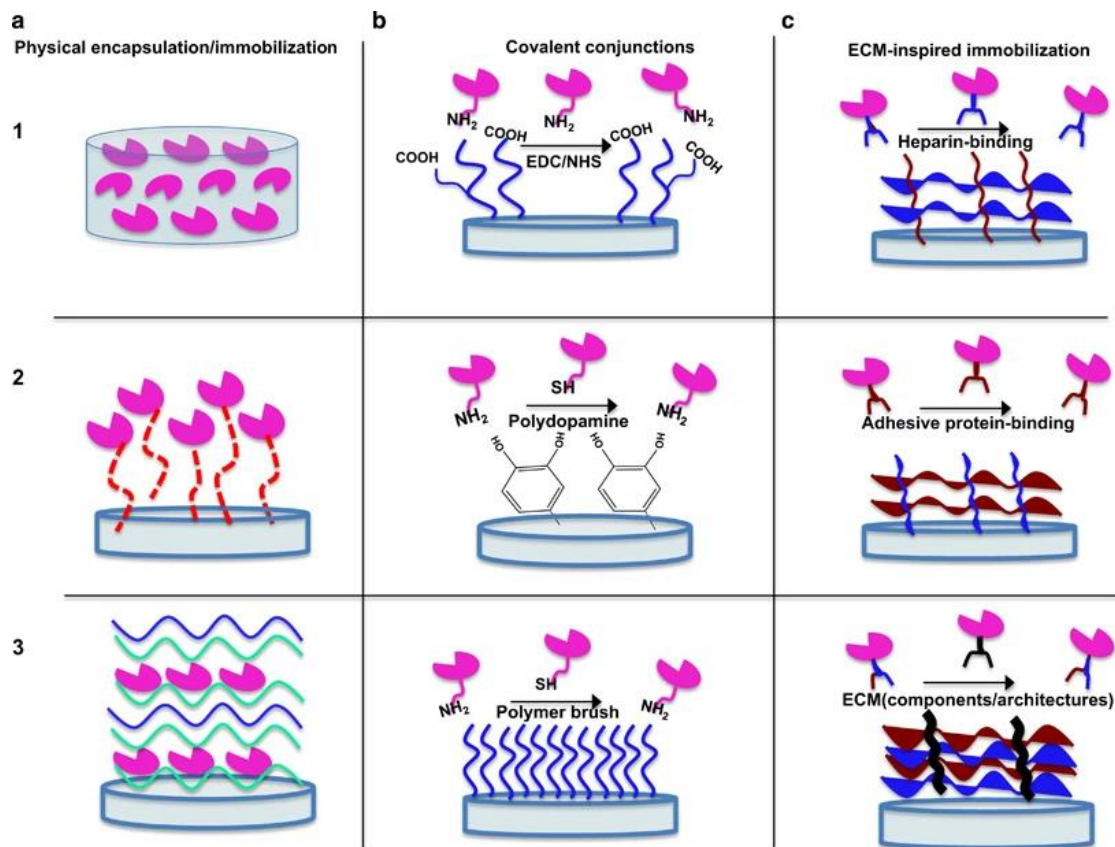


**Figure 1:** Different methods to attach or incorporate GFs into biomaterials directly. (a) Physical immobilization methods, including: 1. Encapsulation of GFs within a delivery system, 2. GFs absorption on the matrix's surface, 3. Layer-by-layer assembly. (b) Immobilization of GFs using their functional groups, encompassing: 1. Carbodiimide coupling immobilization, 2. Utilizing mussel-inspired bonding, 3. Other chemical coupling methods. (c) Immobilization techniques inspired by the extracellular matrix (ECM) that facilitate GF orientation on biomaterial surfaces, such as: 1. Employing heparin-based binding strategies, 2. Utilizing adhesive proteins for binding, 3. Utilizing ECM components and hierarchical structures for binding.<sup>50</sup> Image reproduced with permission of the rights holder, SPRINGER NATURE

### 1.2.1. Physical encapsulation/ immobilization of GFs

Mixing the GFs with the polymer precursor before the polymerization process begins is the simplest way for encapsulating GFs in a matrix. For example, VEGF was introduced into gas foaming vesicles for encapsulation into PLGA (poly lactic co glycolic acid) matrix. VEGF released from these scaffolds was shown to be over 70% active for up to 12 days.<sup>57</sup> In another example, alginate scaffolds were developed for the encapsulation TGF- $\beta$ 1, PDGF-BB, and VEGF.<sup>58</sup> These GFs were bound to alginate sulfate

the same way bind to Heparin in ECM thus allowing the delivery of aforementioned GFs in a particular sequence. The results suggested that the angiogenesis induction within alginate that was bound to three GFs was more when compared to the alginate that was bound to one GF following subcutaneous implantation in rats.<sup>50,58</sup>

### 1.2.2. Engineering GFs for covalent attachment to Biomaterials

Covalent linking of growth factors to biomaterials is often used to avoid typical initial burst release from physical encapsulation and improves the persistence of GFs and stability when delivered to cells or tissues.<sup>50</sup> Growth factor release rate depends on biomaterial cleavage or degradation (enzymatic and hydrolytic) of the bond between biomaterials and growth factors. Strategies to attach growth factors to biomaterials with the help of a reactive chemical group have been widely used. For instance, EDC-NHS crosslinking where amide bond is formed between carboxylic acid and amine groups on the substrates like PEG (approved by USFDA), has lower cost, easier delivery and mild reaction conditions.<sup>50,56</sup> For instance, EDC assisted immobilization of BMP-2 on a multilayer polyelectrolyte film was able to promote bone regeneration in femoral defect in a critical sized rat.<sup>50</sup> Although there are many advantages of using EDC-NHS for immobilization of GFs, this chemistry attaches carboxylic acids and primary amines in a randomized manner.

Enzymatic conjugation can enable oriented immobilization of GFs to biomaterials. Like, a fusion protein containing a mutant VEGF variant and a enzymatically attached to fibrin by the help of enzymatic transglutaminase activity of factor 8A. Injectable gels made using this functionalized fibrin helped in limb regeneration in mice.<sup>59,59</sup>

### 1.2.3. ECM inspired GF delivery systems.

In order to achieve GF delivery to cells in a highly regulated manner, it's beneficial to mimic naturally occurring interactions between extracellular matrix (ECM) and GFs. ECM acts a pool of GFs since it has the capacity to bind to many GFs. For example, heparin sulfate in ECM can bind multiple growth factors including VEGF and PDGF.<sup>50,60,61</sup> Hence, biomaterials have been consists of heparin sulfate or the molecules that mimic heparin sulfate, which can improve GF delivery.<sup>60</sup> For example, heparin-bound peptide-nanofibers containing either FGF-2 or VEGF resulted in a notable increase in blood vessel growth in a rat cornea, in comparison to nanofibers that did not possess a heparin-binding domain.<sup>62</sup> In another example, scientists created special hydrogels with heparin, a substance that helps the gels work better. They found that using a larger heparin molecule helped to load and keep TGF-beta1 in the hydrogels for longer. This change also encouraged stem cells to transform into endothelial cells, which then led to the growth of structures that looked like networks of blood vessels inside the hydrogels.<sup>63</sup>

### 1.3. Angiogenesis

In the realm of regenerative medicine, angiogenesis plays an important role by promoting the creation of new blood vessels. This facilitates effective transportation of nutrients, elimination of waste, and provision of oxygen to the regenerating tissues, thereby supporting tissue integration, guiding immune cell migration, and encouraging regenerative signals. Therefore it enhances the viability, functionality, and overall success of the regenerative process.<sup>64</sup>

Angiogenesis, vasculogenesis and arteriogenesis are three different processes involved in forming new blood vessels. New blood vessels developing from the ones existing before is called angiogenesis, and it's the key event in various pathological conditions, for example wound healing, bone repair, and has potential implications in tissue engineering (Figure 2). Blood vessel formation in a developing embryo takes place through vasculogenesis. During the process, endothelial progenitor cells come together to make dense thread-like structures. These structures slowly develop to mature blood vessels. After the fetal development stage, is involved in vascularization of the human body and in tissue repair after trauma or surgery. In the process of arteriogenesis, the existing arteries grow and mature, which supports the formation of arteries throughout the body. Modulation of both angiogenesis and arteriogenesis can be used as a powerful strategy | therapeutic angiogenesis.

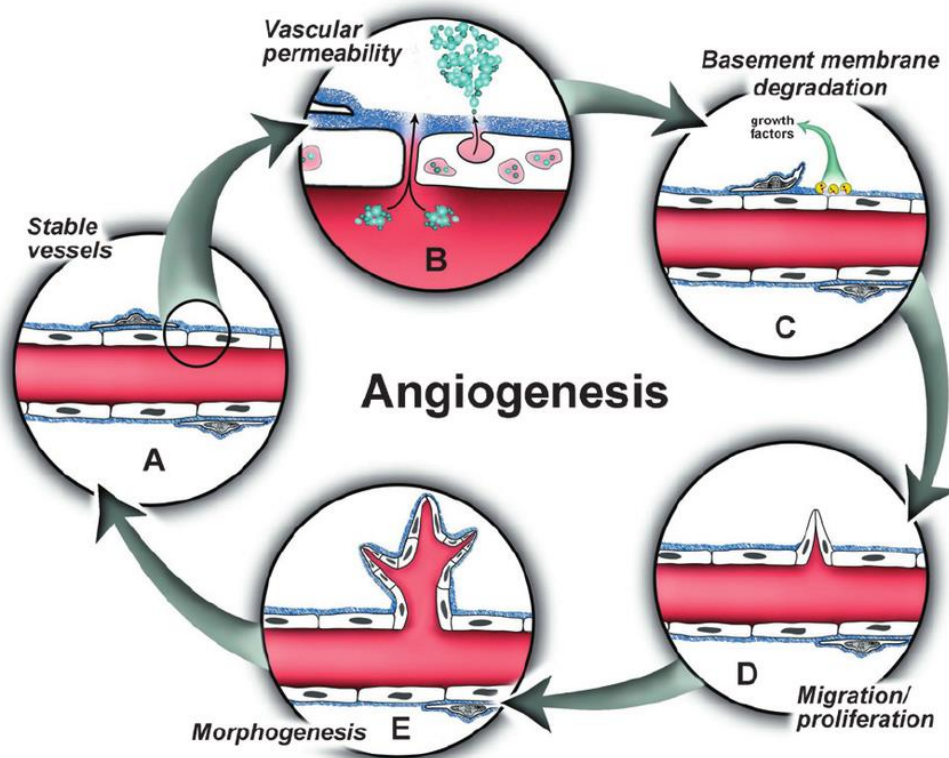


**Figure 2:** The sequence of events in angiogenesis unfolds as follows. During this process, stable blood vessels (a) undergo increased vascular permeability (this phenomenon has been demonstrated in specific scenarios only, as detailed in the accompanying text), leading to the release of plasma proteins (b). Matrix-metalloproteases (MMPs) degrade the extracellular matrix (ECM), liberating pericyte-EC connections and releasing growth factors sequestered within the ECM (c). Subsequently, endothelial cells (ECs) undergo proliferation and migration towards their destination (d), ultimately coalescing to form luminal channels (e). ECM stands for extracellular matrix, and MMPs refer to matrix-metalloproteases, while EC represents endothelial cells. The image is reproduced with permission from the rights holder, SPRINGER NATURE.

## 1.4. Importance of VEGF in angiogenesis

Angiogenic factors are the ones that promote vascularization. The idea of angiogenic factor existence was suggested since they seem to be stimulating angiogenesis in tumors. It was then discovered that normal tissues can also make these factors. There are many different molecules that are thought to help regulate angiogenesis, such as Fibroblast Growth Factor, Tumor Growth Factor-alpha, Tumor Growth Factor-beta and Interleukin-8.<sup>34</sup>

Vascular Endothelial Growth Factor (VEGF) is a GF protein which plays a role in the development of blood vessels and in the healing of wounds. The VEGF-A gene, which is found in humans on chromosome 6, is made up of 8 exons.<sup>34</sup> Different splicing of this gene leads to the production of at least 5 different VEGF molecules that vary in size, ranging from 121 to 206 amino acids. The VEGF165 molecule, which has 165 amino acids, is the most common and biologically active variant. The VEGF121 and VEGF189 molecules are also found in many cells, while the VEGF145 and VEGF206 molecules are less common.<sup>34,35,65</sup> The VEGF165 molecule is a glycoprotein that is a homodimer, binds to heparin, and has a size of 45 kDa. It belongs to a group of proteins called PDGF supergene family, which are characterized by the presence of eight conserved cysteine residues.<sup>35</sup> VEGF binds to two receptors. VEGFR1 and VEGFR-2 were found on cells lining blood vessels. These receptors are activated by VEGF, leading to increased vascular permeability and hence assisting in angiogenesis.<sup>34</sup>

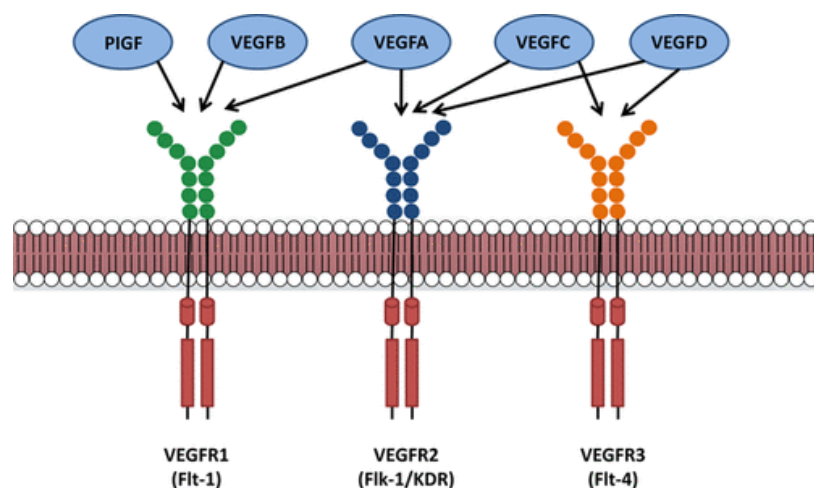


**Figure 3:** VEGF and its receptor mediated pathways.<sup>66</sup> Image reproduced with permission of the rights holder, Wolters Kluwer Health

PI3K/Akt pathway is activated by VEGF. This pathway regulates survival and multiplication of endothelial cells. When VEGF activates the PI3K/Akt pathway, it leads to the upregulation of several downstream targets, including the transcription factor HIF-1 $\alpha$  (Hypoxia inducible factor) and PECAM-1.<sup>32,67-69</sup> Platelet Endothelial Adhesion

molecule is expressed on the surface of endothelial cells. PECAM- acts in response to angiogenic cues by facilitating alignment of endothelial cells.<sup>67,69</sup> PECAM-1 staining provides a way to quantify angiogenesis in experimental models, as its upregulated in endothelial cells undergoing angiogenic transformation.<sup>67</sup>

VEGF can turn on another pathway called the MAPK/ERK pathway. This pathway is important because it helps control whether cells survive, multiply, or change into different types. When VEGF triggers the MAPK/ERK pathway, it sets off a process where certain proteins, like c-Fos and c-Jun, get activated by a chemical change (phosphorylation). These active proteins play a role in controlling genes responsible for forming new blood vessels..<sup>35</sup>

VEGF also activates the Rho/Rho kinase pathway. This pathway regulates cytoskeleton and hence regulate cytoskeleton remodelling.<sup>70-72</sup> Actin is a critical regulator of cell motility and membrane protrusion events, which are key for determining a successful angiogenic response.<sup>71</sup> Due to changes in regulation of cytoskeleton, endothelial cells acquire several new properties along with such as invasiveness and motility during angiogenesis along with morphology change.<sup>71</sup>

Overall, the PI3K/Akt, MAPK/ERK, and Rho/Rho kinase pathways are all involved in the process of angiogenesis and are activated by VEGF to stimulate endothelial cells to form new blood vessels.

VEGF-A exhibits a remarkable degree of conservation across diverse species, spanning from fish to mammals. Furthermore, the VEGFR system, encompassing a soluble variant of VEGFR-1, demonstrates a similar level of conservation from amphibians to mammals. These observations prove that VEGF has a pivotal role in angiogenesis and also in maintaining various tissues, including neural tissues.<sup>34</sup> Moreover, the VEGF-VEGFR system maintains intricate connections with other regulatory systems governing angiogenesis, such as the angiotensin-Tie and Delta (DII4)-Notch systems. Therefore, further exploration of the VEGF-VEGFR system and its interplay with these regulatory networks holds the potential to yield more effective therapeutic strategies for conditions like cancer and other diseases.<sup>34</sup>

## **1.5. Challenges involved in angiogenesis therapies.**

GF-based angiogenic therapies carry the potential for harmful effects. The following text discusses the potential complications that may arise from the use of VEGF.

### **1.5.1. Abnormal growth of blood vessels in tissues not targeted for treatment.**

Angiogenic agents, which enhance the formation of new blood vessels, are believed to stimulate neovascularization in various tissues. However, it may not be possible to ensure that these agents are delivered specifically to the intended target tissue in clinical settings. This raises the possibility of unintended angiogenesis occurring in adjacent or even distant tissues.<sup>15</sup>

When ischemic and healthy canine myocardium were subjected to elevated spatial concentrations of FGF-1. However, the heart tissue deprived of oxygen (ischemic myocardium) showed signs of forming new blood vessels only when it was exposed to a substantial amount of FGF-1 protein for a long time. This indicates that the development of unusual new blood vessels might not happen unless healthy tissue is exposed to angiogenic substances from outside for an extended period..<sup>73</sup>

Although abnormal blood vessels do not form in normal tissue unless the tissue is exposed to high levels of angiogenic agents, this consideration does not apply to people with coexisting conditions, such as diabetic retinopathy and malignant tumors. In such conditions there is abnormally high expression of cytokine receptors, therefore tissues can undergo new blood vessel formation and hence disease progression.<sup>15</sup>

### **1.5.2. VEGF therapy may lead to the development of dysfunctional blood vessels.**

Another potential concern associated with VEGF therapy is the emergence of functionally atypical blood vessels. For instance, VEGF introduced via a viral vector in mice led to formation of thin-walled and wider blood vessels which lacked pericytes and because of this they had increased permeability. These type of blood vessels are frequently observed in healing wounds and in tumors. Since the VEGF induced blood vessels develop in an environment of immature connective tissue, there are questions raised regarding their functional benefits to the connective tissue.<sup>15</sup>

Intravenous injection of a viral vector carrying the VEGF transgene into mice also caused serious functional consequences, including systemic increases of vascular permeability, multiorgan edema, and high mortality rates. Pretreatment with a viral vector carrying the angiopoietin-1 transgene prevented these effects.

These studies emphasize that creating healthy blood vessels relies on the involvement and functioning of several different genes. For obtaining functional blood vessels simply overexpressing one gene is not enough.

Nearly all solid tumors have increased vascular permeability. VEGF is also known for its ability to increase permeability of vessels.<sup>74</sup> Due to this vessels circulate macromolecules at very low concentrations and is approximately 50,000 times more potent than histamine in this regard. The ability of VEGF to make blood vessels more permeable happens rapidly, often within just a few minutes after it is administered.<sup>74</sup> VEGF also stimulates the expression matrix-degrading enzymes, such as collagenases and plasminogen activators, which helps in the in-vivo angiogenic effects.<sup>75</sup>

Since newly formed blood vessels are typically hyperpermeable, increased vascular permeability is necessary their formation.<sup>35,74,76</sup> It also often precedes angiogenesis in pathological and physiological conditions like tumors, rheumatoid arthritis, wound healing, and corpus luteum formation. When VEGF's ability to increase vascular permeability occurs in a different context than its usual biological environment, it can result in several undesirable effects. For example, activation of blood clotting enzymes and accumulation fibrin in the ECM space can lead to localized swelling.<sup>77</sup>

### **1.5.3. Growth of neoplasms**

Angiogenic agents have the potential to stimulate cellular proliferation and may enhance the growth of tumors. FGF is also known to stimulate growth of different cell types and could also induce growth of a tumor. On the other hand, VEGF induces differentiation in endothelial cells, which express receptors for VEGF. However, some non-endothelial tumor cells express low levels of function VEGF receptors,<sup>15,78</sup> which may allow them to respond to VEGF.

Solid tumors necessitate an increased blood supply, achieved through the process of angiogenesis, to provide the essential nutrients for their growth beyond a minimal size. Consequently, using growth factors to promote angiogenesis in ischemic tissue can promote activation of dormant cells in tumor, even if these agents do not directly influence the proliferation of tumor cells.

High levels of VEGF can induce development of benign tumors and abnormalities in the blood vessels in skeletal muscles or heart. Certain normal tissues, such as the uterus, also express functional VEGF receptors and can respond to exogenous growth factors.<sup>15</sup> However, there is no evidence of malignant transformation in animal studies that have shown tumor development, and agents being tested in clinical trials have passed safety tests.<sup>15</sup>

#### **1.5.4. Hypotension and vasodilation during short term administration of VEGF**

VEGF and FGF growth factors can cause vasodilation and low blood pressure when administered in large doses, which may be due to nitric oxide pathways. This can be a serious issue, as seen in a study where four out of eight pigs with myocardial ischemia developed low blood pressure and died after receiving VEGF protein. In a clinical trial, one patient with coronary artery disease also experienced prolonged low blood pressure after receiving basic FGF in the coronary arteries. However, correct dosing and prolonged VEGF release may minimize this risk.

To summarize, angiogenic agents can also cause serious side effects along with stimulating new blood vessels. Researchers hope to develop methods to target these agents specifically to the tissues that need them, while minimizing the potential for stimulation in nontargeted tissues. Additionally, it seems that ischemic tissues will respond more to angiogenic induction as compared to normal tissue which increases the safety margin. Therefore, it is important to note that angiogenic agents carry risk of potentially serious side effects. However, it is believed that with careful study and proper dosing, the benefits of using these agents in therapeutic settings will outweigh the risks.<sup>15</sup>

#### **1.6. Engineered living materials for smart delivery of drugs.**

In-situ control over release of growth factor over a prolonged period of time is one strategy to minimize the risks. Using Engineered Living Materials (ELMs) as a drug-delivery system is an excellent option for achieving this. The drugs release by living therapeutic materials are produced by organisms in ELM as compared to non-living systems, therefore an unlimited supply of drugs is possible. This also makes it cost-effective because there is no need for manufacturing and packaging the drug. Since the drug is produced fresh, it is ideal for protein-based drugs that get rapidly degraded in the body. Introducing smart capabilities doesn't necessitate an increase in the inherent complexity of the material. It can be done by introducing genetic sensors and switches in bacteria. These benefits make living therapeutic materials highly desirable for various medical scenarios.<sup>79-82</sup>

Microorganisms are used to produce complex biopharmaceuticals on a large scale.<sup>83,84</sup> They are not only designed for drug production but also for delivering the drug on site when needed.<sup>85</sup> However, it can be difficult to control the colonization and growth of these bacteria at the site of the disease, which makes it hard to predict the resulting drug release profiles.<sup>79-82,86,87</sup> This is a problem because the release of growth factors needs to be tightly regulated for growth factor-based therapies. To address these challenges, researchers are looking into the possibility of encapsulating therapeutic

bacteria in polymeric matrices to create engineered living materials (ELMs) for drug delivery with promising early results<sup>79,80,82,87,88</sup>

Polymeric matrices can be used to facilitate the growth of microbial populations, control their growth, and prevent them from escaping the system.<sup>80,87-89</sup> These matrices also have a suitable level of porosity that allows for the exchange of nutrients, metabolites and gases. This approach is expected to be cheaper than traditional drug delivery systems because it does not require external purification, storage, or packaging of drugs. Instead, the drugs can be produced in when needed, this makes ELMs the ideal choice for delivering non-stable protein drugs. There are several potential applications for ELMs in medicine, including therapeutic biofilms,<sup>90</sup> skin patches for wounds,<sup>91,92</sup> adhesive patches containing bacteria for treating intestinal inflammation<sup>90</sup> and self-refilling drug depots for the delivering of therapeutic proteins or antimicrobials.<sup>80</sup>

ELMs often contain engineered bacteria that are embedded on or within a supporting material substrate and respond to external or environmental stimuli (Figure 5). ELMs are commonly developed with *E. coli* since they can be easily engineered and have a wide range of established genetic parts available. Other organisms, such as *Lactococcus lactis* and *Bacillus subtilis*, have also been used to create ELMs for biomedical purposes. However, *E. coli* strains that are free of endotoxins, such as ClearColi, offer the advantages of a large genetic toolbox without triggering immune responses in the body.

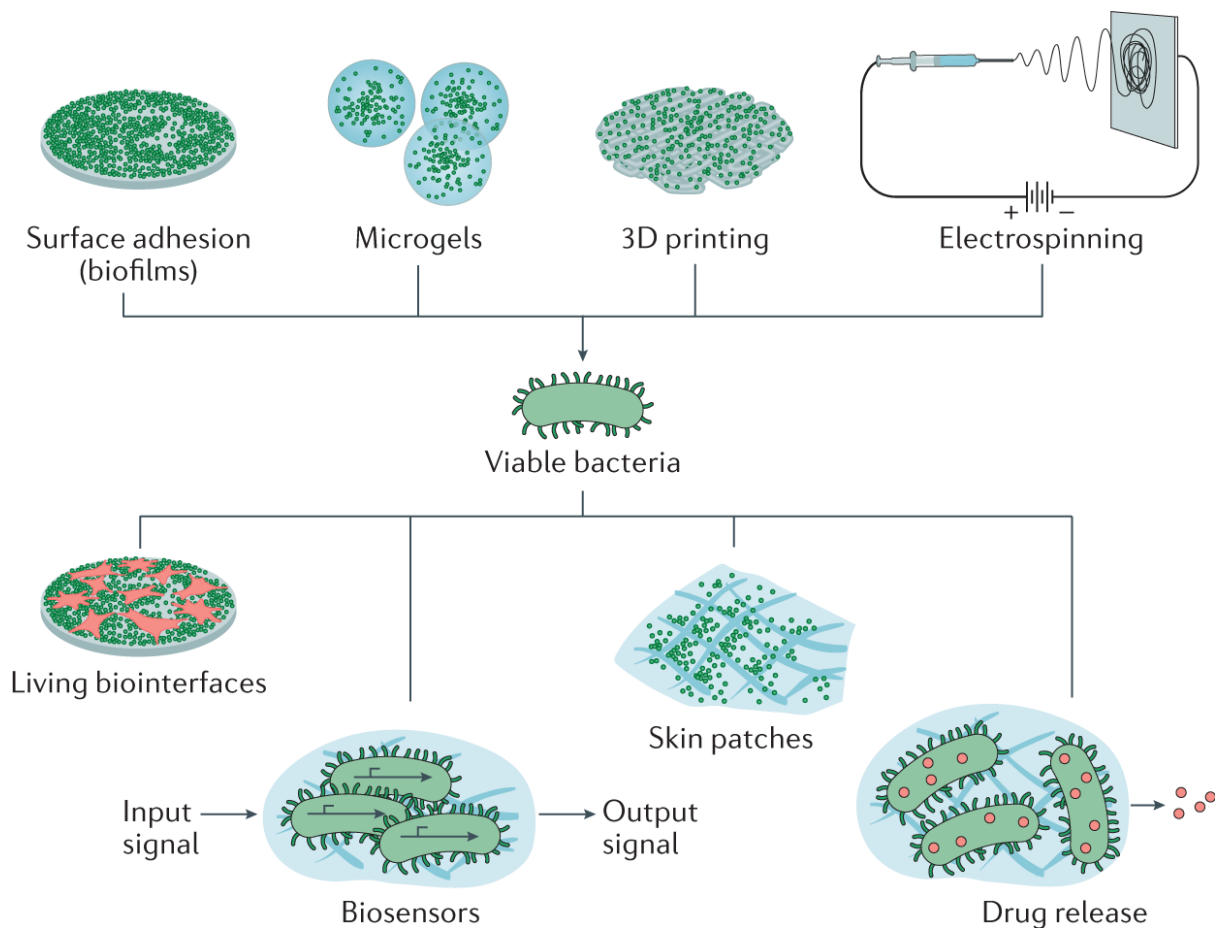


**Figure 5** Living materials are composed of either natural or genetically altered bacteria capable of reacting to outside triggers. These bacteria are incorporated into material surfaces or embedded within the material itself to offer structural reinforcement. Fabrication of ELMs can be done manually or by encapsulating the bacteria in microgels by emulsification. Or by using more sophisticated techniques like 3D printing and electrospinning. The fabricated ELMs can then be used as living bio interfaces, as sensors, as patches for treatment and also as drug release systems<sup>79</sup> Image reproduced with permission of the rights holder, SPRINGER NATURE

In a different approach, ELMs can be prepared from bacteria that self-grow a biofilm. By engineering *E. coli* to secrete curli nanofibers, mechanically stable matrices can be formed, which can attach to tissue. These biofilms can be tailored to produce specific proteins that aid in the treatment of various conditions. For example, modified biofilms expressing trefoil factors can promote intestinal barrier function and epithelial restitution, while biofilms fused with influenza-virus-binding peptides can capture and remove viruses.<sup>93</sup> To regulate biofilm growth, a genetic kill switch can be incorporated, which triggers bacterial lysis once a threshold population density is reached. This control mechanism was employed in the ELM engineered to capture virus particles and prevented excessive biofilm growth.<sup>90</sup>

Microorganisms like *L. lactis* and *E. coli* have been genetically engineered to produce extracellular matrix proteins and growth factors within the biofilm.<sup>23,23,94,95</sup> *L. lactis* biofilms have been made to express fibronectin fragments that interact with mammalian cells through integrin-fibronectin adhesion, serving as a growth substrate for cell proliferation and differentiation. This approach allows for precise control over the differentiation process without relying on external biochemical factors.<sup>95</sup> Similarly, *E. coli* strains have been designed to respond to light stimuli, inducing the production of specific proteins that facilitate interactions with mammalian cells through RGD-integrin interactions.<sup>82</sup>(Figure 6)

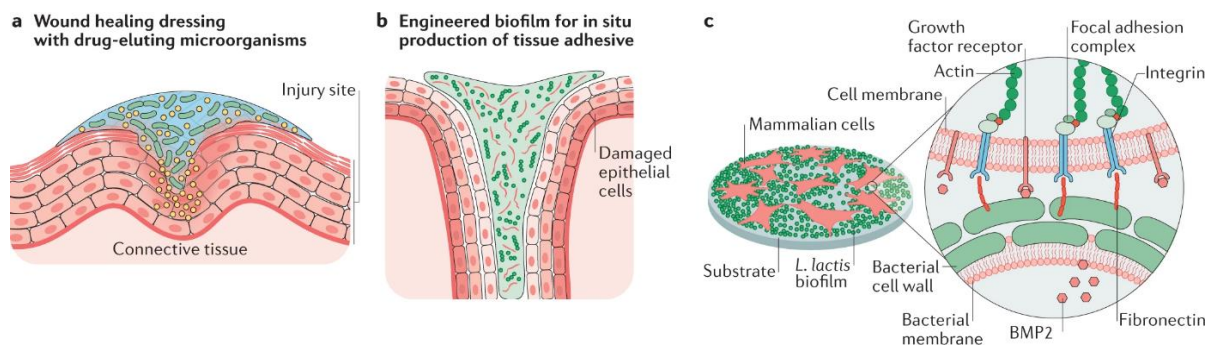


**Figure 6** a. Engineered microorganisms fabricated as wound healing dressings These can assist in wound healing by releasing proteins, drugs or small molecules. *E. coli* was engineered to release CsgA curly fibers in order to assist wound healing by regeneration of the epithelial lining. B. Bacteria can be engineered to make a biofilm for treating inflammation of the intestine. c. *Lactococcus lactis* was engineered to produce a biofilm and mammalian cells were cultured on top of this biofilm. *L. lactis* is capable of producing substances to support proliferation of mammalian cells, like BMP-2<sup>79</sup> Image reproduced with permission of the rights holder, SPRINGER NATURE

Along with the use of bacteria for drug-delivery applications, beneficial bacteria and fungi, such as *Staphylococcus epidermidis* and *B. subtilis*, which work symbiotically with the skin, have been embedded into materials for skin patches.<sup>92</sup> These patches ensured controlled release of the enclosed microorganisms, allowing them to gradually colonize the affected skin area and restore the balance of the skin microbiome. This approach minimizes the risk of dysbiosis, which can occur if the newly introduced microorganisms disproportionately colonize the treatment site.<sup>92</sup>

The use of living materials shows great promise in restoring the skin microbiome, promoting wound healing, and supporting tissue regeneration. These materials provide controlled release, self-growth, and instructive properties, allowing for the gradual colonization of beneficial microorganisms, the formation of mechanically stable matrices, and the production of specific proteins to aid in various therapeutic

applications. These advancements hold significant potential for enhancing skin health, facilitating wound healing, and enabling tissue regeneration.

Other ELM examples are drug-eluting hydrogels that encapsulate penicillin-producing fungi and ontogenetically engineered *E. coli*. In these systems-controlled drug release is possible in response light exposure.<sup>87</sup> Release of drugs in response to light for a month is documented. Additionally, living materials made from encapsulating *B. subtilis* in agarose and in Pluronic F-127 bisurathane have been developed. These gels release antimicrobial drugs for preventing growth of pathogenic bacteria.<sup>96</sup>

Despite these advancements some improvements need to made like, the rate of production and release of drug needs to be improved, and compatibility with immune system needs to be tested by testing these systems in animal models. Nevertheless, since engineered living materials promise to deliver flexible bacterial engineering and materials engineering, it continues to promise for precisely controlled drug delivery systems.

To mitigate the challenges posed by existing ELMs, microorganisms encapsulated in polymeric matrices has been investigated.<sup>79,80,87-89</sup> These matrices create a supportive environment for microorganism survival while preventing their escape. Since the porosity of the matrix can be controlled, the drug released from the material, nutrient and gaseous exchange can be controlled too. Living materials offer advantages over non-living drug-release devices, including in situ drug production and long-term controlled release, potentially reducing costs associated with drug purification and storage. Moreover, living materials can incorporate smart functions by genetically modifying microorganisms with sensors and switches.

## 1.7. References

- (1) Vaidyanathan, L. Growth Factors in Wound Healing – A Review. *Biomedical and Pharmacology Journal* **2021**, *14* (3), 1469–1480.
- (2) *The Role of Growth Factors in Wound Healing : Journal of Trauma and Acute Care Surgery*.  
[https://journals.lww.com/jtrauma/Fulltext/1996/07000/The\\_Role\\_of\\_Growth\\_Factors\\_in\\_Wound\\_Healing.29.aspx](https://journals.lww.com/jtrauma/Fulltext/1996/07000/The_Role_of_Growth_Factors_in_Wound_Healing.29.aspx) (accessed 2023-04-07).
- (3) Steed, D. L. THE ROLE OF GROWTH FACTORS IN WOUND HEALING. *Surgical Clinics of North America* **1997**, *77* (3), 575–586. [https://doi.org/10.1016/S0039-6109\(05\)70569-7](https://doi.org/10.1016/S0039-6109(05)70569-7).
- (4) Ito, Y. Growth Factor Engineering for Biomaterials. *ACS Biomaterials Science & Engineering* **2019**, *5*. <https://doi.org/10.1021/acsbiomaterials.8b01649>.
- (5) Carmeliet, P.; Jain, R. K. Molecular Mechanisms and Clinical Applications of Angiogenesis. *Nature* **2011**, *473* (7347), 298–307. <https://doi.org/10.1038/nature10144>.
- (6) Verheul, H. M.; Pinedo, H. M. The Role of Vascular Endothelial Growth Factor (VEGF) in Tumor Angiogenesis and Early Clinical Development of VEGF-Receptor Kinase Inhibitors. *Clin Breast Cancer* **2000**, *1 Suppl 1*, S80-84. <https://doi.org/10.3816/cbc.2000.s.015>.
- (7) Gacche, R. N.; Meshram, R. J. Angiogenic Factors as Potential Drug Target: Efficacy and Limitations of Anti-Angiogenic Therapy. *Biochim Biophys Acta* **2014**, *1846* (1), 161–179. <https://doi.org/10.1016/j.bbcan.2014.05.002>.
- (8) Senet, P. Bécaplermine gel (Regranex® gel). *Annales de Dermatologie et de Vénérologie* **2004**, *131* (4), 351–358. [https://doi.org/10.1016/S0151-9638\(04\)93614-9](https://doi.org/10.1016/S0151-9638(04)93614-9).
- (9) Ren, X.; Zhao, M.; Lash, B.; Martino, M. M.; Julier, Z. Growth Factor Engineering Strategies for Regenerative Medicine Applications. *Frontiers in Bioengineering and Biotechnology* **2020**, *7*.
- (10) Griffioen, A. W.; Dudley, A. C. The Rising Impact of Angiogenesis Research. *Angiogenesis* **2022**, *25* (4), 435–437. <https://doi.org/10.1007/s10456-022-09849-2>.
- (11) Eelen, G.; Trops, L.; Li, X.; Carmeliet, P. Basic and Therapeutic Aspects of Angiogenesis Updated. *Circulation Research* **2020**, *127* (2), 310–329. <https://doi.org/10.1161/CIRCRESAHA.120.316851>.

- (12) Ng, Y.-S.; D'Amore, P. A. Therapeutic Angiogenesis for Cardiovascular Disease. *Curr Control Trials Cardiovasc Med* **2001**, *2* (6), 278–285. <https://doi.org/10.1186/cvm-2-6-278>.
- (13) Schaper, W. Collateral Circulation: Past and Present. *Basic Res Cardiol* **2009**, *104* (1), 5–21. <https://doi.org/10.1007/s00395-008-0760-x>.
- (14) Karpanen, T.; Bry, M.; Ollila, H. M.; Seppänen-Laakso, T.; Liimatta, E.; Leskinen, H.; Kivelä, R.; Helkamaa, T.; Merentie, M.; Jeltsch, M.; Paavonen, K.; Andersson, L. C.; Mervaala, E.; Hassinen, I. E.; Ylä-Herttuala, S.; Orešič, M.; Alitalo, K. Overexpression of Vascular Endothelial Growth Factor-B in Mouse Heart Alters Cardiac Lipid Metabolism and Induces Myocardial Hypertrophy. *Circulation Research* **2008**, *103* (9), 1018–1026. <https://doi.org/10.1161/CIRCRESAHA.108.178459>.
- (15) Epstein, S. E.; Kornowski, R.; Fuchs, S.; Dvorak, H. F. Angiogenesis Therapy. *Circulation* **2001**, *104* (1), 115–119. <https://doi.org/10.1161/01.CIR.104.1.115>.
- (16) *Vascular endothelial growth factor enhances atherosclerotic plaque progression* | *Nature Medicine*. [https://www.nature.com/articles/nm0401\\_425](https://www.nature.com/articles/nm0401_425) (accessed 2023-10-17).
- (17) Leslie-Barbick, J. E.; Saik, J. E.; Gould, D. J.; Dickinson, M. E.; West, J. L. The Promotion of Microvasculature Formation in Poly(Ethylene Glycol) Diacrylate Hydrogels by an Immobilized VEGF-Mimetic Peptide. *Biomaterials* **2011**, *32* (25), 5782–5789. <https://doi.org/10.1016/j.biomaterials.2011.04.060>.
- (18) Santulli, G.; Ciccarelli, M.; Palumbo, G.; Campanile, A.; Galasso, G.; Ziaco, B.; Altobelli, G. G.; Cimini, V.; Piscione, F.; D'Andrea, L. D.; Pedone, C.; Trimarco, B.; Iaccarino, G. In Vivo Properties of the Proangiogenic Peptide QK. *Journal of Translational Medicine* **2009**, *7* (1), 41. <https://doi.org/10.1186/1479-5876-7-41>.
- (19) Pensa, N. W.; Curry, A. S.; Reddy, M. S.; Bellis, S. L. Sustained Delivery of the Angiogenic QK Peptide through the Use of Polyglutamate Domains to Control Peptide Release from Bone Graft Materials. *J Biomed Mater Res A* **2019**, *107* (12), 2764–2773. <https://doi.org/10.1002/jbm.a.36779>.
- (20) Rodrigo-Navarro, A.; Sankaran, S.; Dalby, M. J.; del Campo, A.; Salmeron-Sanchez, M. Engineered Living Biomaterials. *Nat Rev Mater* **2021**, *6* (12), 1175–1190. <https://doi.org/10.1038/s41578-021-00350-8>.
- (21) Sankaran, S.; del Campo, A. Optoregulated Protein Release from an Engineered Living Material. *Advanced Biosystems* **2019**, *3* (2), 1800312. <https://doi.org/10.1002/adbi.201800312>.
- (22) *Optoregulated Drug Release from an Engineered Living Material: Self-Replenishing Drug Depots for Long-Term, Light-Regulated Delivery* - Sankaran -

- 2019 - Small - Wiley Online Library.  
<https://onlinelibrary.wiley.com/doi/abs/10.1002/sml.201804717> (accessed 2023-05-10).
- (23) *Bacteria-Based Materials for Stem Cell Engineering-Web of Science Core Collection*.  
<https://www.webofscience.com/wos/woscc/full-record/WOS:000448786000028?SID=EUW1ED0DCDu0FV9bothK8ofmyyhNF>  
 (accessed 2023-07-13).
- (24) Johnston, T. G.; Yuan, S.-F.; Wagner, J. M.; Yi, X.; Saha, A.; Smith, P.; Nelson, A.; Alper, H. S. Compartmentalized Microbes and Co-Cultures in Hydrogels for on-Demand Bioproduction and Preservation. *Nat Commun* **2020**, *11* (1), 563. <https://doi.org/10.1038/s41467-020-14371-4>.
- (25) González, L. M.; Mukhitov, N.; Voigt, C. A. Resilient Living Materials Built by Printing Bacterial Spores. *Nat Chem Biol* **2020**, *16* (2), 126–133. <https://doi.org/10.1038/s41589-019-0412-5>.
- (26) Hay, J. J.; Rodrigo-Navarro, A.; Hassi, K.; Moulisova, V.; Dalby, M. J.; Salmeron-Sanchez, M. Living Biointerfaces Based on Non-Pathogenic Bacteria Support Stem Cell Differentiation. *Sci Rep* **2016**, *6* (1), 21809. <https://doi.org/10.1038/srep21809>.
- (27) Mao, A. S.; Mooney, D. J. Regenerative Medicine: Current Therapies and Future Directions. *Proc Natl Acad Sci U S A* **2015**, *112* (47), 14452–14459. <https://doi.org/10.1073/pnas.1508520112>.
- (28) Mason, C.; Dunnill, P. A Brief Definition of Regenerative Medicine. *Regenerative Medicine* **2008**, *3* (1), 1–5. <https://doi.org/10.2217/17460751.3.1.1>.
- (29) *regenerative medicine - Google Search*.  
<https://www.google.com/search?client=firefox-b-d&q=regenerative+medicine>  
 (accessed 2023-04-07).
- (30) *Growth factor delivery using extracellular matrix-mimicking substrates for musculoskeletal tissue engineering and repair - PMC*.  
<https://www.ncbi.nlm.nih.gov/pmc/articles/PMC7773685/> (accessed 2023-01-08).
- (31) *Growth factors, their receptors and development - Hollenberg - 1989 - American Journal of Medical Genetics - Wiley Online Library*.  
<https://onlinelibrary.wiley.com/doi/abs/10.1002/ajmg.1320340109> (accessed 2023-04-07).
- (32) Barrientos, S.; Brem, H.; Stojadinovic, O.; Tomic-Canic, M. Clinical Application of Growth Factors and Cytokines in Wound Healing. *Wound Repair Regen* **2014**, *22* (5), 569–578. <https://doi.org/10.1111/wrr.12205>.

- (33) Stone, W. L.; Leavitt, L.; Varacallo, M. Physiology, Growth Factor. In *StatPearls*; StatPearls Publishing: Treasure Island (FL), 2023.
- (34) Shibuya, M. Vascular Endothelial Growth Factor (VEGF) and Its Receptor (VEGFR) Signaling in Angiogenesis. *Genes Cancer* **2011**, *2* (12), 1097–1105. <https://doi.org/10.1177/1947601911423031>.
- (35) Carmeliet, P. VEGF as a Key Mediator of Angiogenesis in Cancer. *Oncology* **2005**, *69 Suppl 3*, 4–10. <https://doi.org/10.1159/000088478>.
- (36) Crivellato, E. The Role of Angiogenic Growth Factors in Organogenesis. *Int J Dev Biol* **2011**, *55* (4–5), 365–375. <https://doi.org/10.1387/ijdb.103214ec>.
- (37) Cross, M. J.; Claesson-Welsh, L. FGF and VEGF Function in Angiogenesis: Signalling Pathways, Biological Responses and Therapeutic Inhibition. *Trends Pharmacol Sci* **2001**, *22* (4), 201–207. [https://doi.org/10.1016/s0165-6147\(00\)01676-x](https://doi.org/10.1016/s0165-6147(00)01676-x).
- (38) Greenhalgh, D. G. The Role of Growth Factors in Wound Healing. *Journal of Trauma and Acute Care Surgery* **1996**, *41* (1), 159.
- (39) Ren, X.; Zhao, M.; Lash, B.; Martino, M.; Julier, Z. Growth Factor Engineering Strategies for Regenerative Medicine Applications. *Frontiers in Bioengineering and Biotechnology* **2020**, *7*, 469. <https://doi.org/10.3389/fbioe.2019.00469>.
- (40) James, A. W.; LaChaud, G.; Shen, J.; Asatrian, G.; Nguyen, V.; Zhang, X.; Ting, K.; Soo, C. A Review of the Clinical Side Effects of Bone Morphogenetic Protein-2. *Tissue Eng Part B Rev* **2016**, *22* (4), 284–297. <https://doi.org/10.1089/ten.TEB.2015.0357>.
- (41) *Cancer risk after use of recombinant bone morphogenetic protein-2 for spinal arthrodesis - PubMed*. <https://pubmed.ncbi.nlm.nih.gov/24005193/> (accessed 2023-07-24).
- (42) Lowery, J. W.; Rosen, V. Bone Morphogenetic Protein–Based Therapeutic Approaches. *Cold Spring Harb Perspect Biol* **2018**, *10* (4), a022327. <https://doi.org/10.1101/cshperspect.a022327>.
- (43) Tóth, F.; Tózsér, J.; Hegedűs, C. Effect of Inducible BMP-7 Expression on the Osteogenic Differentiation of Human Dental Pulp Stem Cells. *International Journal of Molecular Sciences* **2021**, *22* (12), 6182. <https://doi.org/10.3390/ijms22126182>.
- (44) Ferguson, K. M.; Berger, M. B.; Mendrola, J. M.; Cho, H. S.; Leahy, D. J.; Lemmon, M. A. EGF Activates Its Receptor by Removing Interactions That Autoinhibit Ectodomain Dimerization. *Mol Cell* **2003**, *11* (2), 507–517. [https://doi.org/10.1016/s1097-2765\(03\)00047-9](https://doi.org/10.1016/s1097-2765(03)00047-9).

- (45) Wee, P.; Wang, Z. Epidermal Growth Factor Receptor Cell Proliferation Signaling Pathways. *Cancers (Basel)* **2017**, *9* (5), 52. <https://doi.org/10.3390/cancers9050052>.
- (46) *Fibroblast Growth Factor-2 (FGF-2) Induces Vascular Endothelial Growth Factor (VEGF) Expression in the Endothelial Cells of Forming Capillaries: An Autocrine Mechanism Contributing to Angiogenesis | Journal of Cell Biology | Rockefeller University Press.* <https://rupress.org/jcb/article/141/7/1659/1032/Fibroblast-Growth-Factor-2-FGF-2-Induces-Vascular> (accessed 2023-01-08).
- (47) Lin, Z.; Sugai, J. V.; Jin, Q.; Chandler, L. A.; Giannobile, W. V. Platelet-Derived Growth Factor-B Gene Delivery Sustains Gingival Fibroblast Signal Transduction. *J Periodontal Res* **2008**, *43* (4), 440–449. <https://doi.org/10.1111/j.1600-0765.2008.01089.x>.
- (48) Cao, H.; Shi, K.; Long, J.; Liu, Y.; Li, L.; Ye, T.; Huang, C.; Lai, Y.; Bai, X.; Qin, L.; Wang, X. PDGF-BB Prevents Destructive Repair and Promotes Reparative Osteogenesis of Steroid-Associated Osteonecrosis of the Femoral Head in Rabbits. *Bone* **2023**, *167*, 116645. <https://doi.org/10.1016/j.bone.2022.116645>.
- (49) Karkkainen, M. J.; Petrova, T. V. Vascular Endothelial Growth Factor Receptors in the Regulation of Angiogenesis and Lymphangiogenesis. *Oncogene* **2000**, *19* (49), 5598–5605. <https://doi.org/10.1038/sj.onc.1203855>.
- (50) Wang, Z.; Wang, Z.; Lu, W. W.; Zhen, W.; Yang, D.; Peng, S. Novel Biomaterial Strategies for Controlled Growth Factor Delivery for Biomedical Applications. *NPG Asia Mater* **2017**, *9* (10), e435–e435. <https://doi.org/10.1038/am.2017.171>.
- (51) Enriquez-Ochoa, D.; Robles-Ovalle, P.; Mayolo-Deloisa, K.; Brunck, M. E. G. Immobilization of Growth Factors for Cell Therapy Manufacturing. *Front Bioeng Biotechnol* **2020**, *8*, 620. <https://doi.org/10.3389/fbioe.2020.00620>.
- (52) Vo, T. N.; Kasper, F. K.; Mikos, A. G. Strategies for Controlled Delivery of Growth Factors and Cells for Bone Regeneration. *Adv Drug Deliv Rev* **2012**, *64* (12), 1292–1309. <https://doi.org/10.1016/j.addr.2012.01.016>.
- (53) Hendrikse, S. I. S.; Spaans, S.; Meijer, E. W.; Dankers, P. Y. W. Supramolecular Platform Stabilizing Growth Factors. **2018**.
- (54) Wang, Z.; Wang, Z.; Lu, W. W.; Zhen, W.; Yang, D.; Peng, S. Novel Biomaterial Strategies for Controlled Growth Factor Delivery for Biomedical Applications. *NPG Asia Mater* **2017**, *9* (10), e435–e435. <https://doi.org/10.1038/am.2017.171>.
- (55) Kim, H.; Kumbar, S. G.; Nukavarapu, S. P. Biomaterial-Directed Cell Behavior for Tissue Engineering. *Curr Opin Biomed Eng* **2021**, *17*, 100260. <https://doi.org/10.1016/j.cobme.2020.100260>.

- (56) Masters, K. S. Covalent Growth Factor Immobilization Strategies for Tissue Repair and Regeneration. *Macromolecular Bioscience* **2011**, *11* (9), 1149–1163. <https://doi.org/10.1002/mabi.201000505>.
- (57) Carena, E.; Jordan, O.; Segundo, P. M.-S.; Jiřík, R.; Jr, Z. S.; Borchard, G.; Rosell, A.; Roig, A. Encapsulation of VEGF165 into Magnetic PLGA Nanocapsules for Potential Local Delivery and Bioactivity in Human Brain Endothelial Cells. *J. Mater. Chem. B* **2015**, *3* (12), 2538–2544. <https://doi.org/10.1039/C4TB01895H>.
- (58) Freeman, I.; Cohen, S. The Influence of the Sequential Delivery of Angiogenic Factors from Affinity-Binding Alginate Scaffolds on Vascularization. *Biomaterials* **2009**, *30* (11), 2122–2131. <https://doi.org/10.1016/j.biomaterials.2008.12.057>.
- (59) Zisch, A. H.; Schenk, U.; Schense, J. C.; Sakiyama-Elbert, S. E.; Hubbell, J. A. Covalently Conjugated VEGF--Fibrin Matrices for Endothelialization. *J Control Release* **2001**, *72* (1–3), 101–113. [https://doi.org/10.1016/s0168-3659\(01\)00266-8](https://doi.org/10.1016/s0168-3659(01)00266-8).
- (60) Oliveira, É. R.; Nie, L.; Podstawczyk, D.; Allahbakhsh, A.; Ratnayake, J.; Brasil, D. L.; Shavandi, A. Advances in Growth Factor Delivery for Bone Tissue Engineering. *Int J Mol Sci* **2021**, *22* (2), 903. <https://doi.org/10.3390/ijms22020903>.
- (61) Pieper, J. S.; Hafmans, T.; van Wachem, P. B.; van Luyn, M. J. A.; Brouwer, L. A.; Veerkamp, J. H.; van Kuppevelt, T. H. Loading of Collagen-Heparan Sulfate Matrices with bFGF Promotes Angiogenesis and Tissue Generation in Rats. *J Biomed Mater Res* **2002**, *62* (2), 185–194. <https://doi.org/10.1002/jbm.10267>.
- (62) Hudalla, G. A.; Murphy, W. L. Biomaterials That Regulate Growth Factor Activity via Bioinspired Interactions. *Advanced Functional Materials* **2011**, *21* (10), 1754–1768. <https://doi.org/10.1002/adfm.201002468>.
- (63) Guan, N.; Liu, Z.; Zhao, Y.; Li, Q.; Wang, Y. Engineered Biomaterial Strategies for Controlling Growth Factors in Tissue Engineering. *Drug Deliv* **27** (1), 1438–1451. <https://doi.org/10.1080/10717544.2020.1831104>.
- (64) Jahani, M.; Rezazadeh, D.; Mohammadi, P.; Abdolmaleki, A.; Norooznejhad, A.; Mansouri, K. Regenerative Medicine and Angiogenesis; Challenges and Opportunities. *Adv Pharm Bull* **2020**, *10* (4), 490–501. <https://doi.org/10.34172/apb.2020.061>.
- (65) *The vascular endothelial growth factor (VEGF) isoforms: differential deposition into the subepithelial extracellular matrix and bioactivity of extracellular matrix-bound VEGF - PubMed.* <https://pubmed.ncbi.nlm.nih.gov/8167412/> (accessed 2023-04-11).
- (66) Pandey, A. K.; Singhi, E. K.; Arroyo, J. P.; Ikizler, T. A.; Gould, E. R.; Brown, J.; Beckman, J. A.; Harrison, D. G.; Moslehi, J. Mechanisms of VEGF (Vascular

- Endothelial Growth Factor) Inhibitor–Associated Hypertension and Vascular Disease. *Hypertension* **2018**, *71* (2), e1–e8. <https://doi.org/10.1161/HYPERTENSIONAHA.117.10271>.
- (67) DeLisser, H. M.; Christofidou-Solomidou, M.; Strieter, R. M.; Burdick, M. D.; Robinson, C. S.; Wexler, R. S.; Kerr, J. S.; Garlanda, C.; Merwin, J. R.; Madri, J. A.; Albelda, S. M. Involvement of Endothelial PECAM-1/CD31 in Angiogenesis. *Am J Pathol* **1997**, *151* (3), 671–677.
- (68) Karar, J.; Maity, A. PI3K/AKT/mTOR Pathway in Angiogenesis. *Front Mol Neurosci* **2011**, *4*, 51. <https://doi.org/10.3389/fnmol.2011.00051>.
- (69) Park, S.; DiMaio, T. A.; Scheef, E. A.; Sorenson, C. M.; Sheibani, N. PECAM-1 Regulates Proangiogenic Properties of Endothelial Cells through Modulation of Cell-Cell and Cell-Matrix Interactions. *Am J Physiol Cell Physiol* **2010**, *299* (6), C1468–C1484. <https://doi.org/10.1152/ajpcell.00246.2010>.
- (70) Zhang, W.; Bhetwal, B. P.; Gunst, S. J. Rho Kinase Collaborates with P21-Activated Kinase to Regulate Actin Polymerization and Contraction in Airway Smooth Muscle. *J Physiol* **2018**, *596* (16), 3617–3635. <https://doi.org/10.1113/JP275751>.
- (71) Yadunandanan Nair, N.; Samuel, V.; Ramesh, L.; Marib, A.; David, D. T.; Sundararaman, A. Actin Cytoskeleton in Angiogenesis. *Biology Open* **2022**, *11* (12), bio058899. <https://doi.org/10.1242/bio.058899>.
- (72) Bayless, K. J.; Johnson, G. A. Role of the Cytoskeleton in Formation and Maintenance of Angiogenic Sprouts. *J Vasc Res* **2011**, *48* (5), 369–385. <https://doi.org/10.1159/000324751>.
- (73) Banai, S.; Jaklitsch, M. T.; Casscells, W.; Shou, M.; Shrivastav, S.; Correa, R.; Epstein, S. E.; Unger, E. F. Effects of Acidic Fibroblast Growth Factor on Normal and Ischemic Myocardium. *Circ Res* **1991**, *69* (1), 76–85. <https://doi.org/10.1161/01.res.69.1.76>.
- (74) Nagy, J. A.; Benjamin, L.; Zeng, H.; Dvorak, A. M.; Dvorak, H. F. Vascular Permeability, Vascular Hyperpermeability and Angiogenesis. *Angiogenesis* **2008**, *11* (2), 109–119. <https://doi.org/10.1007/s10456-008-9099-z>.
- (75) Dvorak, H. F. Vascular Permeability Factor/Vascular Endothelial Growth Factor: A Critical Cytokine in Tumor Angiogenesis and a Potential Target for Diagnosis and Therapy. *JCO* **2002**, *20* (21), 4368–4380. <https://doi.org/10.1200/JCO.2002.10.088>.
- (76) Dvorak, H. F. Reconciling VEGF With VPF: The Importance of Increased Vascular Permeability for Stroma Formation in Tumors, Healing Wounds, and Chronic Inflammation. *Frontiers in Cell and Developmental Biology* **2021**, *9*.

- (77) Dvorak, H. F.; Harvey, V. S.; Estrella, P.; Brown, L. F.; McDonagh, J.; Dvorak, A. M. Fibrin Containing Gels Induce Angiogenesis. Implications for Tumor Stroma Generation and Wound Healing. *Lab Invest* **1987**, *57* (6), 673–686.
- (78) Herold-Mende, C.; Steiner, H. H.; Andl, T.; Riede, D.; Buttler, A.; Reisser, C.; Fusenig, N. E.; Mueller, M. M. Expression and Functional Significance of Vascular Endothelial Growth Factor Receptors in Human Tumor Cells. *Lab Invest* **1999**, *79* (12), 1573–1582.
- (79) *Engineered living biomaterials* | *Nature Reviews Materials*. <https://www.nature.com/articles/s41578-021-00350-8> (accessed 2023-07-13).
- (80) *Optoregulated Protein Release from an Engineered Living Material* - Sankaran - 2019 - *Advanced Biosystems* - Wiley Online Library. <https://onlinelibrary.wiley.com/doi/full/10.1002/adbi.201800312> (accessed 2023-07-13).
- (81) *Light-Regulated Pro-Angiogenic Engineered Living Materials* - Dhakane - *Advanced Functional Materials* - Wiley Online Library. <https://onlinelibrary.wiley.com/doi/full/10.1002/adfm.202212695> (accessed 2023-07-13).
- (82) *Toward Light-Regulated Living Biomaterials* - Sankaran - 2018 - *Advanced Science* - Wiley Online Library. <https://onlinelibrary.wiley.com/doi/full/10.1002/advs.201800383> (accessed 2023-07-13).
- (83) Pham, J. V.; Yilma, M. A.; Feliz, A.; Majid, M. T.; Maffetone, N.; Walker, J. R.; Kim, E.; Cho, H. J.; Reynolds, J. M.; Song, M. C.; Park, S. R.; Yoon, Y. J. A Review of the Microbial Production of Bioactive Natural Products and Biologics. *Front Microbiol* **2019**, *10*, 1404. <https://doi.org/10.3389/fmicb.2019.01404>.
- (84) Jozala, A. F.; Geraldés, D. C.; Tundisi, L. L.; Feitosa, V. de A.; Breyer, C. A.; Cardoso, S. L.; Mazzola, P. G.; Oliveira-Nascimento, L. de; Rangel-Yagui, C. de O.; Magalhães, P. de O.; Oliveira, M. A. de; Pessoa, A. Biopharmaceuticals from Microorganisms: From Production to Purification. *Braz J Microbiol* **2016**, *47* (Suppl 1), 51–63. <https://doi.org/10.1016/j.bjm.2016.10.007>.
- (85) *The evolution of commercial drug delivery technologies* | *Nature Biomedical Engineering*. <https://www.nature.com/articles/s41551-021-00698-w> (accessed 2023-07-20).
- (86) Bhise, N. S.; Shmueli, R. B.; Sunshine, J. C.; Tzeng, S. Y.; Green, J. J. Drug Delivery Strategies for Therapeutic Angiogenesis and Antiangiogenesis. *Expert Opin Drug Deliv* **2011**, *8* (4), 485–504. <https://doi.org/10.1517/17425247.2011.558082>.

- (87) Sankaran, S.; Becker, J.; Wittmann, C.; Del Campo, A. Optoregulated Drug Release from an Engineered Living Material: Self-Replenishing Drug Depots for Long-Term, Light-Regulated Delivery. *Small* **2019**, *15* (5), e1804717. <https://doi.org/10.1002/sml.201804717>.
- (88) Dhakane, P.; Tadimarri, V. S.; Sankaran, S. Light-Regulated Pro-Angiogenic Engineered Living Materials. *Advanced Functional Materials* n/a (n/a), 2212695. <https://doi.org/10.1002/adfm.202212695>.
- (89) Bhusari, S.; Kim, J.; Polizzi, K.; Sankaran, S.; Del Campo, A. Encapsulation of Bacteria in Bilayer Pluronic Thin Film Hydrogels: A Safe Format for Engineered Living Materials. *Biomater Adv* **2023**, *145*, 213240. <https://doi.org/10.1016/j.bioadv.2022.213240>.
- (90) *Engineered E. coli Nissle 1917 for the delivery of matrix-tethered therapeutic domains to the gut* | *Nature Communications*. <https://www.nature.com/articles/s41467-019-13336-6> (accessed 2023-07-13).
- (91) González, L. M.; Mukhitov, N.; Voigt, C. A. Resilient Living Materials Built by Printing Bacterial Spores. *Nat Chem Biol* **2020**, *16* (2), 126–133. <https://doi.org/10.1038/s41589-019-0412-5>.
- (92) Lufton, M.; Bustan, O.; Eylon, B.; Shtifman-Segal, E.; Croitoru-Sadger, T.; Shagan, A.; Shabtay-Orbach, A.; Corem-Salkmon, E.; Berman, J.; Nyska, A.; Mizrahi, B. Living Bacteria in Thermoresponsive Gel for Treating Fungal Infections. *Advanced Functional Materials* **2018**, *28* (40), 1801581. <https://doi.org/10.1002/adfm.201801581>.
- (93) Duraj-Thatte, A. M.; Praveschotinunt, P.; Nash, T. R.; Ward, F. R.; Nguyen, P. Q.; Joshi, N. S. Modulating Bacterial and Gut Mucosal Interactions with Engineered Biofilm Matrix Proteins. *Sci Rep* **2018**, *8*, 3475. <https://doi.org/10.1038/s41598-018-21834-8>.
- (94) Saadeddin, A.; Rodrigo-Navarro, A.; Monedero, V.; Rico, P.; Moratal, D.; González-Martín, M. L.; Navarro, D.; García, A. J.; Salmerón-Sánchez, M. Functional Living Biointerfaces. *Adv Healthc Mater* **2013**, *2* (9), 1213–1218. <https://doi.org/10.1002/adhm.201200473>.
- (95) Hay, J. J.; Rodrigo-Navarro, A.; Hassi, K.; Moulisova, V.; Dalby, M. J.; Salmeron-Sanchez, M. Living Biointerfaces Based on Non-Pathogenic Bacteria Support Stem Cell Differentiation. *Sci Rep* **2016**, *6*, 21809. <https://doi.org/10.1038/srep21809>.
- (96) *Engineered Living Biomaterials* | *Nature Reviews Materials*. <https://www.nature.com/articles/s41578-021-00350-8> (accessed 2023-07-13).

- (12) Ng, Y.-S.; D'Amore, P. A. Therapeutic Angiogenesis for Cardiovascular Disease. *Curr Control Trials Cardiovasc Med* **2001**, *2* (6), 278–285. <https://doi.org/10.1186/cvm-2-6-278>.
- (13) Schaper, W. Collateral Circulation: Past and Present. *Basic Res Cardiol* **2009**, *104* (1), 5–21. <https://doi.org/10.1007/s00395-008-0760-x>.
- (14) Karpanen, T.; Bry, M.; Ollila, H. M.; Seppänen-Laakso, T.; Liimatta, E.; Leskinen, H.; Kivelä, R.; Helkamaa, T.; Merentie, M.; Jeltsch, M.; Paavonen, K.; Andersson, L. C.; Mervaala, E.; Hassinen, I. E.; Ylä-Herttuala, S.; Orešič, M.; Alitalo, K. Overexpression of Vascular Endothelial Growth Factor-B in Mouse Heart Alters Cardiac Lipid Metabolism and Induces Myocardial Hypertrophy. *Circulation Research* **2008**, *103* (9), 1018–1026. <https://doi.org/10.1161/CIRCRESAHA.108.178459>.
- (15) Epstein, S. E.; Kornowski, R.; Fuchs, S.; Dvorak, H. F. Angiogenesis Therapy. *Circulation* **2001**, *104* (1), 115–119. <https://doi.org/10.1161/01.CIR.104.1.115>.
- (16) *Vascular endothelial growth factor enhances atherosclerotic plaque progression* / *Nature Medicine*. [https://www.nature.com/articles/nm0401\\_425](https://www.nature.com/articles/nm0401_425) (accessed 2023-10-17).
- (17) Leslie-Barbick, J. E.; Saik, J. E.; Gould, D. J.; Dickinson, M. E.; West, J. L. The Promotion of Microvasculature Formation in Poly(Ethylene Glycol) Diacrylate Hydrogels by an Immobilized VEGF-Mimetic Peptide. *Biomaterials* **2011**, *32* (25), 5782–5789. <https://doi.org/10.1016/j.biomaterials.2011.04.060>.
- (18) Santulli, G.; Ciccarelli, M.; Palumbo, G.; Campanile, A.; Galasso, G.; Ziaco, B.; Altobelli, G. G.; Cimini, V.; Piscione, F.; D'Andrea, L. D.; Pedone, C.; Trimarco, B.; Iaccarino, G. In Vivo Properties of the Proangiogenic Peptide QK. *Journal of Translational Medicine* **2009**, *7* (1), 41. <https://doi.org/10.1186/1479-5876-7-41>.
- (19) Pensa, N. W.; Curry, A. S.; Reddy, M. S.; Bellis, S. L. Sustained Delivery of the Angiogenic QK Peptide through the Use of Polyglutamate Domains to Control Peptide Release from Bone Graft Materials. *J Biomed Mater Res A* **2019**, *107* (12), 2764–2773. <https://doi.org/10.1002/jbm.a.36779>.
- (20) Rodrigo-Navarro, A.; Sankaran, S.; Dalby, M. J.; del Campo, A.; Salmeron-Sanchez, M. Engineered Living Biomaterials. *Nat Rev Mater* **2021**, *6* (12), 1175–1190. <https://doi.org/10.1038/s41578-021-00350-8>.

**Chapter 2. Optogenetic engineering of  
bacteria to light-responsively secrete a pro-  
angiogenic protein.**

## 2.1. Introduction

### Engineering bacteria for drug delivery

Bacteria have been engineered as bio factories to produce therapeutics either constitutively or in response to external factors using genetically encoded sensors and switches.<sup>1-5</sup> (Figure 1) With constitutive expression, a few different species have been demonstrated in clinical trials as safe for use in the body, like *E. coli*<sup>5-8</sup>, *L. lactis*<sup>9-11</sup>, *S. typhimurium*<sup>11,12</sup>, etc. Making their therapeutic production responsive to external factors provides the possibility to control release profiles *in situ*. Through such bacterial engineering, they can be directed to disease sites, activated at the desired time and made to release therapeutics with improved efficacy and reduced side effects.<sup>4,13,14</sup> This responsiveness enhances their therapeutic potential and adaptability in complex biological environments.

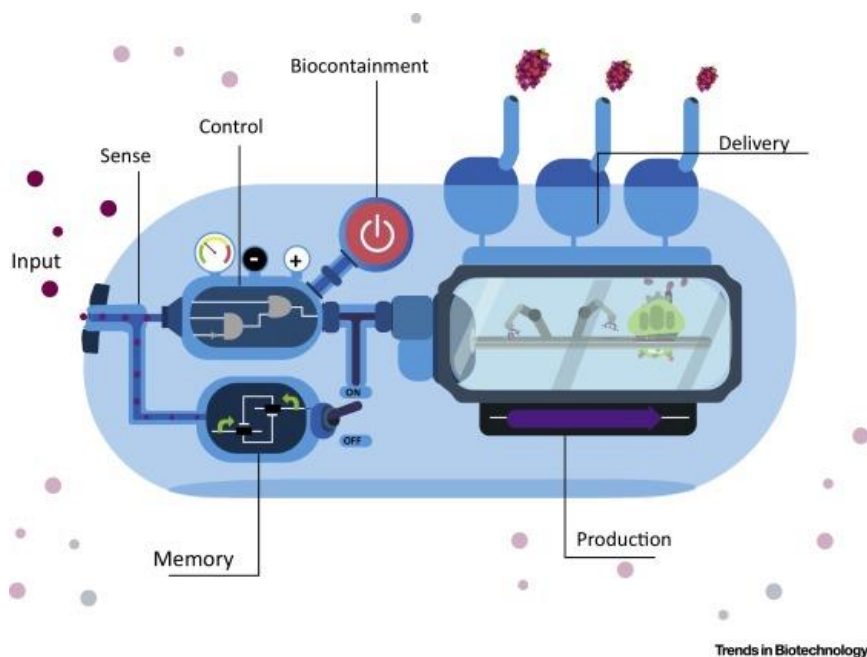


**Figure 1:** Imaginative visualization of bacteria engineered as a biofactory for drug delivery<sup>13</sup> Image reproduced with permission of the rights holder, Elsevier

The clinical studies that have demonstrated safe use of live biotherapeutics freely administered in the body are typically limited to relatively shielded organs in the body such as skin, oral cavity, gastrointestinal and genitourinary tracts. For effective therapeutic impact, large doses of bacteria need to be administered which may lead to risks like (a) severe immune reactions, (b) horizontal gene transfer of the engineered genes through physical contact with other microbes in the body, resulting in unexpected and potentially dangerous modifications in them and (c) tissue damage by colonization of the modified bacteria in non-targeted tissues.<sup>4,14-16</sup>

Encapsulating bacteria in biocompatible materials can circumvent the need for colonization of bacteria within the body and the challenges that come with it. Encapsulated bacteria for therapeutic applications have been explored in the field of engineered living materials (ELMs). There are a few reports of ELMs that incorporate bacteria, which can respond to external stimuli and produce therapeutics.<sup>2,4,13,14</sup> These bacteria are either embedded on the surface or within material substrates that provide structural support. The majority of living materials are based on laboratory strains of *E. coli* due to their ease of genetic modification and the availability of a wide range of established genetic components for engineering purposes. Other organisms such as *L. lactis*, *B. subtilis* and *P. chrysogenum* have also been used in constructing ELMs for biomedical applications. (Table 1). An early instance of an engineered living material designed for drug delivery involved enclosing fungi capable of producing penicillin within a hydrogel made of agar. This structure was positioned between a polyacrylate layer and a nanoporous polycarbonate membrane with a pore diameter of 400 nm. Over a minimum duration of 10 days, the construct steadily dispensed the antibiotic.<sup>18</sup> However, in this system, no genetic programming of the microbe was done to control its drug release. While most studies report the release of anti-microbial drugs from ELMs, one set of studies from the Salmeron-Sanchez lab demonstrates the release of BMP, controlled by an expensive peptide-inducer, nisin.<sup>19,20</sup> Sankaran et al developed agarose-based hydrogels containing ontogenetically engineered *E. coli*, enabling light-regulated release of a fluorescent protein and the drug deoxy violacein.<sup>16</sup> By modulating light exposure, controlled and localized drug production was achieved for over a month without bacterial escape.<sup>16</sup> The endotoxin-free strain of *E. coli* known as ClearColi offers distinct advantages, including a comprehensive genetic toolkit, while avoiding triggering immune responses associated with endotoxins. In this thesis, the ClearColi strain has been employed to develop bacterial hydrogels capable of producing and releasing a pro-angiogenic protein in response to light regulation.

Strain	System	Advantages	Disadvantages
<i>Escherichia coli</i> <sup>21,22</sup> Nissle 1917	Sensing pili for the treatment of Intestinal Bowel Disease	It is a probiotic strain which is easy to engineer	The strain contains endotoxins
<i>Escherichia coli</i> ClearColi <sup>16</sup>	Light- responsive drug delivery	The strain is endotoxin free and is easy to engineer	Does not fall under probiotic category
<i>Lactococcus lactis</i> <sup>23</sup> GN3013	Living bio interfaces	Endotoxin free probiotic strain, good secretor of proteins and can display proteins	Limited genetic toolbox
<i>Bacillus subtilis</i> <sup>24,25</sup>	Low- cost biosensors; skin patches	Robust spore formation	Moderate genetic toolbox
<i>Penicillium</i> <sup>17</sup> <i>chrysogenum</i>	Drug release	Natural producer of penicillin	Limited genetic toolbox
<i>Saccharomyces</i> <sup>26,27</sup> <i>cerevisiae</i>	Biocatalysis, biosensing and bioremediation	Cost-effective. Food grade and big genetic toolbox	Production of ethanol and CO <sub>2</sub> , could be problematic for some medical purposes

2

**Table 1** : Microbial strains employed in Engineered living materials – Its applications along with advantages and disadvantages.<sup>4</sup>

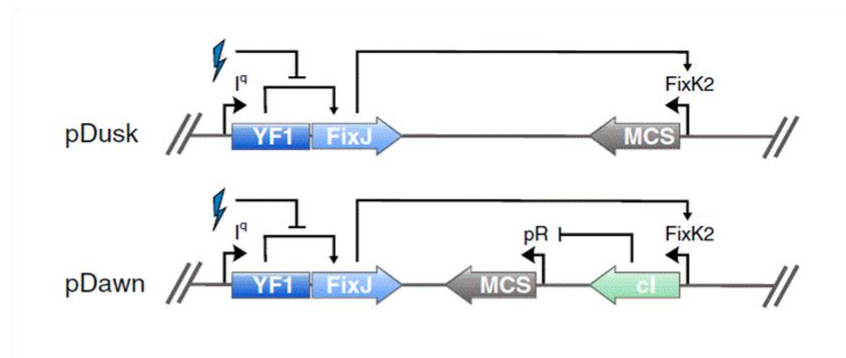
### 2.1.1. Optogenetic control of drug production in bacteria

Bacteria can be programmed with genetic circuits to produce and release a protein when exposed to external factors such as pH<sup>28</sup>, temperature<sup>29–31</sup>, ultrasound<sup>2</sup>, molecular ligands, or light.<sup>14–16,32</sup> Light, among various external stimuli, is particularly convenient to work with, due to its adjustable intensity and wavelength, non-invasiveness and ability for localized drug release with high spatial resolution (as low as ~1  $\mu\text{m}$ ).<sup>15,16,32</sup> It can be applied for specific durations, enabling on-demand delivery.<sup>16</sup> This level of control is essential for achieving targeted therapeutic effects. The manipulation of biological systems using light is referred to as optogenetics, which involves the integration of optical and genetic techniques to introduce light-sensitive proteins for controlling cellular processes in living organisms. Upon exposure to a specific wavelength, the light-sensing domains of the proteins undergo structural alterations, leading to interactions with other molecules or partial folding/unfolding, subsequently regulating downstream biological processes.<sup>33</sup> A prime example of this is the report from Rodriguez et al., which demonstrated the versatility of bacterial optogenetics by engineering *E. coli* to discriminate red, green, and blue (RGB) light, triggering the expression of different genes for each incident wavelength.<sup>33</sup>

pDawn and pDusk are popular plasmid systems that encode blue light-responsive gene expression in bacteria, particularly *E. coli*<sup>34</sup> (shown in Figure 2A). pDusk enables gene expression in the dark, but at a highly reduced rate when exposed to blue light. pDawn was created from pDusk using an inversion module, enabling gene expression to be activated by blue light. Briefly, pDawn contains a light-sensing protein called YF1, which acts as a histidine kinase. When there is no light, YF1 phosphorylates FixJ, which then binds to the FixK2 promoter, triggering the transcription of the *cl* repressor gene (as shown in Figure 2A). The *cl* repressor inhibits transcription from the pR promoter, preventing the expression of a reporter gene. In the presence of light, YF1 remains inactive, preventing the production of the *cl* repressor and allowing transcription of the reporter gene. Implementing pDawn in the laboratory is straightforward, and it can be used in versatile manner. Previous research by Sankaran et al. (2018) demonstrated the potential of using pDawn for light-regulated production and release of a fluorescent protein and a small-molecular drug called deoxyviolacein from bacterial hydrogels (Figure 2B). This research serves as the foundation for the constructs discussed in this thesis.<sup>16,34</sup>

## pDawn and pDusk for light-regulated gene expression

A



B

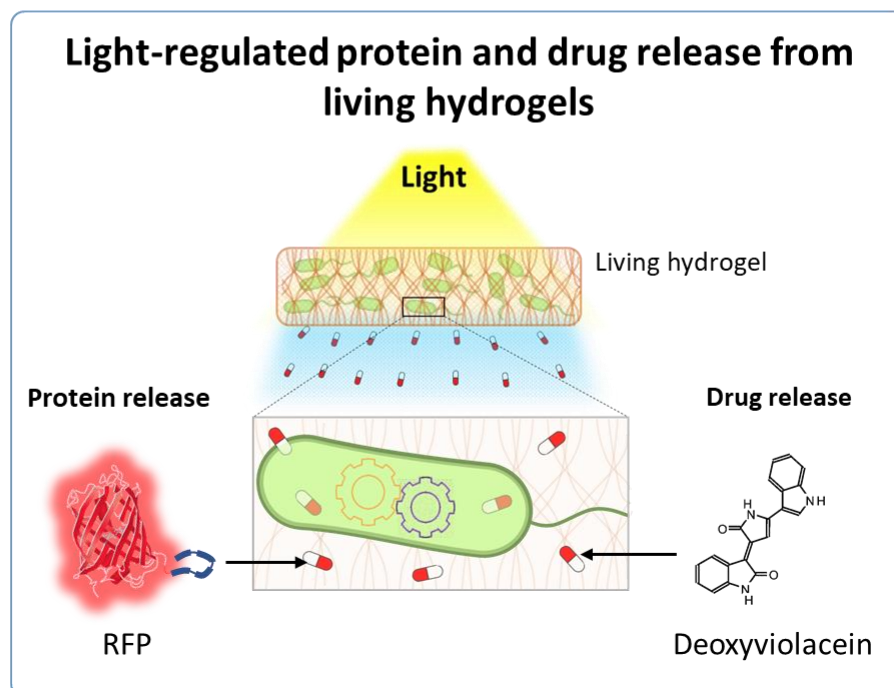


**Figure 2:** A. Diagram illustrating the optogenetic components within the plasmids pDusk for light-inhibited and pDawn for light-induced gene expression in *E. coli*.<sup>34</sup> Image reproduced with permission of the rights holder, Elsevier B. Controlled release of proteins and drugs from hydrogels regulated by light<sup>16</sup> Image reproduced with permission of the rights holder, WILEY

## 2.1.2. Secretion of proteins from *E. coli*

Protein secretion is crucial for bacterial survival as it plays various roles such as aiding in the formation of pili and flagella, releasing extracellular enzymes for polymer degradation to obtain nutrients, and secreting toxins to harm host cells during infections in humans, animals, and plants. It is widely recognized that non-pathogenic *E. coli* strains typically exhibit minimal protein secretion into the extracellular environment during regular growth conditions.<sup>35</sup> In *E. coli*, there are multiple pathways available for protein secretion to the periplasmic space (e.g., Sec, SRP and Tat pathways) (Figure 3), but in order to cross the outer membrane, these proteins need to be genetically fused with transporter proteins.<sup>1,36–38</sup>

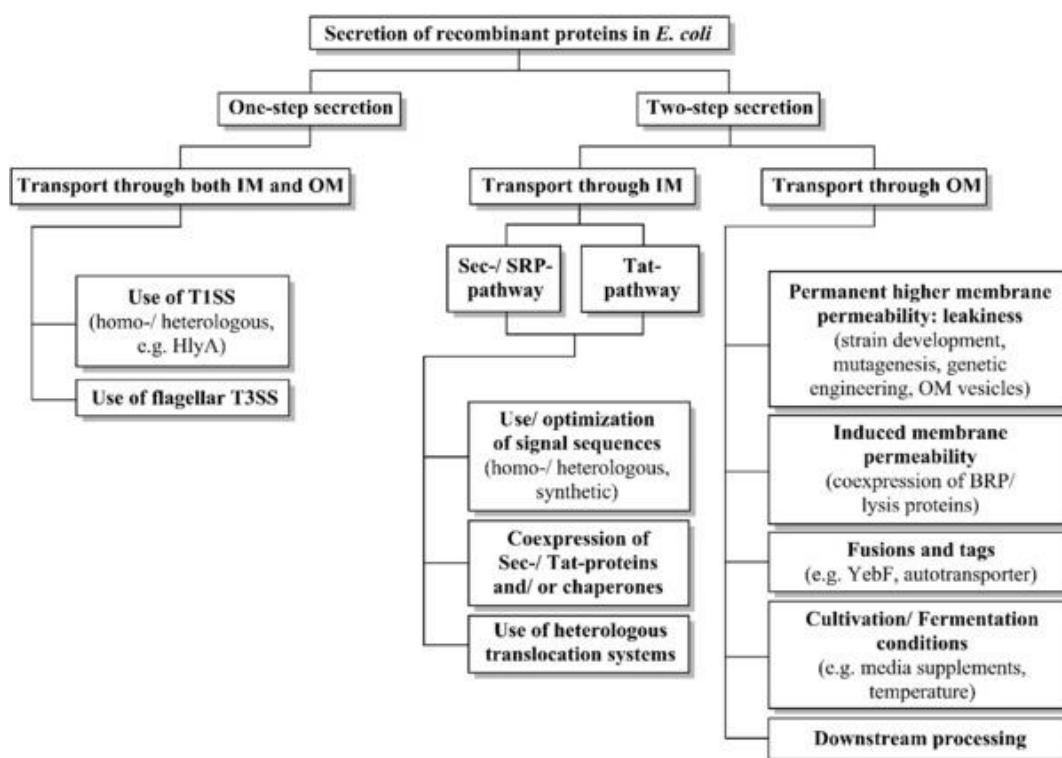


**Figure 3.** Recombinant protein secretion pathways in *E. coli*. One step secretion pathway involves secretion of proteins in one shot that passes through both the inner and outer membrane. In the two-step secretion pathway, transport through inner membrane is via SRP or Tat pathway, whereas transport through the outer membrane occurs if there is higher or induced membrane permeability. Image reproduced with the permission of rights holder, WILEY

Among the transporter proteins found in *E. coli*, YebF is the smallest known naturally occurring soluble protein (10.8 kDa).<sup>1,38,39</sup> On its N-terminal is a Sec-pathway signal

peptide that transports the protein in its unfolded state across the inner membrane into the periplasm. Beyond this, YebF is secreted into the extracellular space through OmpF/OmpC channels (Figure 4). By fusing other proteins to the carboxyl terminus of YebF, researchers have successfully achieved efficient secretion of these "passenger" proteins into the growth media. While the specific function of YebF is still unknown, its utilization as a carrier for transgenic proteins was explored to simplify the purification process of proteins synthesized within *E. coli*.<sup>1,38,40</sup> Experiments have shown that YebF is capable of transporting fusion proteins of different sizes and hydrophilicities from *E. coli* cells to the surrounding medium. Some examples of these proteins include human interleukin-2 (hIL-2) with a size of 15 kDa, alkaline phosphatase weighing 94 kDa, and  $\alpha$ -amylase with a molecular weight of 48 kDa.

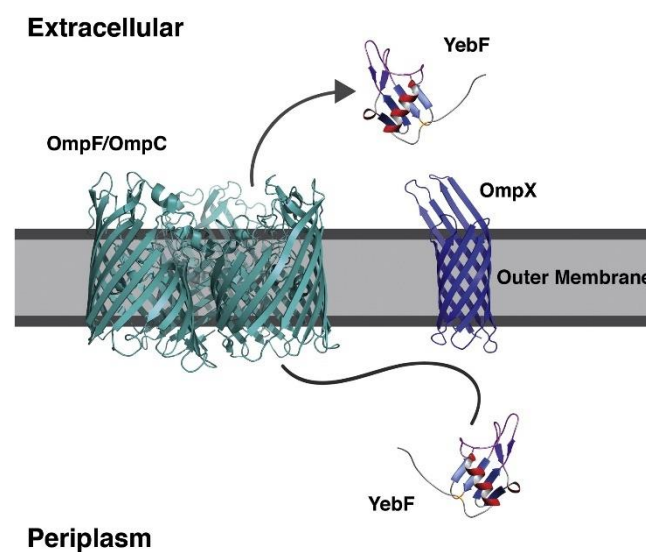


**Figure 4:** Secretion pathway of YebF<sup>38</sup> Image reproduced with permission of the rights holder, ELSEVIER

This chapter describes engineering of light responsive ClearColi for production and secretion of pro-angiogenic protein, YCQ. YCQ was cloned in pDawn in order to produce it in response to light. Angiogenic peptide CBD-QK is fused to YebF to facilitate its export out of ClearColi via the YebF secretion pathway. Since QK needs to bind to the ECM to be functional, the angiogenic peptide was designed with CBD in it, since collagen is found in abundance in extracellular matrix.

## 2.2. Design, cloning and purification of the fusion protein YebF-CBD-QK (YCQ) and the control variant

### 2.2.1. Design, cloning and detection of the His-tag variant

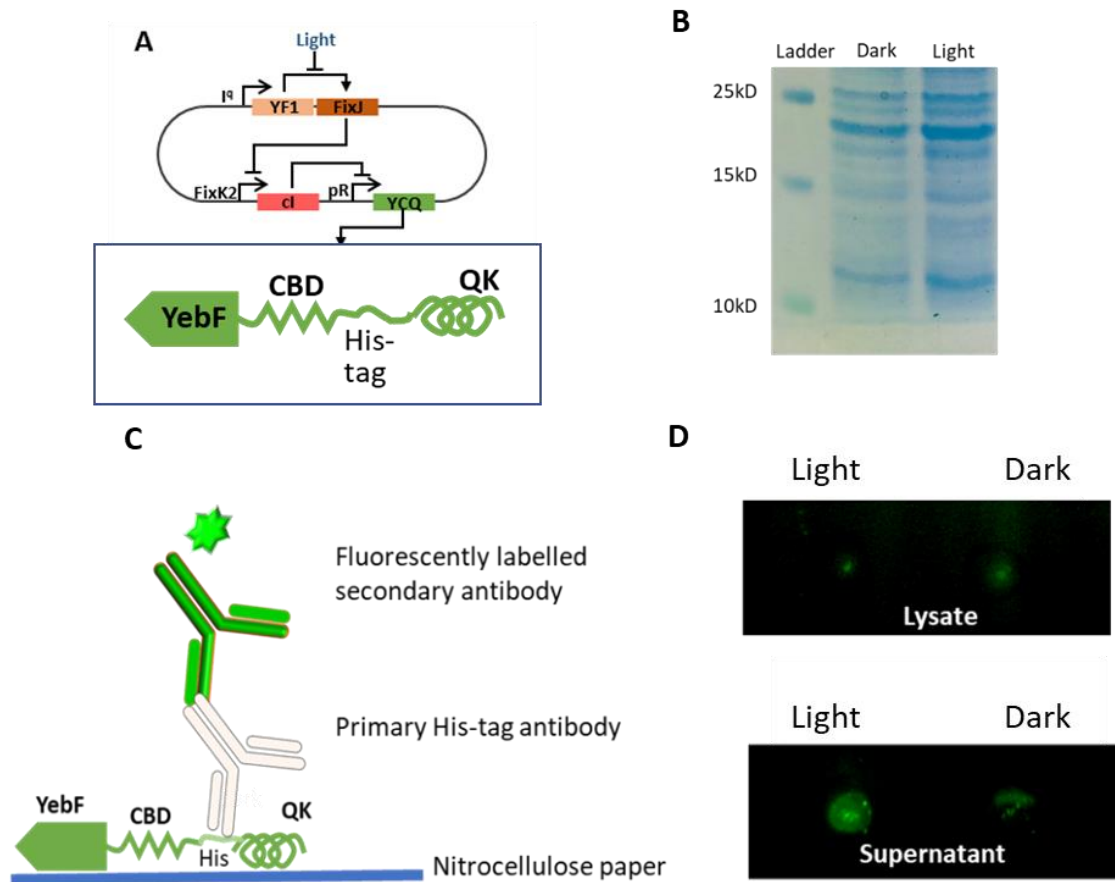


**Figure 5.** A. Design and activity of YCQ: A. Graphical representation of the pDawn-based optogenetic circuit for light-responsive production of YCQ along with scheme highlighting the different domains of the fusion protein. Image reproduced with permission of the rights holder, WILEY B. Production and detection of YCQ secreted by ClearColi. 12% SDS-PAGE gel representing production of YCQ in the ClearColi cell pellet C. Representation of dot blot for detection of YCQ. YCQ was immobilized on a polycarbonate sheet and stained with primary and secondary anti His antibody D. Dot blot indicating the presence of YCQ in the cell lysate and ClearColi YCQ SN induced with light

The pro-angiogenic protein, YCQ, was designed with YebF at the N terminus for secretion followed by a Collagen Binding Domain (CBD) for binding to the mammalian extracellular matrix, a His6-tag for purification and the VEGF-mimetic peptide, QK, at the C terminus (Figure 5 A). It is necessary for YebF to be at the N-terminus, since the signal peptide sequence for transport to the periplasm needs to be at the N-terminus for it to be recognized by the Sec pathway enzymes.<sup>37,38,40</sup> It is also crucial for QK to be at the C-terminus to interact with the VEGF receptors after being secreted.<sup>41</sup> The gene corresponding to the 18.9 kDa YCQ protein was inserted into the multiple cloning site of an optogenetic plasmid, pDawn.<sup>42</sup> A band of expected size was observed in the SDS-PAGE gel (Figure 5B). However, it was surprisingly not possible to purify the protein using a His-tag affinity column. It is speculated that this might be because of the inaccessibility of the intra-chain His6-tag to Ni-NTA anchored to the agarose beads of the chromatography column. In this design, the His6-tag had Gly-Ser-Gly-Ser linkers at both ends. Flexible linkers are generally composed of Gly and Ser residues since they can maintain stability of the linker in a aqueous solution by forming hydrogen bonds, and therefore preventing unfavorable interaction between the linker and protein moieties.<sup>43,44</sup> It is speculated that the GSGS linker might not have provided sufficient flexibility for the His6-tag to be available for Ni-NTA beads and therefore His-tagged YCQ could not be purified.<sup>44</sup>

Detection of secreted YCQ protein was also done using a dot-blot assay (Figure 5C). Lysates and SNs from the dark state and light state (induced) liquid cultures were analyzed by immobilizing them on a polycarbonate sheet. After immobilization the sheets were blocked with BSA and stained with anti-His6-tag primary and AF-488 secondary antibody. YCQ was detected in the SN from the light state culture and low amount of expression was also seen in the dark state SNs as well as lysates from both light and dark states (Figure 5D). However, the results from this assay were inconclusive since non-specific staining was seen in ClearColi wild type lysates. The issue of accessibility of the His6-tag for antibody binding could have also been an issue preventing the generation of a stronger specific signal.

### **2.2.2. Engineering YCQ with Strep tag**

Since the His6-tagged protein could not be purified by affinity chromatography nor could it be specifically detected on a dot-blot, the protein design was modified to bear a Strep-tag instead and (GSGS)<sub>2</sub> linkers were used instead of GSGS to allow more flexibility and accessibility for the Strep-tag<sup>44-46</sup>. This tag binds specifically to Strep-Tactin, a variant of streptavidin, offering improved purification capabilities. The new

design was expected to perform better as Strep-tag has been reported to provide better specificity compared to a His6-tag<sup>47</sup> and the longer linkers would render the tag to be more accessible. The Strep-tag containing YCQ gene was designed *in silico* and purchased as a synthesized double-stranded DNA. This was inserted in the MCS of pDawn by HiFi assembly. In the first design, the sequence for (GSGS)<sub>2</sub> linker on both sides of the Strep-tag was- GGCAGCGGCAGCGGCAGCGGCAGC, which contained repeated codons resulting in mutations and sequencing errors during the cloning process (Figure 6). Genetic rearrangements and mutations are frequently associated with repetitive DNA sequences and might also be a cause for frequent sequencing errors.<sup>48,49</sup> Due to this, the linker codon sequences were modified to GGTAGTGGTAGTGGTAGTGGTAGT, which resulted in successful cloning of Strep-tagged YCQ in pDawn. As a negative control, a similar fusion protein, YCx, was designed bearing a scrambled-QK peptide (GLKEQSPRKHRLG) at the C-terminal, previously shown to be inactive.<sup>41</sup> The gene corresponding to the 18.9 kDa YCQ or YCx protein was inserted into the multiple cloning site of an optogenetic plasmid, pDawn,<sup>34</sup> to achieve light responsive production and secretion.

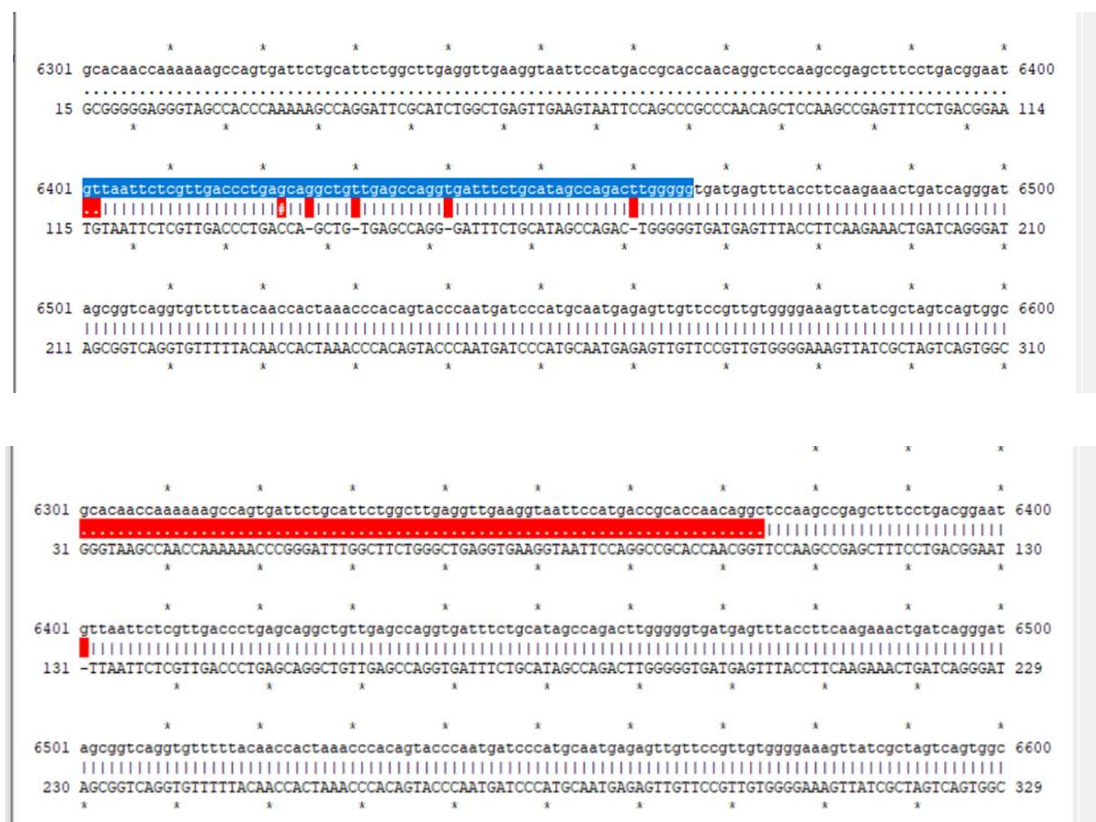


**Figure 6:** Sequencing results of YCQ-His variant showing frequent mutations. The sequence alignment is performed in ApE

Disclaimer: Figure 7, 8, 9 and large parts of the text describing the results of Figure 7,8,9 are taken/adapted from my own published work: Light-Regulated Pro-Angiogenic Engineered Living Materials - Dhakane - Advanced Functional Materials - Wiley Online Library. <https://onlinelibrary.wiley.com/doi/full/10.1002/adfm.202212695> (accessed 2023-07-13).

### 2.2.3. Characterization of YebF-mediated secretion and CBD mediated collagen binding

#### A Design of YCQ



#### B SDS-PAGE analysis of YCQ

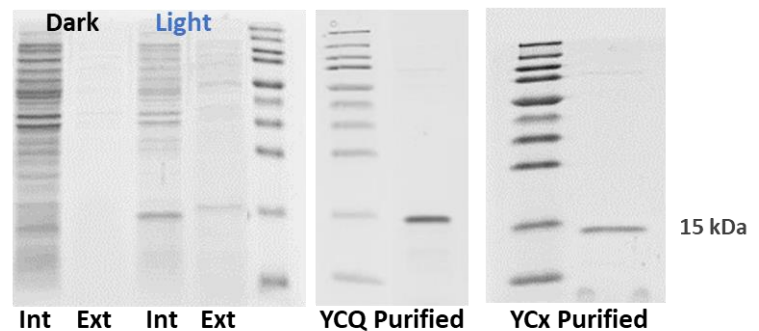


**Figure 7.** Design and activity of YCQ: A. Design of YCQ-strep. B. SDS-PAGE images of the intracellular (Int) and extracellular (Ext) fractions of light-regulated production and secretion of YCQ from engineered bacterial cultures, along with purified YCQ for comparison. Image reproduced with permission of the rights holder, WILEY

To test light-responsive production and secretion, ClearColi pDawn-YCQ was cultivated in liquid LB media until it reached exponential phase of growth ( $\sim 0.5-0.8$  OD<sub>600nm</sub>) and then it was induced with white light for 18 h. Production and secretion of YCQ and YCx was confirmed by SDS-PAGE by running the extracellular and cellular fractions from bacterial cultures grown either in white light or in the dark (Figure 7B). In the light exposed cultures, a band around 15 kDa was observed in both the cellular and extracellular fractions as well as after purification. This lower molecular weight was expected because of cleavage of the 2.2 kDa N-terminal signal peptide of YebF during its secretion into the periplasm through the sec pathway. Western Blot analysis confirmed that this band contained the Strep-tag (Figure 8A). MALDI-TOF mass-spec analysis of the protein purified from the cellular fraction revealed a clear peak at 16.7 kDa confirming cleavage of the signal peptide suggesting that most of the intracellular protein resided in the periplasm (Figure 8B). These results confirmed that YCQ can be light-responsively produced and secreted from ClearColi.

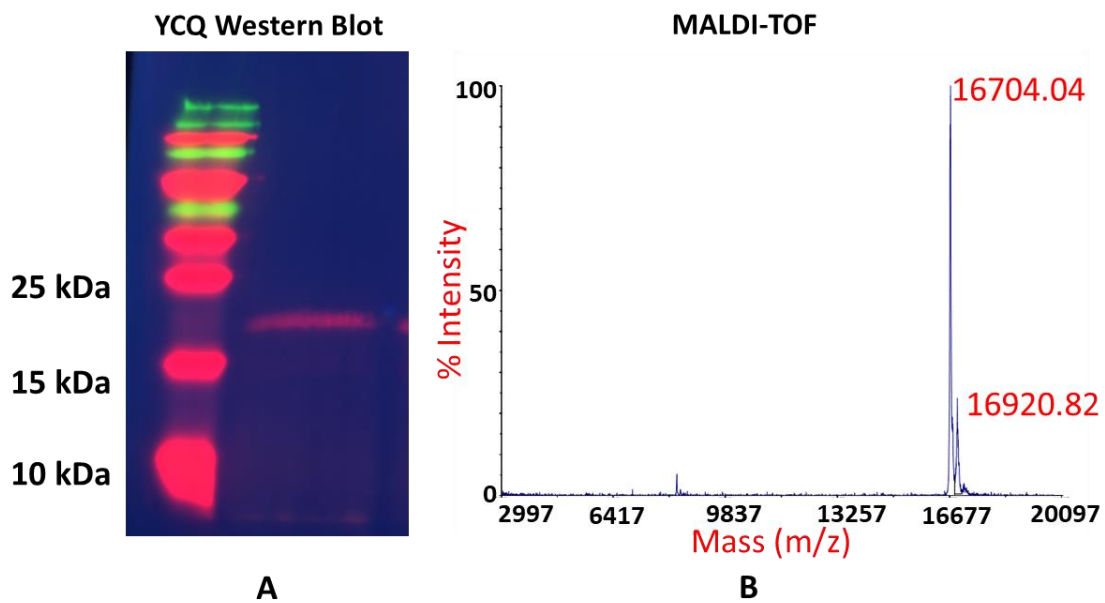


**Figure 8:** Western Blot for confirmation of YCQ. YCQ was stained with fluorescently labelled Q dot streptavidin (red) C. MALDI-TOF MS spectrum of purified YCQ protein; sharp peak at 16.704 kDa confirms the size of YCQ protein after sec-leader peptide cleavage. Image reproduced with permission of the rights holder, WILEY

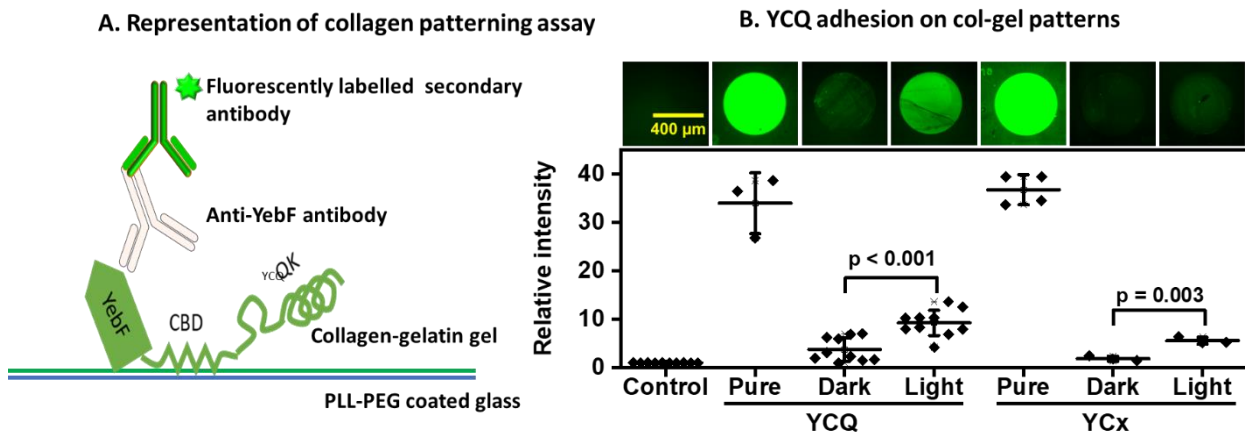


**Figure 9:** YCQ adhesion to Col-Gel Matrices A. Graphical representation of YCQ and YCx adhesion to Col-Gel matrices. B. Fluorescence microscopy images and pattern intensity quantification of the Col-Gel photopatterning assay to verify the ability of YCQ and YCx to adhere to collagen. Staining was done with an Anti-YebF primary antibody and a fluorescently labelled anti rabbit AF-488 secondary antibody. In the Control condition, the patterned Col-Gel surfaces were incubated with supernatants from unmodified ClearColi cultures exposed to light. The symbols in the graph represent the intensity of individual patterned spots from 2 independent experiments (N = 2). The intensities have been normalized to the mean of the control sample. Two sample t-tests were performed between YCQ dark/light and YCx dark/light data sets and p values are given above indicating that their differences are statistically significant. Image reproduced with permission of the rights holder, WILEY

We proceeded to test the capability of the protein to bind collagen using a collagen-gelatin mixture (Col-Gel) in a 3:1 ratio by weight to form a thin film gel that has been reported to mimic the extracellular matrix in wounds where collagen is often degraded to remodel the tissue.<sup>50</sup> Binding of YCQ to collagen was verified by incubating the protein on a photo-patterned substrate of Col-Gel, after which it was immunostained using a primary antibody specific to YebF. Both purified and secreted YCQ and YCx were observed to preferentially adhere to Col-Gel patterned regions (Figure 9B). Analysis of the stained patterns revealed that the intensities of the patterned spots associated with proteins secreted in the presence of light were on average 2.5-fold higher than those cultured in the dark. However, the intensities of spots from light-state protein secretions were on average 3 to 7-fold lower than spots made with 10 nM purified proteins, suggesting that secretion from the overnight cultures was relatively low.

### 2.3. Discussion and Conclusions:

In the initial designs of YCQ, using His tag flagged by GSGS linkers on both the sides possibly did not give accessibility to the His tag for purification. The next design included a strep-tag and 8 amino acid flexible linkers to improve specificity and flexibility. Cloning 8 amino acid flexible linkers with repetitive DNA sequences was not possible because of frequent sequencing errors.<sup>48</sup> YCQ and YCx could be cloned and purified when designed with strep-tag flanking 8 amino acids sequences with non-repetitive codons.

ClearColi was successfully engineered to produce YCQ in response to light. YebF was able to transport 15kD YCQ out of ClearColi, the presence of which was confirmed by SDS-PAGE, western blot and MALDI-TOF. Later, we demonstrated that secreted YCQ can bind to col-gel patterns because of the presence of CBD. Generally, the affinity tag is placed either at the N-terminus or at C-terminus of the protein; in YCQ, it was placed in between CBD and QK because YebF had to be at the N-terminus for its secretory function<sup>1,38,39</sup> and QK was placed at the C-terminus for better accessibility to the VEGF-R. Placing the strep-tag in the middle of the sequence did not lead to insoluble protein and no loss of protein functionality was noticed. YCQ got secreted out of bacterial cells which suggests that YebF was functional, CBD was able to bind to collagen patterns which proved its functionality and the bioactivity of QK is discussed in the next chapters.

While YCQ was secreted from ClearColi, it was noticed on the PAGE gel that a large amount of protein (~80%) was still inside the cell. The cell membrane can be permeabilized by addition of glycine (permeabilizing agent) or co-expressing helper proteins such as bacteriocin-release protein or colicin E1 lysin.<sup>51</sup> However, in some cases this might lead to excessive leakiness or lysis of the bacterial cells causing release of unwanted proteins from the cell.<sup>36,37</sup> Therefore, no such permeabilizing agent was used in the experiments. The secretion efficiency needs to be increased to get higher concentrations of YCQ out of the cell. pelB and CalB are examples of simple amino acid tags where they could be secreted into the medium in gL<sup>-1</sup> scale and 100% of it was secreted into the medium.<sup>52</sup> Low levels of YCQ secretion could also be because *E. Coli* is poor secretor of the proteins.<sup>36</sup> Use of better secretor microorganism like *Bacillus Subtilis* and use of a smaller secretion tag pelB might be able increase secretion efficiency of CBD-QK. This strategy will be explored in the group.

Despite the lower proportion of YCQ secreted from E.Coli, the concentration of still enough for us to test the protein for angiogenesis experiments and for encapsulating

YCQ producing bacteria to create ELMs. The concentration of QK required to induce network formation lies in the nM to  $\mu$ M range, depending on the system use.<sup>41,50,53,54</sup>

Next, YCQ producing ClearColi was encapsulated in PluDa hydrogels to create light-responsive ELMs which is described in the next chapter.

Disclaimer: Large parts of the text of Section 2.4 are taken/adapted from my own published work: Light-Regulated Pro-Angiogenic Engineered Living Materials - Dhakane - Advanced Functional Materials - Wiley Online Library. <https://onlinelibrary.wiley.com/doi/full/10.1002/adfm.202212695> (accessed 2023-07-13).

## 2.4. Materials and Methods

### 2.4.1. Construction of plasmids and bacterial strains:

The YebF-CBD-strep-QK fragment (DNA sequence in Supporting information) was ordered as a g-Block from Eurofins Genomics, and inserted into the plasmid, pDawn (pDawn was a gift from Andreas Moeglich - Addgene plasmid# 43796;; using NEBuilder® HiFi Assembly cloning kit (NEB, E5520S) using following primers-

pDawn Fwd 5'-ataaaagcttAACAAAGCCCGAAAGGAAG-3',

pDawn Rev 5'-ctcttttttCATGGTATATCTCCTTCTTAAAGTTAAAC-3',

YebF-CBD-QK Fwd- 5'- atataccatgAAAAAAGAGGGGCGTTTTTAG-3'

YebF-CBD-QK Rev- 5'- gggctttgttAAGCTTTTATTTTCAGGGTC-3'.

The pDawn YCQ plasmid obtained after cloning was transformed into ClearColi BL21 cells as specified by the provider (BioCat 60810-1-LU). The recombinant pDawn-YCQ was used as a template to construct the pDawn YebF-CBD-Scrambled QK (YCx) mutant (DNA sequence in supporting information) using the HiFi assembly kit obtained from NEB.

pDawn Fwd 5'- CTAGCATAACCCCTTGGG-3',

pDawn Rev 5'- CTAGTAGAGAGCGTTCAC C-3',

YebF-CBD-Scrambled QK Fwd- 5'- cggtgaacgctcttactagAGTCACACTGGCTCACCTTC-3'

YebF-CBD-QK Scrambled Rev- 5'- gccccaaggggttatgctagTTATTGCTCAGCGGTGGC-3'.

pDawn-YCx was also transformed in ClearColi cells as mentioned previously. For storage at -80 °C, glycerol stocks with 30% of glycerol for both clones were made from bacterial cultures grown overnight at 37°C, 250 rpm in the dark from single colonies.

Bacterial culture for protein purification and secretion: 250 mL of *ClearColi* BL21(DE3) pDawn-YCQ or pDawn-YCx cultures were grown in dark for 37°C, 250rpm in LB Miller medium supplemented with 50 µg.mL<sup>-1</sup> of Kanamycin to an OD<sub>600nm</sub> between 0.4 and

0.8. The culture was then induced for 12 h by exposing it to white light for production of YCQ and YCx at 37 °C, 250rpm

Bacterial cultures for ELMs: *ClearColi* BL21(DE3) cultures were grown for 16 h at 37 °C, 250 rpm in LB Miller medium supplemented with 50 µg.mL<sup>-1</sup> of Kanamycin to an OD<sub>600nm</sub> around 0.8. All procedures were performed either in the dark or under orange light.

#### 2.4.2. Purification of YCQ and YCx

*ClearColi* BL21(DE3) with pDawn-YCQ or pDawn YCQx were cultured in LB Miller medium supplemented with Kanamycin. YCQ/YCx production was induced with white light for 16 h. For harvesting the cells, cultures were transferred to 50 mL flacon tubes and centrifuged with an Avanti J-26S XP centrifuge (Beckman Coulter, Indianapolis, USA) using the JLA-10.500 rotor for 20 min at 4000 rpm and 4 °C. The supernatants were discarded, and pellets weighed and stored at -80 °C until further use. For protein extraction, the bacterial pellets were thawed on ice and resuspended in a volume of lysis buffer (100mM TrisCl pH8, 150mM NaCl and 1mM PMSF) having mL magnitude equivalent to 5x the cell pellet weight in g. To lyse the cells, a sonicator (Branson ultrasonics, Gehäuse SFX150) was used with sonication cycles having pulse "ON" for 3 seconds, "OFF" for 5 seconds at 20% power over 6–8 mins. The sonicated solutions were centrifuged at 14000 rpm for 15 mins at 4° C and the supernatants were collected for further purification by affinity-based column chromatography. Supernatants and cell debris were stored for analysis by Sodium dodecyl sulfate-polyacrylamide gel electrophoresis (SDS-PAGE). Since the proteins engineered with a StrepII-tag, columns containing Strep tactin beads (Quiagen, 30004) were used for purification of the protein by affinity chromatography modifying the protocol given by the manufacturer (Quiagen) to optimize pure protein yields. 4 mL of the strep-tactin bead solution was pipetted into a 15 mL falcon tube and was centrifuged at 100 rpm for 2 mins to obtain a strep-tactin bed volume of 2 mL. The beads were washed three times with 5 mL of lysis buffer; the lysis buffer was removed each time by centrifuging the beads at 100 rpm for 2 mins. 5 mL of cell lysate was added onto the strep tactin beads and this assembly was incubated at 4 °C on a rotary shaker for 30 mins to facilitate optimal contact between the beads and cell lysate. The beads were centrifuged at 100 rpm for 2 mins to remove the unbound protein and washed with 5 column volumes (CV) of wash buffer (100 mM TrisCl, 150 mM NaCl and 0.5% tween 20) 3 times by adding 5 CV of wash buffer to the 15 mL falcon and rotating it upside down manually each time; the wash buffer was removed each time by centrifugation of the beads at 100 rpm for

2 mins. The protein was eluted using an elution buffer (100 mM TrisCl, 150 mM NaCl and 2.5 mM Desthiobiotin). The eluted protein was rebuffed in 5 volumes PBS pH 7 and concentrated by using 3 kDa-cutoff centrifugal filter units and centrifugation parameters - 4000 rpm for 45 mins at 4°C. The protein yields for YCQ and YCx were in the range of 6 mg.L<sup>-1</sup> to 20 mg.L<sup>-1</sup>

#### 2.4.4. SDS PAGE analysis of the secreted and purified YCQ

SDS-PAGE (Sodium dodecyl sulfate-Polyacrylamide gel electrophoresis) was used to determine the presence and estimate the molecular weights of proteins. The compositions of all required solutions and buffers are listed in next table

*Composition of buffers and solutions for SDS-PAGE.*

Buffer or Solution	Compound	Final concentration
Sample loading buffer	SDS	6% (m/m)
	Bromophenol blue	0.16% (m/m)
	Tris-HCl	0.1 M
	DTT	0.05 M
	Glycerol (99%)	15% (v/v)
10X running buffer	Tris-HCl	1% (m/m)
	Glycine	1.92 M
	SDS	0.25 M
Staining solution	Coomassie® Brilliant Blue R-250	0.5% (m/m)
	Ethanol (99.8%)	50% (v/v)
	Acetic acid (100%)	10% (v/v)
Destaining solution	Deionised water	-

Preparation of 15% SDS gels is described in the process below:

1) Resolving gel (15%) mix was prepared. It was mixed in the following order.

*Components of resolving gel.*

<b>Components</b>	<b>Volume (mL)</b>
Milli-Q water	4.6
30% Acrylamide mix	10
1 M Tris, pH 8.8	5
10% SDS	0.2
10% Ammonium persulfate (APS)	0.2
Tetramethyl ethylenediamine (TEMED)	0.008

Immediately after APS and TEMED were added to resolving gel mix, it was poured into already set up gel plates apparatus such that 2 cm of space was left for stacking gel. It was made sure to remove bubbles from resolving gel. Isopropanol was poured over the top of the stacking gel which helped in removing the bubbles and prevented the polymerized gel from drying out. The setup was left undisturbed for 30 minutes for gel to completely polymerize. Isopropanol was poured out and its traces were removed by rinsing the edge of the resolving gel with distilled water. Stacking gel (6%) was prepared and they were mixed in the following order:

*Components of stacking gel.*

<b>Chemical substance</b>	<b>Volume (mL)</b>
H <sub>2</sub> O	6.1
30% Acrylamide mix	1.5
1 M Tris, pH 6.8	1.12
10% SDS	0.09
10% APS	0.09
TEMED	0.009

Stacking gel was poured on the top of polymerized resolved gel. Comb was placed in stacking gel to facilitate formation of the wells. The setup was left undisturbed for 30 minutes for gel to completely polymerize.

#### Preparation of samples and running SDS-PAGE:

Polymerized SDS-PAGE Gel was clamped into the apparatus and both the chambers were filled with running buffer. 15  $\mu$ L of samples were mixed with 5  $\mu$ L of 4x Laemmli sample buffer in 0.2 mL PCR tubes. Tubes were incubated at 98 °C for 10 minutes followed by cooling down to 4 °C for a brief period by using a thermocycler PCR instrument to denature the proteins present in the samples. Denatured samples and spectra BR protein ladder (Thermo fisher scientific) were loaded into wells for separation. The gel was allowed to run at 100 V until the dye front reached the bottom of resolving gel (Approximately 90 minutes). Gel was carefully peeled out from the glass plates and washed with water thrice. It was stained in 50 mL of Coomassie brilliant blue stain (Bio-Rad) for 1 hour with gentle shaking at room temperature. Later, gel was destained overnight in ion-free water at room temperature. The destained gel was analysed in Gel-Doc equipment (Cell Biosciences) with a pre-programmed protocol in Flouorochem Q software.

#### **2.4.4. Analysis of the protein with Western Blot and Mass Spectrometry**

After SDS-PAGE, the gel was transferred to the prepare for the blot/gel sandwich instead of staining with Coomassie brilliant blue stain. The gel was soaked in water followed by equilibration in transfer buffer. Filter paper and PVDF membrane (Bio-Rad, Germany) were cut to the same dimensions as of SDS-PAGE gel and were also equilibrated in transfer buffer along with the sponges of the cassette. Gel sandwich was prepared by placing the cassette's black side down on a clean surface. One pre-wetted sponge (in 1X TB) was placed on the black side of the cassette. The filter paper soaked in a transfer buffer was placed on pre wetted sponge. Equilibrated SDS-PAGE gel was placed on the filter paper. PVDF membrane was immerse/soaked in methanol for 15 seconds followed by prewetting in transfer buffer for 2 minutes was positioned on the gel. Another pre-wetted filter paper was placed on the PVDF membrane followed by gently pressing the entire membrane surface with a roller to remove air bubbles. Another Prewetted sponge was placed, and gel cassette was closed with the white latch. The cassette was placed in the module and placed in a tank. Tank was filled with a transfer buffer until the "blotting" mark on the tank. A blue cooling unit

was placed in the tank to facilitate cooling and a stir bar to help maintain even buffer temperature as well as ion distribution in the tank. The blot was run at 100 V for one hour. While the blot was running, snap id 2.0 system was setup by washing the mini blot holder of snap id system connected to vacuum pump with 30 mL of Milli-Q water thrice. Once the blot run was complete, the blotting sandwich was disassembled and the membrane (onto which protein transfer was done) was transferred in between double layered mini blot filter paper pre-soaked (2-3 minutes) in the transfer buffer. Membrane was sandwiched in mini blot filter paper, rolled gently to remove air bubbles. Mini blot paper along with membrane in it was positioned in holder area of snap id. Blocking step: 30 mL of blocking buffer (0.5% non-fat milk powder solution in 1X TBS) was pipetted onto the surface of the mini blot in holder and was left undisturbed for 10 minutes. It was followed by applying vacuum pressure of 430 milli Pa to remove the blocking buffer from mini blot. Washing step: 30 mL of washing buffer (1X TBS) was pipetted onto the surface of mini blot, and vacuum was applied immediately to remove the washing buffer from mini blot. 5 mL of CY5 streptavidin solution (1:500 in TBS) (eBioscience, 0.2 mg/mL) was pipetted onto the membrane followed by 10-minute incubation and 3X washing steps thereafter. Membrane was transferred to Gel doc equipment and was visualised in CY5 pre-programmed RGB blot protocol of FluorochemQ tool.

#### **2.4.5. Patterning of Col-Gel matrix on a Glass Surface to assess binding of YCQ:**

Coating coverslips with PLL-PEG: Glass coverslips were cleaned by treating them with oxygen plasma in a plasma oven (Harrick Plasma, Ithaca, NY, USA) for 5 mins. 50  $\mu\text{L}$  of 0.1  $\text{mg}\cdot\text{mL}^{-1}$  PLL-PEG (PLL (20)-g [3.5]-PEG (5), SuSoS AG, Dübendorf, Switzerland) solution in PBS was placed on a sheet of parafilm. The plasma-treated coverslips were inverted on the drop of PLL-PEG and incubated for 1 h at room temperature (RT).

Cleaning of the photomask: The patterned surface of the photomask was cleaned with acetone, water, ethanol and water by dipping in each solution. It was air dried gently and placed in UVO cleaner (Jelight Company Inc, model no.42) for 5 min, in such a way that the patterned side faced up.

Making patterns using the photomask: After the incubation, the coverslip was released from the parafilm gently by infusing deionised water under the coverslip in such a way that it starts floating. It was rinsed by dipping the patterned surface 5 times in PBS pH 7 solution and dried by draining the excess solution onto a paper towel. 5  $\mu\text{L}$  deionised water was placed on the patterned side of the photomask to reduce friction between the coverslip and patterned surface. The coverslip was carefully picked up with forceps

and placed on the drop of water on the photomask. This assembly was placed in UVO cleaner for 5 mins in a way that the patterned surface in contact with the coverslip faces down. UV exposure cleaves PEG chains at the site of exposure on the glass coverslip. The coverslip was released gently by infusing 100  $\mu\text{L}$  PBS pH 7 beneath it after which it was washed with PBS by dipping it in PBS 5 times. The coverslip was then placed on a 25  $\mu\text{L}$  Col-Gel solution which was prepared by modifying a reported protocol.<sup>50</sup> All stock solutions were made in PBS pH 7. The gels were prepared by mixing 75% v/v of 600  $\mu\text{g mL}^{-1}$  collagen (gibco, A1048301) and 25% v/v of 600  $\mu\text{g mL}^{-1}$  gelatin (SigmaAldrich, 9000-70-8) solution. The two solutions were mixed by manually stirring with the pipette tip in the Eppendorf tube without pipetting it. The gels were allowed to polymerize at 37 °C, 5% CO<sub>2</sub> for 1 hour followed by 4°C incubation overnight. The coverslips were released from the parafilm surface by infusing 200  $\mu\text{L}$  deionised water and washed by dipping them 10 times in 1X PBS with the help of a tweezer.

Incubation of protein solutions and staining of the patterned surface: Supernatants from overnight induced (light) and uninduced (dark) YCQ and YCx were collected by centrifuging the bacterial culture at 4000 rpm for 20 mins. The supernatants were filter sterilized using 0.4  $\mu\text{m}$  syringe filters (Carl roth, SE2M230104). The coverslips with Col-Gel patterns were then incubated with either filtered supernatants or 10 nM purified solutions of YCQ and YCx by inverting the coverslips on 25  $\mu\text{L}$  drops of the protein solutions. This assembly was incubated for one hour at RT. After the incubation, glass coverslips were released gently from the photomask by infusing 100  $\mu\text{L}$  of PBS between glass surface and the parafilm. The coverslips were picked up with forceps and dipped in PBS 5 times to remove the unbound protein. The patterned glass surfaces with immobilized proteins were then incubated with anti-YebF primary antibody (Athena ES, AES-0313) by placing the patterned coverslip on 25  $\mu\text{L}$  1:500 diluted antibody (in 1% BSA) on parafilm. After incubation at RT for 1 h, the coverslips were released as mentioned before and all the patterned surfaces were then incubated with 1:500 diluted AF-488 Goat anti rabbit secondary antibody (ThermoFischer, A-11008) for 1 h at RT. Patterned surfaces were washed with PBS as mentioned before and were placed on a glass slide by placing 10  $\mu\text{L}$  of PBS on the glass slide and inverting the patterned surface on it. YCQ or YCx stained Col-Gel patterns were visualised using a Nikon Ti-Eclipse microscope (Nikon Instruments Europe B.V., Germany).

Sequence of the His-tag variant

TTTAACTTTAAGAAGGAGATATACATATGAAAAAAGAGGGGCGTTTTTAGGGCTGTTGTTGG  
TTTTCTGCCTGCGCATCAGTTTTTCGCTGCCAATAATGAAACCAGCAAGTCGGTCACTTTCCCAA  
GTGTGAAGATCTGGATGCTGCCGGAATTGCCGCGAGCGTAAAACGTGATTATCAACAAAATCG  
CGTGGCGCGTTGGGCAGATGATCAAAAAATTGTCGGTCAGGCCGATCCCGTGGCTTGGGTCA  
GTTTGCAGGACATTCAGGGTAAAGATGATAAATGGTCAGTACCGCTAGCCGTGCGTGGTAAAA  
GTGCCGATATTCATTACCAGGTCAGCGTGGACTGCAAAGCGGGAATGGCGGAATATCAGCGG  
CGTCTCGAGGACGATGACGATAAGGGTACCACTGGAGGATGGCGCGAACCGAGCTTTATGGT  
GCTGAGCGGGCGGCGGCAGCCACCACCACCACCACCAGGCAGCGATATTGGCAAATATAAAC  
TGCAGTATCTGGAACAGTGGACCCTGAAATAAAGCTT

YebF-CBD-Strep-QK g-block sequence

TTTAACTTTAAGAAGGAGATATACCATGAAAAAAGAGGGGCGTTTTTAGGGCTGTTGTTG  
GTTTCTGCCTGCGCATCAGTTTTTCGCTGCCAATAATGAAACCAGCAAGTCGGTCACTTTCCCA  
AAGTGTGAAGATCTGGATGCTGCCGGAATTGCCGCGAGCGTAAAACGTGATTATCAACAAA  
ATCGCGTGGCGCGTTGGGCAGATGATCAAAAAATTGTCGGTCAGGCCGATCCCGTGGCTTG  
GGTCAGTTTGCAGGACATTCAGGGTAAAGATGATAAATGGTCAGTACCGCTAGCCGTGCGT  
GGTAAAAGTGCCGATATTCATTACCAGGTCAGCGTGGACTGCAAAGCGGGAATGGCGGAA  
TATCAGCGGCGTGGTACCACTGGAGGATGGCGCGAACCGAGCTTTATGGTGCTGAGCGGC  
GGCGGCAGCGGCAGCGGCAGCGGCAGCTGGAGCCACCCGCAATTTGAGAAAGGCAGCGG  
CAGCGGCAGCGGCAGCGATATTGGCAAATATAAACTGCAGTATCTGGAACAGTGGACCCTG  
AAATAAAAGCTTAACAAAGCCCGAAAGGAAG

Gene sequence of YCQ : YebF-CBD-Streptag-QK (linker modified)

GTTTAACTTTAAGAAGGAGATATACCATGAAAAAAGAGGGGCGTTTTTAGGGCTGTTGTT  
GGTTTCTGCCTGCGCATCAGTTTTTCGCTGCCAATAATGAAACCAGCAAGTCGGTCACTTTCC  
AAAGTGTGAAGATCTGGATGCTGCCGGAATTGCCGCGAGCGTAAAACGTGATTATCAACAA  
AATCGCGTGGCGCGTTGGGCAGATGATCAAAAAATTGTCGGTCAGGCCGATCCCGTGGCTT  
GGGTCAGTTTGCAGGACATTCAGGGTAAAGATGATAAATGGTCAGTACCGCTAGCCGTGCG  
TGGTAAAAGTGCCGATATTCATTACCAGGTCAGCGTGGACTGCAAAGCGGGAATGGCGGA  
ATATCAGCGGCGTGGTACCACTGGAGGATGGCGCGAACCGAGCTTTATGGTGCTGAGCGG  
CGGCGGTTTCGGGGTCGGGATCGGGATCATGGAGCCACCCGCAATTTGAGAAAGGCTCGGG

CTCGGGGAGTGGAAGTGATATTGGCAAATATAAACTGCAGTATCTGGAACAGTGGACCCTG  
AAATAAAAGCTTAACAAA

Gene sequence of YCx: YebF-CBD-Streptag-Scrambled QK

AAGGAGATATACCATGAAAAAAAAAGAGGGGCGTTTTTAGGGCTGTTGTTGGTTTCTGCCTGC  
GCATCAGTTTTCGCTGCCAATAATGAAACCAGCAAGTCGGTCACTTCCCAAAGTGTGAAGA  
TCTGGATGCTGCCGGAATTGCCGCGAGCGTAAAACGTGATTATCAACAAAATCGCGTGGCG  
CGTTGGGCAGATGATCAAAAAATTGTCGGTCAGGCCGATCCCGTGGCTTGGGTCAGTTTGC  
AGGACATTCAGGGTAAAGATGATAAATGGTCAGTACCGCTAGCCGTGCGTGGTAAAAGTGC  
CGATATTCATTACCAGGTCAGCGTGGACTGCAAAGCGGGAATGGCGGAATATCAGCGGCGT  
GGTACCACTGGAGGATGGCGCGAACCGAGCTTTATGGTGCTGAGCGGCGGCGGTAGTGGT  
AGTGGTAGTGGTAGTTGGAGCCACCCGCAATTTGAGAAAGGCTCGGGCTCGGGGAGTGGA  
AGTGGCTTACGTCATAAGCGTCCGTCACAAGAGAAATTGGGTTAAAAGCTTAAC

## 2.5. References

- (1) Zhang, G.; Brokx, S.; Weiner, J. H. Extracellular Accumulation of Recombinant Proteins Fused to the Carrier Protein YebF in Escherichia Coli. *Nat Biotechnol* **2006**, *24* (1), 100–104. <https://doi.org/10.1038/nbt1174>.
- (2) Abedi, M. H.; Yao, M. S.; Mittelstein, D. R.; Bar-Zion, A.; Swift, M. B.; Lee-Gosselin, A.; Barturen-Larrea, P.; Buss, M. T.; Shapiro, M. G. Ultrasound-Controllable Engineered Bacteria for Cancer Immunotherapy. *Nat Commun* **2022**, *13* (1), 1585. <https://doi.org/10.1038/s41467-022-29065-2>.
- (3) Fu, S.; Zhang, R.; Gao, Y.; Xiong, J.; Li, Y.; Pu, L.; Xia, A.; Jin, F. Programming the Lifestyles of Engineered Bacteria for Cancer Therapy. *National Science Review* **2023**, *10* (5), nwad031. <https://doi.org/10.1093/nsr/nwad031>.
- (4) Omer, R.; Mohsin, M. Z.; Mohsin, A.; Mushtaq, B. S.; Huang, X.; Guo, M.; Zhuang, Y.; Huang, J. Engineered Bacteria-Based Living Materials for Biotherapeutic Applications. *Front Bioeng Biotechnol* **2022**, *10*, 870675. <https://doi.org/10.3389/fbioe.2022.870675>.
- (5) Piñero-Lambea, C.; Ruano-Gallego, D.; Fernández, L. Á. Engineered Bacteria as Therapeutic Agents. *Current Opinion in Biotechnology* **2015**, *35*, 94–102. <https://doi.org/10.1016/j.copbio.2015.05.004>.
- (6) Puurunen, M. K.; Vockley, J.; Searle, S. L.; Sacharow, S. J.; Phillips, J. A.; Denney, W. S.; Goodlett, B. D.; Wagner, D. A.; Blankstein, L.; Castillo, M. J.; Charbonneau, M. R.; Isabella, V. M.; Sethuraman, V. V.; Riese, R. J.; Kurtz, C. B.; Brennan, A. M. Safety and Pharmacodynamics of an Engineered E. Coli Nissle for the Treatment of Phenylketonuria: A First-in-Human Phase 1/2a Study. *Nat Metab* **2021**, *3* (8), 1125–1132. <https://doi.org/10.1038/s42255-021-00430-7>.
- (7) Piñero-Lambea, C.; Bodelón, G.; Fernández-Periáñez, R.; Cuesta, A. M.; Álvarez-Vallina, L.; Fernández, L. Á. Programming Controlled Adhesion of E. Coli to Target Surfaces, Cells, and Tumors with Synthetic Adhesins. *ACS Synth. Biol.* **2015**, *4* (4), 463–473. <https://doi.org/10.1021/sb500252a>.
- (8) McKay, R.; Hauk, P.; Quan, D.; Bentley, W. E. Development of Cell-Based Sentinels for Nitric Oxide: Ensuring Marker Expression and Unimodality. *ACS Synth. Biol.* **2018**, *7* (7), 1694–1701. <https://doi.org/10.1021/acssynbio.8b00146>.
- (9) Chandran, C.; Tham, H. Y.; Rahim, R. A.; Lim, S. H. E.; Yusoff, K.; Song, A. A.-L. Lactococcus Lactis Secreting Phage Lysins as a Potential Antimicrobial against Multi-Drug Resistant Staphylococcus Aureus. *PeerJ* **2022**, *10*, e12648. <https://doi.org/10.7717/peerj.12648>.

- (10) *Oral delivery of a Lactococcus lactis expressing extracellular TGF $\beta$ R2 alleviates hepatic fibrosis* | SpringerLink. <https://link.springer.com/article/10.1007/s00253-021-11485-7> (accessed 2023-08-03).
- (11) Liang, K.; Liu, Q.; Li, P.; Han, Y.; Bian, X.; Tang, Y.; Kong, Q. Endostatin Gene Therapy Delivered by Attenuated Salmonella Typhimurium in Murine Tumor Models. *Cancer Gene Ther* **2018**, *25* (7), 167–183. <https://doi.org/10.1038/s41417-018-0021-6>.
- (12) Hyun, J.; Jun, S.; Lim, H.; Cho, H.; You, S.-H.; Ha, S.-J.; Min, J.-J.; Bang, D. Engineered Attenuated Salmonella Typhimurium Expressing Neoantigen Has Anticancer Effects. *ACS Synth. Biol.* **2021**, *10* (10), 2478–2487. <https://doi.org/10.1021/acssynbio.1c00097>.
- (13) Pedrolli, D. B.; Ribeiro, N. V.; Squizzato, P. N.; de Jesus, V. N.; Cozetto, D. A.; Team AQA Unesp at iGEM 2017. Engineering Microbial Living Therapeutics: The Synthetic Biology Toolbox. *Trends Biotechnol* **2019**, *37* (1), 100–115. <https://doi.org/10.1016/j.tibtech.2018.09.005>.
- (14) Rodrigo-Navarro, A.; Sankaran, S.; Dalby, M. J.; del Campo, A.; Salmeron-Sanchez, M. Engineered Living Biomaterials. *Nat Rev Mater* **2021**, *6* (12), 1175–1190. <https://doi.org/10.1038/s41578-021-00350-8>.
- (15) *Light-Regulated Pro-Angiogenic Engineered Living Materials - Dhakane - Advanced Functional Materials - Wiley Online Library*. <https://onlinelibrary.wiley.com/doi/full/10.1002/adfm.202212695> (accessed 2023-05-10).
- (16) *Optoregulated Drug Release from an Engineered Living Material: Self-Replenishing Drug Depots for Long-Term, Light-Regulated Delivery - Sankaran - 2019 - Small - Wiley Online Library*. <https://onlinelibrary.wiley.com/doi/abs/10.1002/sml.201804717> (accessed 2023-05-10).
- (17) Gerber, L. C.; Koehler, F. M.; Grass, R. N.; Stark, W. J. Incorporation of Penicillin-Producing Fungi into Living Materials to Provide Chemically Active and Antibiotic-Releasing Surfaces. *Angewandte Chemie* **2012**, *124* (45), 11455–11458. <https://doi.org/10.1002/ange.201204337>.
- (18) Witte, K.; Rodrigo-Navarro, A.; Salmeron-Sanchez, M. Bacteria-Laden Microgels as Autonomous Three-Dimensional Environments for Stem Cell Engineering. *Materials Today Bio* **2019**, *2*, 100011. <https://doi.org/10.1016/j.mtbio.2019.100011>.
- (19) Hay, J. J.; Rodrigo-Navarro, A.; Petaroudi, M.; Bryksin, A. V.; García, A. J.; Barker, T. H.; Dalby, M. J.; Salmeron-Sanchez, M. Bacteria-Based Materials for Stem Cell

- Engineering. *Adv Mater* **2018**, *30* (43), e1804310. <https://doi.org/10.1002/adma.201804310>.
- (20) Hay, J. J.; Rodrigo-Navarro, A.; Hassi, K.; Moulisova, V.; Dalby, M. J.; Salmeron-Sanchez, M. Living Biointerfaces Based on Non-Pathogenic Bacteria Support Stem Cell Differentiation. *Sci Rep* **2016**, *6*, 21809. <https://doi.org/10.1038/srep21809>.
- (21) Mimee, M.; Nadeau, P.; Hayward, A.; Carim, S.; Flanagan, S.; Jerger, L.; Collins, J.; McDonnell, S.; Swartwout, R.; Citorik, R. J.; Bulović, V.; Langer, R.; Traverso, G.; Chandrakasan, A. P.; Lu, T. K. An Ingestible Bacterial-Electronic System to Monitor Gastrointestinal Health. *Science* **2018**, *360* (6391), 915–918. <https://doi.org/10.1126/science.aas9315>.
- (22) Petersen, A. M.; Schjørring, S.; Gerstrøm, S. C.; Krogfelt, K. A. Treatment of Inflammatory Bowel Disease Associated E. Coli with Ciprofloxacin and E. Coli Nissle in the Streptomycin-Treated Mouse Intestine. *PLoS One* **2011**, *6* (8), e22823. <https://doi.org/10.1371/journal.pone.0022823>.
- (23) Kim, S.; Kim, Y.; Lee, S.; Kim, Y.; Jeon, B.; Kim, H.; Park, H. Live Biotherapeutic Lactococcus Lactis GEN3013 Enhances Antitumor Efficacy of Cancer Treatment via Modulation of Cancer Progression and Immune System. *Cancers (Basel)* **2022**, *14* (17), 4083. <https://doi.org/10.3390/cancers14174083>.
- (24) González, L. M.; Mukhitov, N.; Voigt, C. A. Resilient Living Materials Built by Printing Bacterial Spores. *Nat Chem Biol* **2020**, *16* (2), 126–133. <https://doi.org/10.1038/s41589-019-0412-5>.
- (25) *Living Bacteria in Thermoresponsive Gel for Treating Fungal Infections - Lufton - 2018 - Advanced Functional Materials - Wiley Online Library*. <https://onlinelibrary.wiley.com/doi/full/10.1002/adfm.201801581> (accessed 2023-07-27).
- (26) Gilbert, C.; Tang, T.-C.; Ott, W.; Dorr, B. A.; Shaw, W. M.; Sun, G. L.; Lu, T. K.; Ellis, T. Living Materials with Programmable Functionalities Grown from Engineered Microbial Co-Cultures. *Nat Mater* **2021**, *20* (5), 691–700. <https://doi.org/10.1038/s41563-020-00857-5>.
- (27) Yuan, S.-F.; Yi, X.; Johnston, T. G.; Alper, H. S. De Novo Resveratrol Production through Modular Engineering of an Escherichia Coli–Saccharomyces Cerevisiae Co-Culture. *Microbial Cell Factories* **2020**, *19* (1), 143. <https://doi.org/10.1186/s12934-020-01401-5>.
- (28) Mei, L.; He, F.; Zhou, R.-Q.; Wu, C.-D.; Liang, R.; Xie, R.; Ju, X.-J.; Wang, W.; Chu, L.-Y. Novel Intestinal-Targeted Ca-Alginate-Based Carrier for PH-Responsive Protection and Release of Lactic Acid Bacteria. *ACS Appl. Mater. Interfaces* **2014**, *6* (8), 5962–5970. <https://doi.org/10.1021/am501011j>.

- (29) Xiong, L. L.; Garrett, M. A.; Buss, M. T.; Kornfield, J. A.; Shapiro, M. G. Tunable Temperature-Sensitive Transcriptional Activation Based on Lambda Repressor. *ACS Synth Biol* **2022**, *11* (7), 2518–2522. <https://doi.org/10.1021/acssynbio.2c00093>.
- (30) Piraner, D. I.; Abedi, M. H.; Moser, B. A.; Lee-Gosselin, A.; Shapiro, M. G. Tunable Thermal Bioswitches for in Vivo Control of Microbial Therapeutics. *Nat Chem Biol* **2017**, *13* (1), 75–80. <https://doi.org/10.1038/nchembio.2233>.
- (31) Nuss, A. M.; Schuster, F.; Roselius, L.; Klein, J.; Bücker, R.; Herbst, K.; Heroven, A. K.; Pisano, F.; Wittmann, C.; Münch, R.; Müller, J.; Jahn, D.; Dersch, P. A Precise Temperature-Responsive Bistable Switch Controlling Yersinia Virulence. *PLOS Pathogens* **2016**, *12* (12), e1006091. <https://doi.org/10.1371/journal.ppat.1006091>.
- (32) Ohlendorf, R.; Möglich, A. Light-Regulated Gene Expression in Bacteria: Fundamentals, Advances, and Perspectives. *Front Bioeng Biotechnol* **2022**, *10*, 1029403. <https://doi.org/10.3389/fbioe.2022.1029403>.
- (33) Fernandez-Rodriguez, J.; Moser, F.; Song, M.; Voigt, C. A. Engineering RGB Color Vision into Escherichia Coli. *Nat Chem Biol* **2017**, *13* (7), 706–708. <https://doi.org/10.1038/nchembio.2390>.
- (34) Ohlendorf, R.; Vidavski, R. R.; Eldar, A.; Moffat, K.; Möglich, A. From Dusk till Dawn: One-Plasmid Systems for Light-Regulated Gene Expression. *Journal of Molecular Biology* **2012**, *416* (4), 534–542. <https://doi.org/10.1016/j.jmb.2012.01.001>.
- (35) Shokri, A.; Sandén, A. M.; Larsson, G. Cell and Process Design for Targeting of Recombinant Protein into the Culture Medium of Escherichia Coli. *Appl Microbiol Biotechnol* **2003**, *60* (6), 654–664. <https://doi.org/10.1007/s00253-002-1156-8>.
- (36) Secretion of Recombinant Proteins from E. Coli. <https://doi.org/10.1002/elsc.201700200>.
- (37) Blight, M. A.; Chervaux, C.; Holland, I. B. Protein Secretion Pathways in Escherichia Coli. *Current Opinion in Biotechnology* **1994**, *5* (5), 468–474. [https://doi.org/10.1016/0958-1669\(94\)90059-0](https://doi.org/10.1016/0958-1669(94)90059-0).
- (38) Prehna, G.; Zhang, G.; Gong, X.; Duszyk, M.; Okon, M.; McIntosh, L. P.; Weiner, J. H.; Strynadka, N. C. J. A Protein Export Pathway Involving Escherichia Coli Porins. *Structure* **2012**, *20* (7), 1154–1166. <https://doi.org/10.1016/j.str.2012.04.014>.
- (39) Weiner, J.; Zhang, G. Protein Production Method Utilizing YebF. US20060246539A1, November 2, 2006.

- <https://patents.google.com/patent/US20060246539A1/en> (accessed 2023-01-05).
- (40) Burdette, L. A.; Leach, S. A.; Wong, H. T.; Tullman-Ercek, D. Developing Gram-Negative Bacteria for the Secretion of Heterologous Proteins. *Microbial Cell Factories* **2018**, *17* (1), 196. <https://doi.org/10.1186/s12934-018-1041-5>.
- (41) Van Hove, A. H.; Antonienko, E.; Burke, K.; Brown, E.; Benoit, D. S. W. Temporally Tunable, Enzymatically Responsive Delivery of Proangiogenic Peptides from Poly(Ethylene Glycol) Hydrogels. *Adv Healthc Mater* **2015**, *4* (13), 2002–2011. <https://doi.org/10.1002/adhm.201500304>.
- (42) Ohlendorf, R.; Vidavski, R. R.; Eldar, A.; Moffat, K.; Möglich, A. From Dusk till Dawn: One-Plasmid Systems for Light-Regulated Gene Expression. *Journal of Molecular Biology* **2012**, *416* (4), 534–542. <https://doi.org/10.1016/j.jmb.2012.01.001>.
- (43) van Rosmalen, M.; Krom, M.; Merkx, M. Tuning the Flexibility of Glycine-Serine Linkers To Allow Rational Design of Multidomain Proteins. *Biochemistry* **2017**, *56* (50), 6565–6574. <https://doi.org/10.1021/acs.biochem.7b00902>.
- (44) Chen, X.; Zaro, J.; Shen, W.-C. Fusion Protein Linkers: Property, Design and Functionality. *Adv Drug Deliv Rev* **2013**, *65* (10), 1357–1369. <https://doi.org/10.1016/j.addr.2012.09.039>.
- (45) Chen, X.; Zaro, J.; Shen, W.-C. Fusion Protein Linkers: Effects on Production, Bioactivity, and Pharmacokinetics. In *Fusion Protein Technologies for Biopharmaceuticals*; John Wiley & Sons, Ltd, 2013; pp 57–73. <https://doi.org/10.1002/9781118354599.ch4>.
- (46) Bachmann, M. Linker Peptide and Its Use in Fusion Proteins. WO2012017069A1, February 9, 2012. <https://patents.google.com/patent/WO2012017069A1/en> (accessed 2023-05-09).
- (47) *Benefits of Strep-tag® vs His-tag purification*. IBA Lifesciences. <https://www.iba-lifesciences.com/strep-tag-vs-his-tag> (accessed 2023-05-09).
- (48) Lovett, S. T. Encoded Errors: Mutations and Rearrangements Mediated by Misalignment at Repetitive DNA Sequences. *Molecular Microbiology* **2004**, *52* (5), 1243–1253. <https://doi.org/10.1111/j.1365-2958.2004.04076.x>.
- (49) Bzymek, M.; Lovett, S. T. Instability of Repetitive DNA Sequences: The Role of Replication in Multiple Mechanisms. *Proc Natl Acad Sci U S A* **2001**, *98* (15), 8319–8325. <https://doi.org/10.1073/pnas.111008398>.

- (50) Chan, T. R.; Stahl, P. J.; Li, Y.; Yu, S. M. Collagen-Gelatin Mixtures as Wound Model, and Substrates for VEGF-Mimetic Peptide Binding and Endothelial Cell Activation. *Acta Biomater* **2015**, *15*, 164–172. <https://doi.org/10.1016/j.actbio.2015.01.005>.
- (51) Flores-Santos, J. C.; Moguel, I. S.; Monteiro, G.; Pessoa, A.; Vitolo, M. Improvement in Extracellular Secretion of Recombinant L-Asparaginase II by Escherichia Coli BL21 (DE3) Using Glycine and n-Dodecane. *Braz J Microbiol* **2021**, *52* (3), 1247–1255. <https://doi.org/10.1007/s42770-021-00534-y>.
- (52) Kim, S.-K.; Park, Y.-C.; Lee, H. H.; Jeon, S. T.; Min, W.-K.; Seo, J.-H. Simple Amino Acid Tags Improve Both Expression and Secretion of Candida Antarctica Lipase B in Recombinant Escherichia Coli. *Biotechnol Bioeng* **2015**, *112* (2), 346–355. <https://doi.org/10.1002/bit.25361>.
- (53) Santulli, G.; Ciccarelli, M.; Palumbo, G.; Campanile, A.; Galasso, G.; Ziaco, B.; Altobelli, G. G.; Cimini, V.; Piscione, F.; D'Andrea, L. D.; Pedone, C.; Trimarco, B.; Iaccarino, G. In Vivo Properties of the Proangiogenic Peptide QK. *Journal of Translational Medicine* **2009**, *7* (1), 41. <https://doi.org/10.1186/1479-5876-7-41>.
- (54) *Tethering QK peptide to enhance angiogenesis in elastin-like recombinamer (ELR) hydrogels* | SpringerLink. <https://link.springer.com/article/10.1007/s10856-019-6232-z> (accessed 2022-10-26).

**Chapter 3. Secure encapsulation and  
characterization of engineered bacteria in bilayer  
thick-film hydrogel constructs**

### 3.1. Introduction

In ELMs created for biosensing or drug delivery purposes, bacteria are often enclosed in hydrogels. These hydrogels must provide a supportive environment for the microorganisms to grow and carry out their functions, while also preventing them from escaping into the surrounding environment.<sup>1-4</sup>

The growth and metabolic activity of bacteria depends on the composition and physical properties of the hydrogel.<sup>5</sup> Bacteria grow and metabolize at a slower pace in physically crosslinked hydrogels, such as agarose<sup>6,7</sup> and alginate<sup>7</sup> as compared to liquid cultures. If sufficient nutrients are present, the bacteria will eventually grow out of the hydrogel and into the surrounding medium. Bacterial growth in chemically crosslinked hydrogels such as poly (ethylene glycol diacrylate)<sup>8</sup> or poly(acrylamide)<sup>9</sup> is limited to small mechanically confined colonies, regardless of nutrient concentration.

Recent studies have demonstrated that hydrogels composed of Pluronic F127 diacrylate (PluDA) are well-suited for bacterial encapsulation.<sup>10,11</sup> This triblock co-polymer, at a concentration of 30 wt% in water, forms a gel at room temperature through the physical assembly of polymeric micelles (Figure 1A and 1B). The network can be further stabilized through radical polymerization of the acrylate groups. These form covalent crosslinks in the hydrogel matrix, thereby increasing its stiffness and preventing the gel from dissolving in water or the bacteria from uncontrollably modifying the network. This is critical for preventing bacterial escape from the gel while ensuring the viability and functionality of the encapsulated bacteria. Furthermore, it is possible to tune the mechanical properties of these hydrogels and thereby the behavior of the bacteria encapsulated in them by varying the molar ratio of chemically cross-linkable PluDA and non-acrylated Pluronic F127 (Plu). Previous studies have shown that bacterial colony growth and protein production rates could be influenced by varying the PluDA:Plu molar ratio from 0% to 100% (PluDA0 – PluDA100).<sup>5</sup> An equimolar ratio of both polymers (PluDA50) yielded hydrogels in which the highest protein production rate was observed over the short-term (<12 h). However, hydrogels with lower chemical crosslinking degrees suffered from greater swelling and leaching of non-crosslinked polymer. Furthermore, even though the chemically crosslinked networks mechanically restricted bacterial growth, when these bacterial gels were incubated in medium, considerable outgrowth of the bacteria from the gels was seen. This is due to bacteria at the periphery of the hydrogel being able to

grow into colonies that reach the interface with the medium and escape from the gel. These limitations must be overcome to create ELM constructs suitable for drug delivery applications.

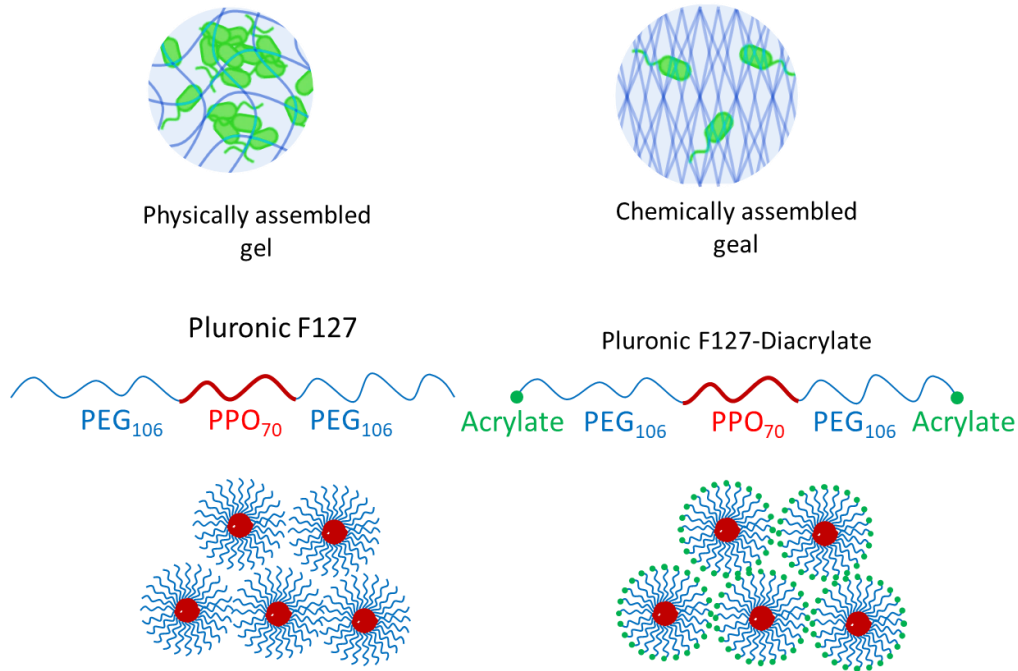


**Figure 1.** A. Bacterial encapsulation in a physically crosslinked gel as opposed to a chemically crosslinked gel. B. Micelles of physically crosslinked Pluronic and chemically crosslinked micelles of Pluronic diacrylate

Many examples of ELMs demonstrate the functionality of bacteria inside the material but do not address the need for containment, thereby limiting their potential use in applicable technological solutions. One simple way to address both the growth and containment requirements of ELMs is by using a bilayer design, such as core-shell particles or compartments. For example, Tang et al. developed beads that encapsulate *E. coli* using  $\text{Ca}^{2+}$  crosslinked alginate as the core material and alginate/poly(acrylamide) double network in the shell. The encapsulated bacteria remained contained for at least 14 days. Similarly, Liu et al. developed poly(acrylamide)-alginate compartments covered by a polydimethylsiloxane (PDMS) elastomer layer to encapsulate genetically modified *E. coli*

in liquid cultures. The resulting living sensor prevented bacterial escape for at least 3 days (Figure 2).

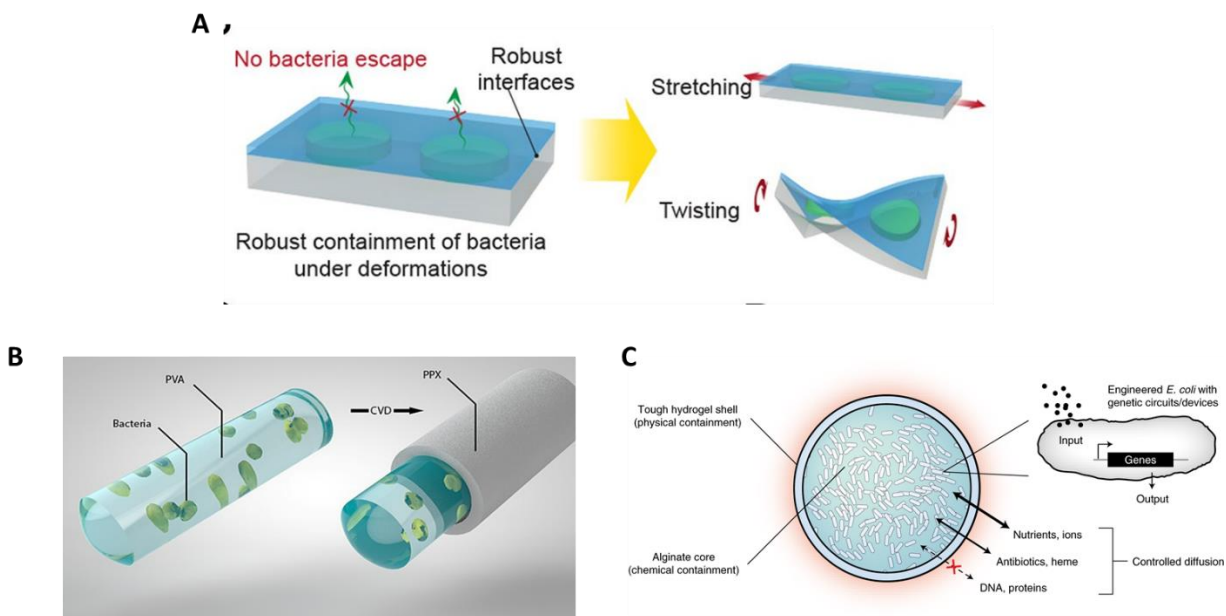


**Figure 2: Bilayer ELMs:** A. This illustration showcases the impressive flexibility and durability of hydrogel-elastomer hybrids, effectively preventing any leakage of cells from the living device, even when subjected to significant deformations. The images demonstrate how the living device can withstand uniaxial stretching of more than 1.8 times its original length and twisting of over 180° while retaining its structural integrity. B. Here, we present the concept of immobilizing whole cell biocatalysts within microfibers composed of a PVA core and a PPX shell. C. The DEPCOS platform ensures secure biocontainment through a core-shell hydrogel design. The sturdy yet semipermeable hydrogel shell acts as a protective barrier, physically containing the contents and shielding them from external influences. Inside the core of the hydrogel made from alginate, vital nutrients required for the growth and sustenance of microorganisms are enclosed, allowing for the containment of chemicals. Modified cells, armed with genetic circuits, react to environmental signals and produce the intended results. Nutrients, biomolecules, and other materials enter or exit the bead in a selective manner based on their molecular size and electric charge.... Image reproduced with permission of the rights holder, SPRINGER NATURE

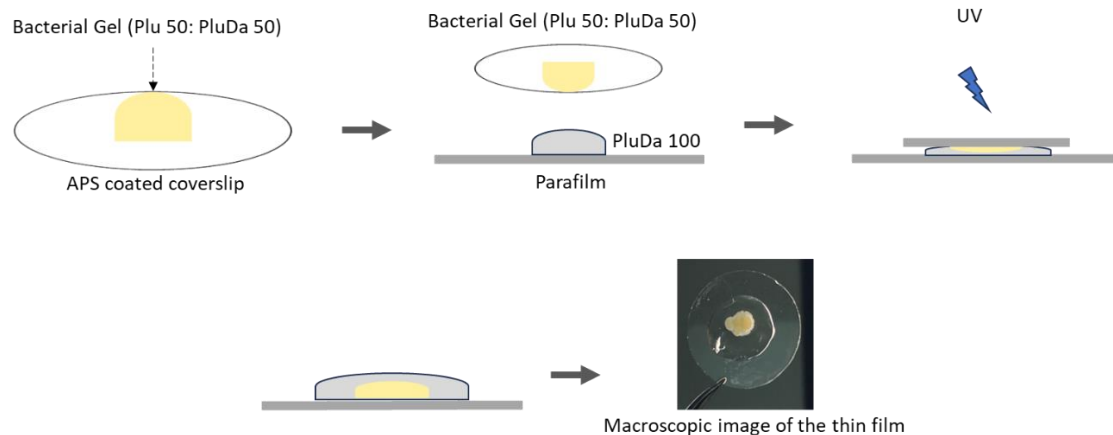
In a different investigation, Connell and colleagues employed photo-crosslinked gelatin shells paired with viscous gelatin cores to form compartments. Within these compartments, microorganisms such as *Staphylococcus aureus* and *Pseudomonas*

*aeruginosa* were cultivated, enabling intricate molecular-level interactions with neighboring compartments. Liu and co-researchers developed tattoos utilizing *E. coli* enclosed within Pluronic hydrogels. These hydrogels were further coated with a second layer composed of Sylgard 184 (Dow Corning) and Silgel 613 (Wacker) elastomers. Their experimentation successfully demonstrated the sustained viability and functionality of the encapsulated bacteria for a duration of up to 8 hours. Knierim and collaborators encapsulated *Micrococcus luteus* and *Nitrobacter winogradskyi* within poly(vinylalcohol) fibers. This encapsulation served the purposes of gold sequestration and nitrite bioremediation, respectively. The encapsulated bacteria were then enveloped with a poly(p-xylylene) shell through a process of chemical vapor deposition. The thickness of this protective shell directly correlated with the reduction in the escape of bacteria. These instances underscore the adaptability and efficacy of bilayer designs for confining bacteria within Electrochemical Microbial Systems (ELMs). In this chapter, we leveraged these design principles and fabricated a bilayer ELM encapsulating YCQ producing bacteria. We securely encapsulated ClearColi in bilayer hydrogel films and demonstrated that they can release YCQ in a light dependent manner for up to 20 days.

### 3.2. Encapsulation of bacteria in thin film scaffolds

Following the ELM design where *E.Coli* was encapsulated in a bilayer thin film format to ensure bacterial survival but prevent their escape to the surroundings,<sup>12</sup> hydrogels were fabricated in a bilayer format, with bacteria encapsulated in a core layer (PluDA50) and surrounded by a protective shell layer (PluDA100). To make the ELMs compatible for microscopy imaging and biochemical assays, they were made in the form of discs bonded to acryloxypropyl silane (3-APS) coated glass cover slips. These constructs were fabricated in a stepwise manner, wherein the bacterial gel was first formed on the glass then coated with the shell hydrogel (Figure 3A, B). Chemical cross-linking of the acrylate groups in the gels was done using a photo-initiator (Irgacure 2959) that could be activated using 365 nm light, which is orthogonal to the blue light required to activate YCQ production in the bacteria. The duration (1 min) and power (6 mW.cm<sup>-2</sup>) of the 365 nm irradiation was selected based on a previous report<sup>5</sup> that identified conditions, which ensured complete cross-linking, while minimally affecting the bacteria.

To make bilayer thin films, the bacterial gel precursor solution was pipetted onto a 13mm coverslip and the shell polymer solution was pipetted onto flattened parafilm, allowing physical gelation to occur at room temperature. After physical gelation the glass coverslip having bacterial gel was flipped onto the parafilm. Then, both layers were photopolymerized in a single 1 min exposure step and the parafilm was removed. The volumes of the inner and outer layers were 2 and 30  $\mu$ L, respectively, and the film's outer diameter was approximately 11 mm, while the inner diameter ranged from 2 to 3 mm. 300  $\mu$ L of media was added on the thin films in order to nourish the bacteria. Bacteria was activated by 160  $\mu$ W/cm<sup>2</sup> blue light irradiation as 1 sec/min pulses. However, YCQ could not be detected in the surrounding medium of the thin films even after 15 days, possibly due to the small volume of the bacterial core compared to the volume of medium required to cover the whole construct. The size of the core could not be reliably increased in this manual fabrication method since it led to leakage of bacteria from the thin films, possibly due to incomplete coverage of the bacterial core by the shell. Thus, alterations to the fabrication method were needed to increase the proportion of the bacterial volume in the bilayer construct.



S

**Figure 3:** The process for fabricating bilayer thin films involves several steps. Initially, a mixture of PluDA50 and bacteria is deposited as a droplet onto an acryl-terminated coverslip, which is then pressed onto a larger droplet of PluDA100 situated on a parafilm surface. Both droplets are dispensed from solutions kept at a low temperature (on ice), and the bilayer is allowed to naturally solidify at room temperature. Subsequently, exposure to UV light activates the formation of covalent bonds between the two layers. The macroscopic image displays the bilayer thin film containing ClearColi engineered to produce YCQ, captured after 15 days of encapsulation..<sup>11</sup>

### 3.3 Methodologies to fabricate bilayer thick films with defined geometries and PluDA compositions

#### 3.3.1. Fabricating the molds for making ELMs

To increase bacterial core size and hence concentration of YCQ secreted in the surrounding medium, thicker bilayer ELM constructs were designed with the help of PDMS molds. In order to make manually fabricated ELMs in a reproducible manner, PDMS molds of varying diameters ranging from 12 mm to 18 mm were fabricated. The volume of PDMS needed for obtaining a desired thickness of the mold was calculated and the mixture was poured into flat-bottomed glass petri dishes of known radii. After baking it for 2 hours at 98 °C, solidified PDMS molds were scraped out from the petri dishes and holes of desired diameter were punched in them using wad punch set (BOEHM, 832 100)

The bilayer hydrogel construct was made on a 3-APS coated 25 mm coverslip. Three different combinations of core and shell diameter were tested. 12 mm core-18mm Shell, 14mm core-18mm shell and 16 mm core and 18 mm shell. These constructs were fabricated by placing PDMS molds on silanized coverslips and pipetting in the

corresponding amount of gel precursor solution in the mold(Figure 4A). The bacterial gel was photopolymerized at 365nm for 1 min, after this the shell solution was added and both the core and shell were allowed to photopolymerize at 365nm for 2mins. The thickness of the core was 0.3 mm and thickness of shell was 0.5 mm for all three constructs. Once the bilayer thick films were fabricated, they were transferred to a 12-well plate.

The composition of Plu and PluDA polymers used in the fabrication of the hydrogel layers played a crucial role in determining the containment capacity of the ELMs. Initial set of experiments were carried out using PluDA50 for the bacterial core gel and PluDA100 for the shell gel, similar to the compositions used in the thin-film constructs. While this might have enabled optimal bacterial performance, the constructs always leaked within 5 days (Figure 4B), possibly due to differential swelling between the core and shell compromising the integrity of the construct. To avoid this, the entire construct was fabricated using only PluDA100 which stopped bacterial leakage (Figure 4C) for a longer period of time (15-20 days).<sup>11</sup>

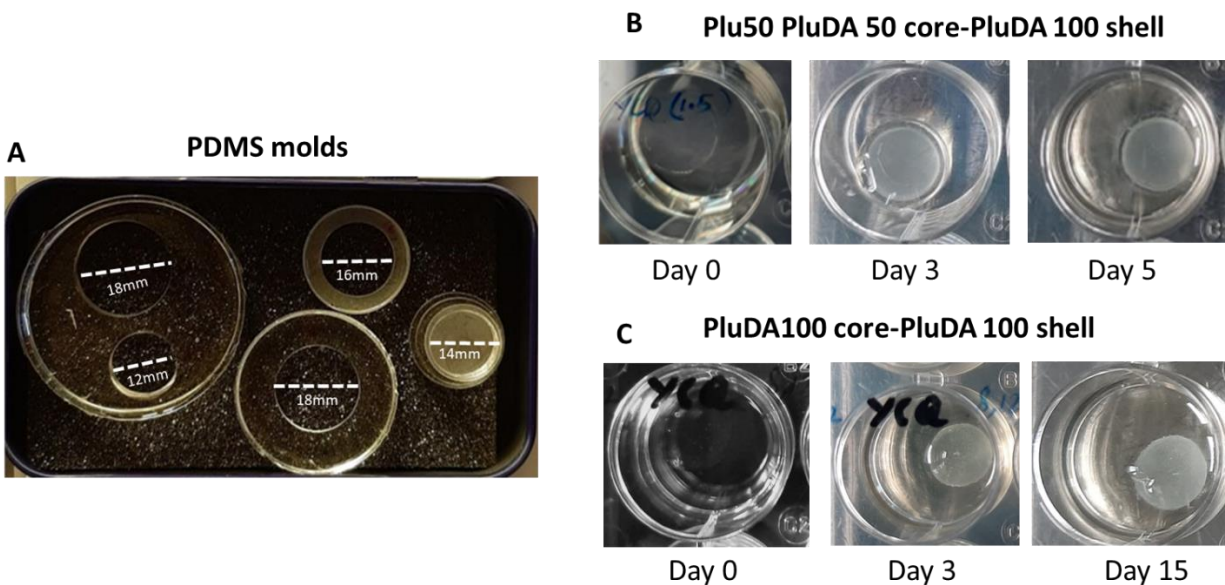


**Figure 4:** ELM Fabrication A. PDMS molds of different diameters used in fabrication of ELMs of varying inner and outer diameter B. ELMs fabricated using Plu50 PluDA50 for the core and PluDA100 for the shell. Bacterial growth in the core is observed from day 0 to day 3; ELMs leaked thereafter and growth leaked bacteria can be seen on day 5 in the media C. ELMs fabricated using PluDA 100 for the core and PluDA100 for the shell.

Disclaimer: Figure 5,6,7,8 and 9 and large parts of the text describing the results of Figure 5,6,7,8 and 9 are taken/adapted from my own published work: Light-Regulated Pro-Angiogenic Engineered Living Materials - Dhakane - Advanced Functional Materials - Wiley Online Library. <https://onlinelibrary.wiley.com/doi/full/10.1002/adfm.202212695> (accessed 2023-07-13). Bacterial growth in the core is observed from day 0 to day 3; ELMs did not leak after 15 days of incubation

The 25mm bilayer thick films were fabricated with 47  $\mu\text{L}$  of PluDA100 for the core and 127  $\mu\text{L}$  for the shell. They were placed in 12 well plates and required 600  $\mu\text{L}$  of media to cover up the whole construct. To minimize material consumption, the bilayer thick film ELMs for the tests were fabricated on a 13 mm coverslip. 23  $\mu\text{L}$  bacterial gel solutions were pipetted into the PDMS molds of radius 3 mm and height of 0.7 mm to make the core layer. 60  $\mu\text{L}$  PluDA was pipetted into a concentric PDMS mold of radius 5 mm and height 1 mm to cover the bacterial core layer (Figure 5A). Crosslinking was done as mentioned before for 25mm constructs. These constructs were then transferred to a 24 well plate and submerged in 300  $\mu\text{L}$  medium. In this format, of 0.1  $\text{OD}_{600\text{nm}}$ , resulted in an initial population of  $\sim 10^6$  bacterial cells ( $8 \times 10^8 \text{ cfu.mL}^{-1}$ ). ELM constructs in this format needed less amount of polymer and did not leak for 15 days (Figure 5B). Hence, all the experiments hereafter were carried out using the 13 mm ELM constructs.

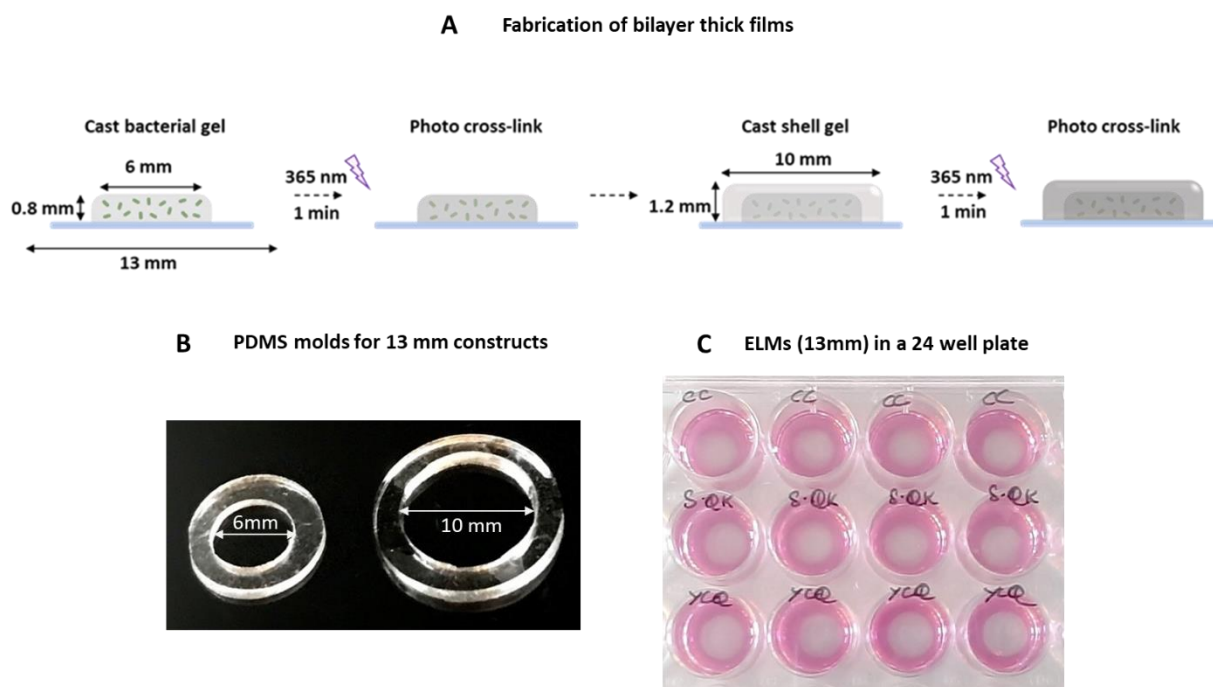


**Figure 5:** A. Graphical representation of manual fabrication of ELM. The scheme depicts the steps involved in the making of the bilayer ELMs, along with relevant dimensions of

the core and shell layers. B. Fabrication A. PDMS molds for ELM fabrication B. ELMs in a 24 well plate suspended in growth supporting media C. ELMs in a 24 well plate suspended in growth supporting media. All the constructs were incubated at 37°C for 15 days. They were continuously illuminated with blue light pulses 2sec/min.

### 3.3.2. Media optimization for ELMs

To test the performance of the ELMs in conditions suitable for mammalian cells, we incubated them in HUVEC-compliant M199 medium. Under these conditions, bacteria were found to not grow, neither in the encapsulated form nor in liquid culture. The concentration of glucose and NaCl in the bacterial growth media (LB Miller) is 1% w/v and 1% w/v respectively. This is higher than the concentration of these two components in M199 media (0.1%w/v glucose and 0.68% w/v). To support bacterial growth, higher glucose and sodium chloride concentrations were added to the medium to reach a final concentration of 0.5 % w/v for glucose and 1.56 % w/v for sodium chloride (Figure 6). This medium composition, named as M199+++ worked the best to support bacterial growth in cell culture media and was used for the following experiments.

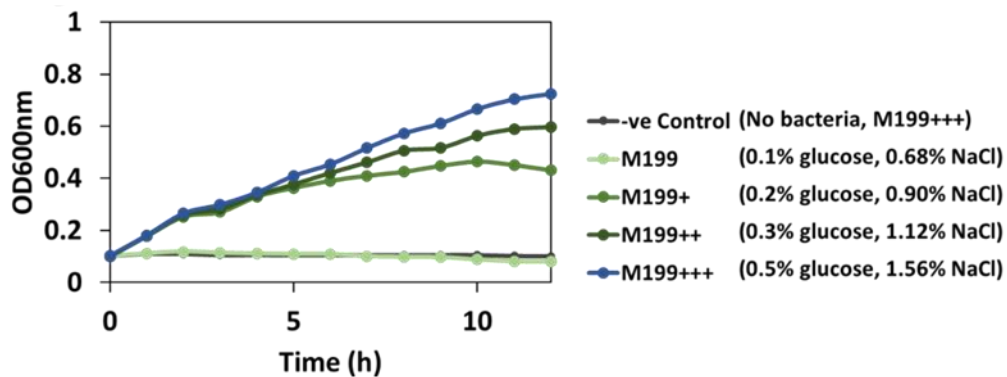


**Figure 6:** Bacterial growth ( $OD_{600nm}$ ) measurement in liquid cultures of HUVEC-compatible media at 37 °C in a microplate reader. All values are means of technical triplicates (standard deviations were negligible). C. ELMs in a 24 well plate suspended in growth supporting media

Incubation of the ELMs in M199+++ medium at 37 °C resulted in the entrapped bacteria growing from single cells to spherical colonies in 24 h (Figure 8), in line with our previous

reports studying bacterial growth in PluDA hydrogel constructs. No leakage or outgrowth of the bacteria into the medium was observed for at least 15 days (Figure 7)

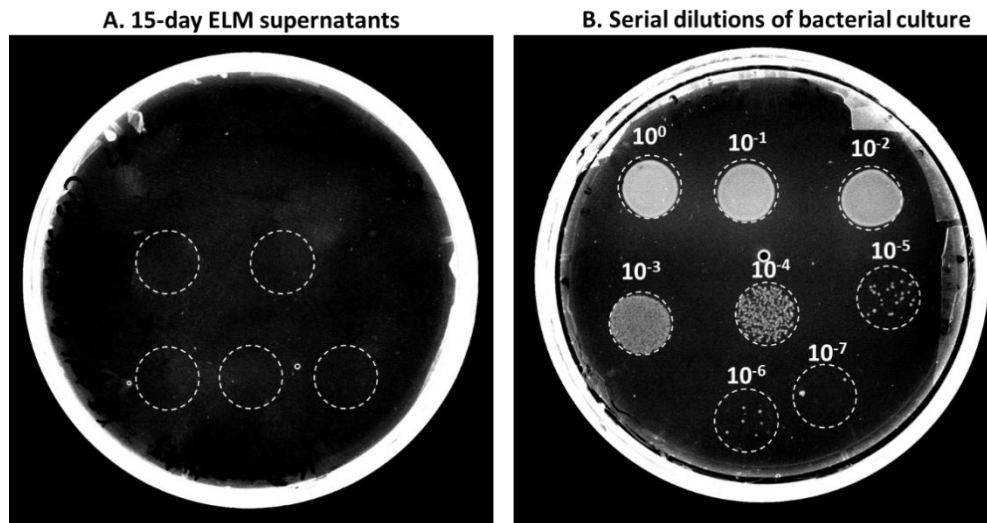


**Figure 7:** Agar plating method to detect potential leakage of bacteria from ELM constructs. A. Supernatants from 15-day old ELM constructs were collected, 20  $\mu\text{L}$  of them were spotted on an LB-NaCl agar plate (white dashed circles) and incubated for 24 h at 37  $^{\circ}\text{C}$ . The absence of colonies indicates that no leakage has occurred. B. Serial dilutions of a bacterial culture were made to test the sensitivity of this assay. The bacterial culture had an initial  $\text{OD}_{600\text{nm}}$  of 1 and labels above the white dashed circles indicate the degree of dilution. Since 1  $\text{OD}_{600\text{nm}}$  corresponds to approximately  $8 \times 10^8$  CFU/mL, the assay is sensitive enough to detect bacterial densities down to 8 CFU/mL.

### 3.4. Characterization of bacterial growth in the hydrogel core

Brightfield microscopic images were taken to characterize bacterial growth in the bilayer thick film constructs (Figure 8). Monitoring the quality of the hydrogels to produce leak-proof hydrogels involved microscopic analysis of hydrogels at regular intervals to check for growth/leakage of bacteria.

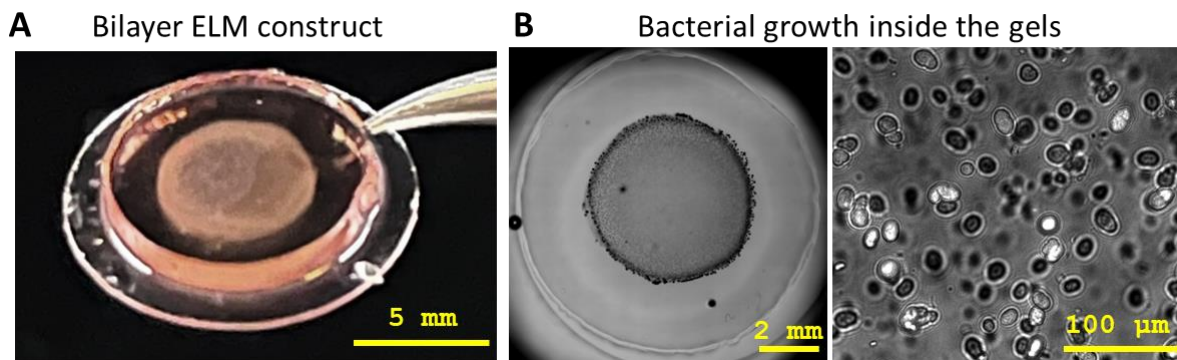


**Figure 8:** A. Macroscopic image of the ELM held by a tweezer. B. Brightfield microscopy stitched image of the ELM with bacteria grown in the core layer (left) along with a magnified image of 6-day grown bacterial colonies.

Since YCQ has a strep-tag, production of YCQ within ELMs was confirmed by staining them on day 6 with Q-dot streptavidin 546 (1:500 dilution) by incubating in the solution for 1 hour at 37 °C followed by washing them with PBS three times for 1 hour each at 37 °C. Fluorescent patches were seen in ClearColi YCQ ELM constructs possibly due to staining of high concentrations of YCQ secreted around the bacterial colonies (Figure 9). In the control ELM containing wild type ClearColi stained using the same protocol, no such fluorescent patches were observed.

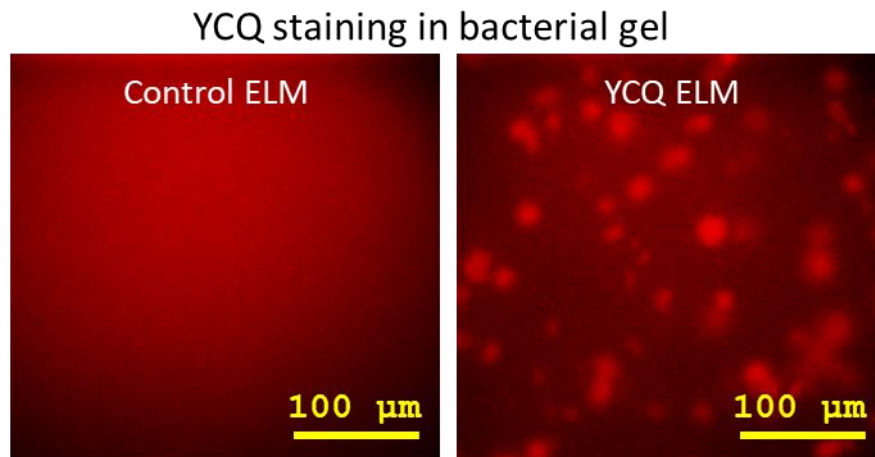


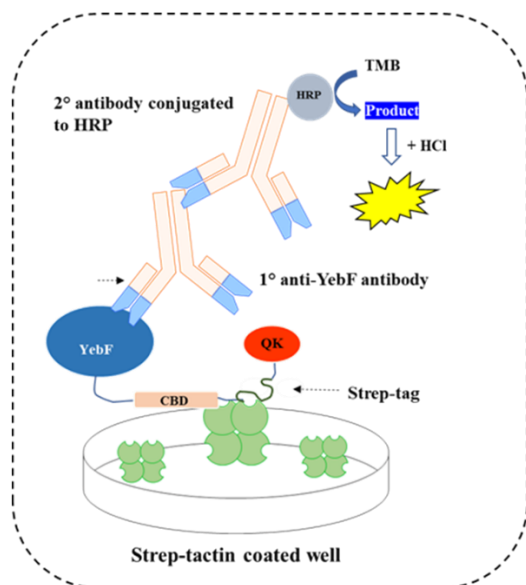
**Figure 9:** Epifluorescence microscopic images of hydrogels stained with Qdot 565 streptavidin on day 6; (a) ClearColi wt encapsulated hydrogel showing no binding of streptavidin; (b) ClearColi-YCQ encapsulated hydrogel red fluorescent spots representing the binding of streptavidin to YCQ molecules present in the bacterial core

### **3.5. Studying light regulated YCQ release and bioactivity from the bacterial hydrogels**

#### **3.5.1. Establishing ELISA-based assay to quantify YCQ release into the medium**

Indirect ELISA was chosen as a method of detection of YCQ secreted from the constructs because of specificity and sensitivity of this detection method. Strep-Tactin coated ELISA plates were used in order to capture YCQ from the media surrounding the ELM constructs. Anti-YebF primary antibody was used that selectively bound to YebF from YCQ and HRP-conjugated secondary antibody was for colorimetric detection. Various concentrations (1:250, 1:500, 1:750, 1:1000) of primary (anti-YebF rabbit antibody) and secondary (HRP-conjugated anti-rabbit) antibodies were tested to determine the optimal concentration that would provide reliable results within the detection limit and with reproducible outcomes. The optimal dilution for both the antibodies was found to be 1:500. To improve the accuracy and specificity of indirect ELISA, an extra blocking step was added to the standard plot optimization process. The Strep-tactin coated plate was first treated with a blocking buffer to mask all available sites of the well plate except for the coated molecules. Then, after addition of YCQ, another blocking step was performed to increase the sensitivity of the assay. A standard plot was made using serial diluted concentrations of purified YCQ (Chapter 2; section 2.4.2.) as the samples (Figure 10). The concentrations used were: 0.306 nM, 0.612 nM, 1.25 nM, 2.5 nM, 5 nM, 10 nM, and 20 nM. Within this range, the response of the assay was linear and a slope for quantifying secreted YCQ concentrations was found by fitting the data with a straight line.

### A. Representation of ELISA for detection of YCQ



### B. Standard curve for YCQ quantification

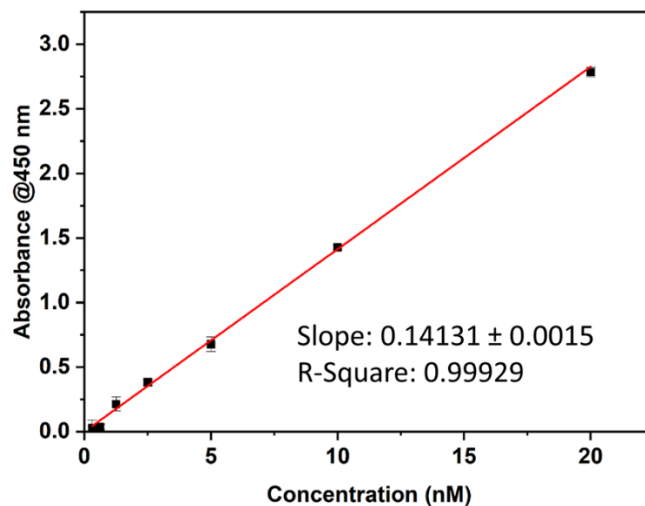


**Figure 10:** ELISA standard plot for YCQ quantification. A. Representation of ELISA for quantification of YCQ. YCQ was immobilized on the surface of strep-tactin coated 96 well plates and stained with rabbit anti-YebF primary antibody followed by AF-488 goat anti rabbit secondary antibody. B. Standard curve generated using purified YCQ

### 3.6. Quantification of light-switchable and light-tunable release of YCQ

#### 3.6.1. YCQ Quantification from hydrogels

The pDawn system in *E. coli* controls protein production in a light responsive manner. However, the relationship between light pulse duration and protein expression may depend on several factors, like strength of the promoter, the stability of the mRNA and protein products, and the metabolic state of the ClearColi cells. To determine the optimal light pulse duration, experiments with different pulse durations and measurements of resulting protein expression levels was done.

To characterize release of YCQ from ELMs in a light-switchable and light-tunable manner, they were induced by irradiating the hydrogels with blue light at 470 nm with 170  $\mu\text{W}/\text{cm}^2$  power. YCQ release was studied for 3 different durations of pulse cycles: 1 second/minute, 2 second/minute and 10 second/minute pulses, over the period of 10 days. ELMs were moved from Light to Dark conditions every two days for 1 second/minute and 2 second/min pulse cycle; for 10 sec/min pulse cycles ELMs were continuously irradiated for 12 days.

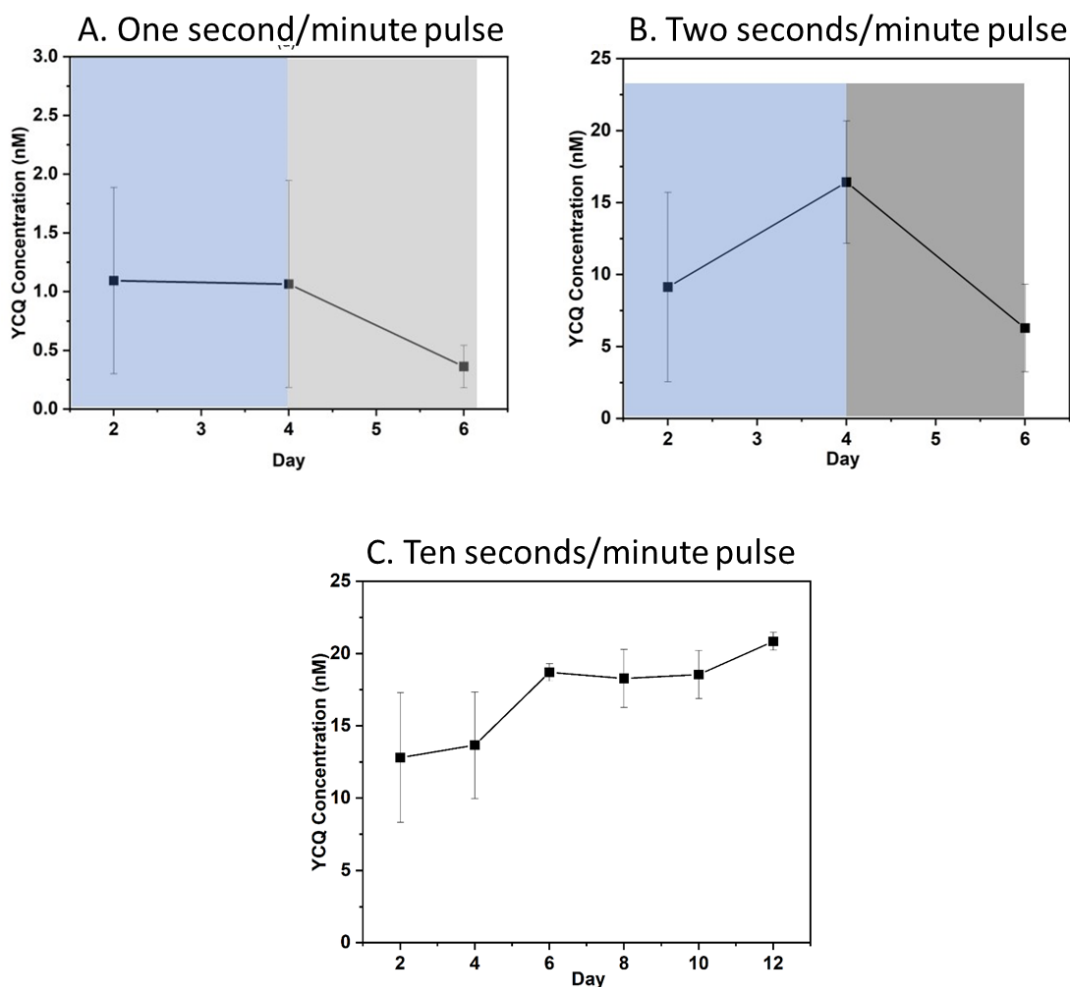


**Figure 11:** Quantification of YCQ release from hydrogels at 1 sec/min pulsed irradiation using ELISA; (A) Hydrogels have been irradiated with light from day 0 to day 4 and in dark from day 4 to day 6 (N=3)(B) Quantification of YCQ release from hydrogels at 2 sec/min pulsed irradiation using ELISA; Hydrogels have been irradiated with light from day 0 to day 4 and in dark from day 4 to day 6 (Blue background in image indicates irradiation and grey background indicates no light condition)(N=3) (C) Quantification of sustained release of YCQ from hydrogels across a span of 12 days at 10 sec/min pulsed irradiation using ELISA(N=3)

From the quantification data of 1 sec/min condition in (Figure 11) low concentrations of YCQ (0.5nM-2nM) was detected at day 2 and day 4. After irradiating them for 4 days ELMs were placed in dark for following 2 days and YCQ production dropped down to less than 0.5nM The duration of dosing/irradiation was doubled to 2 sec/min pulse to study the effect of increased duration on the YCQ production and release from the hydrogels.

Release of YCQ from ELMs increased by 6 – 12-folds when irradiated with 2 sec/min pulses. Release of YCQ on day 2 and 4 was in a similar range: 3nM-21nM In this dosing condition, substantial increase of YCQ release in LIGHT phase and with significant decline in DARK phase is evident.

It was noted from the two previous conditions of 1 sec/min and 2 sec/min that it is possible to tune the YCQ production and. The next aim was to find a higher pulse irradiation point to analyze if saturation point of YCQ production can be detected and to attain sustained release of YCQ at higher concentrations.

In 10 sec/min pulsed dosing experiment, hydrogels were irradiated with blue light on all days except from day 4 – 6 during which they were protected from light exposure but there was no decline in YCQ production unlike the previous dosing conditions. One of the reasons for this anomaly could be the dark state leaky expression and possibility that encapsulated bacteria was induced up to its saturation point during the irradiation in initial four days due to which higher amounts of YCQ was produced by the bacteria which got eventually released when the hydrogels were shifted into the dark state. Also, the protein release levels were comparable to the 2 sec/min condition, suggesting that increased exposure to light did not improve expression levels but could have affected the stability of the optogenetic circuit. The takeaway from 10 sec/min dosing condition was that sustained release of YCQ seemed achievable but such high light dosing was not needed.

The conclusion from the results obtained in different dosing conditions was that YCQ production from the ELM constructs is tunable and switchable.

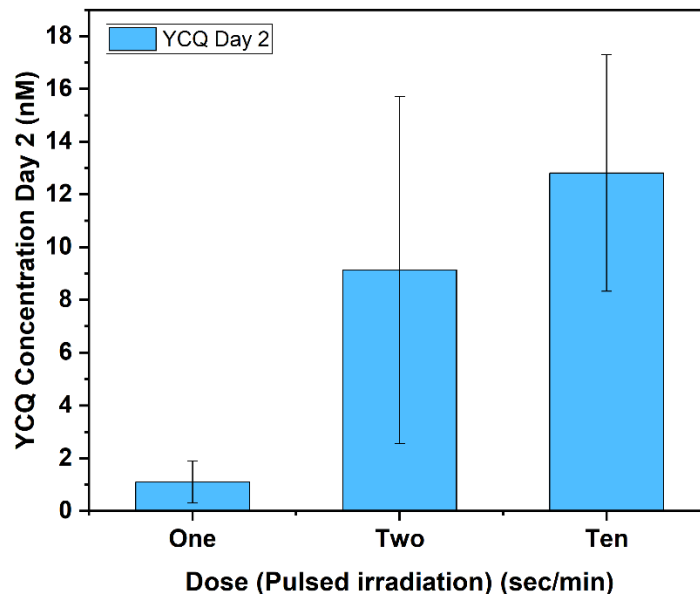


**Figure 12:** Graph illustrating the effect of dosing (pulsed irradiations) on ELMs showing increased YCQ release upon increase in light exposure time

Disclaimer: Figure 13 and large parts of the text describing the results of Figure 13 are taken/adapted from my own published work: Light-Regulated Pro-Angiogenic Engineered Living Materials - Dhakane - Advanced Functional Materials - Wiley Online Library. <https://onlinelibrary.wiley.com/doi/full/10.1002/adfm.202212695> (accessed 2023-07-13).

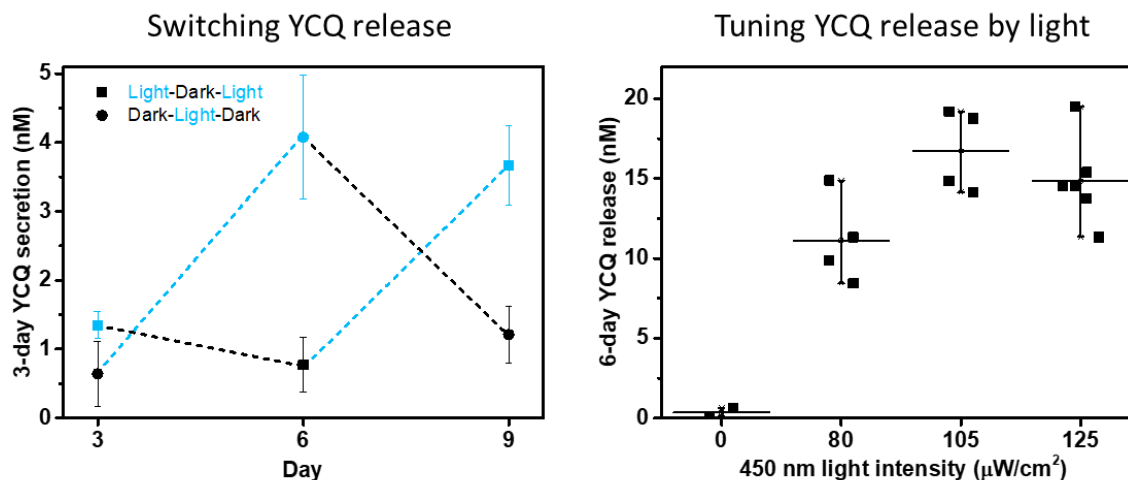


**Figure 13:** Light regulation of YCQ release from ELMs: A. Graphical representation of the ELM setup including blue light irradiation from below. The ELM constructs were placed in 24 well-plate wells containing 300 $\mu\text{L}$  of optimized M199 medium on top of an optowell device for pulsed irradiation at 450 nm (2sec On, 1 min OFF) B. Light switchable control over YCQ release from ELMs. The lines in blue represent durations when samples were placed in light and the lines in black represent durations when samples were placed in the dark. The first blue and black symbols at 3 days were placed in light and dark, respectively till the measurement was made. Symbols represent means values from individual ELM samples and whiskers represent standard deviation C. Tunable release of YCQ by varying intensities of pulsed blue light irradiation from ELMs. Intensities of 0 $\mu\text{W}/\text{cm}^2$ , 80  $\mu\text{W}/\text{cm}^2$ , 105  $\mu\text{W}/\text{cm}^2$  and 125  $\mu\text{W}/\text{cm}^2$  were used. Symbols represent individual ELM samples; horizontal bars represent means and whiskers represent standard deviation.

Next, the capability of switching and tuning YCQ release from the ELMs using light was tested. After preparation, the ELMs were incubated in dark at 28 °C for 16 h, allowing the bacteria to grow into colonies before inducing them with light. Induction of protein expression was maintained by pulsed irradiation with blue light (2 s on, 1 min off, 450nm wavelength, 200  $\mu\text{W}/\text{cm}^2$  power) (Figure 13A). To test the possibility to switch YCQ release ON and OFF, one set of constructs were exposed to blue light for 3 days and another set was left in the dark for the same time at 37 °C (Figure 13B). On day 3, YCQ quantification revealed that the amount released in light (~1.4 nM) was only slightly higher than what was released in the dark (~0.6 nM). The low level of YCQ release in light might be due to bacterial growth continuing to occur in the gel during this period or partial trapping of the protein in the gel. After this, the ELMs that had been exposed to light pulses were placed in the dark and vice versa for another 3 days. At this point, a major

difference in production levels were seen between ELMs exposed to light pulses (~4 nM) compared to those left in the dark (~0.7 nM). Once again, the irradiation conditions were switched for these ELM samples for another 3 days and it was clearly seen that those exposed to light pulses released considerably more YCQ in light (~3.8 nM) compared to those in dark (~1.1 nM). Furthermore, these results clearly demonstrated that the ELMs could be switched from OFF to ON or ON to OFF state using light. Next, to test the possibility of tuning the amount of YCQ release by varying light intensities, ELMs were induced with pulsed blue light (2s on, 1 min off) with intensities of 0  $\mu\text{W}/\text{cm}^2$ , 80  $\mu\text{W}/\text{cm}^2$ , 105  $\mu\text{W}/\text{cm}^2$  or 125  $\mu\text{W}/\text{cm}^2$  for 6 days (Figure 3C). The media surrounding ELMs was collected on day 6 from Control (unmodified bacteria) and YCQ-releasing ELMs and was analysed with ELISA (Materials and Methods). ELMs kept in dark (0  $\mu\text{W}/\text{cm}^2$ ) released <1 nM YCQ, those exposed to 80  $\mu\text{W}/\text{cm}^2$  released 8-15 nM, 105  $\mu\text{W}/\text{cm}^2$  released 14-19 nM and 125  $\mu\text{W}/\text{cm}^2$  released 11-20nM of YCQ (Figure 13C). These results are suggestive of tunable control over protein production in ELMs using varying intensities of light within a range of 1 – 20 nM, although smaller deviations under each condition are desirable.

### 3.7. Conclusion and Discussion

Indirect ELISA was optimized for detection of YCQ. This method is more sensitive and specific as compared to dot blot. Various methods are used for detection of secreted proteins like, SDS-PAGE, Mass spectrometry. However, the concentration of samples needed for such techniques is higher (1-25mM) as compared to what was secreted from the ELMs(1-20nM).<sup>13</sup> Therefore a more sensitive technique like ELISA was needed for detection of secreted YCQ. Detectable amount of YCQ was released from the thick film bilayer constructs when compared with the thin film bilayer constructs where YCQ secretion could not be detected.

In the bilayer thick film format inner layer made up of PluDa was able to support the growth of E. Coli while the outer layer was able to act as shell and it prevented escape of ClearColi for 15 days. YCQ production in the ELMs was confirmed by staining the ELMs with Q-dot streptavidin and YCQ secretion from ELMs was confirmed with ELISA. Bilayer thick films were able to secrete detectable amount of YCQ when compared to bilayer thin format. This is due to the greater number (10X) of bacteria encapsulated in the thick films when compared to thin film ELMs.

With the bilayer thick film ELM's, the possibility of repeatedly turning ON and OFF the release of YCQ for up to 9 days was demonstrated. A variable amount of YCQ was released with different light intensities within the range of 1-20nM in 6 days. It is desirable to improve the rate of protein released from ELM's and the precision. The fabrication of ELMs was done manually, and this can lead to experimental errors despite our efforts to minimize them. Fabrication errors can be minimized using automated methods like 3D printing of ELMs,<sup>14</sup> which will be explored in future studies in the group. As mentioned in the previous chapter low level of protein secretion could be because E. Coli is poor secretor of protein of<sup>15</sup> and PluDa hydrogels have a relatively high polymer content of 30%, which might result in slow protein diffusion.<sup>16</sup> These issues will be addressed in future studies in the group by using lower polymer concentration and by introducing soluble fibers in the polymer.<sup>17</sup>

In spite of all the challenges faced during fabrication of ELMs, a light regulated ELM was fabricated in this study which was able to contain ClearColi for around 15 days and release YCQ in the physiologically relevant range. The YCQ released from ELMs was tested for angiogenesis inducing capabilities and is described in the next chapter.

Disclaimer: Section 3.8 is taken/adapted from my own published work: Light-Regulated Pro-Angiogenic Engineered Living Materials - Dhakane - Advanced Functional Materials - Wiley Online Library. <https://onlinelibrary.wiley.com/doi/full/10.1002/adfm.202212695> (accessed 2023-07-13).

### 3.8. Materials and Methods:

#### 3.8.1. Fabrication of ELMS

1. Silanizing glass coverslips: Glass coverslips (13 mm) were arranged in a Teflon holder with a removable handle (custom made) for washing steps in a beaker. The Teflon holder with coverslips was suspended in a beaker with 99% ethanol and was sonicated for 10 mins. Then, it was washed with ultrapure water followed by 99% ethanol. The Teflon holder handle was removed and the base holding the cover slips was slid into a 50 mL falcon tube containing 20 mL of 95% ethanol, 4% ultrapure water and 1% 3-APS (3-(Trimethoxysilyl)propyl acrylate, Sigma-Aldrich, 4369-14-6) such that coverslips were completely immersed in the solution. After incubation overnight at RT, the coverslips were washed 3 times with deionised water to remove excess APS and transferred into a beaker with ultrapure water and stored in it till further use.

2. Preparation of Polydimethylsiloxane (PDMS) moulds: A beaker in which PDMS moulds were to be made was sonicated for 3 mins with 99 % ethanol in it. 10 g SYLGARD™ 184 silicone elastomer base (Dow chemicals, USA) was added to beaker on a weighing balance and (1 gram) SYLGARD™ 184 silicone elastomer curing agent (cross linker) (Dow chemicals, USA, 1023993) was also added and mixed thoroughly using a spatula. The Beaker with the PDMS-crosslinker mixture was placed in a vacuum-desiccator (DN 150 Duran) for up to 10 mins to remove air from the mixture. The beaker was then removed from the desiccator after confirmation of absence of bubbles in mixture. The volume of the PDMS mixture was calculated to obtain moulds of dimensions depicted in **Figure 2** and Figure S4 and poured into glass petri dishes. These were then placed in a hot air oven at 95 °C for 2 h for polymerization. They were taken out after 2 h and left undisturbed at room temperature overnight. Solidified PDMS moulds were scraped out from glass flasks and holes of desired diameter were punched with wad punch set (BOEHM, 832100).

3. Preparation of Pluronic diacrylate solution: Pluronic diacrylate (PLU-DA) was obtained from the group of Prof. del Campo, who synthesized it as previously reported.<sup>31</sup> 30% w/v Pluronic diacrylate (PLU-DA) + 0.02% w/v IRGACURE 2959 (2-Hydroxy-4'-(2-hydroxyethoxy)-2-methylpropiophenone, Sigma Aldrich, 410896-10G) solution was prepared for construct fabrication. 3 g PLU-DA and 20 mg IRGACURE 2959 photo initiator

were dissolved in ultrapure water in an amber coloured glass bottle and the final volume was adjusted to 10 mL. The PLU-DA solution was kept on a rotary shaker at 4 °C overnight for complete dissolution of contents. PLU-DA was stored in the same amber glass bottle at 4 °C until further use.

4. Fabrication of ELMs: 5 mL bacterial cultures at their exponential phase ( $OD_{600} = 0.5-0.8$ ) were centrifuged at 4000 rpm for 10 mins at room temperature. Pellets were resuspended in M199 cell culture media and was made up to an  $OD_{600}$  of 1 after measuring it in a Nanodrop One device. Bacterial suspensions were prepared by mixing 90% v/v PLU-DA and 10% v/v bacterial culture ( $OD_{600} = 1$ ) such that the final density of bacteria in PLU-DA mixture was 0.1  $OD_{600}$ . Solutions containing PLU-DA were always handled on ice to prevent their physical gelation. 3-APS coated coverslips were placed on disinfected paraffin paper in a petri dish. A cylindrical PDMS mould with 6 mm diameter was placed on the coverslips with conformal contact. 22  $\mu$ L bacterial gel solutions were pipetted into the PDMS moulds to make a core layer of radius 3 mm and height of 0.7 mm. It was left undisturbed for 2 mins at room temperature for the PLU-DA to form a physical gel. The PDMS + coverslip setup was transferred to a Gel-Doc (Biozym Scientific GmbH, FluorChemQ) and the PLU-DA-Bacterial mixture was cross-linked by irradiating it with low intensity UV transillumination (365 nm) for a duration of 60 seconds. The whole setup was transferred back to a sterile hood and left undisturbed for 2 mins after which the PDMS mould was removed from the coverslip. A PDMS mould of 10 mm diameter was then placed on the same coverslip to produce a protective PLU-DA shell to prevent the leakage of bacteria from the ELM. 60  $\mu$ L PLUDA was pipetted onto the PLU-DA bacterial core layer such that it formed a shell layer covering the entire surface of the core with a diameter of 10 mm and height of 1 mm. The PDMS and coverslip setup was transferred to the Gel-Doc and cross-linked by UV transillumination for a duration of 90 seconds. The whole setup was transferred back to the sterile hood and the PDMS mould was removed from the coverslip. This ELM construct was transferred into a well in a 24-well plate and 300  $\mu$ L M199 cell culture media supplemented with additional 0.4% w/v glucose and 0.88% w/v NaCl was pipetted into the well. The 24-well plates with hydrogel constructs was placed in an incubator (28 °C) for 16 hours in dark. For reversible light switching experiments.: one 24-well plate was kept in light (blue light irradiation device; pulse: 2 s ON, 1min OFF; 200  $\mu$ Wcm<sup>-1</sup>) for 3 days and then moved to dark for 3 days followed by a period of light again for 3 days. The other 24 well plate was kept in dark for 3 days and then switched to light (same irradiation parameters as mentioned before) for 3 days followed by a period of dark for 3 days. Surrounding media was collected from each well

after every 3 days and ELMs were replenished with 300  $\mu\text{L}$  fresh media. For light tuning experiments: the 24 well plate containing ELMs was kept on an optoWELL irradiation device (Opto biolabs), which was programmed to irradiate wells with blue light pulses (2 s ON; 1 min OFF, 450 nm) of intensities of 0  $\mu\text{W}\cdot\text{cm}^{-2}$ , 80  $\mu\text{W}\cdot\text{cm}^{-2}$ , 105  $\mu\text{W}\cdot\text{cm}^{-2}$  and 125  $\mu\text{W}\cdot\text{cm}^{-2}$  (corresponding to 3%, 6% and 9% in the device settings) for 6 days. The volume of media surrounding ELM was decreased in 3 days from 300  $\mu\text{L}$  to 250  $\mu\text{L}$  due to evaporation. It was replenished by adding 50  $\mu\text{L}$  fresh media to it. The surrounding media containing secreted protein was collected at day 6 for quantification with ELISA (see point vi)

### 3.8.2. Analysis of ELMs

1. Qdot Streptavidin staining of ELMs: ELMs in 24-well plate wells were washed with PBS thrice. Qdot 655 Streptavidin conjugate (Thermo Fisher scientific, Germany, Q10121MP) was used to stain the hydrogels. The staining solution was prepared in the ratio of 1:500 in 2% w/v BSA. 300  $\mu\text{L}$  staining solution was added to each ELM construct and was incubated at 37  $^{\circ}\text{C}$  for 2 hours. The well plate was completely wrapped with aluminium foil to avoid photobleaching during incubation. The antibody solution was pipetted out from wells and constructs were washed with 300  $\mu\text{L}$  PBS thrice. Then constructs were analysed by Nikon epifluorescence microscope and overlay images of both brightfield as well as the 561 nm red channel were captured.

2. Analysis of ELM supernatant by ELISA: ELISA was performed using Strep-tactin coated 96 well plates (iba-life sciences) with the following protocol:

- i. An initial blocking step was performed with 100  $\mu\text{L}$  of 2% w/v BSA added to the wells and the well-plate left overnight at 4  $^{\circ}\text{C}$  or for 1 h at 37  $^{\circ}\text{C}$ .
- ii. The wells were then washed by pipetting out the blocking solution and washing with 100  $\mu\text{L}$  wash buffer (PBS + 0.1% w/v Tween-20) thrice.
- iii. 100  $\mu\text{L}$  samples were added to the wells and left to incubate for 1 hour at room temperature followed by 3x washing step.
- iv. Another blocking step was performed where 100  $\mu\text{L}$  of 2% w/v BSA was added to wells and left for 1 h at room temperature followed by 3x washing step.
- v. Primary antibody treatment: Rabbit Anti-YebF antibody (Athena enzyme systems, USA) was prepared in the ratio of 1:500 in 2% w/v BSA. 100  $\mu\text{L}$  antibody solution

was added to wells and left at room temperature for 1 hour followed by 3x washing step.

- vi. Secondary antibody treatment: Goat anti-Rabbit IgG conjugated with horseradish peroxidase (Invitrogen) was used as secondary antibody in the ratio of 1:500 in BSA 1% w/v. 100  $\mu$ L secondary antibody solution was added to wells and left at room temperature for 1 hour followed by 4x washing step.
- vii. Substrate treatment: 100  $\mu$ L Tetramethylbenzidine (TMB) (Sigma-Aldrich, Germany) substrate was added to each well and was left undisturbed until stable blue color developed.
- viii. Stopping step: 100  $\mu$ L, 1 M Hydrochloric acid (HCl) was added to wells to stop the reaction and it resulted in yellow coloration of solution which was measured within 30 mins.
- ix. The absorbance of test samples was measured at 450 nm by using *iControl 2000* software of Tecan plate reader and resulting data was analysed.

Using serial dilutions of the purified proteins in the optimized M199 medium, a standard curve was plotted. The slope of this standard curve enabled determination of the molar concentrations of ELM-released YCQ or YCx.

### 3.9. References

- (1) Rodrigo-Navarro, A.; Sankaran, S.; Dalby, M. J.; del Campo, A.; Salmeron-Sanchez, M. Engineered Living Biomaterials. *Nat Rev Mater* **2021**, *6* (12), 1175–1190. <https://doi.org/10.1038/s41578-021-00350-8>.
- (2) Knierim, C.; Enzeroth, M.; Kaiser, P.; Dams, C.; Nette, D.; Seubert, A.; Klingl, A.; Greenblatt, C. L.; Jérôme, V.; Agarwal, S.; Freitag, R.; Greiner, A. Living Composites of Bacteria and Polymers as Biomimetic Films for Metal Sequestration and Bioremediation. *Macromolecular Bioscience* **2015**, *15* (8), 1052–1059. <https://doi.org/10.1002/mabi.201400538>.
- (3) Bhusari, S.; Kim, J.; Polizzi, K.; Sankaran, S.; del Campo, A. Encapsulation of Bacteria in Bilayer Pluronic Thin Film Hydrogels: A Safe Format for Engineered Living Materials. *Biomaterials Advances* **2023**, *145*, 213240. <https://doi.org/10.1016/j.bioadv.2022.213240>.
- (4) Tang, T.-C.; Tham, E.; Liu, X.; Yehl, K.; Rovner, A. J.; Yuk, H.; de la Fuente-Nunez, C.; Isaacs, F. J.; Zhao, X.; Lu, T. K. Hydrogel-Based Biocontainment of Bacteria for Continuous Sensing and Computation. *Nat Chem Biol* **2021**, *17* (6), 724–731. <https://doi.org/10.1038/s41589-021-00779-6>.
- (5) *Regulating Bacterial Behavior within Hydrogels of Tunable Viscoelasticity - Bhusari - 2022 - Advanced Science - Wiley Online Library*. <https://onlinelibrary.wiley.com/doi/full/10.1002/advs.202106026> (accessed 2023-05-05).
- (6) Eun, Y.-J.; Utada, A.; Copeland, M. F.; Takeuchi, S.; Weibel, D. B. Encapsulating Bacteria in Agarose Microparticles Using Microfluidics for High-Throughput Cell Analysis and Isolation. *ACS Chem Biol* **2011**, *6* (3), 260–266. <https://doi.org/10.1021/cb100336p>.
- (7) Jeong, Y.; Irudayaraj, J. Hierarchical Encapsulation of Bacteria in Functional Hydrogel Beads for Inter- and Intra- Species Communication. *Acta Biomater* **2023**, *158*, 203–215. <https://doi.org/10.1016/j.actbio.2023.01.003>.
- (8) Lee, K. G.; Park, T. J.; Soo, S. Y.; Wang, K. W.; Kim, B. I. I.; Park, J. H.; Lee, C.-S.; Kim, D. H.; Lee, S. J. Synthesis and Utilization of E. Coli-Encapsulated PEG-Based Microdroplet Using a Microfluidic Chip for Biological Application. *Biotechnol Bioeng* **2010**, *107* (4), 747–751. <https://doi.org/10.1002/bit.22861>.
- (9) Sankaran, S.; Becker, J.; Wittmann, C.; Del Campo, A. Optoregulated Drug Release from an Engineered Living Material: Self-Replenishing Drug Depots for Long-Term,

- Light-Regulated Delivery. *Small* **2019**, *15* (5), e1804717. <https://doi.org/10.1002/sml.201804717>.
- (10) *Regulating Bacterial Behavior within Hydrogels of Tunable Viscoelasticity* - Bhusari - 2022 - *Advanced Science* - Wiley Online Library. <https://onlinelibrary.wiley.com/doi/full/10.1002/advs.202106026> (accessed 2023-05-10).
- (11) Bhusari, S.; Kim, J.; Polizzi, K.; Sankaran, S.; Del Campo, A. Encapsulation of Bacteria in Bilayer Pluronic Thin Film Hydrogels: A Safe Format for Engineered Living Materials. *Biomater Adv* **2023**, *145*, 213240. <https://doi.org/10.1016/j.bioadv.2022.213240>.
- (12) Bhusari, S.; Kim, J.; Polizzi, K.; Sankaran, S.; del Campo, A. Encapsulation of Bacteria in Bilayer Pluronic Thin Film Hydrogels: A Safe Format for Engineered Living Materials. *Biomaterials Advances* **2023**, *145*, 213240. <https://doi.org/10.1016/j.bioadv.2022.213240>.
- (13) Zheng, J.; Ren, X.; Wei, C.; Yang, J.; Hu, Y.; Liu, L.; Xu, X.; Wang, J.; Jin, Q. Analysis of the Secretome and Identification of Novel Constituents from Culture Filtrate of *Bacillus Calmette-Guérin* Using High-Resolution Mass Spectrometry\*. *Molecular & Cellular Proteomics* **2013**, *12* (8), 2081–2095. <https://doi.org/10.1074/mcp.M113.027318>.
- (14) Johnston, T. G.; Yuan, S.-F.; Wagner, J. M.; Yi, X.; Saha, A.; Smith, P.; Nelson, A.; Alper, H. S. Compartmentalized Microbes and Co-Cultures in Hydrogels for on-Demand Bioproduction and Preservation. *Nat Commun* **2020**, *11* (1), 563. <https://doi.org/10.1038/s41467-020-14371-4>.
- (15) Kleiner-Grote, G. R. M.; Risse, J. M.; Friehs, K. Secretion of Recombinant Proteins from *E. Coli*. *Eng Life Sci* **2018**, *18* (8), 532–550. <https://doi.org/10.1002/elsc.201700200>.
- (16) Cleary, J.; Bromberg, L. E.; Magner, E. Diffusion and Release of Solutes in Pluronic-g-Poly(Acrylic Acid) Hydrogels. *Langmuir* **2003**, *19* (22), 9162–9172. <https://doi.org/10.1021/la034822w>.
- (17) Müller, M.; Becher, J.; Schnabelrauch, M.; Zenobi-Wong, M. Nanostructured Pluronic Hydrogels as Bioinks for 3D Bioprinting. *Biofabrication* **2015**, *7* (3), 035006. <https://doi.org/10.1088/1758-5090/7/3/035006>.

**Chapter 4. 2D network-formation assay  
with HUVECs to study the bioactivity of  
YCQ**

#### 4.1. In vitro models test the angiogenic potential of new molecules.

The study of angiogenesis has grown over the past 40 years in pursuit of solving numerous cardiovascular pathologies. Despite an increasing number of *in vitro* and *in vivo* experimental techniques to study angiogenesis, a 'gold standard' angiogenesis assay does not exist.<sup>1</sup> This is because angiogenesis is a complex process that involves several steps, including the proliferation, migration, and differentiation of endothelial cells and the interaction between these cells and extracellular matrix components.<sup>1-4</sup> Because of the complexity of this process, creating a reliable and reproducible *in vitro* model that can mimic angiogenesis is a challenging first step<sup>1,4</sup> to validate a new pro-angiogenic technology.

The cell source is a critical factor to consider in the design of an *in vitro* angiogenesis model. Human Umbilical Cord Vascular Endothelial Cells (HUVECs) are frequently used in studies related to angiogenesis due to their widespread availability and extensive research history.<sup>5-8</sup> These cells are taken from the umbilical cord, which is a good source of blood vessels, and possess many characteristics of endothelial cells in their natural environment. HUVECs are better suited to imitating the behavior of endothelial cells *in vivo* because of their complexity. HUVECs can form network like structures in a laboratory setting and respond to angiogenic signals in a manner consistent with that of endothelial cells in the body.<sup>9,10</sup>

Although primary human endothelial cells may provide more physiologically relevant results, they are challenging to isolate and maintain in culture.<sup>5,6</sup> HUVECs may have different properties compared to other endothelial cells, which can affect the performance and interpretation of experiments. They may have limited proliferative capacity and a shorter lifespan in culture (reliable passages <8), making it difficult to maintain a continuous supply of cells for long-term or repeated experiments.<sup>11</sup>

There are several assays available to study angiogenesis, such as network formation, migration, and proliferation assays. Endothelial cell network formation assays are commonly used to study how blood vessels are formed and organized.<sup>12-15</sup> In these assays, endothelial cells, which line the inside of blood vessels, are grown either on a 2D surface or in a 3D material. The cells multiply, move, and connect with each other to create networks that resemble real blood vessels. Network formation assays provide a practical and reliable way to assess how potential drugs or therapeutic compounds affect the development of blood vessels. The ability to visualize and measure the

formation of these networks using imaging techniques offers valuable data for gaining insights into the complexities of angiogenesis.

The choice of underlying matrix that supports cell adhesion, spreading and angiogenic differentiation must be carefully considered. Different types of matrices reported for studying angiogenesis through network formation assays are described here:

Matrigel™: Using a basement matrix is a common method in the study of anchorage-dependent differentiation, particularly in *in vitro* assays that investigate the angiogenic functions of endothelial cells. Matrigel™ is a commercially available matrix (since 1984) of natural polymers commonly used to mimic the extracellular matrix (ECM) for studies involving mammalian cells<sup>2</sup> It is derived from the basement membrane of Engelbreth-Holm-Swarm mouse tumors, which is a thin layer of extracellular matrix (ECM) that is made up of collagen type IV, entactin, perlecan, and laminin. Matrigel™ contains a high amount of laminin and mimics the complex extracellular environment found in the basement membrane. Notably, it is one of the *in vitro* model membranes for studying angiogenesis related phenomena.<sup>16</sup> Matrigel™ effectively mimics the natural microenvironment found in living tissues, facilitating cell growth and differentiation through its complex mixture of basement membrane proteins and growth factors. The ease of use and versatility of Matrigel™ allows researchers to effortlessly design cell culture assays tailored to various research needs, such as cell invasion assays and drug screening.<sup>12,13</sup> However, there are some disadvantages when using Matrigel for network formation assays. Its batch variability necessitates cautious validation of each batch, as inconsistent results may occur. Limited control over matrix composition: While Matrigel's complex composition is advantageous for studying angiogenesis, it also limits researcher's control over the specific components of the matrix. This lack of control may hinder the study of certain aspects of angiogenesis, where precise manipulation of the matrix is required.<sup>12,13</sup>

Gelatin Methacrylate: Gelatin methacrylate (GelMA) hydrogels are a type of semi-synthetic hydrogel that have been used in the study of angiogenesis.<sup>17,18</sup> They are composed of a crosslinked network of gelatin functionalized with methacrylate groups and can be easily engineered to have tunable mechanical and biochemical properties. GelMA hydrogels can be modified to mimic the mechanical and biochemical properties of the *in vivo* microenvironment, which can enhance the relevance of the results obtained using these hydrogels.<sup>19</sup> They can support the attachment and proliferation of

various types of cells, including endothelial cells, smooth muscle cells, and fibroblasts.<sup>20</sup> GelMA hydrogels can also be used to deliver growth factors and signaling molecules to cells, allowing study of the effects of these molecules on angiogenesis.<sup>21</sup> Overall, GelMA hydrogels have been shown to be a useful tool for studying angiogenesis *in vitro* and have the potential to be developed towards tissue engineering and regenerative medicine applications. However, using GelMA gels have limited bioactivity for driving angiogenesis, necessitating supplementation with additional factors.<sup>18,21,22</sup>

Collagen-Fibrin Matrices: Collagen-fibrin gels have been used in the study of angiogenesis in the context of mimicking the ECM at a site of wound healing<sup>23,3</sup> While fibrin and type I collagen are key components of the microenvironment that surround cells and tissues, fibrin is involved in blood clotting and promotes angiogenesis during wound healing and tumor growth.<sup>24,3</sup> In contrast, type I collagen, which is a major component of normal skin, has been shown to have limited angiogenic activity on its own<sup>2,25</sup> Combining these two structural proteins enables the fabrication of an *in vitro* model systems suitable for studying angiogenesis related phenomena.

These gels can be customized to different mechanical and biochemical properties that mimic the extracellular matrix (ECM) in healing wounds. These gels are beneficial for this purpose because they closely mimic the native extracellular matrix (ECM), the structural support system for cells in the body, and can be customized to different mechanical and biochemical properties. Collagen-fibrin gels also stimulate cell growth and differentiation and are biocompatible. Fibrin, originates from fibrinogen, which can exhibit variations in composition and properties between individuals and over time within the same individual. These differences in fibrinogen content and characteristics contribute to differences in the gelation kinetics and mechanical properties of fibrin gels from one batch to another. Consequently, such batch-to-batch variability in fibrin gels can result in inconsistent experimental outcomes and pose challenges in replicating research findings.<sup>14,15</sup>

Collagen-Gelatin Gels: Both collagen<sup>26,27</sup> and gelatin<sup>28,29</sup> have been tested independently as well as in combination with each other<sup>30</sup> for their capability to induce angiogenesis in endothelial cells. To be useful as scaffolds for cells, collagen-gelatin films must be stable enough to support cell attachment and growth. A model hydrogel system that mimics wounds and is suitable for studying angiogenesis is the collagen-gelatin (Col-Gel) hydrogel system.<sup>3,16,23,25,30</sup> This model is based on the fact that the ECM in wounds is

highly disrupted and contains both intact and disrupted collagen networks. The gelatin in this combination mimics the disrupted collagen network. Furthermore, it has been shown that VEGF-mimetic peptides can be anchored to the hydrogel through collagen binding domains and promote angiogenic responses in endothelial cells (Figure 1).<sup>30</sup>

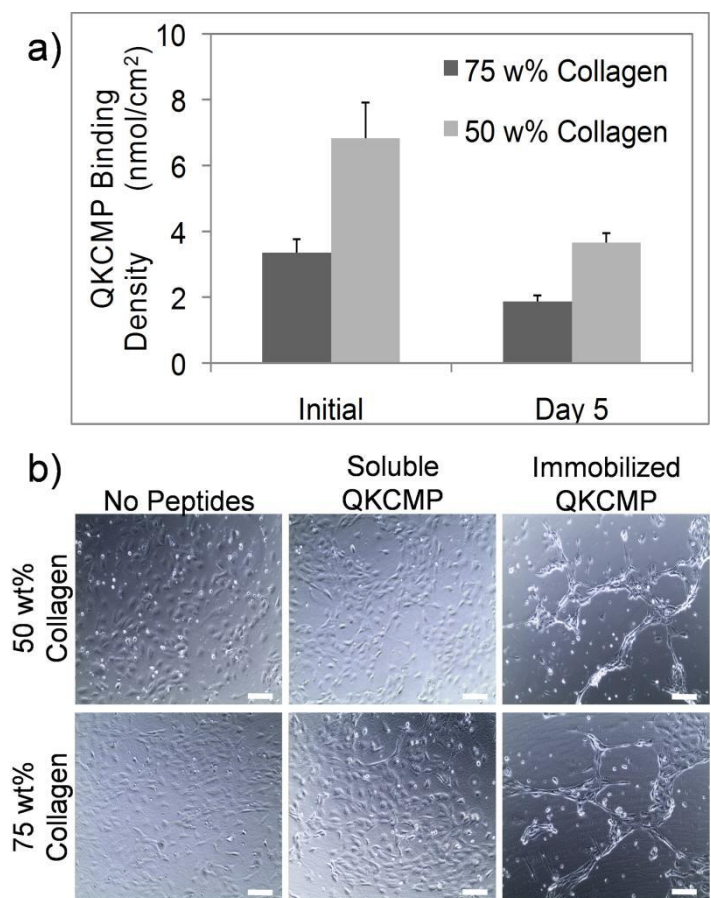


**Figure 1:** a) Assessment QKCMP attachment to Col-Gel films. The evaluation encompassed Col-Gel combination films with collagen contents of 75% or 50% by weight. The error bars indicate the standard deviation ( $\pm$ SD).

b) Observation of HUVEC cell morphology one day after seeding on Col-Gel films under different conditions: without QKCMP, with soluble QKCMP, and with QKCMP immobilized. The scale bars represent a length of 100 micrometers. Image reproduced with permission of the rights holder, Elsevier

Gathering the knowledge about different types of matrices used for network formation assays provided an insight about which matrices might be the candidates for screening the most suitable matrix for testing the activity of YCQ. This chapter describes the

screening of matrices, for testing YCQ, optimization of protein presentation strategy and the staining protocol for developing a robust and reliable network formation assay.

## 4.2. Screening of matrices for the angiogenesis assay

### 4.2.1. Matrigel™

The cell lysates of unmodified *ClearColi* and YCQ-producing *ClearColi* were used in these experiments because optimization of cell experiments was done parallel to optimization of YCQ protein secretion from *ClearColi*. At this point YCQ production from *ClearColi* was optimized but the secretion was still not optimized. The Matrigel solution (10  $\mu$ L) was deposited in the bottom chamber of an Ibidi angiogenesis well plate and after 30 mins of incubation at 37 °C and 5% CO<sub>2</sub>, it formed a solid gel. Bacterial lysates or VEGF solutions (10 ng/mL) were added to Matrigel before polymerization. To test whether such immobilization was needed, comparative samples were prepared where the bacterial lysates (10  $\mu$ L) or VEGF (10ng/mL) were included directly in the cell culture medium and not allowed to first be immobilized to the matrix. When HUVECs stained with green fluorescence Cell Tracker™ dye were seeded on these matrices, they underwent morphology changes leading to network formation within one to two hours in all cases, including the control matrices, which were not exposed to additional proteins or lysates (Figure 2). While network formation was expected in the presence of VEGF and YCQ-containing bacterial lysates, monolayer cell sheets were expected in the presence of the lysate of unmodified *ClearColi* and on the control matrices. This indicated that on our Matrigel matrices, network formation occurred naturally and was not hindered by molecular components present in the *ClearColi* lysate. Because of this, it was concluded that network formation did not occur specifically in response to YCQ or VEGF on the matrices where these proteins were present.

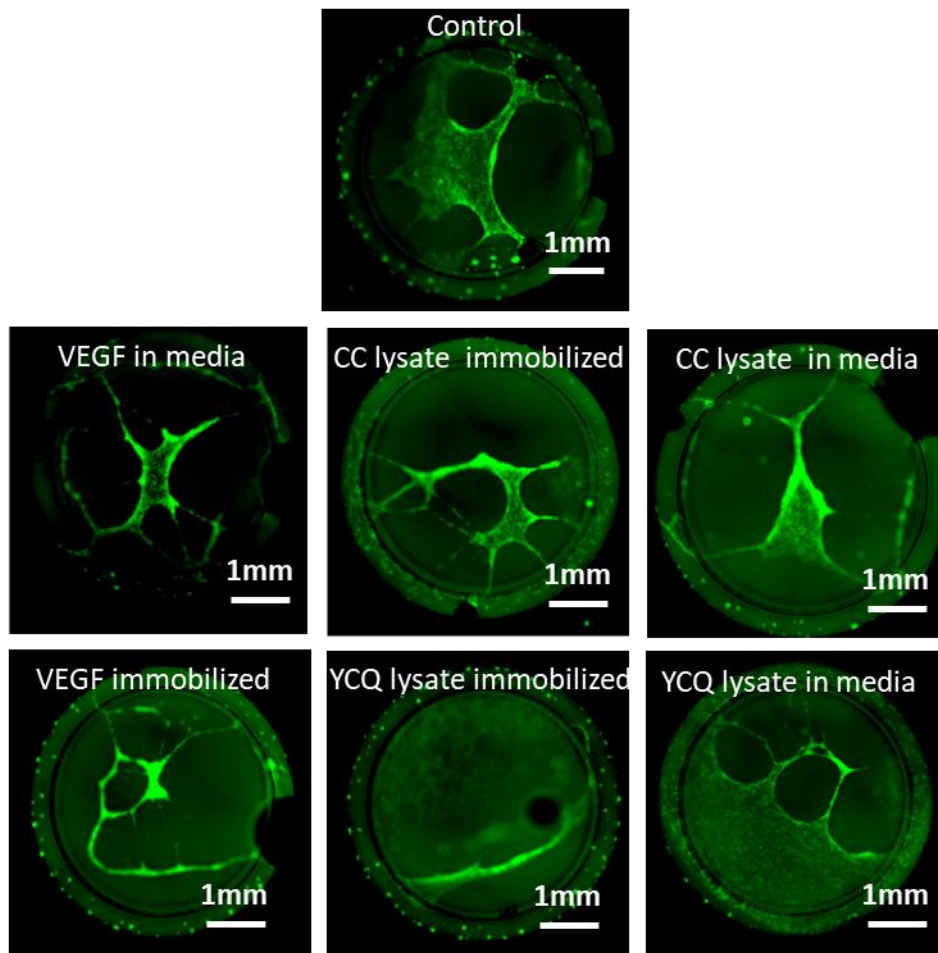


**Figure 2:** Epifluorescence images of HUVECs after 3 hours of incubation on the Matrigel. Substrates were functionalized with Pure VEGF (10ng/ml), cell lysate of unmodified ClearColi, cell lysate of Clear YCQ producing ClearColi. The activity of same samples was also tested when solubilized in media. The media used for these experiments was supplemented with ECGS. HUVECs were stained with Green fluorescent CellTracker™ dye before the assay

#### 4.2.2. Gelatin Methacrylate hydrogels

GelMA was chemically synthesized in the lab by Dr. Jun Feng chemically modifying gelatin with methacrylic anhydride, which introduces methacrylate groups onto the gelatin molecule. The modified gelatin can then be crosslinked to form a hydrogel using photopolymerization.<sup>21,31</sup> The functionality of GelMA obtained after this process was 70% (determined by MS, data not shown). To make the hydrogel precursor solution, GelMA was dissolved in HUVEC media at a concentration of 5% w/v at 4°C. The solution

was then cast in the bottom chamber of an Ibidi angiogenesis well plate and maintained at 37°C in a viscous gel state. Chemical cross-linking of the methacrylate groups was driven by UV light (365nm wavelength) in the presence of a photo initiator (Irgacure 2959) for 1 min, after which a stable gel was obtained, visually determined by indenting it with a pipette tip.

To investigate angiogenesis, VEGF, bFGF and fibronectin were encapsulated as positive controls in the GelMA hydrogels by mixing it in the monomer solution before crosslinking of substrates. The growth factors, VEGF and bFGF, stimulate proliferation and migration of endothelial cells, leading to the formation of endothelial cell networks when added to the matrix.<sup>32,33</sup> Fibronectin can bind to integrin receptors on the surface of endothelial cells, activating signaling pathways that promote cell adhesion, migration, and proliferation. The growth factors were added to the matrix to mimic the conditions necessary for angiogenesis to occur in vivo.<sup>34,35</sup> HUVEC cells were seeded on these gels at a high density ( $2 \times 10^5$  cells/mL) and observed for 18 h. However, during this period, it was observed that the cells did not spread on the GelMA surfaces irrespective of the presence or absence of additional growth factors or fibronectin (Figure 3). While GelMA hydrogels have been used for angiogenesis studies, even with HUVECs, these studies were largely in a 3D setting with the cells encapsulated within the gels. It is unclear whether the GelMA surfaces lack the necessary mechanical properties or molecular recognition sites, or microstructure needed for HUVEC cells to spread on them in 2D. Since the cells were unable to adhere and spread on these surfaces under multiple different conditions, further experimentation was not pursued with them.

## Gelatin Methacrylate Gels

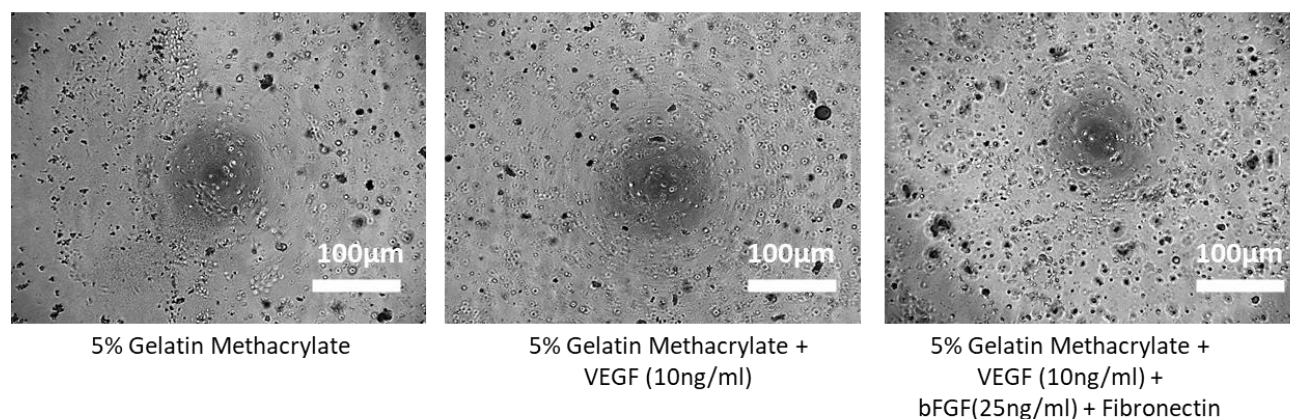


**Figure 3:** Brightfield images of HUVECs after 12 hours incubation on Gelatin Methacrylate hydrogels. VEGF, bFGF and Fibronectin (10 ng/ml of each) were encapsulated in GelMA gels

### 4.2.3 Collagen-fibrin Gels

Based on previous reports, collagen-fibrin gels were made by mixing 70% collagen and 30% fibrin (Vol/Vol).<sup>23,36</sup> The concentration of Collagen and Fibrin used was 2 mg/ml to mimic the proportion of these proteins in the ECM.<sup>14</sup>

The Collagen-fibrin gels were functionalized with VEGF, bFGF and fibronectin by encapsulating them and incubating for 1 hour at 37°C, and HUVECs were seeded on them. All the substrates including control substrates induced network formation. This might be due to the fact that fibrin is a natural component in blood clotting and tissue repair with the potentially innate capacity to induce network formation in endothelial cells.<sup>36</sup> Thus, the intrinsic angiogenic potential of fibrin makes it difficult to distinguish between the effect of an experimental substance from the effect of fibrin gel itself. Because of this, further experimentation was not continued with these collagen-fibrin gels.<sup>36</sup>

## Collagen Fibrin Gels

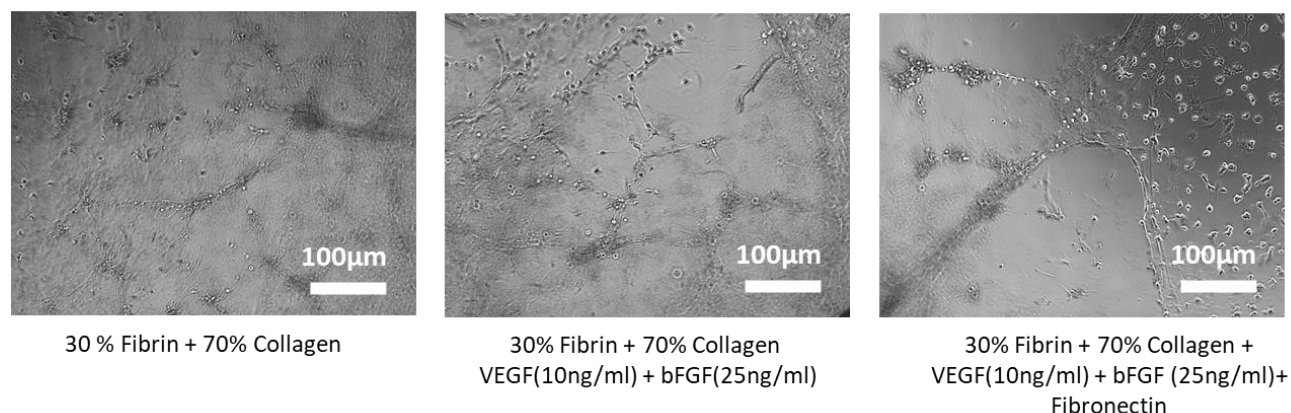


**Figure 4:** Brightfield images of HUVECs after 18 hours of seeding them on the collagen fibrin substrates. Substrates were functionalized with VEGF (10ng/ml) and bFGF (25ng/ml) by encapsulating them. VEGF and bFGF were added to the substrates before polymerization.

### 4.2.4. Collagen-Gelatin gels for angiogenesis

An existing protocol was modified to make a suitable collagen-gelatin matrix.<sup>30</sup> Col-Gel gels made using 75% collagen (600ug/ml) and 25% Gelatin (600µg/ml)<sup>30</sup> were unstable and could not support cell attachment and growth (Figure 5). These gels started degrading/dissolving soon after HUVECs were seeded. While collagen forms fibers and can form gels with sufficient stability over time<sup>37</sup>, gelatin does not form fibers, resulting in poor thermal stability.<sup>38</sup> Previous reports suggest that the stability of these gels can be increased by increasing the collagen concentration.<sup>39</sup> Thus, to improve the mechanical stability of the gels, the concentrations of collagen and gelatin solutions were increased to 2 mg/ml. Next, collagen-gelatin gels were chosen to test YCQ for its ability to induce network formation in endothelial cells. Both collagen<sup>26,27</sup> and gelatin<sup>28,29</sup> have been tested independently as well as in combination with each other<sup>30</sup> for their capability to induce angiogenesis in endothelial cells. In order to be useful as scaffolds for cells, collagen-gelatin films must be stable enough to support cell attachment and growth. The gels started degrading soon after HUVECs were added to the substrates.

### Collagen Gelatin Gels

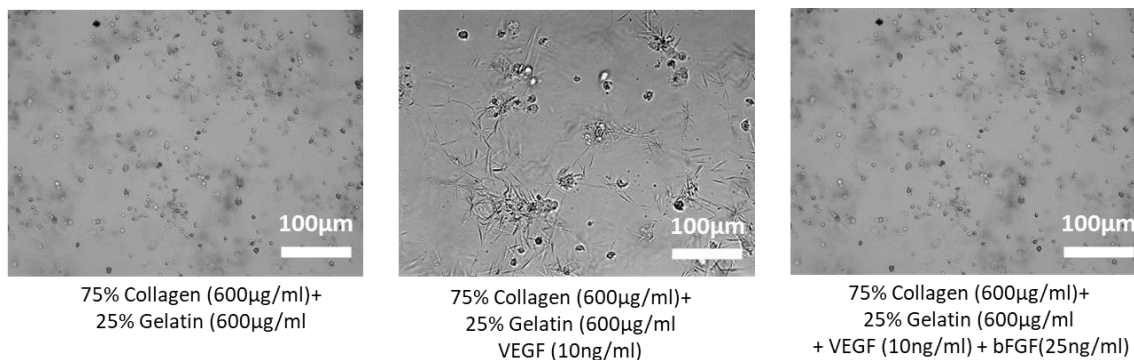


**Figure 5:** Use of 600 µg/ml Col-Gel gels to test the right conditions for network formation. Control wells contain only Col-Gel whereas the test wells have 10ng of VEGF and 25ng bFGF. The BF images were taken 12 hours after incubation of HUVECs on Collagen-fibrin gels.

These 2mg/ml Col-Gel gels were found to have sufficient stability to support endothelial cell attachment (Figure 6). As is suggestive from a previous report,<sup>30</sup> this is possibly due to the formation of stable collagen fibers, which create a mesh-like structure to which gelatin can physically adhere, making it difficult for them to separate and dissolve into solution.<sup>30</sup> Col-Gel gels made using 75% collagen (2mg/ml) and 25% Gelatin (2mg/ml) While collagen forms fibers and has good mechanical properties<sup>37</sup>, gelatin does not form fibers and has low mechanical strength and thermal stability.<sup>38</sup> The stability of these films can be increased by increasing the collagen concentration. When the collagen content was 75% collagen concentration was increased to 2mg/ml, the films were stable enough to support endothelial cell attachment (Figure 6). This is likely due to the formation of stable collagen fibers, which create a mesh-like structure that prevents the dissolution of the loose gelatin chains. The collagen fibers may also physically cross-link the gelatin strands, making it difficult for them to separate and dissolve into solution.<sup>30</sup>

## Collagen Gelatin Gels

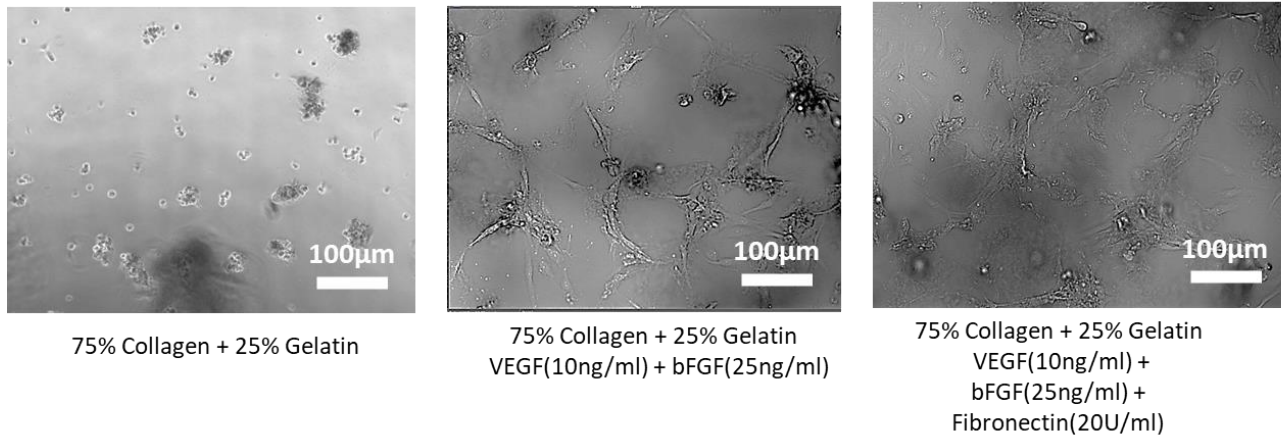


**Figure 6:** Use of 2 mg/mL Col-Gel gels to test for right conditions for network formation. Control wells contain only Col-Gel whereas the test wells have 10ng of VEGF, 25ng bFGF and Fibronectin (25U/ml). The BF images were taken 12 hours after incubation of HUVECs on Collagen-fibrin gels.

As seen in Figure 6, HUVECs exhibited contrasting response on the control gels as compared to the gels in which VEGF and bFGF (10ng/ml of both) were encapsulated by adding it to the monomer solution before polymerization at 37 °C for 1h followed by overnight incubation at 4°C. On the control gels, HUVECs could not spread and receded into scattered morphology. On the gels which had encapsulated VEGF + bFGF, HUVECs underwent network formation morphology in 16 h after seeding. Similar effects were observed for the gels which had encapsulated VEGF, bFGF and Fibronectin. Addition of VEGF and bFGF to the Col-Gel gels supported their survival and induced network formation. Addition of Fibronectin to this did not seem to have any further impact on HUVEC morphology. At this stage, the Col-Gel gels were supporting network formation but HUVECs still died in the absence of the growth factors. Based on previous studies,<sup>30</sup>we speculated that cell survival in the absence of growth factors could be improved by optimizing the gel formation method.

Previous studies have shown that collagen gels are more stable when they are polymerized at a cold temperature of 4°C.<sup>37,40</sup>This is suggested to be because collagen molecules form more stable triple helices at lower temperatures, resulting in a more compact and homogenous gel structure with better mechanical properties. The slow polymerization rate at low temperatures allows collagen molecules to assemble more uniformly, further contributing to the stability and mechanical strength of the gel.<sup>35,47</sup>

Once the initial gel formation has occurred, the collagen structure can be further stabilized by keeping it at a lower temperature, such as 4°C.<sup>41</sup> At this temperature, and cross-linking of the collagen fibers slows down, allowing the collagen to become even more stable and create a stronger network.<sup>37,41</sup>

While encapsulation of growth factors has shown success in promoting angiogenesis in some cases<sup>33,42,43</sup>, it failed to produce consistent promising results in our experiments, .it limits the amount of growth factor that can be released over time.<sup>44-46</sup> It was necessary to explore different strategies of growth factor presentation to promote network formation in a consistent manner. Since surface immobilization can overcome limitations posed by encapsulation of VEGF such as poor interaction with the cell specific receptor and poor release profile, it was tested as the next strategy for using the Col-Gel as a model to assess the angiogenic potential of YCQ.

Disclaimer: Figure 7 and large parts of the text describing the results of Figure 7 are taken from my own published work: *Light-Regulated Pro-Angiogenic Engineered Living Materials - Dhakane - Advanced Functional Materials - Wiley Online Library*. <https://onlinelibrary.wiley.com/doi/full/10.1002/adfm.202212695> (accessed 2023-07-13).

### 4.3. Surface Immobilization of YCQ

Surface immobilization of growth factors can increase the bioactivity of growth factors by enabling them to interact more effectively with specific receptors on cell surfaces.<sup>44–48</sup> It is a versatile and straightforward approach that can be applied to different surfaces, including scaffolds and implants. These benefits make surface immobilization a promising option for delivering growth factors.

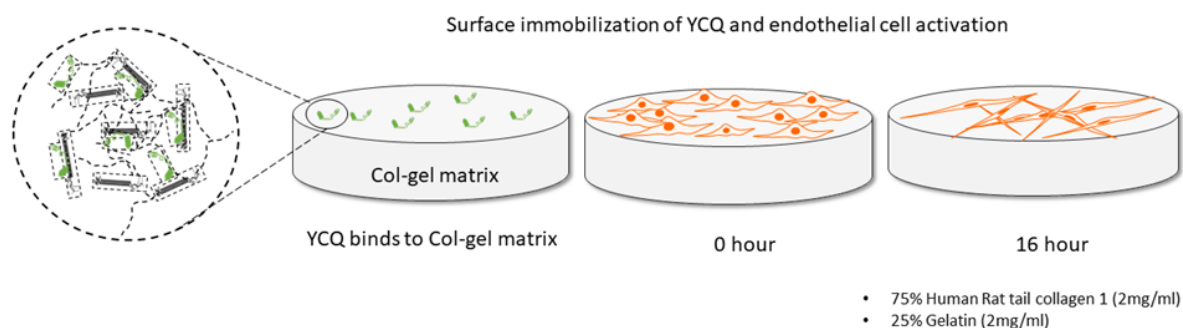


**Figure 7:** Col-Gel wound healing model for promotion of angiogenesis in HUVECs. YCQ is immobilized on the surface of col-gel gels. HUVECs undergo morphological change and form cell networks within 16 hours of seeding them on the col-gel YCQ gels

We tested the activity of pure YCQ by immobilizing it on the surface of Col-Gel matrix. For this, first, 2 mg/mL Col-Gel gels were prepared by allowing them to polymerize at 37 °C for one hour followed by 4°C overnight incubation. Then VEGF and YCQ solutions were incubated on the surface of the Col-Gel gels for 1 hour at 37 °C, after which they were removed, and the gels were washed with PBS. Following this, HUVECs were seeded on the surface of the gels and their network formation was assessed. The control gel, on which no proteins were incubated, did not induce network formation in HUVECs within 3 hours of seeding. It was observed that on gels where YCQ was surface-immobilized, network formation occurred within 3 hours while on gels where YCQ was encapsulated, network formation took 12 hours to occur. Furthermore, the networks had better definition in the surface-immobilized samples compared to the encapsulated

samples. Notably, surface-immobilized VEGF (10ng/ml) failed to induce network formation, possibly since VEGF binds to the ECM via a Heparin-Binding Domain<sup>45,49</sup> and the Col-Gel gels do not contain Heparin in it.

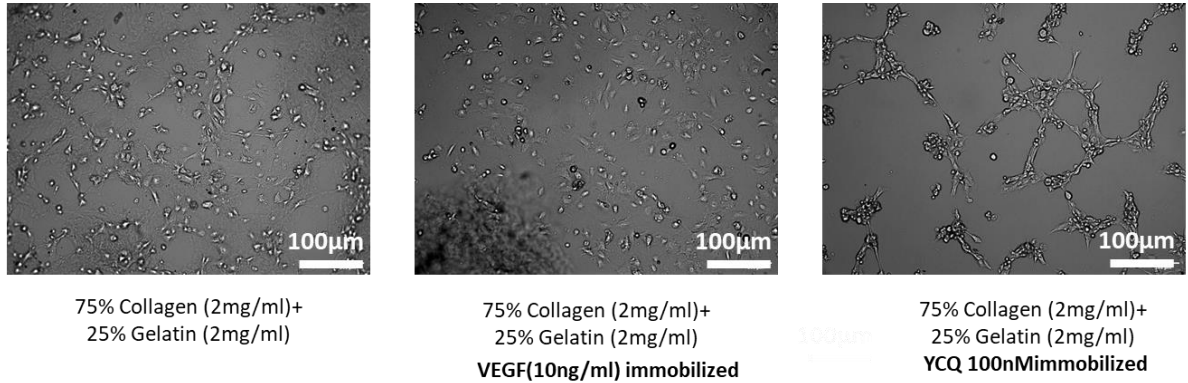


**Figure 8:** Brightfield images of HUVECs seeded on Col-Gel substrates. Substrates were functionalized with VEGF (10ng/ml) or YCQ (100nM) by immobilizing them on the surface of col-gel gels after complete polymerization. For surface immobilization, VEGF and YCQ were added on to the substrates and incubated for 1 hour at 37°C followed by washing with PBS once

#### 4.4. Establishment of fixation, immunostaining, and image analysis protocols

While brightfield microscopy can be used to visualize some of the gross morphological features of angiogenic structures, such as their length or branching pattern, it may not provide detailed information on the specific cell types or molecular components involved in the process. Therefore, staining can significantly enhance the ability to analyze and interpret the results of an angiogenesis cell assay, and enable visualization of specific components such as PECAM-1<sup>50,51</sup>, actin and nucleus<sup>17,52,53</sup>.

PECAM-1 or Platelet Endothelial Cell Adhesion Molecule-1 is a transmembrane glycoprotein that is expressed on the surface of endothelial cells. It is widely used as a marker to identify endothelial cells and is involved in angiogenesis. When new blood vessels are formed from existing ones, endothelial cells are activated to multiply and move towards the location where the new vessel will be formed. As these cells move, they create new connections between cells to build the new vessel.<sup>50,51</sup> PECAM-1 plays a role in these processes by encouraging endothelial cells to attach and move towards each other, as well as promoting the formation of connections between adjacent cells. Studies have shown that PECAM-1 expression is increased in endothelial cells during angiogenesis in 2D as well as 3D cell experiments, and that blocking PECAM-1 can inhibit angiogenesis.<sup>50,51,54</sup> Therefore, PECAM-1 is considered an important factor in studying the effect of growth factors that induce angiogenesis.

Studying actin expression is crucial in the process of angiogenesis. Actin is a cytoskeletal protein that plays a vital role in regulating cell shape, adhesion, and motility, all of which are essential for the formation of new blood vessels.<sup>52,53</sup> During network formation, endothelial cells undergo structural changes. Actin filaments provide the structural support for these changes, allowing endothelial cells to migrate and create new network-like structures. Actin staining can provide information on the organization and distribution of actin filaments within endothelial cells during angiogenesis.<sup>52,53,55</sup> Actin staining can be used to visualize the formation of new network structures and the migration of endothelial cells.

Listed are important factors that were considered while optimizing staining protocol for HUVEC 2D networks:

- Specificity: To ensure the immunostaining only detects the target protein or antigen of interest and does not cross-react with other proteins or antigens in the sample, validated and specific primary antibodies were used and assessed with proper controls.<sup>56,57</sup>
- Sensitivity: To ensure the staining detects low levels of the target protein or antigen, while minimizing background staining, optimization of the antibody concentration, incubation times, and detection methods was done.<sup>56,58</sup>
- Reproducibility: To maximize the consistency of results between different samples and experiments, a reliably detailed protocol was established and executed using validated reagents.<sup>58</sup>
- Localization: It must accurately localize the target protein or antigen within the tissue sample, providing information on its cellular or subcellular distribution by proper fixation and permeabilization of the tissue samples.<sup>59</sup>
- Interpretation: It must allow accurate and objective interpretation of the results, considering the staining intensity, pattern, and distribution.

In a preliminary protocol, all HUVEC samples on Col-Gel gels were fixed with 4% PFA for 30 mins and stained with anti-PECAM-1 antibody overnight at 4°C overnight, followed by staining them with AF-546 anti-rabbit secondary antibody, phalloidin and DAPI. Anti-PECAM-1 primary and secondary antibodies were used to stain PECAM-1 present on the membrane of HUVECs. Since the samples were not permeabilized prior to staining, anti CD31 antibody and phalloidin could not pass through the intact HUVECs efficiently, and since they were not permeabilized and blocked with BSA prior to staining them, this resulted in a lot of background staining (Figure 9). Background staining made it difficult to analyze and interpret the results of the staining experiment.

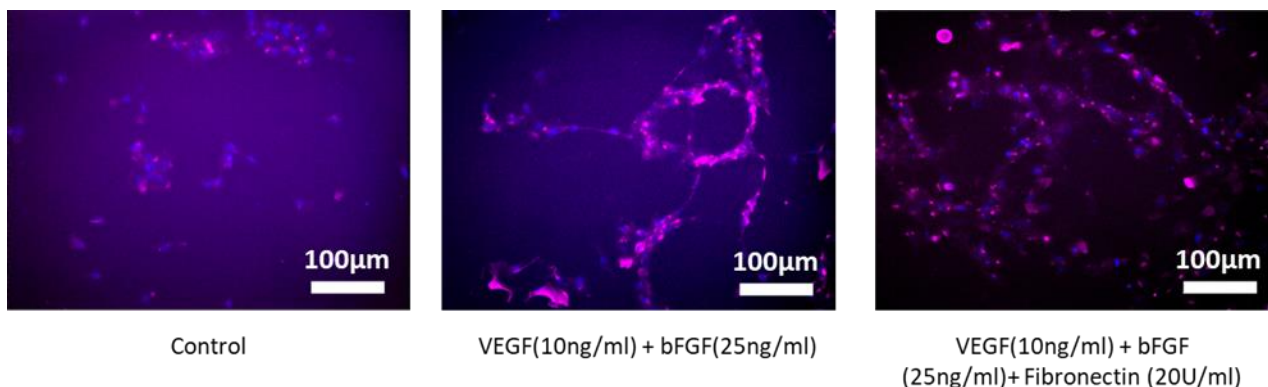


**Figure 9:** Epifluorescence images of HUVECs after 16 h of incubation on Col-Gel gels encapsulated with VEGF (10ng/ml), bFGF (25ng/ml) and fibronectin (20U/ml). HUVECs are labelled with PECAM-1 antibody (magenta), DAPI (cyan) to stain the nucleus and Phalloidin-AF488 (yellow) to stain actin fibres. No yellow stain can be seen in these channels because phalloidin could not enter the cells. Channel brightness and contrasts were adjusted for optimal visualization. Scale Bar 200  $\mu$ m

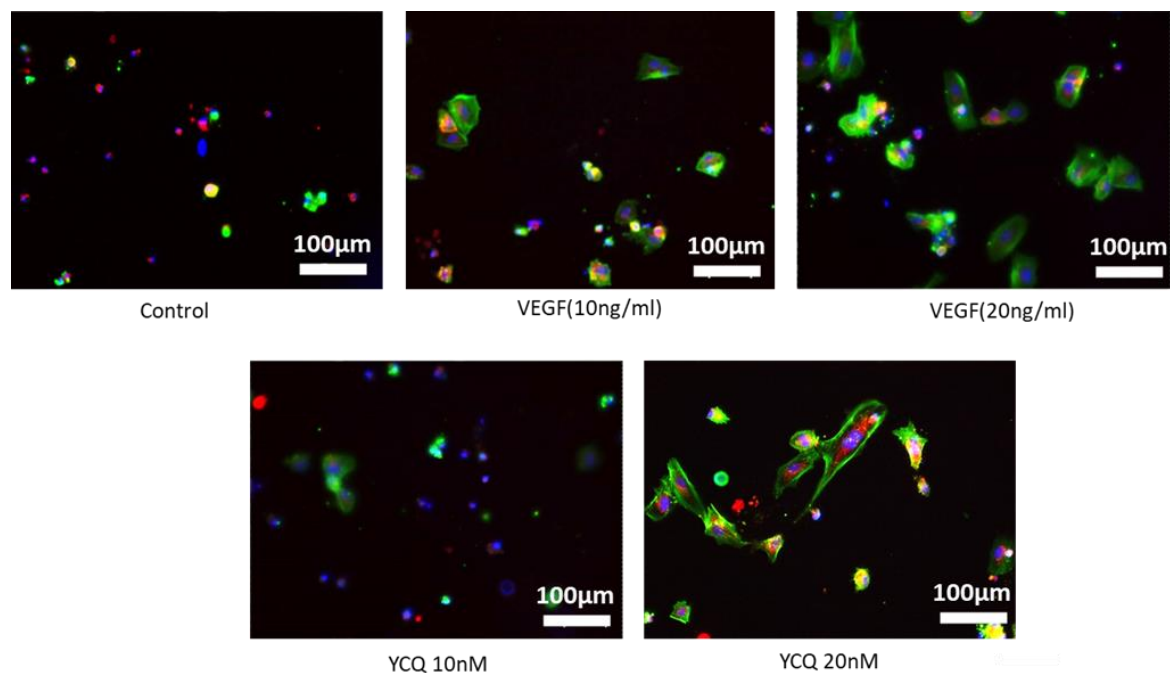


**Figure 10:** Epifluorescence images of HUVECs after 16 h of incubation on col-gel surfaces functionalized with VEGF and bFGF. HUVECs are labelled with PECAM-1 antibody (magenta), DAPI (cyan) to stain the nucleus and Phalloidin-AF488 (yellow) to stain actin fibres. Channel brightness and contrasts were adjusted for optimal visualization

For better visualization of the stained components in the cells, they were stained by following a previously published protocol.<sup>60</sup> HUVECs were fixed for 30 mins with 4% PFA, permeabilizing the cells with 0.5% Triton X and blocking them with 5% BSA prior to adding the anti-PECAM-1 antibody. the antibodies were able to penetrate HUVECs but integrity of HUVECs were compromised (figure 10). Fixing HUVECs for 30 mins lead to disintegration of networks and cellular structure and thereby not allowing proper visualization (Figure 10). The samples fixed for 30 mins with 4% PFA led to detachment of some of the cells from the substrate. It is known that longer fixation time with PFA might lead to degradation of more labile components in the sample, for example some

of the proteins and enzymes that are important to maintain structural integrity of the sample.<sup>18</sup> To retain structural integrity of the HUVECs on Col-Gel substrates, it was needed reduce the time needed for fixing HUVECs.<sup>56</sup> Next, HUVECs were fixed for 10 mins with PFA followed by permeabilizing the cells with 0.5% Triton X and blocking them with 5% BSA prior to adding the anti-PECAM-1 antibody. Antibodies were able to penetrate HUVECs but integrity of HUVECs were compromised.

Although the timing for fixing the cells was less the concentration of Triton-X was high (0.5%). In this case, adding more Triton-X than required for permeabilization can compromise the integrity of the cell membrane and hence can cause cell lysis.<sup>53,57</sup> Figure 11 shows leaked cellular components (marked in circles) that could have been a result cell lysis. In the next staining optimization step concentration of Triton-X was reduced from 0.5% to 0.1 % (Figure 12)

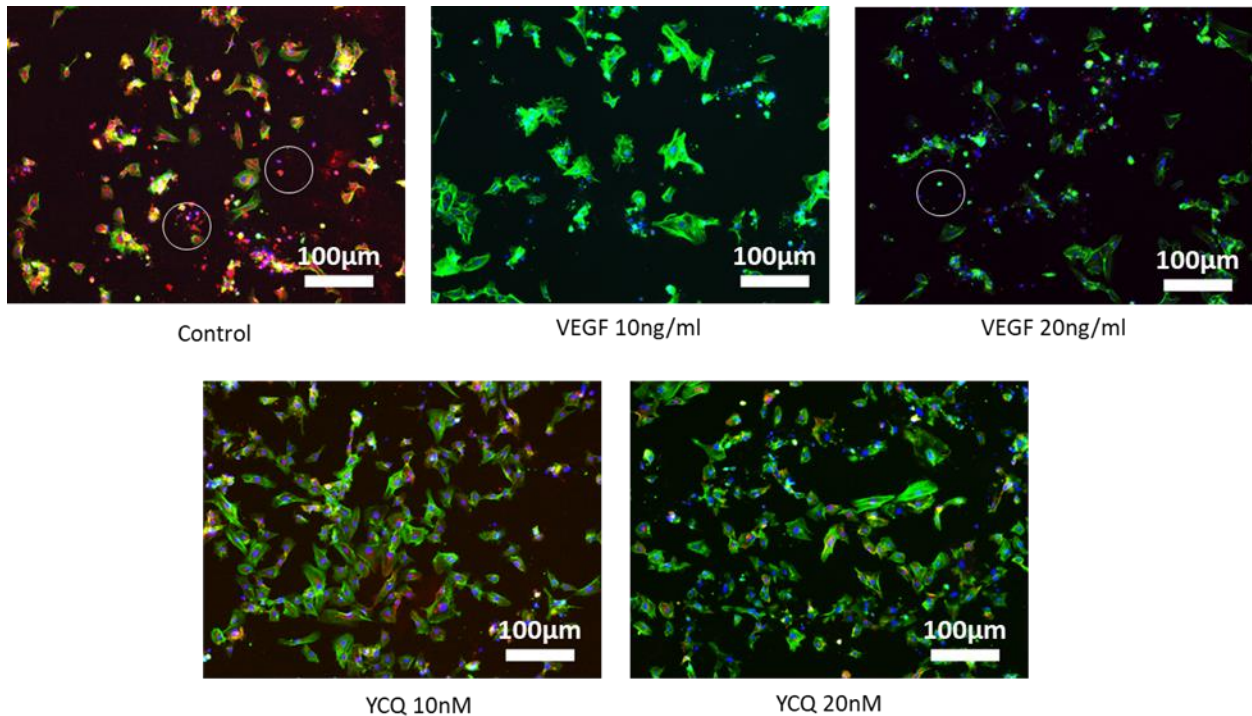


**Figure 11:** Optimization of collagen-gelatin gel staining. HUVECs were fixed for 30 mins with PFA and permeabilized with 0.5% Triton X stabilized with 0.1% Triton X. Leaked cellular components are marked in circles.

This helped in preserving the integrity of the cell membrane and it was observed that the cellular components do not leak after lowering the concentration of Triton-X.

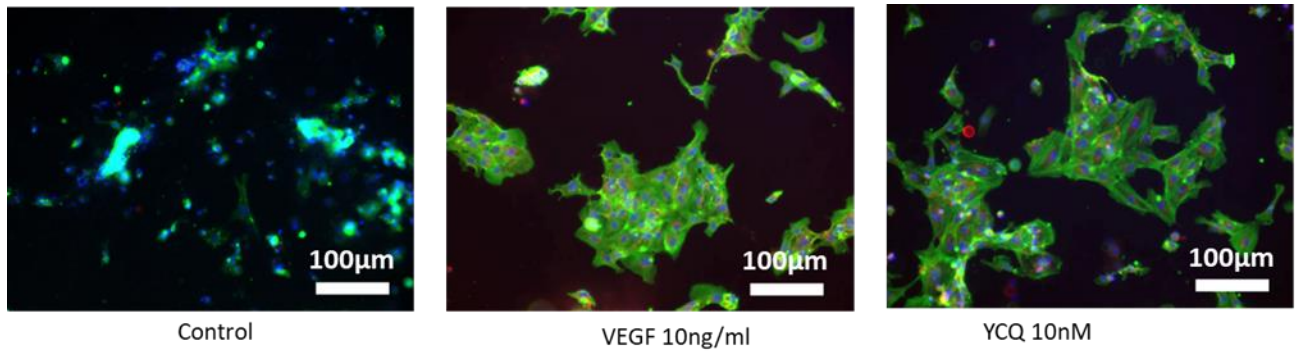


**Figure 12::** Optimization of collagen-gelatin gel staining. HUVECs were fixed for 10 mins with PFA and permeabilized with 0.1% Triton X permeabilized with 0.1% Triton-X

#### 4.6. Network formation capabilities of light-responsively secreted YCQ from liquid culture and pure YCQ

In our study, cultures of bacteria that light-responsively secrete YCQ and YCx were grown in dark until they reached OD<sub>600nm</sub> of 0.5 and then under light or dark conditions overnight. Cell-free supernatants (SN) from these cultures were then collected, filter sterilized and incubated on Col-Gel surfaces for the proteins to bind with the matrix (Figure 13). As positive controls, 10 nM of purified YCQ was immobilized on the surface, whereas and 10 ng/ $\mu$ L VEGF encapsulated in the col-gel matrix(Figure 13). When HUVECs were seeded on these Col-Gel surfaces, it was observed that those incubated with the negative control conditions of YCx dark, YCx light- and YCQ dark-state supernatants, cells retained monolayer cobblestone morphology over the same period (Figure 13).

Disclaimer: Figure 13, 14 ,15, 16 and 17 and large parts of the text describing the results of those figures are taken from my own published work: *Light-Regulated Pro-Angiogenic Engineered Living Materials - Dhakane - Advanced Functional Materials - Wiley Online Library*. <https://onlinelibrary.wiley.com/doi/full/10.1002/adfm.202212695> (accessed 2023-07-13).

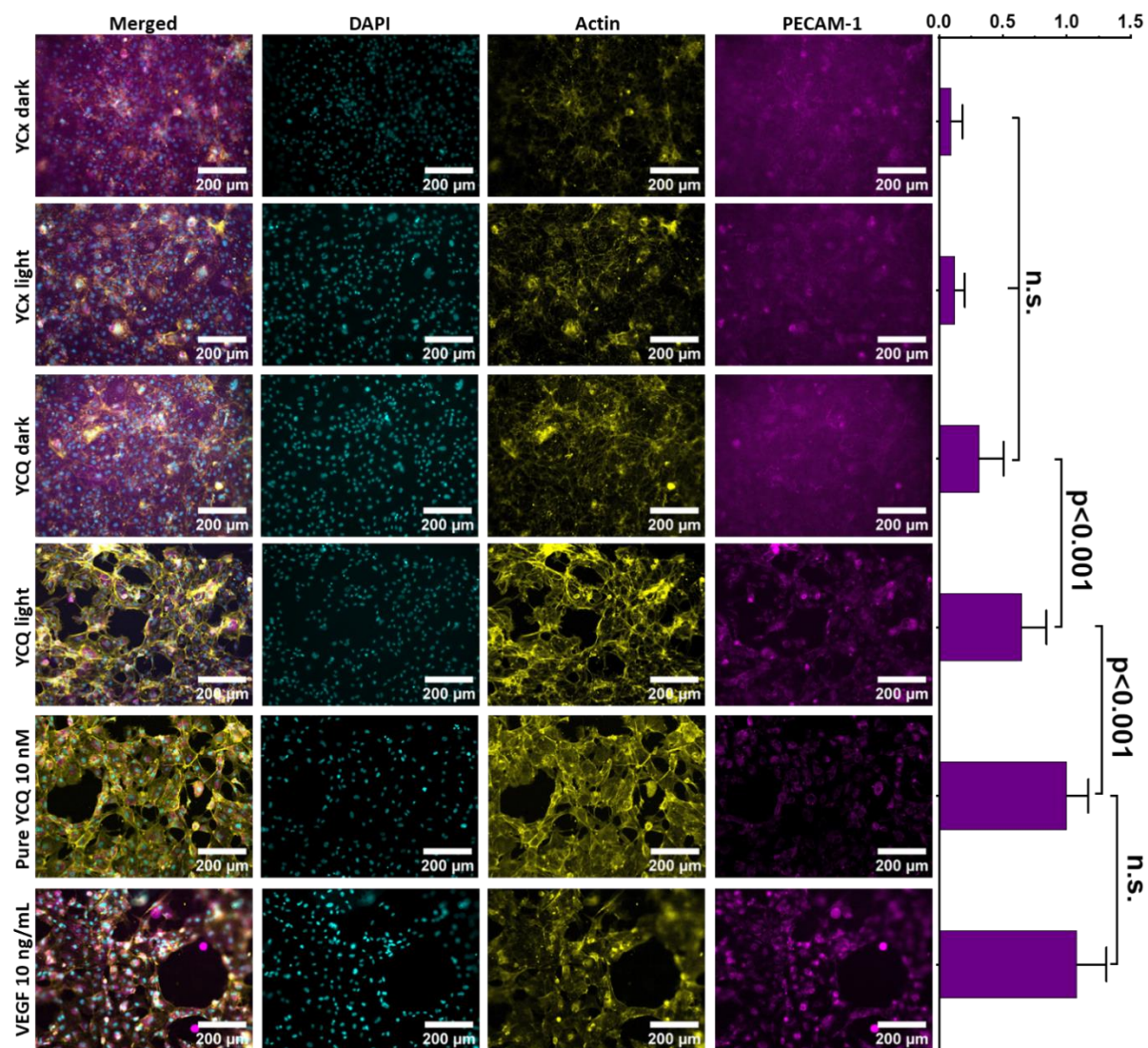


**Figure 13:** Fluorescence microscopy images of HUVECs grown for 16 h on Col-Gel surfaces incubated with supernatants of different bacterial cultures grown with or without light and with purified YCQ and VEGF as positive controls. The cells were stained for PECAM-1 (magenta), actin (yellow) and DNA (cyan). Brightness and contrast of each channel has been adjusted for optimal visualization. The graph represents intracellular PECAM-1 signal intensity after 16 hours of seeding HUVECs from experimental duplicates. Bar lengths represent mean values and whiskers represent standard deviation from at least 2 experimental replicates and 2 images in each replicate. The data was normalized to the mean value of Pure YCQ 10 nM. ANOVA was performed to

test for statistical significance of differences between different samples (n.s. = no significance)

Additional control substrates incubated with unmodified *ClearColi* supernatants, pure YCx 10 nM, and pure YCQ 1 nM were also found to yield similar results (Figure 14). On the other hand, those modified with light-activated YCQ supernatants, pure YCQ and VEGF promoted the cells to undergo a modest degree of network formation in 16 h.

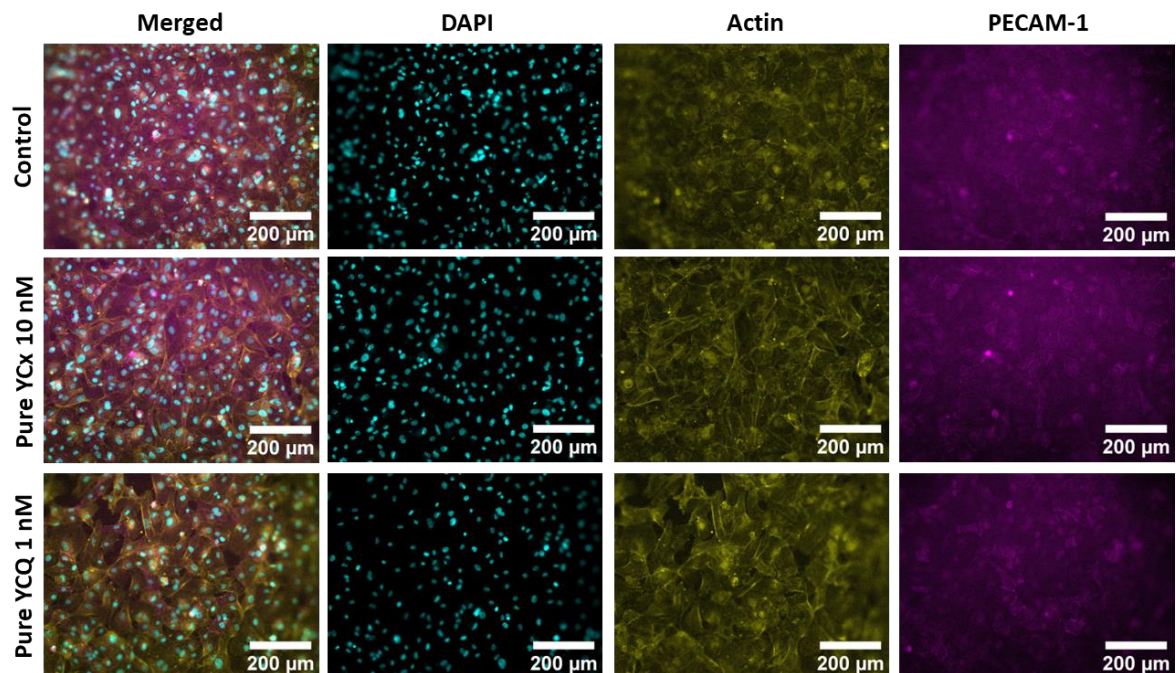


**Figure 14:** Epifluorescence images of HUVECs after 16 h of incubation on col-gel surfaces functionalized with unmodified *ClearColi* liquid culture supernatant (Control), pure YCx 10 nM, and pure YCQ 1nM supernatants. HUVECs are labelled with PECAM-1 antibody (magenta), DAPI (cyan) to stain the nucleus and Phalloidin-AF488 (yellow) to stain actin fibers. Channel brightness and contrasts were adjusted for optimal visualization.

A much stronger and quicker (3 h) network formation was observed when the Col-Gel matrices modified with a higher YCQ concentration of 100 nM (Figure 15), similar to what has been observed by others.<sup>39</sup> This indicates that YCQ immobilized on Col-Gel matrices is able to promote network formation in HUVEC cultures but only to a modest degree at the concentrations released by the bacterial cultures. Immunostaining analysis revealed a moderate upregulation of PECAM-1 in cells that formed networks compared to the those that formed a monolayer (Figure 15). These features correlate with the initiation of the angiogenesis process, in line with previous reports.<sup>40,41</sup> All together, these results confirmed that YCQ performed the secretion, collagen-binding and angiogenesis functions it was designed for.

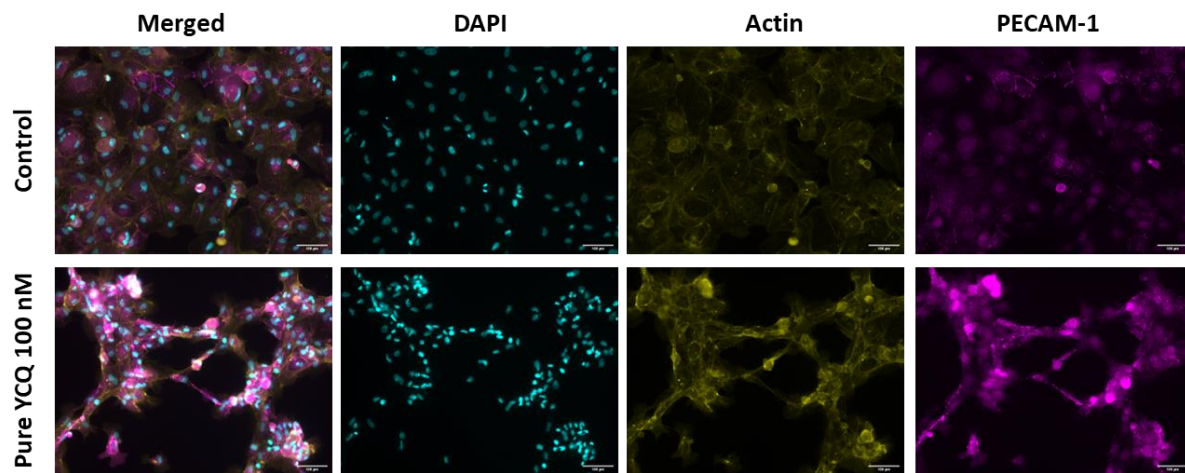


**Figure 15:** Epifluorescence images of HUVECs after 3 h of incubation on col-gel surfaces functionalized with unmodified ClearColi culture supernatant (Control) and pure YCQ 100 nM. HUVECs are labelled with PECAM-1 antibody (magenta), DAPI (cyan) to stain the nucleus and Phalloidin-AF488 (yellow) to stain actin fibers.

#### 4.7. Network formation capabilities of light-responsively secreted YCQ from ELMs

Next, we tested the bioactivity of YCQ released from the ELMs after 6 days of pulsed blue light irradiation at  $105 \mu\text{w}\cdot\text{cm}^{-2}$  and concentration  $>10 \text{ nM}$ . As controls, ELMs containing unmodified bacteria and YCx-producing bacteria were also made. The supernatants from the ELMs were incubated with Col-Gel surfaces after which the network formation assay using HUVECs was performed. On 3 out of 4 Col-Gel surfaces incubated with light-exposed YCQ-releasing ELMs, HUVECs were seen to form networks in 16 h, while this did not occur in all other conditions, where HUVECs were seen to grow as monolayers with cobblestone morphology (**Figure 16**). Notably, this cobblestone morphology was also seen on Col-Gel surfaces incubated with dark-state YCQ-releasing ELMs ( $<1 \text{ nM YCQ}$ ), indicating that the light-induced fold change of YCQ release was sufficient to elicit different responses from the HUVECs. Based on imaging of immunoassayed cells, the HUVECs that underwent network formation showed an increase in the expression PECAM-1 when compared to the control samples (**Figure 16**). While there are a few small regions in the control conditions like YCQ dark where the PECAM-1 fluorescence intensity is comparable to that in the YCQ light condition, the quantification reveals that the differences between these conditions are significant. This is a clear indication that the cells were undergoing angiogenic differentiation, in agreement with the results from previous reports.<sup>61,62</sup>

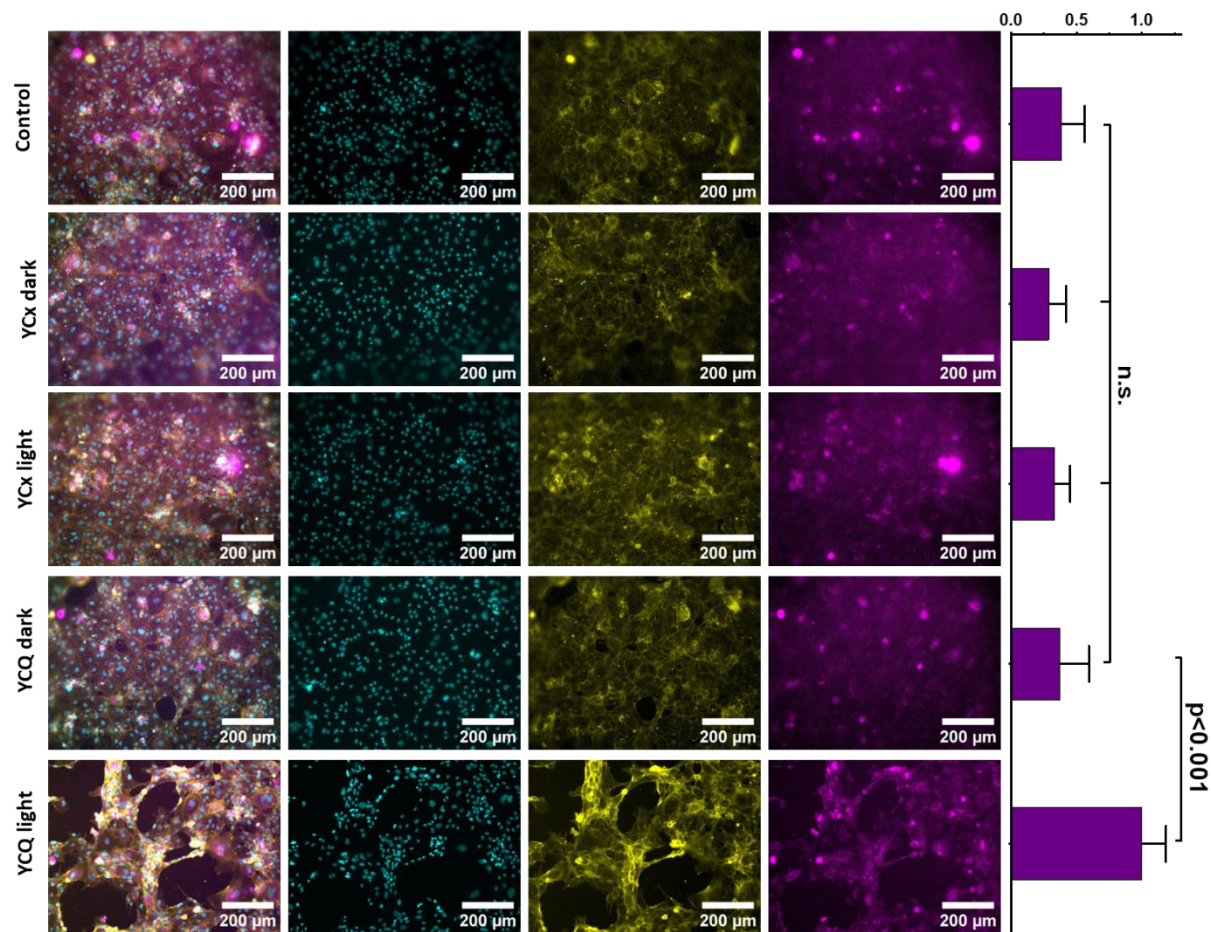


**Figure 16:** Epifluorescence images of HUVECs cultured for 16 hours on Col-Gel surfaces that were incubated in supernatants from ELMs containing unmodified ClearColi (Control), YCx-expressing and YCQ-expressing bacteria kept in dark or exposed to blue light pulses (2 s ON, 1 min OFF; 105  $\mu\text{W}\cdot\text{cm}^{-2}$ ) for 6 days. The cells were stained for PECAM-1 (magenta), actin (yellow) and DNA (cyan). Brightness and contrast of each channel has been adjusted for optimal visualization. The graph represents intracellular PECAM-1 signal intensity after 16 hours of seeding HUVECs from experimental triplicates (supernatant derived from 3 individual ELM constructs). Bar lengths represent mean values and whiskers represent standard deviation. The data was normalized to the mean value of YCQ light.

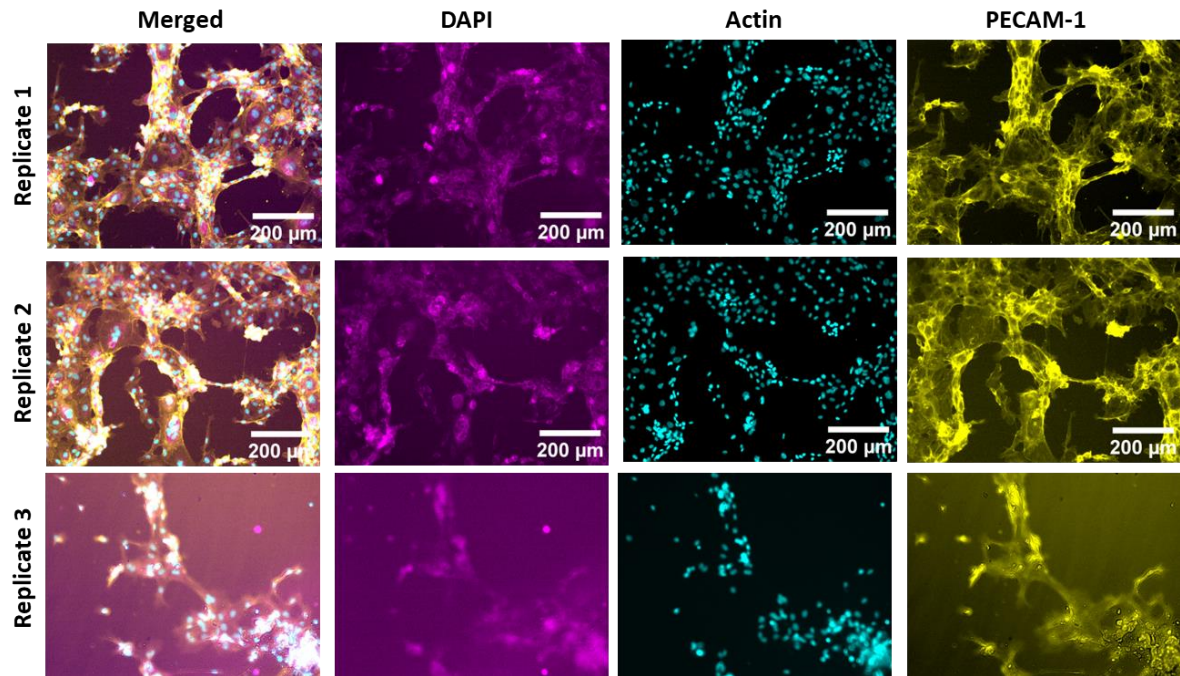


**Figure 17:** Epifluorescence images of HUVECs cultured for 16 hours on Col-Gel surfaces that were incubated in supernatants from ELMs containing YCQ bacteria exposed to blue light pulses (2 s ON, 1 min OFF;  $105 \mu\text{W}\cdot\text{cm}^{-2}$ ) for 6 days. The cells were stained for PECAM-1 (magenta), actin (yellow) and DNA (cyan).

#### 4.8. Discussion and conclusions

High levels of collagen remodeling is seen in humans during physiological events like bone renewal, and also in pathological conditions, such as arthritis, tumor growth and chronic wounds. Collagen exists locally both in native and denatured gelatin-like states at the wound healing sites.<sup>30</sup> Because collagen is the major component of ECM and its present in most of the tissues, therefore it is the most promising target for therapeutic applications. In this study we tested Fibrin-collagen, Collagen-Gelatin and GelMA matrices for designing developing a network formation assay. The Col-Gel was found to be the best system amongst the three tested due to batch-to-batch consistency, survival of HUVECs on the Gels and reproducibility of the results. An existing protocol was modified to create Col-Gel films and YCQ was immobilized on the surface of Col-Gel films.<sup>30</sup>

The ability of QK peptide to substitute VEGF in stimulating network formation is well-established. QK stimulates the same endothelial cell behaviors as recombinant VEGF and has comparable neovascularization potential in in-vitro as well as in-vivo models.<sup>63-66</sup> Consistent with these results, we observed that YCQ can induce network formation in endothelial cells, which is an early sign of angiogenesis. The activity of QK was proven in its pure form, when secreted from ClearColi liquid culture and when secreted from light activated ELMs.

Prominent issues in the design of angiogenic biomaterials are controlled and localized delivery of angiogenic factors.<sup>60</sup> This study highlights the potential of ELM to be able to release QK in a light-controlled manner which in turn can induce network formation in-vitro.

Disclaimer: Section 4.8 is taken from my own published work: *Light-Regulated Pro-Angiogenic Engineered Living Materials - Dhakane - Advanced Functional Materials - Wiley Online Library*. <https://onlinelibrary.wiley.com/doi/full/10.1002/adfm.202212695> (accessed 2023-07-13).

## 4.8. Materials and methods

### 4.8.1. HUVEC network formation assay:

#### **1. Cell Culture Conditions:**

HUVECs (PromoCell C-12205) were cultured on cell culture flasks coated with 0.2% gelatin and M199 media (Sigma M4530) supplemented with 20% FBS (Gibco 10270), 100 U/L penicillin, 100 mg/L streptomycin, Sodium heparin (Sigma, H-3393) and Endothelial Cell growth Supplement (Sigma E2759) was used as previously described. HUVECs between passages 2 to 7 were used for the experiments

**2. Bacterial culture conditions:** For obtaining the cell lysates that have been tested in the present study, CC Wt, CC YCQ, CC YCx were cultivated in dark at 32°C and 250 rpm until they reached the OD<sub>600</sub> 0.5, after which they were induced for production of YCQ and YCx with light (information about the lamp)

#### **3. Preparation of substrates for angiogenesis**

A. Preparation of Matrigel: To prepare the substrate Corning Matrigel was thawed on ice for 30 mins. The test substances (VEGF 10 ng/ml, 2 µL CC and CC YCQ lysate) were mixed in the Matrigel solution in desired concentrations. 10 µL of Matrigel with encapsulated growth factors and cell lysates was pipetted into an angiogenesis well plate. It was allowed to polymerize for 1 hour at 37°C.

B. Preparation of Gelatin Methacrylate substrates: GelMA was dissolved in HUVEC media at a concentration of 5% w/v at 4°C. The test substances (VEGF 10 ng/ml, 2 µL CC and CC YCQ lysate in 10 µL of GelMA solution) were mixed in solution. The solution was then cast in the bottom chamber of an Ibidi angiogenesis well plate and maintained at 37°C in a viscous gel state for 10 mins. Chemical cross-linking of the methacrylate groups was driven by UV light (365 nm wavelength) in the presence of a photoinitiator (Irgacure 2959) for 1 min, after which a stable gel was obtained, visually determined by indenting it with a pipette tip.

C. Preparation of Fibrin-Collagen Gels: Solutions of fibrinogen, collagen (2 mg mL<sup>-1</sup>) and thrombin (20 U mL<sup>-1</sup>) were mixed in the ratio of 7:2:1. The test substances (VEGF

10ng/ml, 2µL CC and CC YCQ lysate in 10µL of gel) were mixed in solution. It was allowed to polymerize at 37°C for 1 hour.

D. Preparation of Col-Gel surfaces: All stock solutions were made in PBS pH 7. The gels were prepared by mixing 75% v/v of 2mg.mL<sup>-1</sup> collagen (gibco, A1048301) and 25% v/v of 2mg.mL<sup>-1</sup> gelatin (SigmaAldrich, 9000-70-8) solution. The two solutions were mixed by manually stirring with the pipette tip in the Eppendorf tube without pipetting it. 10 µL of this solution was added into the 15 well angiogenesis well plates (ibidi, 81506). The gels were allowed to polymerize at 37 °C, 5% CO<sub>2</sub> for 1 hour followed by overnight incubation at 4°C.

**4. Encapsulation of YCQ and VEGF:** Solutions of VEGF and YCQ were mixed with the col-gels before their polymerization. Col-Gel were incubated 1 h at 37 °C in a CO<sub>2</sub> incubator followed by incubation at 4°C overnight

**5. Immobilization of secreted YCQ on Col-Gel surfaces:** 10 µL of the SN collected from ELMs were incubated on the Col-Gel surface for 1 h at 37 °C in a CO<sub>2</sub> incubator. The supernatants were removed with a pipette and the Col-Gel surfaces were washed with 50 µL PBS once to remove unbound proteins.

**6. HUVEC seeding:** (50 µL of 2×10<sup>5</sup> cells.mL<sup>-1</sup>) HUVECs (P3-P7) were seeded on the Col-Gel surfaces and the plate was incubated at 37 °C and 5% CO<sub>2</sub> for 16 hours. The culture was then fixed with 4% aqueous PFA solution for 15 mins, washed with PBS and blocked with 5% w/v BSA solution for 1 h. Cells were permeabilized with 0.1% w/v Triton X-100 for 15 mins and incubated with monoclonal goat anti-rabbit PECAM-1 primary antibody (1:500 in 1% w/v BSA, Abcam) overnight and washed with PBS. This was followed by incubation with anti-rabbit Alexa flour-488 secondary antibody (1:500 in water, Thermo Fisher Scientific) for 1 h. Subsequently, cells were washed with PBS and nuclei were stained with DAPI (1:500 in water, Life Technology) and actin fibers were labelled with TRITC-phalloidin (1:500 in water, Thermo Fisher Scientific). Samples were washed thrice with PBS and imaged with a Nikon epifluorescence microscope at 10X magnification using excitation wavelengths of 405 nm (900 ms excitation), 488 nm (100 ms excitation), and 565 nm (100 ms excitation) and 20% incident light intensity. Images were captured using NIS-Elements software and processed as follows for inclusion in the figures: Image processing and analysis was done using Fiji edition of ImageJ (Image J Java 1.8.0). Brightness and contrast for the DAPI (Cyan, 405 nm) and Actin (Yellow, 488 nm) were adjusted in their respective LUT histograms to the same range for all the images in an

individual experiment. For PECAM-1, since Anti-PECAM-1 agglomeration at some places created bright spots to different degrees, the brightness and contrast in the LUT histograms were manually adjusted for each image based on the maximum intensity within the cells that were not caused by the agglomerates and the minimum intensity in the cell-free background. This way ensured the best possible visualization of PECAM-1 expression in all the cells.

## **7. PECAM-1 analysis -**

Quantification of PECAM-1 fluorescence intensity was done using Fiji Edition of ImageJ (ImageJ Java 1.8.0). Mean grey values within the cells were determined by manual selection and (the agglomerates which created bright spots were excluded from the measurement) and was subtracted from the mean grey value of the background.

## **8. Statistical Analysis**

All image processing for quantification of PECAM-1 intensities was performed using the Fiji edition of ImageJ on Raw microscopy images. All data processing and analyses were done using Origin 2022 software. Details of sample sizes, replicates and statistical tests for quantified data are provided in the figure captions. Significant differences were determined by testing for the null hypothesis using a Two sample t-test when comparing 2 sample sets (Figure 1C) and using one-way ANOVA with the Tukey test for means comparison when comparing more than 3 samples sets (Figure 2, 4, 5). The p values are given directly in the figures and p values above 0.05 are indicated as non-significant (n.s.) in Figures 2, 5.

## 4.9. References

- (1) Staton, C. A.; Reed, M. W. R.; Brown, N. J. A Critical Analysis of Current in Vitro and in Vivo Angiogenesis Assays. *Int J Exp Pathol* **2009**, *90* (3), 195–221. <https://doi.org/10.1111/j.1365-2613.2008.00633.x>.
- (2) Tahergorabi, Z.; Khazaei, M. A Review on Angiogenesis and Its Assays. *Iran J Basic Med Sci* **2012**, *15* (6), 1110–1126.
- (3) Peterson, A. W.; Caldwell, D. J.; Rioja, A. Y.; Rao, R. R.; Putnam, A. J.; Stegemann, J. P. Vasculogenesis and Angiogenesis in Modular Collagen–Fibrin Microtissues. *Biomater. Sci.* **2014**, *2* (10), 1497–1508. <https://doi.org/10.1039/C4BM00141A>.
- (4) Tomanek, R. J.; Schatteman, G. C. Angiogenesis: New Insights and Therapeutic Potential. *The Anatomical Record* **2000**, *261* (3), 126–135. [https://doi.org/10.1002/1097-0185\(20000615\)261:3<126::AID-AR7>3.0.CO;2-4](https://doi.org/10.1002/1097-0185(20000615)261:3<126::AID-AR7>3.0.CO;2-4).
- (5) Nguyen, L. T.; Tran, N. T.; Than, U. T. T.; Nguyen, M. Q.; Tran, A. M.; Do, P. T. X.; Chu, T. T.; Nguyen, T. D.; Bui, A. V.; Ngo, T. A.; Hoang, V. T.; Hoang, N. T. M. Optimization of Human Umbilical Cord Blood-Derived Mesenchymal Stem Cell Isolation and Culture Methods in Serum- and Xeno-Free Conditions. *Stem Cell Research & Therapy* **2022**, *13* (1), 15. <https://doi.org/10.1186/s13287-021-02694-y>.
- (6) Crampton, S. P.; Davis, J.; Hughes, C. C. W. Isolation of Human Umbilical Vein Endothelial Cells (HUVEC). *J Vis Exp* **2007**, No. 3, 183. <https://doi.org/10.3791/183>.
- (7) Baudin, B.; Bruneel, A.; Bosselut, N.; Vaubourdolle, M. A Protocol for Isolation and Culture of Human Umbilical Vein Endothelial Cells. *Nat Protoc* **2007**, *2* (3), 481–485. <https://doi.org/10.1038/nprot.2007.54>.
- (8) *Culture of Human Endothelial Cells Derived from Umbilical Veins. IDENTIFICATION BY MORPHOLOGIC AND IMMUNOLOGIC CRITERIA - PMC.* <https://www.ncbi.nlm.nih.gov/pmc/articles/PMC302542/> (accessed 2023-04-20).
- (9) Adair, T. H.; Montani, J.-P. *Angiogenesis Assays*; Morgan & Claypool Life Sciences, 2010.
- (10) Medina-Leyte, D. J.; Domínguez-Pérez, M.; Mercado, I.; Villarreal-Molina, M. T.; Jacobo-Albavera, L. Use of Human Umbilical Vein Endothelial Cells (HUVEC) as a Model to Study Cardiovascular Disease: A Review. *Applied Sciences* **2020**, *10* (3), 938. <https://doi.org/10.3390/app10030938>.
- (11) Liao, H.; He, H.; Chen, Y.; Zeng, F.; Huang, J.; Wu, L.; Chen, Y. Effects of Long-Term Serial Cell Passaging on Cell Spreading, Migration, and Cell-Surface Ultrastructures

- of Cultured Vascular Endothelial Cells. *Cytotechnology* **2014**, *66* (2), 229–238. <https://doi.org/10.1007/s10616-013-9560-8>.
- (12) Staton, C. A.; Reed, M. W. R.; Brown, N. J. A Critical Analysis of Current in Vitro and in Vivo Angiogenesis Assays. *Int J Exp Pathol* **2009**, *90* (3), 195–221. <https://doi.org/10.1111/j.1365-2613.2008.00633.x>.
- (13) *In Vitro Matrigel Angiogenesis Assays* | SpringerLink. <https://link.springer.com/protocol/10.1385/1-59259-143-4:205> (accessed 2023-07-17).
- (14) Feng, X.; Tonnesen, M. G.; Mousa, S. A.; Clark, R. A. F. Fibrin and Collagen Differentially but Synergistically Regulate Sprout Angiogenesis of Human Dermal Microvascular Endothelial Cells in 3-Dimensional Matrix. *Int J Cell Biol* **2013**, *2013*, 231279. <https://doi.org/10.1155/2013/231279>.
- (15) Peterson, A. W.; Caldwell, D. J.; Rioja, A. Y.; Rao, R. R.; Putnam, A. J.; Stegemann, J. P. Vasculogenesis and Angiogenesis in Modular Collagen-Fibrin Microtissues. *Biomater Sci* **2014**, *2* (10), 1497–1508. <https://doi.org/10.1039/C4BM00141A>.
- (16) Khoo, C. P.; Micklem, K.; Watt, S. M. A Comparison of Methods for Quantifying Angiogenesis in the Matrigel Assay in Vitro. *Tissue Eng Part C Methods* **2011**, *17* (9), 895–906. <https://doi.org/10.1089/ten.TEC.2011.0150>.
- (17) Nikkhah, M.; Eshak, N.; Zorlutuna, P.; Annabi, N.; Castello, M.; Kim, K.; Dolatshahi-Pirouz, A.; Edalat, F.; Bae, H.; Yang, Y.; Khademhosseini, A. Directed Endothelial Cell Morphogenesis in Micropatterned Gelatin Methacrylate Hydrogels. *Biomaterials* **2012**, *33* (35), 9009–9018. <https://doi.org/10.1016/j.biomaterials.2012.08.068>.
- (18) Im, G.-B.; Lin, R.-Z. Bioengineering for Vascularization: Trends and Directions of Photocrosslinkable Gelatin Methacrylate Hydrogels. *Frontiers in Bioengineering and Biotechnology* **2022**, *10*.
- (19) *Cell-laden microengineered gelatin methacrylate hydrogels* - Google Search. <https://www.google.com/search?client=firefox-b-e&q=Cell-laden+microengineered+gelatin+methacrylate+hydrogels> (accessed 2023-03-13).
- (20) Nichol, J. W.; Koshy, S.; Bae, H.; Hwang, C. M.; Yamanlar, S.; Khademhosseini, A. Cell-Laden Microengineered Gelatin Methacrylate Hydrogels. *Biomaterials* **2010**, *31* (21), 5536–5544. <https://doi.org/10.1016/j.biomaterials.2010.03.064>.
- (21) Bupphathong, S.; Quiroz, C.; Huang, W.; Chung, P.-F.; Tao, H.-Y.; Lin, C.-H. Gelatin Methacrylate Hydrogel for Tissue Engineering Applications—A Review on Material

Modifications. *Pharmaceuticals* **2022**, *15* (2), 171.  
<https://doi.org/10.3390/ph15020171>.

- (22) Heltmann-Meyer, S.; Steiner, D.; Müller, C.; Schneidereit, D.; Friedrich, O.; Salehi, S.; Engel, F. B.; Arkudas, A.; Horch, R. E. Gelatin Methacryloyl Is a Slow Degrading Material Allowing Vascularization and Long-Term Use in Vivo. *Biomed. Mater.* **2021**, *16* (6), 065004. <https://doi.org/10.1088/1748-605X/ac1e9d>.
- (23) Feng, X.; Tonnesen, M. G.; Mousa, S. A.; Clark, R. A. F. Fibrin and Collagen Differentially but Synergistically Regulate Sprout Angiogenesis of Human Dermal Microvascular Endothelial Cells in 3-Dimensional Matrix. *Int J Cell Biol* **2013**, *2013*, 231279. <https://doi.org/10.1155/2013/231279>.
- (24) Veith, A. P.; Henderson, K.; Spencer, A.; Sligar, A. D.; Baker, A. B. Therapeutic Strategies for Enhancing Angiogenesis in Wound Healing. *Adv Drug Deliv Rev* **2019**, *146*, 97–125. <https://doi.org/10.1016/j.addr.2018.09.010>.
- (25) Twardowski, T.; Fertala, A.; Orgel, J. P. R. O.; San Antonio, J. D. Type I Collagen and Collagen Mimetics as Angiogenesis Promoting Superpolymers. *Curr Pharm Des* **2007**, *13* (35), 3608–3621. <https://doi.org/10.2174/138161207782794176>.
- (26) Kirkpatrick, N. D.; Andreou, S.; Hoying, J. B.; Utzinger, U. Live Imaging of Collagen Remodeling during Angiogenesis. *American Journal of Physiology-Heart and Circulatory Physiology* **2007**, *292* (6), H3198–H3206. <https://doi.org/10.1152/ajpheart.01234.2006>.
- (27) Schor, A. M.; Ellis, I.; Schor, S. L. Collagen Gel Assay for Angiogenesis. In *Angiogenesis Protocols*; Murray, J. C., Ed.; Methods in Molecular Medicine™; Humana Press: Totowa, NJ, 2001; pp 145–162. <https://doi.org/10.1385/1-59259-143-4:145>.
- (28) Dreesmann, L.; Ahlers, M.; Schlosshauer, B. The Pro-Angiogenic Characteristics of a Cross-Linked Gelatin Matrix. *Biomaterials* **2007**, *28* (36), 5536–5543. <https://doi.org/10.1016/j.biomaterials.2007.08.040>.
- (29) Zambuto, S. G.; Clancy, K. B. H.; Harley, B. A. C. A Gelatin Hydrogel to Study Endometrial Angiogenesis and Trophoblast Invasion. *Interface Focus* **2019**, *9* (5), 20190016. <https://doi.org/10.1098/rsfs.2019.0016>.
- (30) Chan, T. R.; Stahl, P. J.; Li, Y.; Yu, S. M. Collagen-Gelatin Mixtures as Wound Model, and Substrates for VEGF-Mimetic Peptide Binding and Endothelial Cell Activation. *Acta Biomater* **2015**, *15*, 164–172. <https://doi.org/10.1016/j.actbio.2015.01.005>.

- (31) Sun, M.; Sun, X.; Wang, Z.; Guo, S.; Yu, G.; Yang, H. Synthesis and Properties of Gelatin Methacryloyl (GelMA) Hydrogels and Their Recent Applications in Load-Bearing Tissue. *Polymers (Basel)* **2018**, *10* (11), 1290. <https://doi.org/10.3390/polym10111290>.
- (32) Goto, F.; Goto, K.; Weindel, K.; Folkman, J. Synergistic Effects of Vascular Endothelial Growth Factor and Basic Fibroblast Growth Factor on the Proliferation and Cord Formation of Bovine Capillary Endothelial Cells within Collagen Gels. *Lab Invest* **1993**, *69* (5), 508–517.
- (33) Arkudas, A.; Tjiawi, J.; Bleiziffer, O.; Grabinger, L.; Polykandriotis, E.; Beier, J. P.; Stürzl, M.; Horch, R. E.; Kneser, U. Fibrin Gel-Immobilized VEGF and bFGF Efficiently Stimulate Angiogenesis in the AV Loop Model. *Mol Med* **2007**, *13* (9–10), 480–487. <https://doi.org/10.2119/2007-00057.Arkudas>.
- (34) Kumar, V. B. S.; Viji, R. I.; Kiran, M. S.; Sudhakaran, P. R. Angiogenic Response of Endothelial Cells to Fibronectin. In *Biochemical Roles of Eukaryotic Cell Surface Macromolecules*; Sudhakaran, P. R., Surolia, A., Eds.; Advances in Experimental Medicine and Biology; Springer: New York, NY, 2012; pp 131–151. [https://doi.org/10.1007/978-1-4614-3381-1\\_10](https://doi.org/10.1007/978-1-4614-3381-1_10).
- (35) *Fibronectin promotes the elongation of microvessels during angiogenesis in vitro - Nicosia - 1993 - Journal of Cellular Physiology - Wiley Online Library*. <https://onlinelibrary.wiley.com/doi/abs/10.1002/jcp.1041540325> (accessed 2023-04-18).
- (36) van Hinsbergh, V. W.; Collen, A.; Koolwijk, P. Role of Fibrin Matrix in Angiogenesis. *Ann N Y Acad Sci* **2001**, *936*, 426–437. <https://doi.org/10.1111/j.1749-6632.2001.tb03526.x>.
- (37) Shoulders, M. D.; Raines, R. T. COLLAGEN STRUCTURE AND STABILITY. *Annu Rev Biochem* **2009**, *78*, 929–958. <https://doi.org/10.1146/annurev.biochem.77.032207.120833>.
- (38) Bigi, A.; Panzavolta, S.; Rubini, K. Relationship between Triple-Helix Content and Mechanical Properties of Gelatin Films. *Biomaterials* **2004**, *25* (25), 5675–5680. <https://doi.org/10.1016/j.biomaterials.2004.01.033>.
- (39) Sarrigiannidis, S. O.; Rey, J. M.; Dobre, O.; González-García, C.; Dalby, M. J.; Salmeron-Sanchez, M. A Tough Act to Follow: Collagen Hydrogel Modifications to Improve Mechanical and Growth Factor Loading Capabilities. *Mater Today Bio* **2021**, *10*, 100098. <https://doi.org/10.1016/j.mtbio.2021.100098>.

- (40) Fujii, K. K.; Taga, Y.; Takagi, Y. K.; Masuda, R.; Hattori, S.; Koide, T. The Thermal Stability of the Collagen Triple Helix Is Tuned According to the Environmental Temperature. *Int J Mol Sci* **2022**, *23* (4), 2040. <https://doi.org/10.3390/ijms23042040>.
- (41) J. Holder, A.; Badiei, N.; Hawkins, K.; Wright, C.; R. Williams, P.; J. Curtis, D. Control of Collagen Gel Mechanical Properties through Manipulation of Gelation Conditions near the Sol–Gel Transition. *Soft Matter* **2018**, *14* (4), 574–580. <https://doi.org/10.1039/C7SM01933E>.
- (42) Li, Y.; Liu, Y.; Bai, H.; Li, R.; Shang, J.; Zhu, Z.; Zhu, L.; Zhu, C.; Che, Z.; Wang, J.; Liu, H.; Huang, L. Sustained Release of VEGF to Promote Angiogenesis and Osteointegration of Three-Dimensional Printed Biomimetic Titanium Alloy Implants. *Front Bioeng Biotechnol* **2021**, *9*, 757767. <https://doi.org/10.3389/fbioe.2021.757767>.
- (43) Abraham, S.; Sanjay, G.; Majiyd, N. A.; Chinnaiah, A. Encapsulated VEGF121-PLA Microparticles Promote Angiogenesis in Human Endometrium Stromal Cells. *Journal of Genetic Engineering and Biotechnology* **2021**, *19* (1), 23. <https://doi.org/10.1186/s43141-021-00118-1>.
- (44) Wang, Z.; Wang, Z.; Lu, W. W.; Zhen, W.; Yang, D.; Peng, S. Novel Biomaterial Strategies for Controlled Growth Factor Delivery for Biomedical Applications. *NPG Asia Mater* **2017**, *9* (10), e435–e435. <https://doi.org/10.1038/am.2017.171>.
- (45) *Design principles for therapeutic angiogenic materials | Nature Reviews Materials*. <https://www.nature.com/articles/natrevmats20156> (accessed 2023-04-20).
- (46) Shakya, A.; Imado, E.; Nguyen, P. K.; Matsuyama, T.; Horimoto, K.; Hirata, I.; Kato, K. Oriented Immobilization of Basic Fibroblast Growth Factor: Bioengineered Surface Design for the Expansion of Human Mesenchymal Stromal Cells. *Sci Rep* **2020**, *10* (1), 8762. <https://doi.org/10.1038/s41598-020-65572-2>.
- (47) Backer, M. V.; Patel, V.; Jehning, B. T.; Claffey, K. P.; Backer, J. M. Surface Immobilization of Active Vascular Endothelial Growth Factor via a Cysteine-Containing Tag. *Biomaterials* **2006**, *27* (31), 5452–5458. <https://doi.org/10.1016/j.biomaterials.2006.06.025>.
- (48) Fernandes-Cunha, G. M.; Lee, H. J.; Kumar, A.; Kreymerman, A.; Heilshorn, S.; Myung, D. Immobilization of Growth Factors to Collagen Surfaces Using Pulsed Visible Light. *Biomacromolecules* **2017**, *18* (10), 3185–3196. <https://doi.org/10.1021/acs.biomac.7b00838>.

- (49) Zhao, W.; McCallum, S. A.; Xiao, Z.; Zhang, F.; Linhardt, R. J. Binding Affinities of Vascular Endothelial Growth Factor (VEGF) for Heparin-Derived Oligosaccharides. *Biosci Rep* **2012**, *32* (1), 71–81. <https://doi.org/10.1042/BSR20110077>.
- (50) Cao, G.; O'Brien, C. D.; Zhou, Z.; Sanders, S. M.; Greenbaum, J. N.; Makrigiannakis, A.; DeLisser, H. M. Involvement of Human PECAM-1 in Angiogenesis and in Vitro Endothelial Cell Migration. *American Journal of Physiology-Cell Physiology* **2002**, *282* (5), C1181–C1190. <https://doi.org/10.1152/ajpcell.00524.2001>.
- (51) Park, S.; DiMaio, T. A.; Scheef, E. A.; Sorenson, C. M.; Sheibani, N. PECAM-1 Regulates Proangiogenic Properties of Endothelial Cells through Modulation of Cell-Cell and Cell-Matrix Interactions. *Am J Physiol Cell Physiol* **2010**, *299* (6), C1468–C1484. <https://doi.org/10.1152/ajpcell.00246.2010>.
- (52) Pasquier, E.; Tuset, M.-P.; Sinnappan, S.; Carnell, M.; Macmillan, A.; Kavallaris, M.  $\gamma$ -Actin Plays a Key Role in Endothelial Cell Motility and Neovessel Maintenance. *Vasc Cell* **2015**, *7*, 2. <https://doi.org/10.1186/s13221-014-0027-2>.
- (53) Bayless, K. J.; Johnson, G. A. Role of the Cytoskeleton in Formation and Maintenance of Angiogenic Sprouts. *J Vasc Res* **2011**, *48* (5), 369–385. <https://doi.org/10.1159/000324751>.
- (54) *Light-Regulated Angiogenesis via a Phototriggerable VEGF Peptidomimetic - Nair - 2021 - Advanced Healthcare Materials - Wiley Online Library.* <https://onlinelibrary.wiley.com/doi/full/10.1002/adhm.202100488> (accessed 2023-04-27).
- (55) Yadunandanan Nair, N.; Samuel, V.; Ramesh, L.; Marib, A.; David, D. T.; Sundararaman, A. Actin Cytoskeleton in Angiogenesis. *Biology Open* **2022**, *11* (12), bio058899. <https://doi.org/10.1242/bio.058899>.
- (56) Zhou, J. 9. Specificity and Sensitivity of Immunohistochemistry: In *9. Specificity and sensitivity of immunohistochemistry*; De Gruyter, 2017; pp 97–104. <https://doi.org/10.1515/9783110531398-009>.
- (57) Nowak-Sliwinska, P.; Alitalo, K.; Allen, E.; Anisimov, A.; Aplin, A. C.; Auerbach, R.; Augustin, H. G.; Bates, D. O.; van Beijnum, J. R.; Bender, R. H. F.; Bergers, G.; Bikfalvi, A.; Bischoff, J.; Böck, B. C.; Brooks, P. C.; Bussolino, F.; Cakir, B.; Carmeliet, P.; Castranova, D.; Cimpean, A. M.; Cleaver, O.; Coukos, G.; Davis, G. E.; De Palma, M.; Dimberg, A.; Dings, R. P. M.; Djonov, V.; Dudley, A. C.; Dufton, N. P.; Fendt, S.-M.; Ferrara, N.; Fruttiger, M.; Fukumura, D.; Ghesquière, B.; Gong, Y.; Griffin, R. J.; Harris, A. L.; Hughes, C. C. W.; Hultgren, N. W.; Iruela-Arispe, M. L.; Irving, M.; Jain, R. K.; Kalluri, R.; Kalucka, J.; Kerbel, R. S.; Kitajewski, J.; Klaassen, I.; Kleinmann, H. K.;

- Koolwijk, P.; Kuczynski, E.; Kwak, B. R.; Marien, K.; Melero-Martin, J. M.; Munn, L. L.; Nicosia, R. F.; Noel, A.; Nurro, J.; Olsson, A.-K.; Petrova, T. V.; Pietras, K.; Pili, R.; Pollard, J. W.; Post, M. J.; Quax, P. H. A.; Rabinovich, G. A.; Raica, M.; Randi, A. M.; Ribatti, D.; Ruegg, C.; Schlingemann, R. O.; Schulte-Merker, S.; Smith, L. E. H.; Song, J. W.; Stacker, S. A.; Stalin, J.; Stratman, A. N.; Van de Velde, M.; van Hinsbergh, V. W. M.; Vermeulen, P. B.; Waltenberger, J.; Weinstein, B. M.; Xin, H.; Yetkin-Arik, B.; Yla-Herttuala, S.; Yoder, M. C.; Griffioen, A. W. Consensus Guidelines for the Use and Interpretation of Angiogenesis Assays. *Angiogenesis* **2018**, *21* (3), 425–532. <https://doi.org/10.1007/s10456-018-9613-x>.
- (58) Piña, R.; Santos-Díaz, A. I.; Orta-Salazar, E.; Aguilar-Vazquez, A. R.; Mantellero, C. A.; Acosta-Galeana, I.; Estrada-Mondragon, A.; Prior-Gonzalez, M.; Martinez-Cruz, J. I.; Rosas-Arellano, A. Ten Approaches That Improve Immunostaining: A Review of the Latest Advances for the Optimization of Immunofluorescence. *International Journal of Molecular Sciences* **2022**, *23* (3), 1426. <https://doi.org/10.3390/ijms23031426>.
- (59) O’Hurley, G.; Sjöstedt, E.; Rahman, A.; Li, B.; Kampf, C.; Pontén, F.; Gallagher, W. M.; Lindskog, C. Garbage in, Garbage out: A Critical Evaluation of Strategies Used for Validation of Immunohistochemical Biomarkers. *Molecular Oncology* **2014**, *8* (4), 783–798. <https://doi.org/10.1016/j.molonc.2014.03.008>.
- (60) Nair, R. V.; Farrukh, A.; del Campo, A. Light-Regulated Angiogenesis via a Phototriggerable VEGF Peptidomimetic. *Advanced Healthcare Materials* **2021**, *10* (14), 2100488. <https://doi.org/10.1002/adhm.202100488>.
- (61) Nair, R. V.; Farrukh, A.; Campo, A. del. Light-Regulated Angiogenesis via a Phototriggerable VEGF Peptidomimetic. *Advanced Healthcare Materials* **2021**, *10* (14), 2100488. <https://doi.org/10.1002/adhm.202100488>.
- (62) Cao, G.; O’Brien, C. D.; Zhou, Z.; Sanders, S. M.; Greenbaum, J. N.; Makrigiannakis, A.; DeLisser, H. M. Involvement of Human PECAM-1 in Angiogenesis and in Vitro Endothelial Cell Migration. *American Journal of Physiology-Cell Physiology* **2002**, *282* (5), C1181–C1190. <https://doi.org/10.1152/ajpcell.00524.2001>.
- (63) Santulli, G.; Ciccarelli, M.; Palumbo, G.; Campanile, A.; Galasso, G.; Ziaco, B.; Altobelli, G. G.; Cimini, V.; Piscione, F.; D’Andrea, L. D.; Pedone, C.; Trimarco, B.; Iaccarino, G. In Vivo Properties of the Proangiogenic Peptide QK. *Journal of Translational Medicine* **2009**, *7* (1), 41. <https://doi.org/10.1186/1479-5876-7-41>.
- (64) Chan, T. R.; Stahl, P. J.; Li, Y.; Yu, S. M. Collagen-Gelatin Mixtures as Wound Model, and Substrates for VEGF-Mimetic Peptide Binding and Endothelial Cell Activation. *Acta Biomater* **2015**, *15*, 164–172. <https://doi.org/10.1016/j.actbio.2015.01.005>.

- (65) Pensa, N. W.; Curry, A. S.; Reddy, M. S.; Bellis, S. L. Sustained Delivery of the Angiogenic QK Peptide through the Use of Polyglutamate Domains to Control Peptide Release from Bone Graft Materials. *J Biomed Mater Res A* **2019**, *107* (12), 2764–2773. <https://doi.org/10.1002/jbm.a.36779>.
- (66) *Tethering QK peptide to enhance angiogenesis in elastin-like recombinamer (ELR) hydrogels* | SpringerLink. <https://link.springer.com/article/10.1007/s10856-019-6232-z> (accessed 2022-10-26).
- (67) Johnston, T. G.; Yuan, S.-F.; Wagner, J. M.; Yi, X.; Saha, A.; Smith, P.; Nelson, A.; Alper, H. S. Compartmentalized Microbes and Co-Cultures in Hydrogels for on-Demand Bioproduction and Preservation. *Nat Commun* **2020**, *11* (1), 563. <https://doi.org/10.1038/s41467-020-14371-4>.
- (68) Secretion of Recombinant Proteins from E. Coli. <https://doi.org/10.1002/elsc.201700200>.
- (69) Cleary, J.; Bromberg, L. E.; Magner, E. Diffusion and Release of Solutes in Pluronic-g-Poly(Acrylic Acid) Hydrogels. *Langmuir* **2003**, *19* (22), 9162–9172. <https://doi.org/10.1021/la034822w>.
- (70) Freudl, R. Protein Secretion in Gram-Positive Bacteria. *J Biotechnol* **1992**, *23* (3), 231–240. [https://doi.org/10.1016/0168-1656\(92\)90072-h](https://doi.org/10.1016/0168-1656(92)90072-h).
- (71) Müller, M.; Becher, J.; Schnabelrauch, M.; Zenobi-Wong, M. Nanostructured Pluronic Hydrogels as Bioinks for 3D Bioprinting. *Biofabrication* **2015**, *7* (3), 035006. <https://doi.org/10.1088/1758-5090/7/3/035006>.

## Conclusion and Outlook

This research shows the potential for the development of remotely controlled Engineered Living Materials (ELMs) that can induce angiogenic differentiation in human endothelial cells in a light-regulated manner. This was achieved by optogenetically engineering the endotoxin free bacteria (ClearColi) to synthesize and release a collagen-binding VEGF mimetic peptide fusion protein known as YCQ, in response to blue light stimulus. The engineered bacterial strain was securely encapsulated within bilayer hydrogel constructs. The study also demonstrates the potential to repeatedly activate and deactivate the release of YCQ over a span of 9 days, adjusting the quantity released by modulating intensities of light within the range of 1 – 20 nM over a 6-day period. The YCQ released during from liquid cell culture as well as from ELMs demonstrated its ability to bind effectively to Col-Gel matrices, mimicking the extracellular matrix (ECM) found in wounds that are healing. This binding led to the promotion of network formation in HUVEC cultures, providing clear evidence of the cells undergoing angiogenic differentiation. Importantly, it is noteworthy that the minimal leaky expression of YCQ in the absence of light was insufficient to induce such angiogenic differentiation. This observation underscores the successful control and regulation of the Engineered Living Materials (ELM) within the pertinent functional range of YCQ, validating its efficacy in targeted applications.

Moreover, the precision in fabricating bilayer ELMs and the protein release rate from them needs to be improved. Although we implemented strategies to avoid and minimize experimental errors, they can occur during manual fabrication of ELMs constructs leading to variabilities. Fabrication of ELMs can be automated by usage of 3D printing methods to minimize the errors in fabrication<sup>67</sup>; this will be explored in further studies in the group. The amount of YCQ released from ELMs is low and this is expected to be caused by two main reasons – (i) Secretion of proteins by *E. coli* is poor<sup>68</sup> (ii) the concentration of PluDa used for fabrication of ELMs is relatively high (30%) which might lead to slower diffusion of proteins from the ELM to its surrounding media.<sup>69</sup> Both the aspects will be dealt with in future studies by (i) usage of probiotic gram positive bacteria like lactic acid bacteria and *B. subtilis*, which are great secretors of protein<sup>70</sup> (ii) fabricating bilayer ELMs with lower concentration of polymer – PluDa or by introducing soluble fillers to increase porosity of the matrix.<sup>71</sup> Although there are limitations and the drugs release system can be improved, the results distinctively highlight that ELMs can

attain long term release and in-situ control over long term release of the pro-angiogenic protein.

# Priyanka Dhakane

Saarbrücken, 66123, Germany

priyanka.dhakane@leibniz-inm.de

## Professional Summary

### Experience

**Researcher- Material SynBio**, 1/2023 - Present

**INM-Leibniz Institute for New Materials** – Saarbrücken, Germany

- Developing mi-RNA based bacterial sensor for detection of Cervical Cancer

**PhD student - Bioprogrammable Materials**, 10/2018 – 12/2022

**INM-Leibniz Institute for New Materials** – Saarbrücken, Germany

- I developed Living therapeutic materials for the light-controlled release of angiogenesis promoting QK. I engineered *E. coli* to release QK in response to light and gained experience in the field of Engineered Living Materials by working on an interdisciplinary project that involves Synthetic Biology, Material Science and Cell Biology
- Supervised two Master students towards successful completion of their dissertation

**Freelance Biology Teacher**, 06/2016 – 08/2018

**Self-employed** – Mumbai, India

- worked as a freelance Biology teacher for trained students for all Indian medical entrance examination

**Research Assistant**, 06/2015 – 07/2016

**Indian Institute of Technology (IIT)** – Bombay, India

- worked on a project entitled Structural and functional basis of antibiotic biosynthesis regulation by TetR family proteins in *Streptomyces fradiae*. The project aimed at studying structure and function of five candidate genes and m-RNA expression profile in order to design the regulatory network.

**Master thesis**, 10/2014 – 06/2015

**Indian Institute of Technology (IIT) - Bombay** – Mumbai, India

- worked on elucidating the Role of transcription regulator, TyIP, in tylosin biosynthesis involved in *Streptomyces fradiae*. I learnt skills like Molecular Cloning, Protein purification, protein crystallography and Macro-molecular docking

### Education

**2015 St. Xavier's College - Autonomous** – Mumbai

**Masters in Biotechnology**

- GPA: 3.35 out of 4
- Courses taken: Genomes and Transcriptomes, Immunology, Membrane studies, Biochemistry, Metabolomics, Clinical Immunology, Drug designing, Nanotechnology Animal Cell Biotechnology, Developmental Biology, Bioinformatics, Research Methodology and Entrepreneurship

**2012 KET's V.G. Vaze College, University of Mumbai** – Mumbai

**Bachelor of Science Biotechnology**

- Score: 63.07% average of three years
- Molecular Biology, Medicinal Microbiology, Immunology, Cell Biology, Animal Cell Biology, Chemistry and Zoology

### Published work

Dhakane, P., Tadimarri, V.S. and Sankaran, S. (2023) 'Light-regulated Pro-angiogenic Engineered Living Materials', *Advanced Functional Materials*. doi:10.1002/adfm.202212695.

### Manuscript in preparation

- Priyanka Dhakane, Shrikrishnan Sankaran. "Photoswitchable ICAM for immunological synapse studies." 2022

### Conference presentations:

- Dhakane, Priyanka Zhang, Jingnan del Campo, Aránzazu Sankaran, Shrikrishnan. Photoswitchable ICAM1 for Immunological synapse studie. In: **Cell Physics 2021**, Saarland University . Saarland University ; 2021: 60 C.11.

- Dhakane, Priyanka Tadimarri, V.S.del Campo, Aránzazu Sankaran, Shrikrishnan. Living therapeutic materials to release angiogenesis-promoting QK that can bind to ECM collagen. **German Conference on Synthetic Biology (GCSB21) - Engineering Living Systems, September 13-17, 2021**, virtual
- Dhakane, Priyanka Tadimarri, V.S. del Campo, Aránzazu Sankaran, Shrikrishnan. Living therapeutic materials for sustained drug release. **Designer Biology Conference, September 8-10, 2021, virtual**
- Dhakane, Priyanka Sankaran, Shrikrishnan del Campo, Aránzazu. Streptomyces albus based living therapeutic materials for sustained drug release. **Synthetic Biology, September 12-13, 2019**, University
- Sankaran, Shrikrishnan Dhakane, Priyanka del Campo, Aránzazu. Bacterial confinement in hydrogels to develop living therapeutic materials. In: **Cell Physics 2019, October 9-11, 2019**, Saarland University . Saarland University ; 2019: 94 C.45.
- Sankaran, Shrikrishnan Dhakane, Priyanka, Shardul Dey, Sourik Blanch-Asensio, M.Riedel, FlorianTadimarri, Varun Saidel Campo, Aránzazu. Living therapeutic materials - hydrogel confined bacteria for smart drug delivery. **May 5, 2022, Bharathiar University Coimbatore**

## **Scientific Publications**

Dhakane, P., Tadimarri, V.S. and Sankaran, S. (2023) 'Light-regulated Pro-angiogenic Engineered Living Materials', *Advanced Functional Materials*. doi:10.1002/adfm.202212695

P. Dhakane, V. S. Tadimarri, S. Sankaran  
INM – Leibniz Institute for New Materials  
Campus D2 2, 66123 Saarbrücken, Germany  
E-mail: shrikrishnan.sankaran@leibniz-inm.de

P. Dhakane, V. S. Tadimarri  
Chemistry Department  
Saarland University  
66123 Saarbrücken, Germany  
The ORCID identification number(s) for the author(s) of this

Published in: *Advanced Functional Materials*

Doi: doi:10.1002/adfm.202212695

Published: 05 May 2023

Priyanka Dhakane: First author

- Conceptualization of the project
- Designed and performed the experiments
- Verified the analytical methods
- Troubleshooting and optimization of the protocols
- Visualized the next steps for better results
- Image processing and analysis
- Data Processing and analysis
- Trained the master student: VaunSai Tadimarri, supervised him personally in the lab while he was performing the experiments and troubleshooting of the results he got
- Writing and editing the original manuscript - Light-Regulated Pro-Angiogenic Engineered Living Materials - Dhakane - *Advanced Functional Materials* - Wiley Online Library.

<https://onlinelibrary.wiley.com/doi/full/10.1002/adfm.202212695>  
(accessed 2023-07-13).

Dr Shrikrishnan Sankaran: Corresponding author

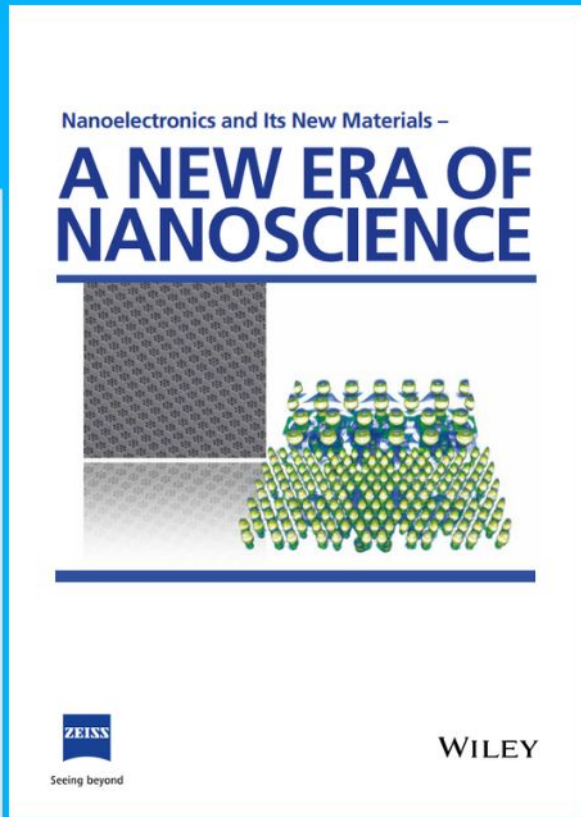
- Conceived the presented idea
- Encouraged the investigation
- Discussed the results
- Edited the manuscript

VarunSai Tadimarri: Second author

- Performed experiments to optimize the encapsulation and ELISA
- Discussion of the results



# Nanoelectronics and Its New Materials – A NEW ERA OF NANOSCIENCE



**Discover the recent advances in electronics research and fundamental nanoscience.**

Nanotechnology has become the driving force behind breakthroughs in engineering, materials science, physics, chemistry, and biological sciences. In this compendium, we delve into a wide range of novel applications that highlight recent advances in electronics research and fundamental nanoscience. From surface analysis and defect detection to tailored optical functionality and transparent nanowire electrodes, this eBook covers key topics that will revolutionize the future of electronics.

To get your hands on this valuable resource and unleash the power of nanotechnology, simply download the eBook now. Stay ahead of the curve and embrace the future of electronics with nanoscience as your guide.



Seeing beyond

**WILEY**

# Light-Regulated Pro-Angiogenic Engineered Living Materials

Priyanka Dhakane, Varun Sai Tadimarri, and Shrikrishnan Sankaran\*

Regenerative medicine aims to restore damaged cells, tissues, and organs, for which growth factors are vital to stimulate regenerative cellular transformations. Major advances have been made in growth factor engineering and delivery like the development of robust peptidomimetics and controlled release matrices. However, their clinical applicability remains limited due to their poor stability in the body and need for careful regulation of their local concentration to avoid unwanted side-effects. In this study, a strategy to overcome these limitations is explored using engineered living materials (ELMs), which contain live microorganisms that can be programmed with stimuli-responsive functionalities. Specifically, the development of an ELM that releases a pro-angiogenic protein in a light-regulated manner is described. This is achieved by optogenetically engineering bacteria to synthesize and secrete a vascular endothelial growth factor peptidomimetic (QK) linked to a collagen-binding domain. The bacteria are securely encapsulated in bilayer hydrogel constructs that support bacterial functionality but prevent their escape from the ELM. In situ control over the release profiles of the pro-angiogenic protein using light is demonstrated. Finally, it is shown that the released protein is able to bind collagen and promote angiogenic network formation among vascular endothelial cells, indicating the regenerative potential of these ELMs.

extracellular matrix (ECM) and interact with the receptors on the surfaces of other cells. These receptor-specific interactions trigger signal transduction pathways that promote events such as cell growth, proliferation, differentiation, cell migration, adhesion and survival.<sup>[2-4]</sup> For instance, vascular endothelial growth factor (VEGF), and platelet derived growth factor (PDGF) strongly stimulate blood vessel formation by activating integrin, NOTCH and WNT signaling for endothelial cell differentiation and increasing the permeability of endothelial cell layers.<sup>[5]</sup> Thus, growth factors are powerful tools in regenerative medicine. However, due to their potency in driving cellular transformations, their concentration and localization need to be carefully regulated. Failing to do so can cause overstimulation or off-site differentiation of cells, leading to necrosis or tumorigenesis.<sup>[6,7]</sup> This is exemplified by the long list of severe side-effects plaguing the few clinically approved growth factor-based medical products like PDGF-based Regnarex (side effects include increased risk of systemic cancer, skin rash and cel-

lulitis).<sup>[8]</sup> Apart from unwanted side effects, growth factors are also complex bulky proteins often with poor stability, making them expensive to produce, purify, store, and deliver at effective doses.<sup>[7,9]</sup> These technical challenges have thus far limited the clinical applicability of growth factor-based therapies despite over 3 decades of research demonstrating their potential.<sup>[10]</sup>

These issues are being addressed through 2 major strategies – i) use of drug release systems ensuring localized and controlled supply of the growth factor over time and ii) development of short and robust variants mimicking a desired function of the growth factors. This is particularly exemplified by advances in VEGF-based therapies. This growth factor plays a prominent role in stimulating the sprouting of new blood vessels from existing ones to supply oxygen to tissues suffering from hypoxia.<sup>[11,12]</sup> VEGF based therapies are being explored for peripheral vascular disease (PVD) that causes severe blockage of arteries of the lower extremities, leads to high limb amputation and mortality rates and generally results in poor prognosis.<sup>[13]</sup> In animal models of PVD, increasing VEGF levels to enhance collateral flow around blocked blood vessel has been achieved by intramuscular injection and vascular infusion of an adenoviral vector encoding VEGF.<sup>[14]</sup> Overexpression or overstimulation by VEGF in laboratory animals has been shown to lead to a variety of side-effects like formation of leaky vessels, metabolic dysfunction, transient edema, increase in atherosclerotic plaques and

## 1. Introduction

Regenerative medicine is a rapidly developing research field focused on accelerating the repair of damaged cells, tissues, and organs to restore normal function and circumvent the need for transplantation.<sup>[1]</sup> In healing processes, growth factors play a major role in stimulating cells and orchestrate transformations in them necessary for regeneration. They are proteins that are secreted by cells, can bind to the surrounding

P. Dhakane, V. S. Tadimarri, S. Sankaran  
INM – Leibniz Institute for New Materials  
Campus D2 2, 66123 Saarbrücken, Germany  
E-mail: shrikrishnan.sankaran@leibniz-inm.de

P. Dhakane, V. S. Tadimarri  
Chemistry Department  
Saarland University  
66123 Saarbrücken, Germany

 The ORCID identification number(s) for the author(s) of this article can be found under <https://doi.org/10.1002/adfm.202212695>.

© 2023 The Authors. Advanced Functional Materials published by Wiley-VCH GmbH. This is an open access article under the terms of the Creative Commons Attribution License, which permits use, distribution and reproduction in any medium, provided the original work is properly cited.

DOI: 10.1002/adfm.202212695

uncontrolled neoangiogenesis (increased risk of cancer).<sup>[15,16]</sup> Controlled release of VEGF through implantable devices is challenged by the protein's complexity and low serum stability, leading to high costs, low packing densities and poor control over its release.<sup>[17]</sup> Thus, despite its promise, clinical application of VEGF for PVD has been severely limited by these issues.<sup>[18,19]</sup>

A cheaper, shorter and more robust alternative to VEGF under investigation is the peptidomimetic, QK (KLTWQE-LYQLKYGI), that has been shown to promote formation and organization of capillaries both in vitro<sup>[20]</sup> and in vivo.<sup>[21]</sup> The peptide has higher potency to drive angiogenic morphogenesis in endothelial cells when immobilized on hydrogel matrices compared to its soluble form.<sup>[20,22]</sup> This mimics the activity of VEGF when immobilized to heparan sulphate in the ECM. Furthermore, such immobilization ensures that the pro-angiogenic activity is spatially confined. Recently, sustained release of QK from bone graft materials for up to 6 days was shown to induce angiogenic differentiation in vascular endothelial cells.<sup>[23]</sup> Thus, QK has shown great promise for promoting blood vessel formation similar to VEGF. For effective treatment of PVD with wide variabilities in disease profiles and progression among patients, it is desirable to develop a versatile strategy to deliver QK where and when it is required in a cost-effective manner.

Recently, a unique strategy to achieve low-cost and in situ controllable drug release has been explored in the form of engineered living materials (ELMs). In ELMs, living cells are combined with non-living materials to create composites with programmable and life-like capabilities.<sup>[24]</sup> ELMs for drug delivery have been made encapsulating within hydrogels, bacteria genetically engineered to produce and release drugs on demand, remotely controlled by external stimuli like chemical inducers or light. The bacteria in these ELMs are expected to thrive on nutrients available at the disease site and can be triggered to produce and secrete drugs at desired doses when needed. Using hydrogels made of agarose, Pluronic F127 or collagen and bacteria like *E. coli*, *L. lactis*, and *B. subtilis*, therapeutic ELMs have been made in the form of discs, films, patches and 3D printed structures to suit different therapeutic needs.<sup>[25–29]</sup> While most studies report the release of anti-microbial drugs from ELMs, one set of studies from the Salmeron-Sanchez lab demonstrates the release of BMP, controlled by a peptide-inducer, nisin.<sup>[27,30]</sup>

In this study, an ELM capable of in situ tunable release of a collagen-binding QK fusion protein is described. For the first time, we demonstrate light controlled release of an active growth factor peptidomimetic from ELMs fabricated in a secure bilayer encapsulation format that prevents bacterial escape/outgrowth.<sup>[31]</sup> We show that QK secretion can be sustained in a physiologically relevant range of concentrations (5 – 25 nM) for at least 9 days in a light-controlled manner and that it can induce angiogenic differentiation in endothelial cells.

## 2. Results and Discussion

### 2.1. Light-Responsive Production, Secretion, and Bioactivity of QK

For this study, *ClearColi*, an endotoxin-free variant of *E. coli*, was engineered to light-responsively synthesize and secrete a QK-bearing fusion protein (YCQ) as shown in Figure 1A.

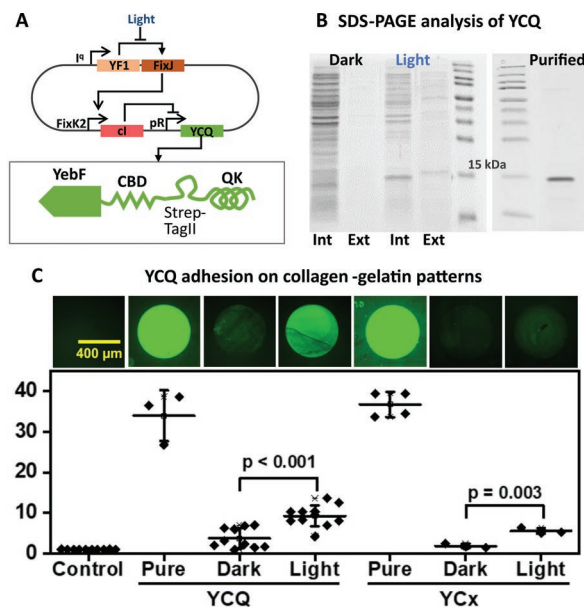


**Figure 1.** Design and activity of YCQ: A). Graphical representation of the pDawn-based optogenetic circuit for light-responsive production of YCQ along with scheme highlighting the different domains of the fusion protein. B). SDS-PAGE images of the intracellular (Int) and extracellular (Ext) fractions of light-regulated production and secretion of YCQ from engineered bacterial cultures, along with purified YCQ for comparison. C). Fluorescence microscopy images and pattern intensity quantification of the Col-Gel photopatterning assay to verify the ability of YCQ and YCx to adhere to collagen. Staining was done with an Anti-YebF primary antibody and a fluorescently labelled anti rabbit AF-488 secondary antibody. In the Control condition, the patterned Col-Gel surfaces were incubated with supernatants from unmodified *ClearColi* cultures exposed to light. The symbols in the graph represents the intensity of individual patterned spots from 2 independent experiments (N = 2). The intensities have been normalized to the mean of the control sample. Two sample t-tests were performed between YCQ dark/light and YCx dark/light data sets and p values are given above indicating that their differences are statistically significant.

This YCQ fusion protein contained i) YebF, a carrier protein aiding secretion from *E. coli*,<sup>[32,33]</sup> ii) a collagen-binding domain (CBD, sequence – WREPSFMVLS)<sup>[34]</sup> to facilitate immobilization of QK to the extracellular matrix, iii) a Strep-TagII peptide (WSHPQFEK) for purification and staining<sup>[35]</sup> and iv) the QK peptide. Notably, this design allowed for YebF to be at the N-terminal and QK at the C-terminal, which is necessary for their functionality. As a negative control, a similar fusion protein, YCx, was designed bearing a scrambled-QK peptide (GLKEQSPRKHRLG) at the C-terminal, previously shown to be inactive.<sup>[36]</sup> The gene corresponding to the 18.9 kDa YCQ or YCx protein was inserted into the multiple cloning site of an optogenetic plasmid, pDawn,<sup>[37]</sup> to achieve light responsive production and secretion. This was confirmed through SDS-PAGE by running the extracellular and cellular fractions from bacterial cultures grown either in white light or in the dark (Figure 1B). In the light exposed cultures, a band  $\approx$ 15 kDa was observed in both the cellular and extracellular fractions as well as after purification. This lower molecular weight was expected as a consequence of cleavage of the 2.2 kDa N-terminal signal peptide of YebF during its secretion into the periplasm through

the sec pathway. Western Blot analysis confirmed that this band contained the StrepII-tag (Figure S1, Supporting information). MALDI-TOF mass-spec analysis of the protein purified from the cellular fraction revealed a clear peak at 16.7 kDa confirming cleavage of the signal peptide suggesting that most of the intracellular protein resided in the periplasm (Figure S1, Supporting Information). These results confirmed that YCQ can be light-responsively produced and secreted from *ClearColi*. We proceeded to test the capability of the protein to bind collagen and trigger angiogenic differentiation in vascular endothelial cells. For these assays, we used a collagen-gelatin mixture (Col-Gel) in a 3:1 ratio by weight to form a thin film gel that has been reported to mimic the extracellular matrix in wounds where collagen is often degraded to remodel the tissue.<sup>[38]</sup> Binding of YCQ to collagen was verified by incubating the protein on a photo-patterned substrate of Col-Gel, after which it was immunostained using a primary antibody specific to YebF. Both purified and secreted YCQ and YCx were observed to preferentially adhere to Col-Gel patterned regions (Figure 1C). Analysis of the stained patterns revealed that the intensities of the patterned spots associated with proteins secreted in the presence of light were on average 2.5 fold higher than those cultured in the dark. However, the intensities of spots from light-state protein secretions were on average 3 to 7 fold lower than spots made with 10 nM purified proteins, suggesting that secretion from the overnight cultures was relatively low.

Next, we tested the ability of YCQ-bound Col-Gel matrices to induce angiogenic differentiation in Human Umbilical Vein Endothelial Cell (HUVEC) cultures using a network formation assay.<sup>[38]</sup> In this assay, Col-Gel matrices mimic disrupted collagen networks found in wounds and are used as model substrates to study angiogenesis-related events. A tell-tale sign of angiogenic differentiation in endothelial cells in 2D is the transformation of their culture from a monolayer into networks with larges gaps in between. Col-Gel matrices have been used to show that such network formation with HUVECs occurs in the presence of collagen-bound QK.<sup>[38]</sup> This assay can be used to identify genes and pathways that are involved in the promotion or inhibition of angiogenesis in a rapid, reproducible, and quantitative manner. In our study, cultures of bacteria that light-responsively secrete YCQ and YCx were grown in dark until they reached OD<sub>600nm</sub> of 0.5 and then under light or dark conditions overnight. Cell-free supernatants (SN) from these cultures were then collected, filter sterilized and incubated on Col-Gel surfaces for the proteins to bind with the matrix (Figure S2, Supporting Information). As positive controls, 10 nM of purified YCQ and 10 ng μL<sup>-1</sup> VEGF<sup>[39]</sup> were similarly incubated on the Col-Gel surfaces. When HUVECs were seeded on these Col-Gel surfaces, it was observed that those incubated with the negative control conditions of YCx dark, YCx light- and YCQ dark-state supernatants, cells retained monolayer cobblestone morphology over the same period (Figure 2). Additional control substrates incubated with unmodified ClearColi supernatants, pure YCx 10 nM, and pure YCQ 1 nM were also found to yield similar results (Figure S3, Supporting Information). On the other hand, those modified with light-activated YCQ supernatants, pure YCQ and VEGF promoted the cells to undergo a modest degree of network formation in 16 h. A much stronger and quicker (3 h) network formation was observed when the

Col-Gel matrices modified with a higher YCQ concentration of 100 nM (Figure S4, Supporting Information), similar to what has been observed by others.<sup>[39]</sup> This indicates that YCQ immobilized on Col-Gel matrices is able to promote network formation in HUVEC cultures but only to a modest degree at the concentrations released by the bacterial cultures. Immunostaining analysis revealed a moderate upregulation of PECAM-1 in cells that formed networks compared to the those that formed a monolayer (Figure 2). These features correlate with the initiation of the angiogenesis process, in line with previous reports.<sup>[40,41]</sup> All together, these results confirmed that YCQ performed the secretion, collagen-binding and angiogenesis functions it was designed for.

## 2.2. Engineered Living Material Design and Fabrication

To fabricate our ELMs, we encapsulated the bacteria in acrylate modified Pluronic F127 hydrogels, commonly used in medically relevant ELM reports.<sup>[31,42]</sup> ensure bacterial survival but prevent their escape to the surroundings, 30% wv<sup>-1</sup> Pluronic F127-diacrylate (PluDA) hydrogels were fabricated in a bilayer format, with bacteria encapsulated in a core layer and surrounded by a protective shell layer. To make the ELMs compatible for microscopy imaging and biochemical assays, they were made in the form of discs bonded to acryloxypropyl silane coated glass cover slips. These constructs were fabricated in a stepwise manner, wherein the bacterial gel was first formed on the glass then coated with the shell hydrogel (Figure 3A,B). Chemical cross-linking of the acrylate groups in the gels was done using a photo-initiator (Irgacure 2959) that could be activated using 365 nm light, which is orthogonal to the blue light required to activate YCQ production in the bacteria. The duration (1 min) and power (6 mW cm<sup>-2</sup>) of the 365 nm irradiation was selected based on a previous report<sup>[31]</sup> that identified conditions, which ensured complete cross-linking, while minimally affecting the bacteria. To ensure that the ELMs had well-defined and reproducible dimensions, ring-shaped PDMS moulds (Figure S5, Supporting Information) were used to form the core (dia 6 mm, h 0.8 mm) and shell (dia 13 mm, h 1.2 mm). In this format, the bacterial gel has a volume of almost 23 μL with an initial bacterial density of 0.1 OD<sub>600nm</sub>, resulting in an initial population of ≈10<sup>6</sup> bacterial cells (1 OD<sub>600nm</sub> = 8 × 10<sup>8</sup> cfu mL<sup>-1</sup> for *E. coli*). To test the performance of the ELMs in conditions suitable for mammalian cells, we decided to incubate them in HUVEC-compliant M199 medium. However, the bacteria were found to not grow in this medium, even in liquid culture. To support bacterial growth, the increasing glucose and sodium chloride concentrations were tested and the final concentrations in the medium were increased from 0.1 to 0.5% w/v for glucose and from 0.68 to 1.56% w/v for sodium chloride (Figure S5, Supporting Information). Incubation of the ELMs in this medium at 37 °C resulted in the entrapped bacteria growing from single cells to spherical colonies in 24 h (Figure 3C), in line with our previous reports studying bacterial growth in PluDA hydrogel constructs.<sup>[31,40]</sup> No leakage or outgrowth of the bacteria into the medium was observed for at least 15 days, verified by brightfield microscopy (Figure S6, Supporting Information). Bacterial colonies producing YCQ were stained with fluorescently labelled

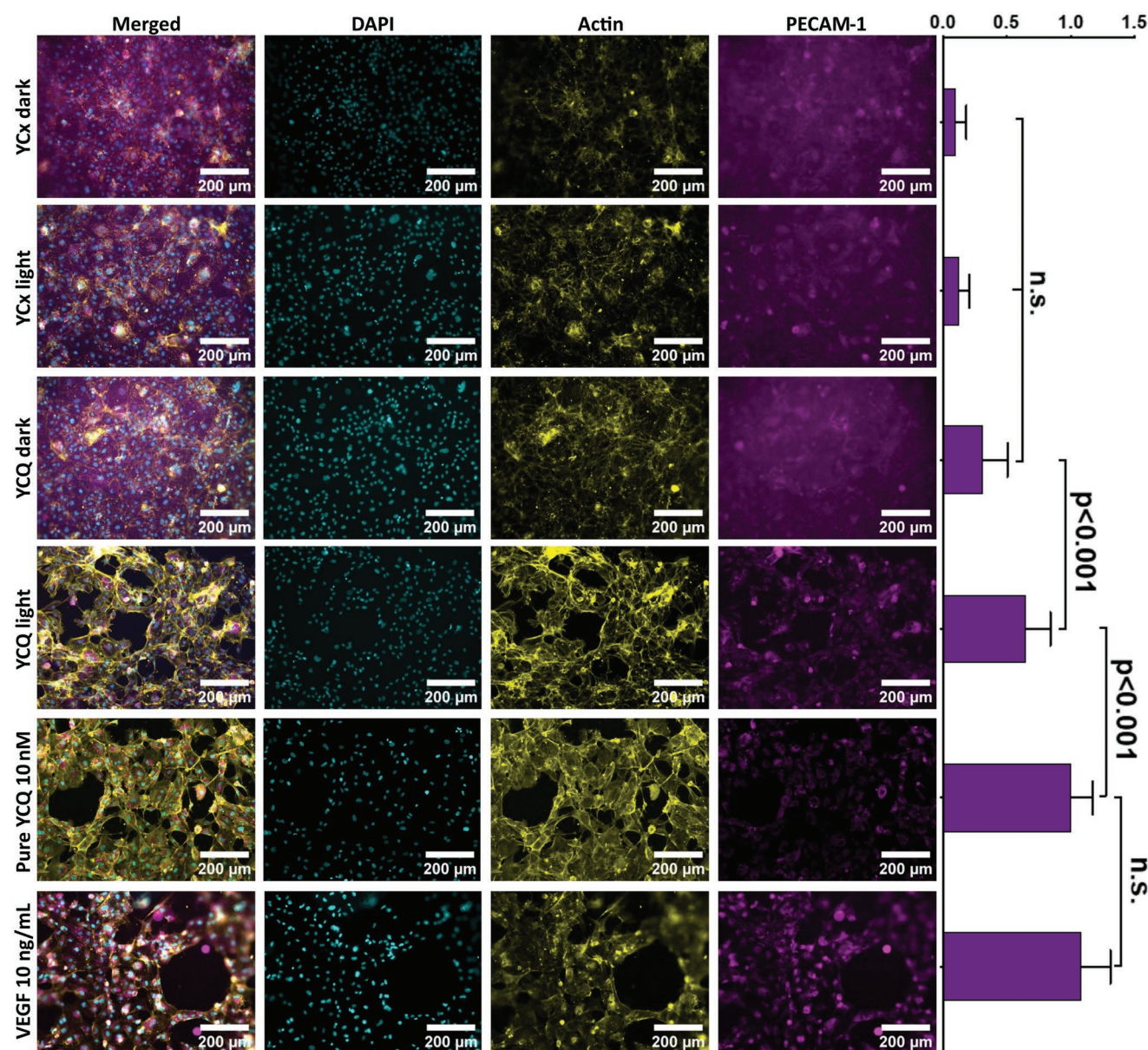


**Figure 2.** Fluorescence microscopy images of HUVECs grown for 16 h on Col-Gel surfaces incubated with supernatants of different bacterial cultures grown with or without light and with purified YCQ and VEGF as positive controls. The cells were stained for PECAM-1 (magenta), actin (yellow), and DNA (cyan). Brightness and contrast of each channel has been adjusted for optimal visualization. The graph represents intracellular PECAM-1 signal intensity after 16 h of seeding HUVECs from experimental duplicates. Bar lengths represent mean values and whiskers represent standard deviation from at least 2 experimental replicates and 2 images in each replicate. The data was normalized to the mean value of Pure YCQ 10 nM. ANOVA was performed to test for statistical significance of differences between different samples (n.s. = no significance).

streptavidin and could be observed as diffuse patches by fluorescence microscopy. These patches represent staining of high concentrations of secreted YCQ around the bacterial colonies (Figure 3D). In comparison, no such patches were observed in gels containing unmodified bacteria (Control).

### 2.3. Light-Regulated Release of Active YCQ from ELMs

Next, we tested the capability of switching and tuning YCQ release from the ELMs using light. After preparation, the

ELMs were incubated in dark at 28°C for 16 h, allowing the bacteria to grow into colonies before inducing them with light. Induction of protein expression was maintained by pulsed irradiation with blue light (2 s on, 1 min off, 450 nm wavelength, 200  $\mu\text{W}\cdot\text{cm}^{-2}$  power) (Figure 4A). The release of YCQ from these bilayer ELM constructs was quantified using a sandwich ELISA assay with a Streptactin-coated plate and a primary antibody specific to YebF (Figure S7, Supporting Information). To test the possibility of switching YCQ release ON and OFF, one set of constructs were exposed to blue light for 3 days and another set was left in the dark for the same time at

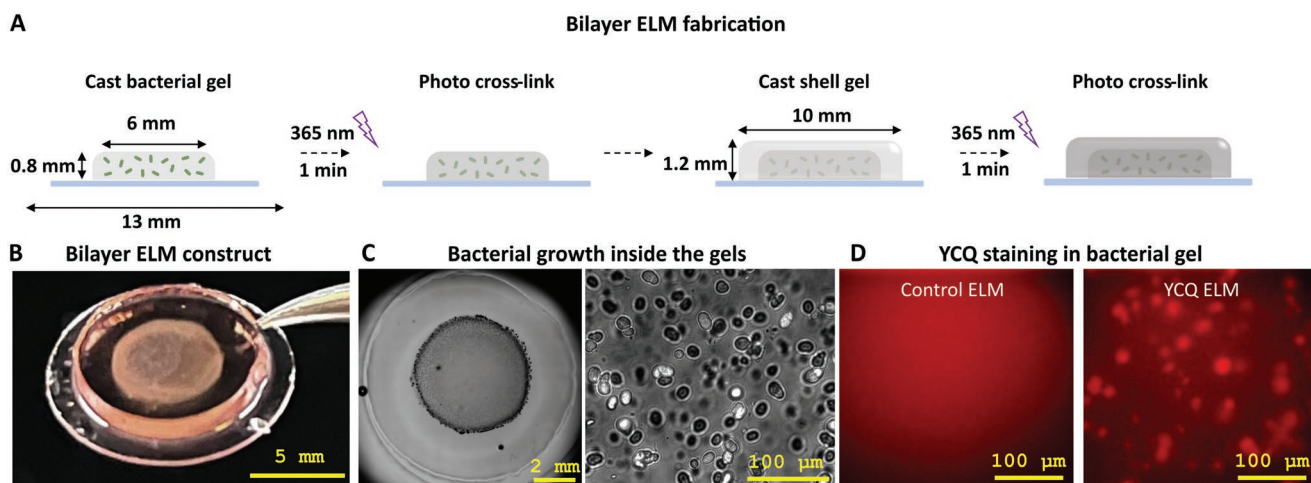


**Figure 3.** Engineered living material design and fabrication. A). Graphical representation of manual fabrication of ELM. The scheme depicts the steps involved in the making of the bilayer ELMs, along with relevant dimensions of the core and shell layers. B). Macroscopic image of the ELM held by a tweezer. C). Brightfield microscopy stitched image of the ELM with bacteria grown in the core layer (left) along with a magnified image of 6 day grown bacterial colonies. D). Qdot streptavidin staining of YCQ-producing ELM. *ClearColi* YCQ colonies are stained red indicating YCQ production within ELM; control ELM has unmodified *ClearColi*.

37 °C (Figure 4B). On day 3, YCQ quantification revealed that the amount released in light ( $\approx 1.4$  nM) was only slightly higher than what was released in the dark ( $\approx 0.6$  nM). The low level of YCQ release in light might be due to bacterial growth continuing to occur in the gel during this period or partial trapping of the protein in the gel, as previously reported by us.<sup>[31,43]</sup> After this, the ELMs that had been exposed to light pulses were placed in the dark and vice versa for another 3 days. At this point, a major difference in production levels were seen between ELMs exposed to light pulses ( $\approx 4$  nM) compared to those left in the dark ( $\approx 0.7$  nM). Once again, the irradiation conditions were switched for these ELM samples for another 3 days and it was clearly seen that those exposed to light pulses released considerably more YCQ in light ( $\approx 3.8$  nM) compared to those in dark ( $\approx 1.1$  nM). Furthermore, these results clearly

demonstrated that the ELMs could be switched from OFF to ON or ON to OFF state using light. To test the sensitivity of YCQ release to different light intensities, ELMs were induced with pulsed blue light (2 s on, 1 min off) with intensities of 0, 80, 105, or 125  $\mu\text{W cm}^{-2}$  for 6 days (Figure 4C). The media surrounding ELMs was collected on day 6 from Control (unmodified bacteria) and YCQ-releasing ELMs and was analyzed with ELISA (Materials and Methods Section: E, Figure S4, Supporting Information). ELMs kept in dark (0  $\mu\text{W cm}^{-2}$ ) released  $<1$  nM YCQ, those exposed to 80  $\mu\text{W cm}^{-2}$  released 8–15 nM, 105  $\mu\text{W cm}^{-2}$  released 14–19 nM, and 125  $\mu\text{W cm}^{-2}$  released 11–20 nM of YCQ (figure 4C). Statistical analysis (ANOVA) revealed significant differences in YCQ release between the 0, 80, and 105  $\mu\text{W cm}^{-2}$  conditions. This suggests that the ELMs are highly responsive to light within this range and precise

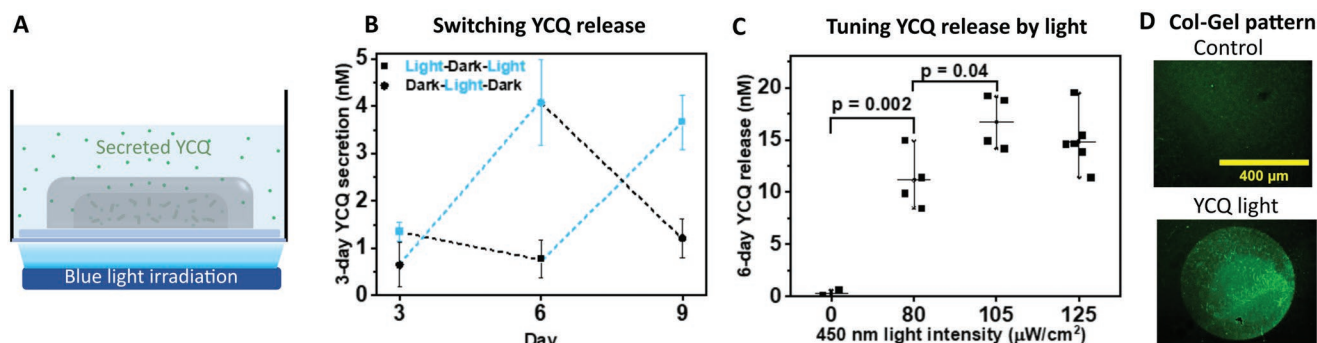


**Figure 4.** Light regulation of YCQ release from ELMs: A). Graphical representation of the ELM setup including blue light irradiation from below. The ELM constructs were placed in 24 well-plate wells containing 300  $\mu\text{L}$  of optimized M199 medium on top of an optowell device for pulsed irradiation at 450 nm (2 s On, 1 min OFF). B). Light switchable control over YCQ release from ELMs. The lines in blue represent durations when samples were placed in light and the lines in black represent durations when samples were placed in the dark. The first blue and black symbols at 3 days were placed in light and dark, respectively till the measurement was made. Symbols represent means values from individual ELM samples and whiskers represent standard deviation ( $N = 2, n = 2$ ). C). Tuneable release of YCQ by varying intensities of pulsed blue light irradiation from ELMs. Intensities of 0, 80, 105, and 125  $\mu\text{W cm}^{-2}$  were used. Symbols represent individual ELM samples; horizontal bars represent means and whiskers represent standard deviation. D). Fluorescence microscopy images of the Col-Gel photopatterning assay to verify the ability of ELM-secreted YCQ to adhere to collagen. Control refers to Col-Gel surfaces incubated with supernatants from unmodified *ClearColi* ELMs exposed to light.

control over release concentrations by light intensities could be achieved when the variance in the output from different constructs is minimized. We expect that experimental variabilities can be minimized by switching to an automated ELM fabrication method (e.g., 3D printing<sup>[28]</sup>) and increasing the rate of YCQ secretion, which has been discussed in the conclusions section. Furthermore, the increased variance and lower mean in the 125  $\mu\text{W cm}^{-2}$  condition compared to 105  $\mu\text{W cm}^{-2}$  suggests a possible detrimental effect of blue light on bacterial performance beyond this intensity. This is further supported by the low release concentrations observed in Figure 4B where a light intensity of 200  $\mu\text{W cm}^{-2}$  was used. While further optimization is possible, these results are evidence that YCQ release profiles can be remotely controlled in situ using light. Finally, using the Col-Gel patterning assay, we confirm that YCQ released from the light-irradiated ELM constructs are able to bind to these matrices (Figure 4D).

#### 2.4. Angiogenesis Promoting Capabilities of Light-Responsively Secreted YCQ

Next, we tested the bioactivity of YCQ released from the ELMs after 6 days of pulsed blue light irradiation at 105  $\mu\text{W cm}^{-2}$  and concentration >10 nM. As controls, ELMs containing unmodified bacteria and YC<sub>x</sub>-producing bacteria were also made. The supernatants from the ELMs were incubated with Col-Gel surfaces after which the network formation assay using HUVECs was performed. On 3 out of 4 Col-Gel surfaces incubated with light-exposed YCQ-releasing ELMs, HUVECs were seen to form networks in 16 h, while this did not occur in all other conditions, where HUVECs were seen to grow as monolayers with cobblestone morphology (Figure 5; Figure S8, Supporting Information). Notably, this cobblestone morphology was also seen on Col-Gel surfaces incubated with dark-state YCQ-releasing ELMs (<1 nM YCQ), indicating that the light-induced fold change of

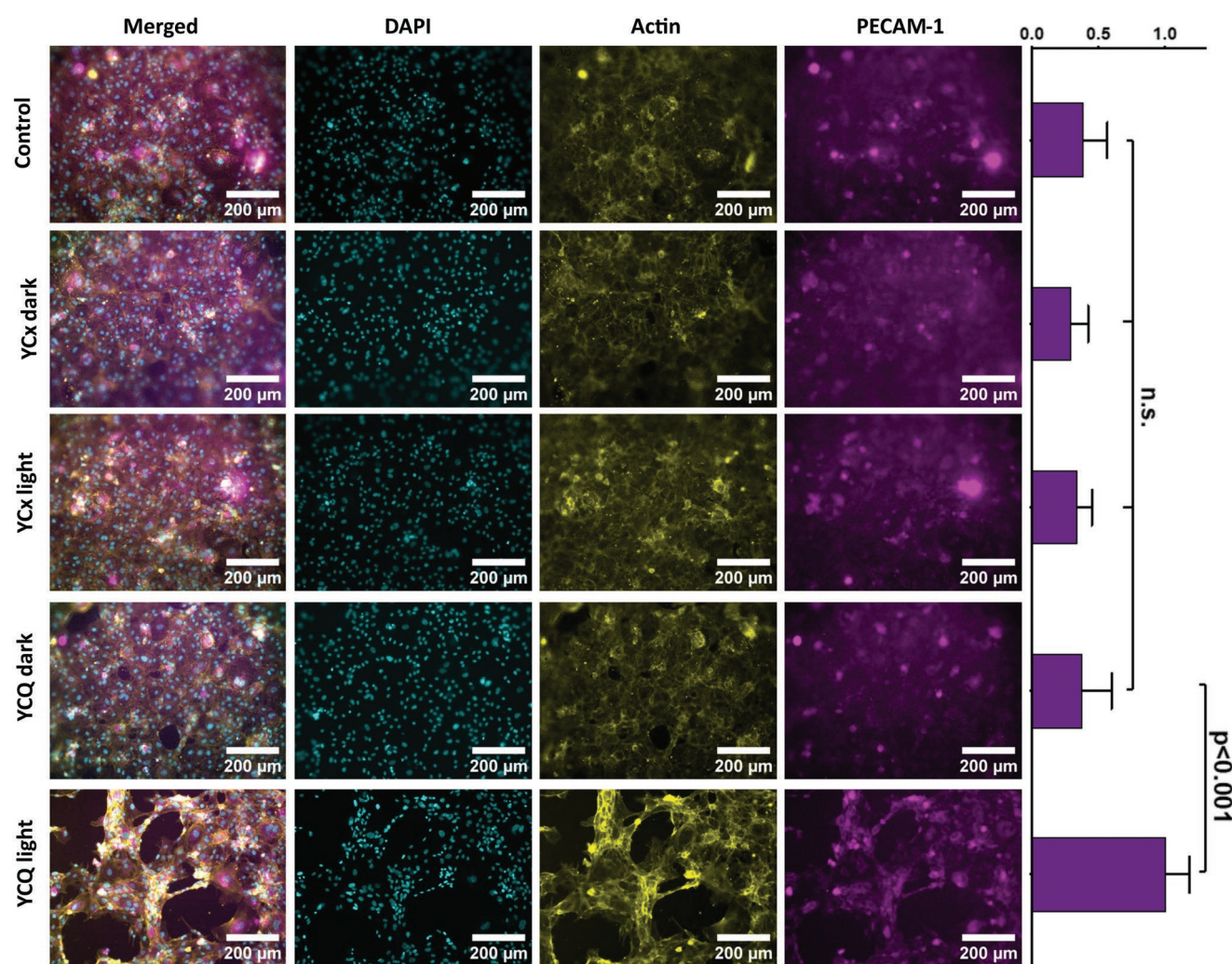


**Figure 5.** Epifluorescence images of HUVECs cultured for 16 h on Col-Gel surfaces that were incubated in supernatants from ELMs containing unmodified *ClearColi* (Control), YC<sub>x</sub>-expressing and YCQ-expressing bacteria kept in dark or exposed to blue light pulses (2 s ON, 1 min OFF; 105  $\mu\text{W cm}^{-2}$ ) for 6 days. The cells were stained for PECAM-1 (magenta), actin (yellow), and DNA (cyan). Brightness and contrast of each channel has been adjusted for optimal visualization. The graph represents intracellular PECAM-1 signal intensity after 16 h of seeding HUVECs from experimental triplicates (supernatant derived from 3 individual ELM constructs). Bar lengths represent mean values and whiskers represent standard deviation. The data was normalized to the mean value of YCQ light.

YCQ release was sufficient to elicit different responses from the HUVECs. Based on imaging of immunostained cells, the HUVECs that underwent network formation showed an increase in the expression PECAM-1 when compared to the control samples (Figure 5). While there are a few small regions in the control conditions like YCQ dark where the PECAM-1 fluorescence intensity is comparable to that in the YCQ light condition, the quantification reveals that the differences between these conditions are significant. This is a clear indication that the cells were undergoing angiogenic differentiation, in agreement with the results from previous reports.<sup>[40,44]</sup>

### 3. Conclusion

This study demonstrates the possibility to develop remote-controlled ELMs capable of promoting angiogenic differentiation of vascular endothelial cell cultures in a light regulated manner. This was realized by optogenetically engineering bacteria to produce and secrete a collagen-binding VEGF peptidomimetic fusion protein, YCQ, in response to blue light and securely encapsulating this strain in bilayer hydrogel constructs. With this ELM, we were able to demonstrate the possibility to repeatedly switch ON and OFF the release of YCQ up to 9 days and vary the amount released with different light intensities within the range of 1 – 20 nM in 6 days. The released YCQ was able to adhere to Col-Gel matrices that simulate the ECM of healing wounds and promote network formation in HUVEC cultures, indicating the cells underwent angiogenic differentiation. Notably, the negligible leaky expression of YCQ in dark was insufficient to promote such angiogenic differentiation, thereby validating the capability of controlling the ELM within relevant ranges of YCQ's functionality.

However, it is desirable to improve the precision and rate of protein released from these ELMs. Variabilities in the system are attributed to experimental errors that can arise during manual fabrication of the ELM constructs despite our strategies to minimize them. This can be further minimized using automated fabrication methods like 3D printing,<sup>[28]</sup> which will be explored in future studies. The low levels of protein release are expected to be caused by 2 factors – i) *E. coli* is a poor secretor of proteins<sup>[45]</sup> and ii) the PluDA hydrogels have a relatively high polymer content of 30%, possibly resulting in slow protein diffusion.<sup>[46]</sup> In future studies, both these aspects will be addressed by i) using gram-positive probiotic bacteria like *B. subtilis* or lactic acid bacteria, which are prolific at protein secretion<sup>[47]</sup> although their genetic toolboxes are poorly equipped compared to *E. coli* and ii) constructing bilayer hydrogels with lower polymer concentrations of PluDA or introducing soluble fillers that increase matrix porosity.<sup>[48]</sup> Despite these limitations, the results in this study clearly highlight the unique advantages that ELMs can offer for regenerative therapies in terms of long-term release of therapeutic proteins and in situ control over release profiles.

### 4. Experimental Section

**Construction of Plasmids and Bacterial Strains:** The YebF-CBD-strep-QK fragment (DNA sequence in Supporting information) was ordered

as gBlock from Eurofins Genomics, and inserted into the plasmid, pDawn (pDawn was a gift from Andreas Moeglich – Addgene plasmid# 43 796; <http://n2t.net/addgene:43796>; RRID:Addgene\_43 796) using NEBuilder® HiFi Assembly cloning kit (NEB, E5520S) using following primers-

pDawn Fwd 5'-ataaaagcttAACAAGCCCCGAAAGGAAG-3',  
pDawn Rev 5'-ctcttttttCATGGTATATCTCCTTCTTAAAGTTAAAC-3',  
YebF-CBD-QK Fwd-5'-ataaccatgAAAAAAGAGGGCGTTTTAG-3'  
YebF-CBD-QK Rev-5'-gggctttgTAAAGCTTTTATTCAGGGTC-3'.

This yielded the pDawn-YCQ plasmid which was then transformed into *ClearColi* BL21(DE3) electrocompetent cells as specified by the provider (BioCat 60810-1-LU). The recombinant pDawn-YCQ was used as a template to construct the pDawn YebF-CBD-Scrambled QK (YCx) mutant (DNA sequence in supporting information) using the NEBuilder® HiFi DNA Assembly Cloning Kit with the following primers:

pDawn Fwd 5'-CTAGCATAACCCCTTGGG-3',  
pDawn Rev 5'-CTAGTAGAGAGCGTTCAC C-3',  
YebF-CBD-Scrambled QK Fwd-5'-cggtgaacgctcttactagAGTCACACT  
GGCTCACCTTC-3'  
YebF-CBD-QK Scrambled Rev-5'-gccccaaggggttagctagTTATTGCTCA  
CGGGTGGC-3'.

pDawn-YCx was then transformed in *ClearColi* BL21(DE3) electrocompetent cells as specified by the provider. For storage at -80 °C, glycerol stocks with 30% of glycerol for both clones were made from bacterial cultures grown overnight at 37 °C, 250 rpm in the dark from single colonies.

**Bacterial culture for protein purification and secretion:** *ClearColi* BL21(DE3) pDawn-YCQ or pDawn-YCx cultures of 250 mL were grown in dark for 37 °C, 250 rpm in LB Miller medium supplemented with 50 µg mL<sup>-1</sup> of Kanamycin to an OD<sub>600nm</sub> between 0.4 and 0.8. The culture was then induced for 12 h by exposing it to white light for production of YCQ and YCx at 37 °C, 250 rpm

**Bacterial cultures for ELMs:** *ClearColi* BL21(DE3) cultures were grown for 16 h at 37 °C, 250 rpm in LB Miller medium supplemented with 50 µg mL<sup>-1</sup> of Kanamycin to an OD<sub>600nm</sub> ≈ 0.8. All procedures were performed either in the dark or under orange light.

**Purification of YCQ and YCx:** *ClearColi* BL21(DE3) with pDawn-YCQ or pDawn YCx were cultured in LB Miller medium supplemented with Kanamycin. YCQ/YCx production was induced with white light for 16 h. For harvesting the cells, cultures were transferred to 50 mL falcon tubes and centrifuged with an Avanti J-26S XP centrifuge (Beckman Coulter, Indianapolis, USA) using the JLA-10.500 rotor for 20 min at 4000 rpm and 4 °C. The supernatants were discarded and pellets weighed and stored at -80 °C until further use. For protein extraction, the bacterial pellets were thawed on ice and resuspended in a volume of lysis buffer (100 mM TrisCl pH8, 150 mM NaCl and 1 mM PMSF) having mL magnitude equivalent to 5x the cell pellet weight in g. To lyse the cells, a sonicator (Branson ultrasonics, Gehäuse SFX150) was used with sonication cycles having pulse "ON" for 3 s, "OFF" for 5 s at 20% power over 6–8 mins. The sonicated solutions were centrifuged at 14 000 rpm for 15 mins at 4 °C and the supernatants were collected for further purification by affinity-based column chromatography. Supernatants and cell debris were stored for analysis by Sodium dodecyl sulfate-polyacrylamide gel electrophoresis (SDS-PAGE). Since the proteins engineered with a StrepII-tag, columns containing Strep tactin beads (Quiagen, 30 004) were used for purification of the protein by affinity chromatography modifying the protocol given by the manufacturer (Quiagen) to optimize pure protein yields. 4 mL of the strep-tactin bead solution was pipetted into a 15 mL falcon tube and was centrifuged at 100 rpm for 2 mins to obtain a strep-tactin bed volume of 2 mL. The beads were washed three times with 5 mL of lysis buffer; the lysis buffer was removed each time by centrifuging the beads at 100 rpm for 2 mins. Cell lysate of 5 mL was added onto the strep tactin beads and this assembly was incubated at 4 °C on a rotary shaker for 30 mins to facilitate optimal contact between the beads and cell lysate. The beads were centrifuged at 100 rpm for 2 mins to remove the unbound protein and washed with 5 column volumes (CV) of wash buffer (100 Mm TrisCl, 150 Mm NaCl, and 0.5% tween 20) 3 times by adding 5 CV of wash buffer to the 15 mL falcon

and rotating it upside down manually each time; the wash buffer was removed each time by centrifugation of the beads at 100 rpm for 2 mins. The protein was eluted using an elution buffer (100 mM TrisCl, 150 mM NaCl, and 2.5 mM Desthiobiotin). The eluted protein was rebuffed in 5 volumes PBS pH 7 and concentrated by using 3 kDa-cutoff centrifugal filter units and centrifugation parameters – 4000 rpm for 45 mins at 4 °C. The protein yields for YCQ and YCx were in the range of 6 to 20 mg L<sup>-1</sup>.

**Patterning of Col-Gel Matrix on a Glass Surface to Assess Binding of YCQ:** Coating coverslips with PLL-PEG: Glass coverslips were cleaned by treating them with oxygen plasma in a plasma oven (Harrick Plasma, Ithaca, NY, USA) for 5 mins. 50 µL of 0.1 mg mL<sup>-1</sup> PLL-PEG (PLL (20)-g [3.5]-PEG (5), SuSoS AG, Dübendorf, Switzerland) solution in PBS was placed on a sheet of parafilm. The plasma-treated coverslips were inverted on the drop of PLL-PEG and incubated for 1 h at room temperature (RT).

**Cleaning of the photomask:** The patterned surface of the photomask was cleaned with acetone, water, ethanol, and water by dipping in each solution. It was air dried gently and placed in UVO cleaner (Jelight Company Inc, model no.42) for 5 min, in such a way that the patterned side faced up.

**Making patterns using the photomask:** After the incubation, the coverslip was released from the parafilm gently by infusing deionized water under the coverslip in such a way that it starts floating. It was rinsed by dipping the patterned surface 5 times in PBS pH 7 solution and dried by draining the excess solution onto a paper towel. 5 µL deionized water was placed on the patterned side of the photomask in order to reduce friction between the coverslip and patterned surface. The coverslip was carefully picked up with forceps and placed on the drop of water on the photomask. This assembly was placed in UVO cleaner for 5 mins in a way that the patterned surface in contact with the coverslip faces down. UV exposure cleaves PEG chains at the site of exposure on the glass coverslip. The coverslip was released gently by infusing 100 µL PBS pH 7 beneath it after which it was washed with PBS by dipping it in PBS 5 times. The coverslip was then placed on a 25 µL Col-Gel solution which was prepared by modifying a reported protocol.<sup>[38]</sup> All stock solutions were made in PBS pH 7. The gels were prepared by mixing 75% v/v of 600 µg mL<sup>-1</sup> collagen (gibco, A1048301), and 25% v/v of 600 µg mL<sup>-1</sup> gelatin (Sigma–Aldrich, 9000-70-8) solution. The two solutions were mixed by manually stirring with the pipette tip in the Eppendorf tube without pipetting it. The gels were allowed to polymerize at 37 °C, 5% CO<sub>2</sub> for 1 h followed by 4 °C incubation overnight. The coverslips were released from the parafilm surface by infusing 200 µL deionized water and washed by dipping them 10 times in 1X PBS with the help of a tweezer.

**Incubation of protein solutions and staining of the patterned surface:** Supernatants from overnight induced (light) and uninduced (dark) YCQ and YCx were collected by centrifuging the bacterial culture at 4000 rpm for 20 mins. The supernatants were filter sterilized using 0.4 µm syringe filters (Carl roth, SE2M230104). The coverslips with Col-Gel patterns were then incubated with either filtered supernatants or 10 nM purified solutions of YCQ and YCx by inverting the coverslips on 25 µL drops of the protein solutions. This assembly was incubated for one hour at RT. After the incubation, glass coverslips were released gently from the photomask by infusing 100 µL of PBS between glass surface and the parafilm. The coverslips were picked up with forceps and dipped in PBS 5 times to remove the unbound protein. The patterned glass surfaces with immobilized proteins were then incubated with anti-YebF primary antibody (Athena ES, AES-0313) by placing the patterned coverslip on 25 µL 1:500 diluted antibody (in 1% BSA) on parafilm. After incubation at RT for 1 h, the coverslips were released as mentioned before and all the patterned surfaces were then incubated with 1:500 diluted AF-488 Goat anti rabbit secondary antibody (ThermoFischer, A-11008) for 1 h at RT. Patterned surfaces were washed with PBS as mentioned before and were placed on a glass slide by placing 10 µL of PBS on the glass slide and inverting the patterned surface on it. YCQ or YCx stained Col-Gel patterns were visualized using a Nikon Ti-Eclipse microscope (Nikon Instruments Europe B.V., Germany).

**Fabrication of ELM:** Silanizing glass coverslips: Glass coverslips (13 mm) were arranged in a Teflon holder with a removable handle (custom made) for washing steps in a beaker. The Teflon holder with coverslips was suspended in a beaker with 99% ethanol and was sonicated for 10 mins. Then, it was washed with ultrapure water followed by 99% ethanol. The Teflon holder handle was removed and the base holding the cover slips was slid into a 50 mL falcon tube containing 20 mL of 95% ethanol, 4% ultrapure water, and 1% 3-APS (3-(Trimethoxysilyl)propyl acrylate, Sigma–Aldrich, 4369-14-6) such that coverslips were completely immersed in the solution. After incubation overnight at RT, the coverslips were washed 3 times with deionized water to remove excess APS and transferred into a beaker with ultrapure water and stored in it till further use.

**Preparation of Polydimethylsiloxane (PDMS) molds:** A beaker in which PDMS molds were to be made was sonicated for 3 mins with 99% ethanol in it. 10 g SYLGARD™ 184 silicone elastomer base (Dow chemicals, USA) was added to beaker on a weighing balance and (1 g SYLGARD™ 184 silicone elastomer curing agent (cross linker) (Dow chemicals, USA, 1 023 993) was also added and mixed thoroughly using a spatula. The Beaker with the PDMS-crosslinker mixture was placed in a vacuum-desiccator (DN 150 Duran) for up to 10 mins to remove air from the mixture. The beaker was then removed from the desiccator after confirmation of absence of bubbles in mixture. The volume of the PDMS mixture was calculated to obtain molds of dimensions depicted in Figure 2 and Figure S4 (Supporting Information) and poured into glass petri dishes. These were then placed in a hot air oven at 95 °C for 2 h for polymerization. They were taken out after 2 h and left undisturbed at room temperature overnight. Solidified PDMS molds were scraped out from glass flasks and holes of desired diameter were punched with pad punch set (BOEHRM, 832 100).

**Preparation of Pluronic diacrylate solution:** Pluronic diacrylate (PLU-DA) was obtained from the group of Prof. del Campo, who synthesized it as previously reported.<sup>[31]</sup> 30% w/v Pluronic diacrylate (PLU-DA) + 0.02% w/v IRGACURE 2959 (2-Hydroxy-4'-(2-hydroxyethoxy)-2-methylpropiophenone, Sigma–Aldrich, 410896-10G) solution was prepared for construct fabrication. 3 g PLU-DA and 20 mg IRGACURE 2959 photo initiator were dissolved in ultrapure water in an amber colored glass bottle and the final volume was adjusted to 10 mL. The PLU-DA solution was kept on a rotary shaker at 4 °C overnight for complete dissolution of contents. PLU-DA was stored in the same amber glass bottle at 4 °C until further use.

**Fabrication of ELMs:** Bacterial cultures of 5 mL at their exponential phase (OD<sub>600</sub> = 0.5–0.8) were centrifuged at 4000 rpm for 10 mins at room temperature. Pellets were resuspended in M199 cell culture media and was made up to an OD<sub>600</sub> of 1 after measuring it in a Nanodrop One device. Bacterial suspensions were prepared by mixing 90% v/v PLU-DA and 10% v/v bacterial culture (OD<sub>600</sub> = 1) such that the final density of bacteria in PLU-DA mixture was 0.1 OD<sub>600</sub>. Solutions containing PLU-DA were always handled on ice to prevent their physical gelation. 3-APS coated coverslips were placed on disinfected paraffin paper in a petri dish. A cylindrical PDMS mold with 6 mm diameter was placed on the coverslips with conformal contact. 22 µL bacterial gel solutions were pipetted into the PDMS molds to make a core layer of radius 3 mm and height of 0.7 mm. It was left undisturbed for 2 mins at room temperature for the PLU-DA to form a physical gel. The PDMS + coverslip setup was transferred to a Gel-Doc (Biozym Scientific GmbH, FluorChemQ) and the PLU-DA-Bacterial mixture was cross-linked by irradiating it with low intensity UV transillumination (365 nm) for a duration of 60 s. The whole setup was transferred back to a sterile hood and left undisturbed for 2 mins after which the PDMS mold was removed from the coverslip. A PDMS mold of 10 mm diameter was then placed on the same coverslip to produce a protective PLU-DA shell to prevent the leakage of bacteria from the ELM. 60 µL PLUDA was pipetted onto the PLU-DA bacterial core layer such that it formed a shell layer covering the entire surface of the core with a diameter of 10 mm and height of 1 mm. The PDMS and coverslip setup was transferred to the Gel-Doc and cross-linked by UV transillumination for a duration of 90 s. The whole setup was transferred back to the sterile hood and the PDMS mold was removed from the

coverslip. This ELM construct was transferred into a well in a 24-well plate and 300  $\mu\text{L}$  M199 cell culture media supplemented with additional 0.4% w/v glucose and 0.88% w/v NaCl was pipetted into the well. The 24-well plates with hydrogel constructs was placed in an incubator (28 °C) for 16 h in dark. For reversible light switching experiments: one 24-well plate was kept in light (blue light irradiation device; pulse: 2 s ON, 1 min OFF; 200  $\mu\text{W cm}^{-1}$ ) for 3 days and then moved to dark for 3 days followed by a period of light again for 3 days. The other 24 well plate was kept in dark for 3 days and then switched to light (same irradiation parameters as mentioned before) for 3 days followed by a period of dark for 3 days. Surrounding media was collected from each well after every 3 days and ELMs were replenished with 300  $\mu\text{L}$  fresh media. For light tuning experiments: the 24 well plate containing ELMs was kept on an optoWELL irradiation device (Opto biolabs), which was programmed to irradiate wells with blue light pulses (2 s ON; 1 min OFF, 450 nm) of intensities of 0, 80, 105 and 125  $\mu\text{W cm}^{-2}$  (corresponding to 3%, 6%, and 9% in the device settings) for 6 days. The volume of media surrounding ELM was decreased in 3 days from 300  $\mu\text{L}$  to 250  $\mu\text{L}$  due to evaporation. It was replenished by adding 50  $\mu\text{L}$  fresh media to it. The surrounding media containing secreted protein was collected at day 6 for quantification with ELISA (see point vi)

**Qdot Streptavidin staining of ELMs:** ELMs in 24-well plate wells was washed with PBS thrice. Qdot 655 Streptavidin conjugate (Thermo Fisher scientific, Germany, Q10121MP) was used to stain the hydrogels. The staining solution was prepared in the ratio of 1:500 in 2% w/v BSA. 300  $\mu\text{L}$  staining solution was added to each ELM construct and was incubated at 37 °C for 2 h. The well plate was completely wrapped with aluminum foil to avoid photobleaching during incubation. The antibody solution was pipetted out from wells and constructs were washed with 300  $\mu\text{L}$  PBS thrice. Then constructs were analyzed by Nikon epifluorescence microscope and overlay images of both brightfield as well as the 561 nm red channel were captured.

**Analysis of ELM supernatant by ELISA:** ELISA was performed using Strep-tactin coated 96 well plates (iba-life sciences) with the following protocol:

An initial blocking step was performed with 100  $\mu\text{L}$  of 2% w/v BSA added to the wells and the well-plate left overnight at 4 °C or for 1 h at 37 °C.

The wells were then washed by pipetting out the blocking solution and washing with 100  $\mu\text{L}$  wash buffer (PBS + 0.1% w/v Tween-20) thrice.

Samples of 100  $\mu\text{L}$  were added to the wells and left to incubate for 1 hour at room temperature followed by 3x washing step.

Another blocking step was performed where 100  $\mu\text{L}$  of 2% w/v BSA was added to wells and left for 1 h at room temperature followed by 3x washing step.

**Primary antibody treatment:** Rabbit Anti-YebF antibody (Athena enzyme systems, USA) was prepared in the ratio of 1:500 in 2% w/v BSA. 100  $\mu\text{L}$  antibody solution was added to wells and left at room temperature for 1 hour followed by 3x washing step.

**Secondary antibody treatment:** Goat anti-Rabbit IgG conjugated with horseradish peroxidase (Invitrogen) was used as secondary antibody in the ratio of 1:500 in BSA 1% w/v. Secondary antibody solution of 100  $\mu\text{L}$  was added to wells and left at room temperature for 1 hour followed by 4x washing step.

**Substrate treatment:** Tetramethylbenzidine (TMB) (Sigma-Aldrich, Germany) substrate of 100  $\mu\text{L}$  was added to each well and was left undisturbed until stable blue color developed.

**Stopping step:** 1 M Hydrochloric acid (HCl) of 100  $\mu\text{L}$  was added to wells to stop the reaction and it resulted in yellow coloration of solution which was measured within 30 mins.

The absorbance of test samples was measured at 450 nm by using *iControl 2000* software of Tecan plate reader and resulting data was analyzed.

Using serial dilutions of the purified proteins in the optimized M199 medium, a standard curve was plotted. The slope of this standard curve enabled determination of the molar concentrations of ELM-released YCQ or YCx.

**HUVEC Network Formation Assay:** Cell Culture Conditions: HUVECs (PromoCell, C-12205) were maintained on cell culture flasks coated

with gelatin (0.2% w/v). Cells were cultured in M199 medium (Sigma, M4530) supplemented with penicillin (1000 U L<sup>-1</sup>), streptomycin (100 mg L<sup>-1</sup>, Sigma), ECGS (Sigma, E2759), sodium heparin (Sigma, H-3393), and 20% w/v fetal bovine serum (FBS, Gibco, 10 270) as previously described.<sup>[40]</sup> HUVECs between passages 2 to 7 were used for the experiments.

**Preparation of Col-Gel surfaces:** Col-Gel surfaces were prepared as mentioned previously (Materials and Methods section C ii). This solution of 10  $\mu\text{L}$  was added into the 15 well angiogenesis well plates (ibidi, 81 506). The gels were allowed to polymerize at 37°C, 5% CO<sub>2</sub> for 1 h followed by overnight incubation at 4 °C.

**Immobilization of secreted YCQ on Col-Gel surfaces:** 10  $\mu\text{L}$  of the SN collected from ELMs were incubated on the Col-Gel surface for 1 h at 37°C in a CO<sub>2</sub> incubator. The supernatants were removed with a pipette and the Col-Gel surfaces were washed with 50  $\mu\text{L}$  PBS once to remove unbound proteins.

**HUVEC seeding:** (50  $\mu\text{L}$  of  $2 \times 10^5$  cells mL<sup>-1</sup>) HUVECs (P3-P7) were seeded on the Col-Gel surfaces and the plate was incubated at 37 °C and 5% CO<sub>2</sub> for 16 h. The culture was then fixed with 4% aqueous PFA solution for 15 mins, washed with PBS and blocked with 5% w/v BSA solution for 1 h. Cells were permeabilized with 0.1% w/v Triton X-100 for 15 mins and incubated with monoclonal goat anti-rabbit PECAM-1 primary antibody (1:500 in 1% w/v BSA, Abcam) overnight and washed with PBS. This was followed by incubation with anti-rabbit Alexa flour-488 secondary antibody (1:500 in water, Thermo Fisher Scientific) for 1 h. Subsequently, cells were washed with PBS and nuclei were stained with DAPI (1:500 in water, Life Technology) and actin fibers were labelled with TRITC-phalloidin (1:500 in water, Thermo Fisher Scientific). Samples were washed thrice with PBS and imaged with a Nikon epifluorescence microscope at 10X magnification using excitation wavelengths of 405 nm (900 ms excitation), 488 nm (100 ms excitation), and 565 nm (100 ms excitation) and 20% incident light intensity. Images were captured using NIS-Elements software and processed as follows for inclusion in the figures: Image processing and analysis was done using Fiji edition of ImageJ (Image J Java 1.8.0). Brightness and contrast for the DAPI (Cyan, 405 nm) and Actin (Yellow, 488 nm) were adjusted in their respective LUT histograms to the same range for all the images in an individual experiment. For PECAM-1, since Anti-PECAM-1 agglomeration at some places created bright spots to different degrees, the brightness and contrast in the LUT histograms were manually adjusted for each image based on the maximum intensity within the cells that were not caused by the agglomerates and the minimum intensity in the cell-free background. This way ensured best possible visualization of PECAM-1 expression in all the cells.

**PECAM-1 analysis – Fiji edition of ImageJ (ImageJ Java 1.8.0).** was used for quantification PECAM-1 fluorescence intensity. Quantification of the fluorescence intensities was done by determining the mean grey value within the cells excluding the bright spots created by agglomerates (by manual selection) and subtracting the mean grey value of the cell-free background.

**Statistical Analysis:** All image processing for quantification of PECAM-1 intensities was performed using the Fiji edition of ImageJ on Raw microscopy images. All data processing and analyses were done using Origin 2022 software. Details of sample sizes, replicates and statistical tests for quantified data were provided in the figure captions. Significant differences were determined by testing for the null hypothesis using a Two sample t-test when comparing 2 sample sets (Figure 1C) and using one-way ANOVA with the Tukey test for means comparison when comparing >3 samples sets (Figure 2, 4, and 5). The p values were given directly in the figures and p values above 0.05 were indicated as non-significant (n.s.) in Figures 2 and 5.

## Supporting Information

Supporting Information is available from the Wiley Online Library or from the author.

## Acknowledgements

The authors acknowledge support from the Leibniz Science Campus on Living Therapeutic Materials, LifeMat and the Deutsche Forschungsgemeinschaft's Collaborative Research Centre, SFB 1027. pDawn was a gift from Andreas Moeglich (Addgene plasmid# 43796; <http://n2t.net/addgene:43796>; RRID:Addgene\_43796). The authors thank Shardul Bhusari, Hafiz Syed Usama Bin Farrukh and Samuel Pearson (INM – Leibniz Institute for New Materials) for chemical synthesis of Pluronic F127 diacrylate and Claudia Fink-Straube (INM – Leibniz Institute for New Materials) and Klaus Hollemeyer (Saarland University) for performing the MALDI-TOF measurements.

Open access funding enabled and organized by Projekt DEAL.

## Conflict of Interest

The authors declare no conflict of interest.

## Data Availability Statement

The data that support the findings of this study are available from the corresponding author upon reasonable request.

## Keywords

angiogenesis, bacteria, engineered living materials, growth factor, optogenetics

Received: November 1, 2022

Revised: March 30, 2023

Published online: May 5, 2023

- [1] C. Mason, P. Dunnill, *Regener. Med.* **2008**, 3, 1.
- [2] R. Goldman, *Adv. Skin Wound Care* **2004**, 17, 24.
- [3] A. T. Grazul-Bilska, M. L. Johnson, J. J. Bilski, D. A. Redmer, L. P. Reynolds, A. Abdullah, K. M. W. Abdullah, *Drugs Today* **2003**, 39, 787.
- [4] M. Atanasova, A. Whitty, *Crit. Rev. Biochem. Mol. Biol.* **2012**, 47, 502.
- [5] P. Carmeliet, R. K. Jain, *Nature* **2011**, 473, 298.
- [6] H. M. Verheul, H. M. Pinedo, *Clin. Breast Cancer* **2000**, 1, S80.
- [7] R. N. Gacche, R. J. Meshram, *Biochim. Biophys. Acta* **2014**, 1846, 161.
- [8] P. Senet, *Ann. Dermatol.* **2004**, 131, 351.
- [9] X. Ren, M. Zhao, B. Lash, M. M. Martino, Z. G. F. E. S. f. R. M. A. Julier, *Front Bioeng. Biotechnol.* **2020**, 7.
- [10] A. W. Griffioen, A. C. Dudley, *Angiogenesis* **2022**, 25, 435.
- [11] M. Potente, H. Gerhardt, P. Carmeliet, *Cell* **2011**, 146, 873.
- [12] M. M. Martino, S. Brkic, E. Bovo, M. Burger, D. J. Schaefer, T. Wolff, L. Gürke, P. S. Briquez, H. M. Larsson, R. Gianni-Barrera, J. A. Hubbell, A. Banfi, *Front Bioeng. Biotechnol.* **2015**, 3, 45.
- [13] S. Takeshita, L. P. Zheng, E. Brogi, M. Kearney, L. Q. Pu, S. Bunting, N. Ferrara, J. F. Symes, J. M. Isner, *J. Clin. Invest.* **1994**, 93, 662.
- [14] I. Vajanto, T. T. Rissanen, J. Rutanen, M. O. Hiltunen, T. T. Tuomisto, K. Arve, O. Närönen, H. Manninen, H. Räsänen, M. Hippeläinen, E. Alhava, *J. Gene. Med.* **2002**, 4, 371.
- [15] W. Schaper, *Basic Res. Cardiol.* **2009**, 104, 5.
- [16] T. Karpanen, M. Bry, H. M. Ollila, T. Seppänen-Laakso, E. Liimatta, H. Leskinen, R. Kivelä, T. Helkamaa, M. Merentie, M. Jeltsch, K. Paavonen, L. C. Andersson, E. Mervaala, I. E. Hassinen, S. Ylä-Herttua, M. Oresic, K. Alitalo, *Circ. Res.* **2008**, 103, 1018.
- [17] G. Eelen, L. Treps, X. Li, P. Carmeliet, *Circ. Res.* **2020**, 127, 310.
- [18] S. E. Epstein, R. Kornowski, S. Fuchs, H. F. Dvorak, *Circulation* **2001**, 104, 115.
- [19] F. L. Celletti, J. M. Waugh, P. G. Amabile, A. Brendolan, P. R. Hilfiker, M. D. Dake, *Nat. Med.* **2001**, 7, 425.
- [20] J. E. Leslie-Barbick, J. E. Saik, D. J. Gould, M. E. Dickinson, J. L. West, *Biomaterials* **2011**, 32, 5782.
- [21] G. Santulli, M. Ciccarelli, G. Palumbo, A. Campanile, G. Galasso, B. Ziaco, G. G. Altobelli, V. Cimini, F. Piscione, L. D. D'Andrea, C. Pedone, B. Trimarco, G. Iaccarino, *J. Transl. Med.* **2009**, 7, 41.
- [22] T. Flora, I. G. de Torre, M. Alonso, J. C. Rodríguez-Cabello, *J. Mater. Sci.: Mater. Med.* **2019**, 30, 30.
- [23] N. W. Pensa, A. S. Curry, M. S. Reddy, S. L. Bellis, *J. Biomed. Mater. Res., Part A* **2019**, 107, 2764.
- [24] A. Rodrigo-Navarro, S. Sankaran, M. J. Dalby, A. del Campo, M. Salmeron-Sanchez, *Nat. Rev. Mater.* **2021**, 6, 1175.
- [25] S. Sankaran, A. del Campo, *Adv. Biosyst.* **2019**, 3, 1800312.
- [26] S. Sankaran, J. Becker, C. Wittmann, A. del Campo, *Small* **2019**, 15, 1804717.
- [27] J. J. Hay, A. Rodrigo-Navarro, M. Petaroudi, A. V. Bryksin, A. J. García, T. H. Barker, M. J. Dalby, M. Salmeron-Sanchez, *Adv. Mater.* **2018**, 30, 1804310.
- [28] T. G. Johnston, S.-F. Yuan, J. M. Wagner, X. Yi, A. Saha, P. Smith, A. Nelson, H. S. Alper, *Nat. Commun.* **2020**, 11, 563.
- [29] L. M. González, N. Mukhitov, C. A. Voigt, *Nat. Chem. Biol.* **2020**, 16, 126.
- [30] J. J. Hay, A. Rodrigo-Navarro, K. Hassi, V. Moulisova, M. J. Dalby, M. Salmeron-Sanchez, *Sci. Rep.* **2016**, 6, 21809.
- [31] S. Bhusari, S. Sankaran, A. del Campo, *Adv. Sci.* **2022**, 9, 2106026.
- [32] G. Zhang, S. Brox, J. H. Weiner, *Nat. Biotechnol.* **2006**, 24, 100.
- [33] Protein Production Method Utilizing Yebf, August 12, **2005**, <https://patents.google.com/patent/EP1791961A1/en>.
- [34] J. A. Andrades, B. Han, J. Becerra, N. Sorgente, F. L. Hall, M. E. Nimni, *Exp. Cell Res.* **1999**, 250, 485.
- [35] T. G. M. Schmidt, A. Skerra, *Nat. Protoc.* **2007**, 2, 1528.
- [36] A. H. Van Hove, E. Antonienko, K. Burke, E. Brown, D. S. W. T. T. Benoit, *Adv. Healthcare Mater.* **2015**, 4, 2002.
- [37] R. Ohlendorf, R. R. Vidavski, A. Eldar, K. Moffat, A. Möglich, *J. Mol. Biol.* **2012**, 416, 534.
- [38] T. R. Chan, P. J. Stahl, Y. Li, S. M. Yu, *Europe PMC* **2015**, 15, 164.
- [39] S. P. Cartland, S. W. Genner, A. Zahoor, M. M. Kavurma, *Int. J. Mol. Sci.* **2016**, 17, 2025.
- [40] R. V. Nair, A. Farrukh, A. d. Campo, *Adv. Healthcare Mater.* **2021**, 10, 2100488.
- [41] Y. Zheng, Z. Chen, Q. Jiang, J. Feng, S. Wu, A. d. Campo, *Nanoscale* **2020**, 12, 13654.
- [42] X. Liu, H. Yuk, S. Lin, G. A. Parada, T.-C. Tang, E. Tham, C. de la Fuente-Nunez, T. K. Lu, X. Zhao, *Adv. Mater.* **2018**, 30, 1704821.
- [43] S. Bhusari, J. Kim, K. Polizzi, S. Sankaran, A. del Campo, *Biomater Adv* **2023**, 145, 213240.
- [44] G. Cao, C. D. O'Brien, Z. Zhou, S. M. Sanders, J. N. Greenbaum, A. Makrigiannakis, H. M. DeLisser, *Am. J. Physiol.-Cell Physiol.* **2002**, 282, C1181.
- [45] G. R. M. Kleiner-Grote, J. M. Risse, K. Friehs, *Eng. Life Sci.* **2018**, 18, 532.
- [46] J. Cleary, L. E. Bromberg, E. Magner, *Langmuir* **2003**, 19, 9162.
- [47] R. Freudl, *J. Biotechnol.* **1992**, 23, 231.
- [48] M. Müller, J. Becher, M. Schnabelrauch, M. Zenobi-Wong, *Biofabrication* **2015**, 7, 035006.

# ADVANCED FUNCTIONAL MATERIALS

## Supporting Information

for *Adv. Funct. Mater.*, DOI: 10.1002/adfm.202212695

Light-Regulated Pro-Angiogenic Engineered Living  
Materials

*Priyanka Dhakane, Varun Sai Tadimarri, and  
Shrikrishnan Sankaran\**

# Supplementary information

## Light-regulated pro-angiogenic engineered living materials

Priyanka Dhakane,<sup>1,2</sup> Varun Sai Tadimarri,<sup>1,2</sup> Shrikrishnan Sankaran<sup>1</sup> \*

Affiliations

<sup>1</sup>INM – Leibniz Institute for New Materials, Campus D2 2, 66123 Saarbrücken, Germany

<sup>2</sup>Chemistry Department, Saarland University, 66123 Saarbrücken, Germany

\*Corresponding author

Email: shrikrishnan.sankaran@leibniz-inm.de

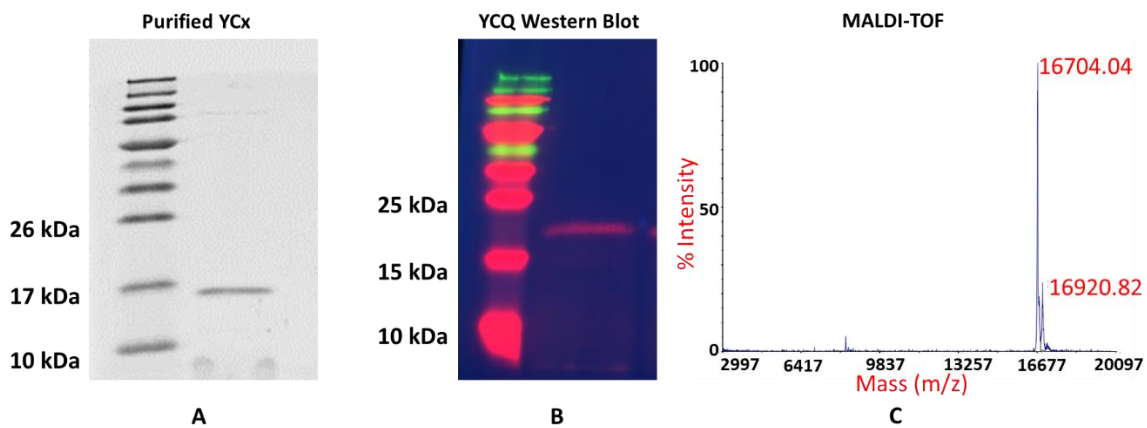
### Gene sequence of YCQ : YebF-CBD-Streptag-QK

```
GTTTAACTTTAAGAAGGAGATATACCATGAAAAAAGAGGGGCGTTTTTAGGGCTGTTGTTGGTTTC
TGCCTGCGCATCAGTTTTTCGCTGCCAATAATGAAACCAGCAAGTCGGTCACTTTCCCAAAGTGTGAA
GATCTGGATGCTGCCGGAATTGCCGCGAGCGTAAAACGTGATTATCAACAAAATCGCGTGGCGCGT
TGGGCAGATGATCAAAAAATTGTCGGTCAGGCCGATCCCGTGGCTTGGGTGAGTTTGCAGGACATT
CAGGGTAAAGATGATAAATGGTCAGTACCGCTAGCCGTGCGTGGTAAAAGTGCCGATATTCATTAC
CAGGTCAGCGTGGACTGCAAAGCGGGAATGGCGGAATATCAGCGGCGTGGTACCACTGGAGGATG
GCGCGAACCGAGCTTTATGGTGTGAGCGGCGGCGGTTCCGGGTCCGGATCCGGATCATGGAGCC
ACCCGCAATTTGAGAAAGGCTCGGGCTCGGGGAGTGGAAGTGATATTGGCAAATATAAACTGCAGT
ATCTGGAACAGTGGACCCTGAAATAAAAGCTTAACAAA
```

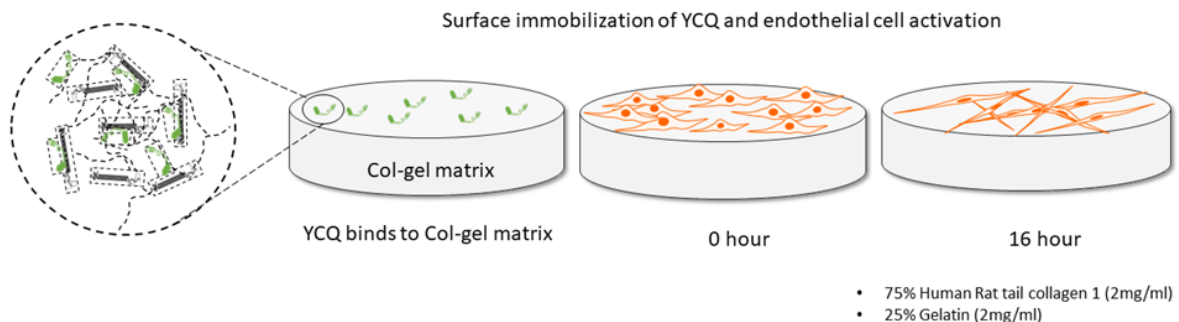
### Gene sequence of YCx: YebF-CBD-Streptag-QK

```
AAGGAGATATACCATGAAAAAAGAGGGGCGTTTTTAGGGCTGTTGTTGGTTTCTGCCTGCGCATC
AGTTTTTCGCTGCCAATAATGAAACCAGCAAGTCGGTCACTTTCCCAAAGTGTGAAGATCTGGATGCT
GCCGGAATTGCCGCGAGCGTAAAACGTGATTATCAACAAAATCGCGTGGCGGTTGGGCAGATGAT
CAAAAAATTGTCGGTCAGGCCGATCCCGTGGCTTGGGTGAGTTTGCAGGACATTCAGGGTAAAGAT
GATAAATGGTCAGTACCGCTAGCCGTGCGTGGTAAAAGTGCCGATATTCATTACCAGGTCAGCGTG
GACTGCAAAGCGGGAATGGCGGAATATCAGCGGCGTGGTACCACTGGAGGATGGCGCGAACCGAG
CTTTATGGTGTGAGCGGCGGCGGTAGTGGTAGTGGTAGTGGTAGTTGGAGCCACCCGCAATTTGA
GAAAGGCTCGGGCTCGGGGAGTGGAAGTGGCTTACGTCATAAGCGTCCGTCAAGAGAAATTGG
GTTAAAAGCTTAAC
```

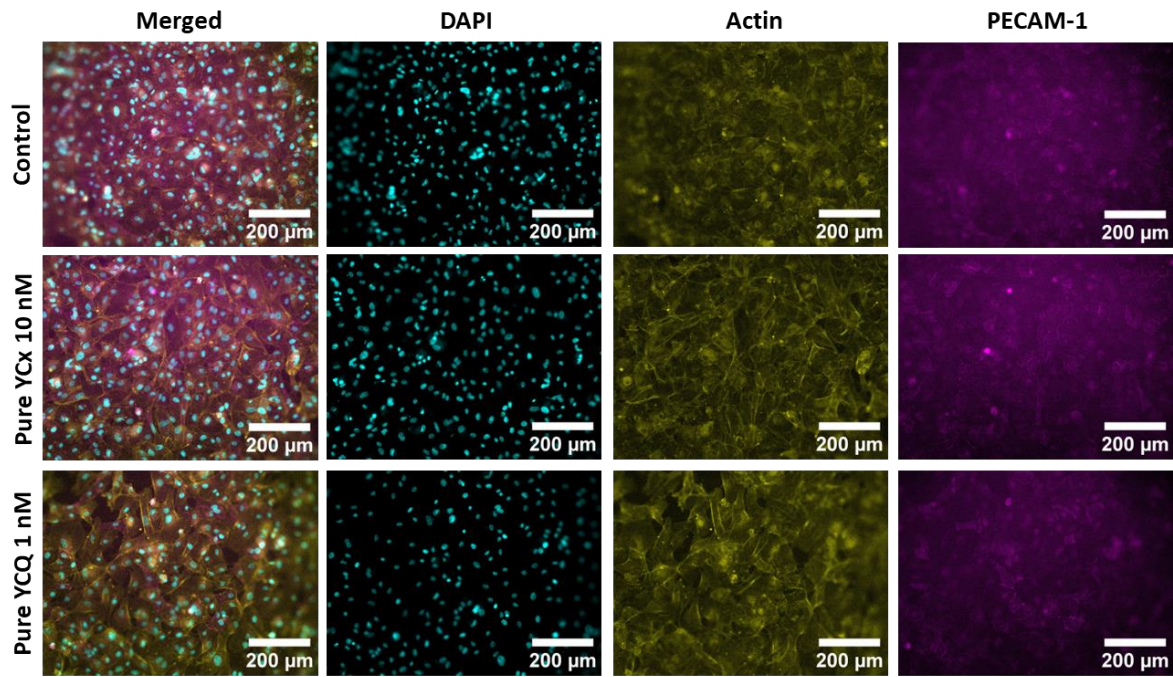
**SDS-PAGE and Western Blot:** YCx and YCQ proteins were purified from 250 mL cultures as mentioned in the Materials and Methods section and 5  $\mu$ L Laemmli 4x buffer was mixed with 15 $\mu$ L of the both the proteins and heated at 95°C for 5 min. 10  $\mu$ L of this was loaded on separate 15% SDS gels and run at 120 V for 60 min. YCx gel was Biosafe Coomassie (Bio-Rad) stained. YCQ gel was wet blotted to a PVDF membrane (Merck Millipore) with Mini Trans-Blot Cell (Bio-Rad) at 100V for 1h. Qdot streptavidin (Thermo Fisher scientific, Germany, Q10121MP) staining was performed with SNAP i.d. 2.0 (Millipore). diluted 1:500 in PBST. Pictures were taken in RGB multiplex mode of Fluorchem Q imager.



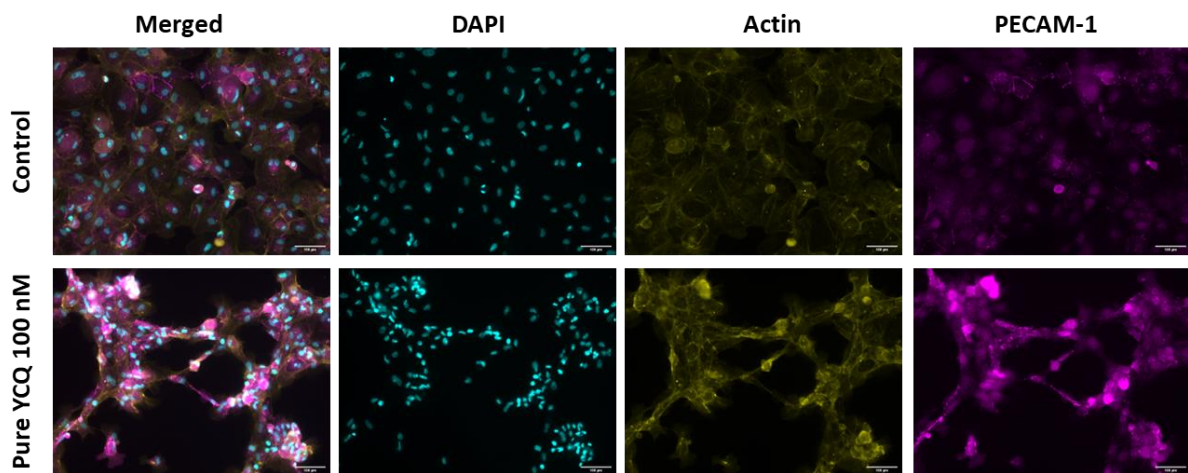
**Figure S1:** A. Purified YCx on 15% Polyacrylamide gel B. Western Blot for confirmation of YCQ. YCQ was stained with fluorescently labelled Q dot streptavidin (red) C. MALDI-TOF MS spectrum of purified YCQ protein; sharp peak at 16.704 kDa confirms the size of YCQ protein after sec-leader peptide cleavage.



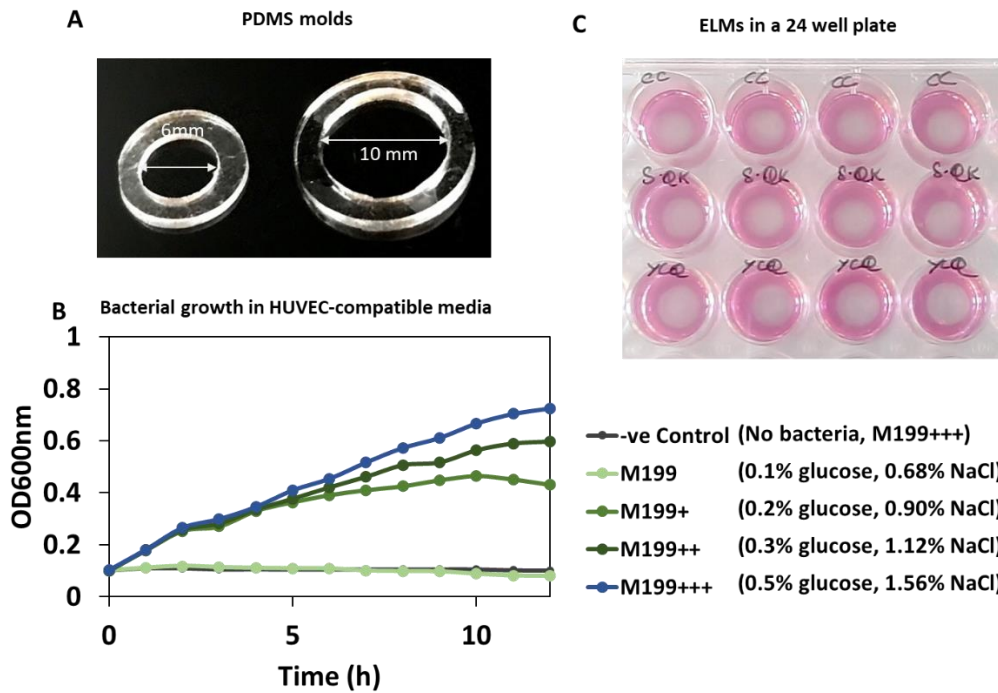
**Figure S2:** Col-Gel wound healing model for promotion of angiogenesis in HUVECs. YCQ is immobilized on the surface of col-gel gels. HUVECs undergo morphological change and from cell networks within 16 hours of seeding the on the col-gel YCQ gels



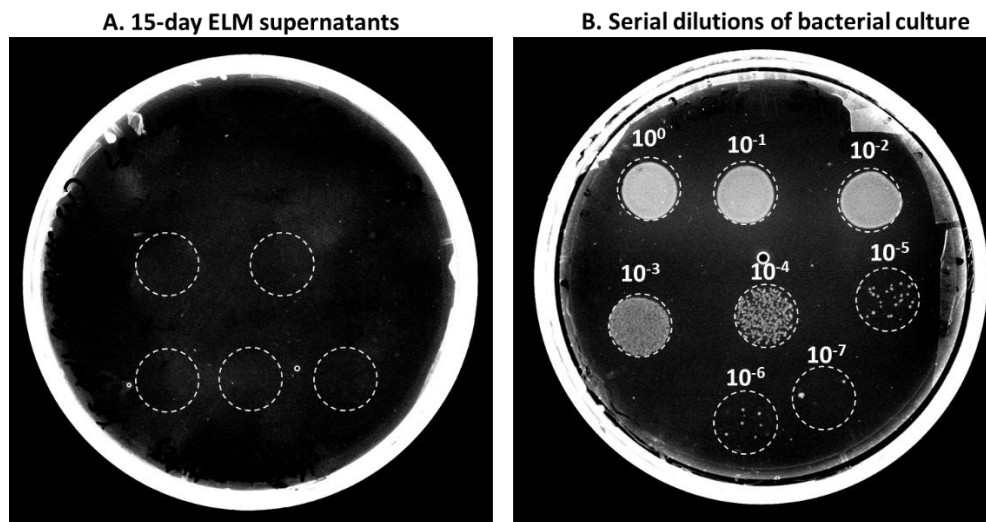
**Figure S3:** Epifluorescence images of HUVECs after 16 h of incubation on col-gel surfaces functionalized with unmodified *ClearColi* liquid culture supernatant (Control), pure YCx 10 nM, and pure YCQ 1nM supernatants. HUVECs are labelled with PECAM-1 antibody (magenta), DAPI (cyan) to stain the nucleus and Phalloidin-AF488 (yellow) to stain actin fibres. Channel brightness and contrasts were adjusted for optimal visualization.



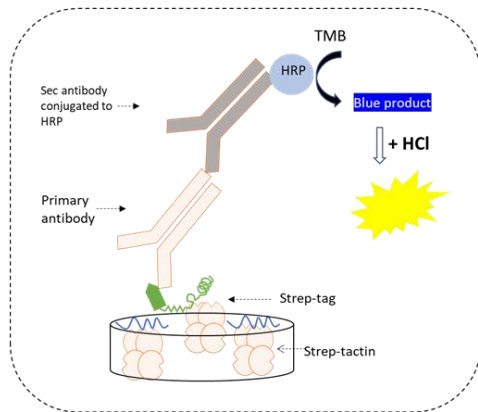
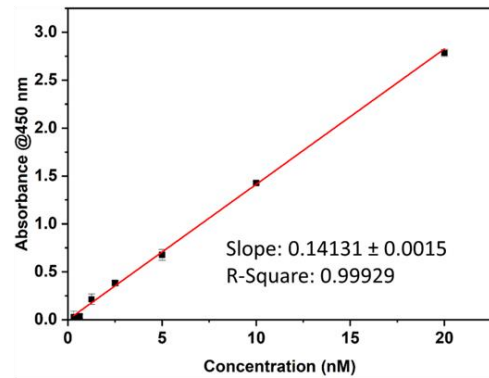
**Figure S4:** Epifluorescence images of HUVECs after 3 h of incubation on col-gel surfaces functionalized with unmodified *ClearColi* culture supernatant (Control) and pure YCQ 100 nM. HUVECs are labelled with PECAM-1 antibody (magenta), DAPI (cyan) to stain the nucleus and Phalloidin-AF488 (yellow) to stain actin fibres.



**Figure S5:** A. PDMS molds for ELM fabrication B. Bacterial growth ( $OD_{600nm}$ ) measurement in liquid cultures of HUVEC-compatible media at 37 °C in a microplate reader. All values are means of technical triplicates (standard deviations were negligible). C. ELMs in a 24 well plate suspended in growth supporting media



**Figure S6:** Agar plating method to detect potential leakage of bacteria from ELM constructs. A. Supernatants from 15-day old ELM constructs were collected, 20  $\mu$ L of them were spotted on an LB-NaCl agar plate (white dashed circles) and incubated for 24 h at 37 °C. The absence of colonies indicates that no leakage has occurred. B. Serial dilutions of a bacterial culture were made to test the sensitivity of this assay. The bacterial culture had an initial  $OD_{600nm}$  of 1 and labels above the white dashed circles indicate the degree of dilution. Since 1  $OD_{600nm}$  corresponds to approximately  $8 \times 10^8$  CFU/mL, the assay is sensitive enough to detect bacterial densities down to 8 CFU/mL.

**A Representation of ELISA for detection of YCQ****B Standard curve for YCQ quantification**

**Figure S7:** A. Representation of ELISA for quantification of YCQ. YCQ was immobilized on the surface of strep-tactin coated 96 well plates and stained with rabbit anti-YebF primary antibody followed by AF-488 goat anti rabbit secondary antibody. B. ELISA standard curve for YCQ quantification

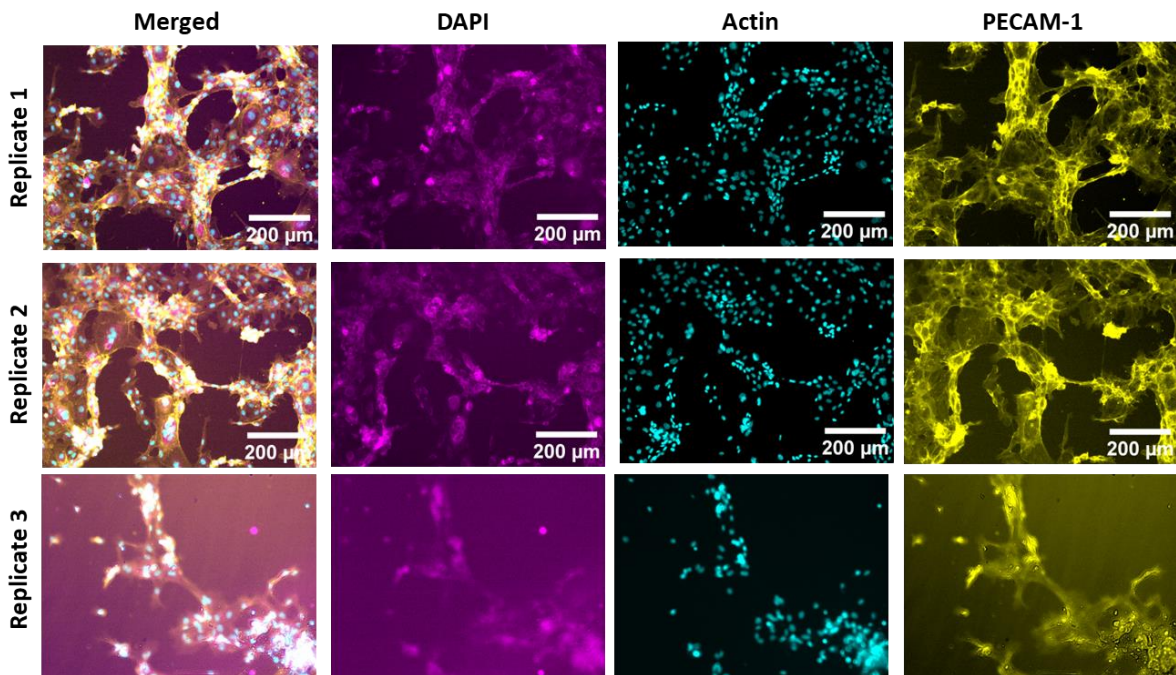


**Figure S8:** Epifluorescence images of HUVECs cultured for 16 hours on Col-Gel surfaces that were incubated in supernatants from ELMs containing YCQ bacteria exposed to blue light pulses (2 s ON, 1 min OFF;  $105 \mu\text{W}\cdot\text{cm}^{-2}$ ) for 6 days. The cells were stained for PECAM-1 (magenta), actin (yellow) and DNA (cyan).